There is something bigger than fact: the underlying spirit,
all it stands for, the mood, the vastness, the wildness.

Emily Carr

University of Alberta

Quaternary glaciation of central Banks Island, NT, Canada

by

Thomas Ryan Lakeman

A thesis submitted to the Faculty of Graduate Studies and Research
in partial fulfillment of the requirements for the degree of

Doctor of Philosophy

Department of Earth and Atmospheric Sciences

Fall 2012
Edmonton, Alberta

For Mom and Dad
Without your tremendous example,
none of this would have been possible.

ABSTRACT

The glacial geology and geomorphology of central Banks Island record the extent and dynamics of the northwest Laurentide Ice Sheet (LIS) during Late Wisconsinan glaciation. Additional stratigraphic exposures document Mid Quaternary environmental changes. Detailed mapping and a new chronology indicate that the island was inundated by the northwest LIS during the Late Wisconsinan. The maximum limit of the ice sheet was offshore on the Beaufort Sea shelf, one of several source regions for floating glacier ice that scoured the Arctic Ocean sea floor to a depth of 450 m. Ice sheet retreat was underway by ~14 cal ka BP when an ice stream withdrew rapidly from M'Clure Strait. A readvance or stillstand 13.75–12.75 cal ka BP resulted in deposition of widespread controlled moraines, comprising the Jesse moraine belt on eastern Banks Island and adjacent Victoria Island. This deposit records predominantly cold-based ice margins giving way to polythermal bed conditions, which were conducive to widespread deposition of controlled moraines and ice stream bedforms. The expansion of warm-based thermal regimes in the northwest LIS followed ice sheet withdrawal from M'Clure Strait and western Amundsen Gulf, suggesting a re-equilibration of regional ice divides in response to rapidly changing ice sheet margins and surface gradients. These reconstructed ice sheet dynamics provide new constraints for assessing the sensitivity of the northwest LIS to past changes in climate and sea level.

Stratigraphic exposures at Morgan Bluffs on eastern Banks Island comprise an archive of Mid to Late Quaternary environmental change. New, detailed

sedimentological analyses and stratigraphic investigations negate the previously reported climatostratigraphy, which involved multiple glacial-interglacial cycles. Instead, three distinct intervals of sedimentation are now recognized. The first records the progradation of a delta, followed by aggradation of a braided river valley perhaps ~1 Ma ago. The second documents a glacier advance across a former marine delta more than 780 ka ago. The third succession is interpreted to record sedimentation by an ice-contact delta into an ice-dammed lake during the last deglaciation, ~12.75 cal ka BP. The revised stratigraphic framework adds important new terrestrial observations to a sparse and fragmentary dataset of Arctic environmental change.

ACKNOWLEDGEMENTS

This research was principally funded by Dr. John England's Natural Sciences and Engineering Research Council (NSERC) Northern Chair and Discovery Grant programs at the University of Alberta. Additional funding from the Canadian Circumpolar Institute (CCI) and Aboriginal Affairs and Northern Development Canada (AANDC) in the form of Circumpolar-Boreal Alberta Research (CBAR) grants and Northern Scientific Training Program (NSTP) grants, respectively, is also acknowledged. The Polar Continental Shelf Program (PCSP) provided logistical support required to access the remote field sites documented in this study. I am particularly grateful to several funding agencies for postgraduate scholarships, including NSERC (Postgraduate Scholarship D3), the Alberta Ingenuity Fund (Alberta Innovates; Ph.D. Graduate Student Scholarship), the Association of Canadian Universities for Northern Studies, and the W. Garfield Weston Foundation (Garfield Weston Doctoral Award for Northern Research). As well, I would like to thank the members of my supervisory committee, John England, Marianne Douglas, Duane Froese, Doug Schmitt, Martin Sharp, and Martyn Unsworth, as well as my external examiner, Chris Stokes, for their interest, valuable comments, and guidance over the course of my program.

I owe special gratitude to my supervisor, John England, who first introduced me to the Arctic in 2003. Your mentorship, encouragement, and humility over the past decade have kept me on an engaging and rewarding path. The vastness, silence, and intimacy of the Arctic have changed me in ways I never thought possible. I consider this a great blessing and privilege, one I hope everyone can experience. For this I shall remain forever thankful.

Many people contributed greatly to extensive fieldwork on Banks Island from 2007 to 2012. A selfless, Vernon Amos, welcomed me to Banks Island and provided stalwart assistance at Stewart Point in 2007. For what it's worth… always watch. Guy Springett provided comradeship and many laughs during a long, arduous field season in 2008. Our paddle down the Thomsen River and our frequent visits by the wolves at Jesse Harbour are cherished adventures. Additional field assistance at Storkerson Bay, Burnett Bay, and Jesse Bay by Stacey Harrison during many snowy days in 2009 is also acknowledged.

Roy Coulthard provided many valuable insights, mentorship, and above all, friendship. Our long conversations over many micro-brewed ales, often straying from science and geomorphology into politics and the magic of *the North*, are sure to be missed. I thank Mark Furze for many fruitful discussions throughout the course of my program and for the opportunity to teach at Grant MacEwan University. I am particularly indebted for his assistance and mentorship in 2010 on Phillips Island. Anna Pienkowski is acknowledged for her keen, satirical sense of humour, and her legendary general kindness. Jessica Vaughan's sheer energy and hilarity contributed much colour to otherwise grey days in the office. I thank Jonathan Doupé for many discussions about cosmogenic nuclides and for organizing Monday morning shinny. Dave Evans helped stimulate my continuing interest in glacial sedimentology and provided many insights that improved my field research in

2008 and 2010. Catherine La Farge offered many encouragements and kindly shared her vast knowledge of Arctic bryophytes (and French cooking!).

Finally, I would like to thank my family. Mom and Dad (Patricia and Gordon Lakeman) fostered in me a great love of the outdoors and a strong independent spirit, without which I would only be a fragment of the person I am today. Thanks also to my brother, Ken, and sister, Katherine, for sharing my interests and for your sense of humour. Ours is the most Canadian family I know. My daughter, Sasha, and new son, Oscar, provided much needed respite from my research. It is a joy being your father and I can't wait to share new Arctic experiences with you in the future. Lastly, I wish to thank my Partner, Chantel Nixon. Your unending support, affection, and patience over these many years, has made our remarkable journey possible. As we move forward to face life's new opportunities, may our love remain, forever, Resolute.

TABLE OF CONTENTS

LIST OF TABLES

LIST OF FIGURES

CHAPTER 1

INTRODUCTION

SCOPE

Many facets of the geological history of the Canadian Arctic Archipelago (CAA; Fig. 1.1) remain enigmatic after more than 200 years of scientific observations. One aspect of notable uncertainty is the history of Late Cenozoic paleoenvironmental change, which includes past variability in tectonics, climate, the Arctic Ocean, sea ice, and the extent and dynamics of former glaciers and ice sheets, to name a few (Trettin, 1991; Harrison et al., 1999, 2011; Dyke et al., 2002; Dyke, 2004; Moran et al., 2006; Miller et al., 2010; Jakobsson et al., 2010a; Polyak et al., 2010). The focus of this dissertation is the Quaternary history of the western CAA, spanning the last 2.6 million years, during which the cyclical growth and decay of continental ice sheets characterized high latitudes (Maslin et al., 1998; Lisiecki and Raymo, 2007; Parrenin et al., 2007). For example, during the last glaciation the circum-Arctic was inundated by the Cordilleran Ice Sheet (CIS); Laurentide Ice Sheet (LIS), Innuitian Ice Sheet (IIS), Greenland Ice Sheet (GIS), Scandinavian Ice Sheet (SIS), and Barents-Kara Ice Sheet (BKIS) as well as thick sea ice in the Arctic Ocean (Clague and James, 2002; Dyke, 2004; Funder et al., 2004; Mangerud et al., 2004; Svendsen et al., 2004; England et al, 2006; Bradley and England, 2008; Fig. 1.2). Recent geophysical surveys in the Arctic Ocean, demonstrating seafloor erosion to depths exceeding 1000 m by Quaternary ice sheets, ice shelves, and icebergs, place important new constraints on the age, size, and extent of these former ice masses (Vogt et al., 1994; Jakobsson, 1999; Polyak et al., 2001, 2007; Kristoffersen et al, 2004; Jakobsson et al., 2005, 2008, 2010b; Engels et al., 2008; Dowdeswell et al., 2010). For example, many erosional scars in the western Arctic Ocean have been attributed to floating or grounded glacier ice originating from ice sheets that formerly occupied the western CAA (Polyak et al., 2001, 2007; Jakobsson et al., 2005, 2008 2010b; Engels et al., 2008).

Complementary to this research in the Arctic Ocean is the consensus that emerged primarily during the past decade in favour of more extensive Late Wisconsinan ice cover in the CAA (Blake, 1970, 1992a, b, 1993; Tushingham, 1991; Blake et al., 1996; Bednarski, 1998; Dyke, 1998, 1999; England, 1998, 1999; Bischof and Darby, 1999; Ó Cofaigh, 1999; Ó Cofaigh et al., 1999, 2000; Smith, 1999; England et al., 2000, 2004, 2006, 2009; Lamoureux and England, 2000; Dyke et al., 2002, 2003; Atkinson, 2003; Hansen, 2003; Atkinson and England, 2004; Dyke, 2004; Stokes et al., 2005, 2006, 2009; Nixon, 2012). The recognition of pervasive Late Wisconsinan glaciation across the CAA is based on widespread evidence of the convergence of the northern LIS, the IIS, the GIS, and several local ice caps (Fig. 1.3), which formed a dynamic ice mass with multiple ice shelves and ice streams (Dyke and Prest, 1987; Hodgson, 1994; Dyke et al., 2002; Atkinson, 2003; Hanson, 2003; Dyke, 2004; DeAngelis and Klemen, 2005, 2007; Stokes et al., 2005, 2006, 2009; England et al., 2006, 2009; Nixon, 2012). Recently, several studies have documented new thicknesses and limits for the northwest Laurentide Ice Sheet in M'Clure Strait (Stokes et al., 2005, 2009; England et al., 2009), in Amundsen Gulf

(Stokes et al., 2006; MacLean et al., 2012), and on the Yukon Coastal Plain (Fritz et al., 2012). This research reinforces the model of a pervasive Late Wisconsinan ice cover across the CAA and further supplants the previous model purporting limited glacier expansion during the last glaciation (Craig and Fyles, 1960; Fyles, 1962; England, 1976, 1978, 1983, 1992, 1996; England and Bradley, 1978; England et al., 1978, 1981, 1991; Boulton, 1979; Vincent, 1982, 1983; Hodgson, 1985; Bell, 1996).

Despite these recent advances, however, the maximum limit of Late Wisconsinan glaciation in the western CAA remains enigmatic (Fig. 1.3). Further, the dynamical changes within the northwest LIS that occasioned deglaciation and the record of postglacial relative sea level change are poorly understood. Constraining these uncertainties using the glacial geomorphology on central and northern Banks Island, NT constitutes the first objective of this thesis. Banks Island is situated in the western CAA (Fig. 1.1) in between Amundsen Gulf and M'Clure Strait, which were formerly occupied by major ice streams of the northwest LIS (Stokes et al., 2005, 2006, 2009; England et al., 2009; MacLean et al., 2012; Fig. 1.3). As such, reconstructions of former ice sheet limits and dynamics on Banks Island will bear directly on past limits, thicknesses, and dynamics of the M'Clure Strait and Amundsen Gulf ice streams, as well as on broad assessments of the northwest LIS during the last glaciation. A revision of the glacial history of Banks Island is also warranted because the last systematic study was conducted two decades prior to the current consensus regarding extensive LGM ice sheets throughout the CAA (Vincent, 1982, 1983). Vincent (1982, 1983) strongly reinforced the paradigm of limited ice extent in the western CAA during the last glaciation (Hobbs, 1945; Jenness, 1952; Wilson et al., 1958; Fyles, 1962; Prest, 1969). Specifically, Vincent

(1982, 1983) purported the existence of an ice age refugium on Banks Island during the Late Wisconsinan (i.e. Harington, 2005; MacPhee, 2007) and identified multiple older Quaternary glaciations that were each successively less extensive (Fig. 1.4). This model stands in stark contrast to newly recognized, extensive LGM ice cover in the western Canadian Arctic (Hanson, 2003; Stokes et al., 2005, 2006, 2009; England et al., 2006, 2009; Fritz et al., 2012; Nixon, 2012; Fig. 1.3) and Late Wisconsinan glacier erosion of the Arctic Ocean seafloor to depths of up to ~450 m (Polyak et al., 2001, 2007; Jakobsson et al., 2005; Jakobsson et al., 2008).

The second focus of this thesis is the stratigraphic evidence of Early Quaternary environmental changes preserved at Morgan Bluffs, eastern Banks Island (Fig. 1.4), and their relationship to former paleoclimates (i.e. glaciations and interglaciations), sea levels, and landscape dynamics. Terrestrial evidence for Quaternary environments preceding Late Wisconsinan glaciation is sparse and generally fragmentary in the CAA (Blake, 1974; Miller et al., 1977; Vincent, 1982, 1983, 1990; Fyles, 1990; Matthews and Ovenden, 1990; Fyles et al., 1994, 1998; Barendregt et al., 1998; Axford et al., 2009). This contrasts markedly with northern Yukon and Alaska where widespread Quaternary sedimentary archives exist (i.e. Péwé, 1975; Hopkins et al., 1982; Kaufman and Brigham-Grette, 1995; Froese et al., 2000, 2008; Brigham-Grette, 2001; Shapiro et al., 2004).

Morgan Bluffs is one of several stratigraphic exposures on Banks Island (Fig. 1.4) purportedly containing sediments relating to multiple Quaternary glaciations and interglaciations of unknown absolute age (Vincent, 1982, 1983, 1990; Barendregt et al., 1998). A climatostratigraphic framework for the multiple exposures was first developed by Vincent (1982, 1983) following initial lithostratigraphic correlations. Subsequently, Vincent et al. (1984), Vincent (1990), and Barendregt et al. (1998) amended this climatostratigraphy using new biostratigraphic and magnetostratigraphic correlations. The latest climatostratigraphic framework proposed by Barendregt et al. (1998) represents a sequence of Early Quaternary environmental change that differs from previous work only in the number of recorded glaciations and interglaciations. To date, a comprehensive description of the sedimentology of the deposits and the occasionally complex stratigraphic relationships within single exposures (i.e. glaciotectonism) has not been completed. As a result, the purported climatostratigraphic framework does not account for rapid vertical and lateral facies changes, which are a hallmark of most Quaternary sedimentary successions (i.e. Evans, 2003). Such a reconsideration of the stratigraphy and sedimentology would supplant the existing climatostratigraphic interpretations of the deposits on Banks Island and add significantly to our understanding of past depositional environments, glaciations, climates, ecosystems, and relative sea level changes.

STRUCTURE AND OBJECTIVES

This dissertation comprises three related field studies from central Banks Island that fundamentally challenge previously reported conclusions and hence contributes new perspectives on the Quaternary evolution of the CAA and our understanding of high-latitude ice sheets.

Chapter 2, *The extent of Late Wisconsinan glaciation and the nature of postglacial relative sea level change on western Banks Island, Canadian Arctic Archipelago*, documents the surficial geology and geomorphology of western Banks

Island. The objectives are to: determine the Late Wisconsinan limit of the LIS on Banks Island; characterize local glacier dynamics during ice sheet retreat; and document the history of postglacial sea level change resulting from glacioisostatic unloading of the crust following deglaciation. A version of this chapter, co-authored by J.H. England, was submitted for publication in *Quaternary Research* on March 1, 2012.

In Chapter 3, *Paleoglaciological insights from the age and morphology of the Jesse moraine belt, western Canadian Arctic*, the ice sheet dynamics that occasioned the deposition of a large moraine belt on eastern Banks Island and on adjacent western Victoria Island (the Jesse moraine belt) are characterized. The objectives are to: describe the geomorphology and sedimentology of the Jesse moraine belt in relation to distal glacial deposits in order to characterize former ice-marginal processes; evaluate spatial and temporal variations in ice-marginal depositional environments to inform estimates of past ice sheet dynamics; and consider potential causal linkages between former ice sheet dynamics and past fluctuations in climate, sea level, and the timing and pattern of regional deglaciation. A version of this chapter, co-authored by J.H. England, was published in *Quaternary Science Reviews* on July 30, 2012.

Chapter 4, *Revision of the early Quaternary stratigraphy at Morgan Bluffs, Banks Island, western Canadian Arctic*, reexamines the stratigraphy of Quaternary sediments comprising Morgan Bluffs, a ~ 6 km long exposure on the north shore of Jesse Bay on eastern Banks Island. The objective is to fundamentally reinvestigate the sedimentology of the Bluffs in order to identify past depositional environments and their relationship to former glaciations and interglaciations, relative sea levels, and landscape dynamics. A version of this chapter, co-authored by J.H. England, is currently in preparation for submission to Boreas.

RATIONALE

Observations of past ice sheet dynamics provide important constraints for geophysical models of extant glaciers and ice sheets (Bentley, 2010; Joughin and Alley, 2011). Improved understanding of ice sheet dynamics provides insights on the past and present behaviour of the Greenland and Antarctic ice sheets, which is critical to developing accurate forecasts of future eustatic sea level rise (Joughin and Alley, 2011; Siddall and Milne, 2012). For example, in its Fourth Assessment Report (AR4), the Intergovernmental Panel on Climate Change (IPCC) forecasted a global rise in sea level of 0.18-0.59 m by 2100. This estimate, however, takes no account of future ice sheet dynamical changes in the Greenland and Antarctic ice sheets, which remain a focus for current research but are, nonetheless, still poorly understood (i.e. Zwally et al., 2002; Hanna et al., 2004; Rignot, 2008; Jacobs et al., 2011; Thomas et al., 2011). As a result, future ice sheet dynamics comprise one of the major sources of uncertainty in future estimates of global sea level rise.

Reconstructions of past ice sheets also help to elucidate the origin and nature of former paleoclimatic and paleoceanographic changes that characterized the last glaciation, including the last glacial-interglacial transition (i.e. Peltier et al., 2006; Clark et al., 2009; Tarasov et al., 2011; Thornalley et al., 2011; Weber et al., 2011). Some of these changes, such as those during the Younger Dryas chronozone, were astonishingly rapid and interhemispheric in scale (Dansgaard et al., 1993; Clark et al., 2002; Broecker et al., 2010). The record of postglacial relative sea level change is also a valuable archive of glacioisostatic crustal adjustments following ice sheet retreat, which bears on estimates of the geophysical properties of the lithosphere and asthenosphere (i.e. Clague and James, 2002; Peltier and Drummond, 2008).

Terrestrial stratigraphic exposures of Quaternary sediments are rare in the CAA but constitute important archives of past environments during widely varying climates. When fully characterized and integrated with other terrestrial records from Yukon, Alaska, and elsewhere, these sediments can help elucidate former rates, magnitudes, and spatial heterogeneities of terrestrial Arctic environmental change, including past variability in Arctic flora/fauna, relative sea level, climate, glaciers and ice sheets, and sea ice, among others. Ultimately, this knowledge provides new perspectives on the natural range of interdependency among various environmental variables. Indeed, such information can constrain geophysical models used to forecast future environmental change (i.e. Lunt et al., 2009). Furthermore, these records inform reconstructions of the Quaternary evolution of the circum-Arctic based on sediment cores from the Arctic Ocean basin (i.e. Moran et al., 2006).

REFERENCES

Atkinson, N. 2003. Late Wisconsinan glaciation of Amund and Ellef Ringnes islands, Nunavut: evidence for the configuration, dynamics and deglacial chronology of the northwest sector of the Innuitian Ice Sheet. Canadian Journal of Earth Sciences 40, 351–363. doi:10.1139/e02-106.

Atkinson, N., England, J. 2004. Postglacial emergence of Amund and Ellef Ringnes islands, Nunavut: implications for the northwest sector of the Innuitian Ice Sheet. Canadian Journal of Earth Sciences 41, 271–283. doi:10.1139/e03-095.

Axford, Y., Briner, J.P., Cooke, C.A., Francis, D.R., Micheluttie, N., Miller, G.H., Smol, J.P., Thomas, E.K., Wilson, C.R., Wolfe, A.P. 2009. Recent changes in a remote Arctic lake are unique within the past 200,000 years. Proceedings of the National Academy of Sciences. doi:10.1073/pnas.0907094106.

Barendregt, R.W., Vincent, J.-S., Irving, E., Baker, J. 1998. Magnetostratigraphy of Quaternary and late Tertiary sediments on Banks Island, Canadian Arctic Archipelago. Canadian Journal of Earth Sciences 35, 147–161. doi:10.1139/e97-094.

Bednarski, J.M. 1998. Quaternary history of Axel Heiberg Island, bordering Nansen Sound, Northwest Territories, emphasizing the Last Glacial Maximum. Canadian Journal of Earth Sciences 35, 520–533. doi:10.1139/e97-124.

Bell, T. 1996. The last glaciation and sea level history of Fosheim Peninsula, Ellesmere Island, Canadian High Arctic. Canadian Journal of Earth Sciences 33, 1075–1086. doi:10.1139/e96-082.

Bentley, M.J., 2010. The Antarctic palaeo record and its role in improving predictions of future Antarctic Ice Sheet change. Journal of Quaternary Science 25, 5–18. doi:10.1002/jqs.1287.

Bischof, J., Darby, D. 1999. Quaternary ice transport in the Canadian Arctic and extent of Late Wisconsinan glaciation in the Queen Elizabeth Islands. Canadian Journal of Earth Sciences 36, 2007–2022. doi:10.1139/e99-096.

Blake, W., Jr. 1970. Studies of glacial history in Arctic Canada. Canadian Journal of Earth Sciences 7, 634–664. doi:10.1139/e70-065.

Blake, W., Jr. 1974. Studies of glacial history in Arctic Canada. II. Interglacial peat deposits on Bathurst Island. Canadian Journal of Earth Sciences 11, 1025–1042. doi:10.1139/e74-102.

Blake, W., Jr. 1992a. Holocene emergence at Cape Herschel, east-central Ellesmere Island, Arctic Canada: implications for ice sheet configuration. Canadian Journal of Earth Sciences 29, 1958–1980. doi:10.1139/e92-153.

Blake, W., Jr. 1992b. Shell-bearing till along Smith Sound, Ellesmere Island-Greenland: age and significance. In: Robertson, A-M., Ringberg, B., Miller, U., Brunnberg, L. (Eds.), Quaternary Stratigraphy, Glacial Morphology and Environmental Change, Vol. 81. Sveriges Geologiska Underso¨ kning, pp. 51–58.

Blake, W., Jr. 1993. Holocene emergence along the Ellesmere Island coast of northernmost Baffin Bay. Norsk Geologisk Tidsskrift 73, 147–160.

Blake, W., Jr., Jackson, H.R., Currie, C.G. 1996. Seafloor evidence for glaciation, northernmost Baffin Bay. Bulletin of the Geological Society of Denmark 23, 157–168.

Boulton, G.S. 1979. A model of Weichselian glacier variation in the North Atlantic regions. Boreas 8, 373–395. doi:10.1111/j.1502-3885.1979.tb00820.x.

Bradley, R.S., England, J.H. 2008. The Younger Dryas and the Sea of Ancient Ice. Quaternary Research 70, 1–10. doi:10.1016/j.yqres.2008.03.002.

Brigham-Grette, J. 2001. New perspectives on Beringian Quaternary palaeogeography, straitgraphy, and glacial history. Quaternary Science Reviews 20, 15–24. doi:10.1016/S0277-3791(00)00134-7.

Broecker, W.S., Denton, G.H., Edwards, R.L., Cheng, H., Alley, R.B., Putnam, A.E. 2010. Putting the Younger Dryas cold event in context. Quaternary Science

Reviews 29,1078–1081. doi:10.1016/j.quascirev.2010.02.019.

Clague, J.J., James, T.S. 2002. History and isostatic effects of the last ice sheet in southern British Columbia. Quaternary Science Reviews 21, 71–87. doi:10.1016/S0277-3791(01)00070-1.

Clark, P.U., Pisias, N.G., Stocker, T.F., Weaver, A.J. 2002. The role of the thermohaline circulation in abrupt climate change. Nature 415, 863–869. doi:10.1038/415863a.

Clark, P.U., Dyke, A.S., Shakun, J.D., Carlson, A.E., Clark, J., Wohlfarth, B., Mitrovica, J.X., Hostetler, S.W., McCabe, A.M. 2009. The Last Glacial Maximum. Science 325, 710–714. doi:10.1126/science.1172873.

Craig, B.G., Fyles, J.G. 1960. Pleistocene geology of Arctic Canada. Geological Survey of Canada, Paper 60-10.

De Angelis, H., Kleman, J. 2005. Palaeo-ice streams in the northern Keewatin sector of the Laurentide Ice Sheet. Annals of Glaciology 42, 135–144. doi:10.3189/172756405781812925.

De Angelis, H., Kleman, J. 2007. Palaeo-ice streams in the Foxe/Baffin sector of the Laurentide Ice Sheet. Quaternary Science Reviews 26, 1313–1331. doi:10.1016/j.quascirev.2007.02.010.

Dowdeswell, J.A., Jakobsson, M., Hogan, K.A., O'Regan, M., Backman, J., Evans, J., Hell, B., Löwemark, L., Marcussen, C., Noormets, R., Ó Cofaigh, C., Sellén, E., Sölvsten, M. 2010. High-resolution geophysical observations of the Yermak Plateau and northern Svalbard margin: implications for ice-sheet grounding and deep-keeled icebergs. Quaternary Science Reviews 29, 3518–3531. doi:10.1016/j.quascirev.2010.06.002.

Dyke, A.S. 1998. Holocene delevelling of Devon Island, Arctic Canada: implications for ice sheet geometry and crustal response. Canadian Journal of Earth Sciences 35, 885–904. doi:10.1139/e98-034.

Dyke, A.S. 1999. The Last Glacial Maximum and the deglaciation of Devon Island: support for an Innuitian Ice Sheet. Quaternary Science Reviews 18, 393–420. doi:10.1016/S0277-3791(98)00005-5.

Dyke, A.S. 2004. An outline of the deglaciation of North America with emphasis on central and northern Canada. In: Ehlers, J., Gibbard, P.L. (Eds.), Quaternary Glaciations, Extent and Chronology. Part II. North America. Developments in Quaternary Science, vol. 2b. Elsevier, Amsterdam.

Dyke, A.S., Prest, V.K. 1987. Late Wisconsinan and Holocene history of the Laurentide Ice Sheet. Géographie physique et Quaternaire 41, 237–263.

Dyke, A.S., Andrews, J.T., Clark, P.U., England, J.H., Miller, G.H., Shaw, J., Veillette, J.J. 2002. The Laurentide and Innuitian ice sheets during the Last Glacial Maximum. Quaternary Science Reviews 21, 9–31. doi:10.1016/S0277-3791(01)00095-6.

Dyke, A.S., Moore, A., Robertson, L. 2003. Deglaciation of North America. In: Geological Survey of Canada, Open File 1574.

Engels, J.L., Edwards, M.H., Polyak, L., Johnson, P.D. 2008. Seafloor evidence for ice shelf flow across the Alaska–Beaufort margin of the Arctic Ocean. Earth Surface Processes and Landforms 33, 1047–1063. doi:10.1002/esp1601.

England, J. 1976. Late Quaternary glaciation of the Queen Elizabeth Islands, Northwest Territories, Canada: alternative models. Quaternary Research 6, 185–202. doi:10.1016/0033-5894(76)90049-1.

England, J. 1978. The glacial geology of northeastern Ellesmere Island, N.W.T., Canada. Canadian Journal of Earth Sciences 15, 603–617. doi:10.1139/e78-065.

England, J. 1983. Isostatic adjustments in a full glacial sea. Canadian Journal of Earth Sciences 20, 895–917. doi:10.1139/e83-081.

England, J. 1992. Postglacial emergence in the Canadian High Arctic: integrating glacioisostasy, eustasy, and late deglaciation. Canadian Journal of Earth Sciences 29, 984–999. doi:10.1139/e92-082.

England, J. 1996. Glacier dynamics and paleoclimatic change during the last glaciation of eastern Ellesmere Island, Canada. Canadian Journal of Earth Sciences 33, 779–799. doi:10.1139/e96-060.

England, J. 1998. Support for the Innuitian Ice Sheet in the Canadian High Arctic during the Last Glacial Maximum. Journal of Quaternary Science 13, 275–280. doi:10.1002/(SICI)1099-1417(199805/06)13:3<275::AID-JQS374>3.0.CO;2-N.

England, J. 1999. Coalescent Greenland and Innuitian ice during the Last Glacial Maximum: revising the Quaternary of the Canadian High Arctic. Quaternary Science Reviews 18, 421–556. doi:10.1016/S0277-3791(98)00070-5.

England, J., Bradley, R.S. 1978. Past glacial activity in the Canadian high arctic. Science 200, 265–270. doi:10.1126/science.200.4339.265.

England, J., Bradley, R.S., Miller, G.H. 1978. Former ice shelves in the Canadian High Arctic. Journal of Glaciology 20, 393–404.

England, J., Bradley, R.S., Stuckenrath, R. 1981. Multiple glaciations and marine transgressions, western Kennedy Channel, Northwest Territories, Canada. Boreas 10, 71–89. doi:10.1111/j.1502-3885.1981.tb00470.x.

England, J., Sharp, M., Lemmen, D.S., Bednarski, J. 1991. On the extent and thickness of the Innuitian Ice Sheet: a postglacial adjustment approach: discussion.

Canadian Journal of Earth Sciences 28, 1689–1695. doi:10.1139/e91-152.

England, J., Smith, I.R., Evans, D.J.A. 2000. The last glaciation of eastcentral Ellesmere Island, Nunavut: ice dynamics, deglacial chronology, and sea level change. Canadian Journal of Earth Sciences 37, 1355–1371. doi:10.1139/e00-060.

England, J., Atkinson, N., Dyke, A.S., Evans, D.J.A., Zreda, M. 2004. Late Wisconsinan buildup and wastage of the Innuitian Ice Sheet across southern Ellesmere Island, Nunavut: dominance of the Greenland Ice Sheet. Canadian Journal of Earth Sciences 41, 39–61. doi:10.1139/e03-082.

England, J.H., Atkinson, H., Bednarski, J., Dyke, A.S., Hodgson, D.A., O Cofaigh, C. 2006. The Innuitian Ice Sheet: configuration, dynamics and chronology. Quaternary Science Reviews 25, 689–703. doi:10.1016/j.quascirev.2005.08.007.

England, J.H., Furze, M.F.A, Doupé, J.P. 2009. Revision of the NW Laurentide Ice Sheet: implications for paleoclimate, the northeast extremity of Beringia, and Arctic Ocean sedimentation. Quaternary Science Reviews 28, 1573–1596. doi:10.1016/j.quascirev.2009.04.006.

Evans, D.J.A. (Ed.) 2003. Glacial Landsystems. Arnold, London.

Fritz, M., Wetterich, S., Schirrmeister, L., Meyer, H., Lantuit, H., Preusser, F., Pollard, W.H. 2012. Eastern Beringia and beyond: Late Wisconsinan and Holocene landscape dynamics along the Yukon Coastal Plain, Canada. Palaeogeography, Palaeoclimatology, Palaeoecology 319-320, 28–45. doi:10.1016/j.palaeo.2011.12.015.

Froese, D.G., Barendregt, R.W., Enkin, R.J., Baker, J. 2000. Paleomagnetic evidence for multiple Late Pliocene-Early Pleistocene glaciations in the Klondike area, Yukon Territory. Canadian Journal of Earth Sciences 37, 863–877. doi:10.1139/cjes-37-6-863.

Froese, D.G., Westgate, J.A., Reyes, A.V., Enkin, R.J., Preece, S.J. 2008. Ancient permafrost and a future, warmer arctic. Science 321, 1648. doi:10.1126/science.1157525.

Funder, S., Jennings, A.E., Kelly, M.J. 2004. Middle and late Quaternary glacial limits in Greenland. In: Ehlers, J., Gibbard, P.L. (Eds.), Quaternary Glaciations, Extent and Chronology. Part II. North America. Developments in Quaternary Science, vol. 2b. Elsevier, Amsterdam.

Fyles, J.G. 1962. Physiography. In: Thorsteinsson, R., Tozer, E.T., Banks, Victoria, and Stefansson Island, Arctic Archipelago. Geological Survey of Canada, Memoir 330, pp. 8–17.

Fyles, J.G. 1990. Beaufort Formation (Late Tertiary) as seen from Prince Patrick Island, Arctic Canada. Arctic 43, 393–403.

Fyles, J.G., Hills, L.V., Matthews, J.V., Jr., Barendregt, R., Baker, J., Irving, E., Jetté, H. 1994. Ballast Brook and Beaufort Formations (Late Tertiary) on northern Banks Island, Arctic Canada. Quaternary International 22/23, 141–171. doi:10.1016/1040-6182(94)90010-8.

Fyles, J.G., McNeil, D.H., Matthews, J.V., Barendregt, R.W., Marincovich, L., Brouwers, E., Bednarski, J., Brigham-Grette, J., Ovenden, L.W., Miller, K.G., Baker, J., Irving, E. 1998. Geology of Hvitland beds (Late Pliocene), White Point lowland, Ellesmere Island, Northwest Territories. Geological Survey of Canada Bulletin 512, 35 pp.

Hanna, E., Huybrechts, P., Steffen, K., Cappelen, J., Huff, R., Shuman, C., Irvine-Flynn, T., Wise, S., Griffiths, M. 2008. Increased runoff from melt from the Greenland

Ice Sheet: a response to global warming. Journal of Climate 21, 331–341. doi:10.1175/2007JCLI1964.1.

Hanson, M. 2003. Late Quaternary Glaciation, Relative Sea Level History and Recent Coastal Submergence of Northeast Melville Island, Nunavut. M.Sc. thesis. University of Alberta, Edmonton, Alberta, Canada.

Harington, C.R. 2005. The eastern limit of Beringia: mammoth remains from Banks and Melville islands, Northwest Territories. Arctic 58, 361–369.

Harrison, J.C., Mayr, U., McNeil, D.H., Sweet, A.R., Eberle, J.J., McIntyre, D.J., Harington, C.R., Chalmers, J.A., Dam, G., Nohr-Hansen, H. 1999. Correlation of Cenozoic sequences of the Canadian Arctic region and Greenland; implications for the tectonic history of northern North America. Bulletin of Canadian Petroleum Geology 47, 223–254.

Harrison, J.C., Brent, T.A., Oakey, G.N. 2011. Baffin Fan and its inverted rift system of Arctic eastern Canada: stratigraphy, tectonics and petroleum resource potential. In: A.M. Spencer, A.F. Embry, D.L. Gautier, A.V. Stoupakavoa, K. Sørensen (Eds.), Arctic Petroleum Geology. Geological Society, London, Memoirs 35, 595–626. doi:10.1144/M35.40.

Hobbs, W.H. 1945. The boundary of the latest glaciation in Arctic Canada. Science 101, 549–551. doi:10.1126/science.101.2631.549.

Hodgson, D.A. 1985. The last glaciation of west-central Ellesmere Island, Arctic Archipelago, Canada. Canadian Journal of Earth Sciences 22, 347–368. doi:10.1139/e85-035.

Hodgson, D.A. 1994. Episodic ice streams and ice shelves during retreat of the northwesternmost sector of the late Wisconsinan Laurentide Ice Sheet over the central Canadian Arctic Archipelago. Boreas 23, 14–28. doi:10.1111/j.1502-3885.1994.tb00582.x.

Hopkins, D.M., Matthews, J.V., Jr., Schweger, C.E., Young, S.B. (Eds.). 1982. Paleoecology of Beringia. New York, Academic Press, 489 pp.

Jacobs, S.S., Jenkins, A., Giulivi, C.F., Dutrieux, P. 2011. Stronger ocean circulation and increased melting under Pine Island Glacier ice shelf. Nature Geoscience 4, 519–523. doi:10.1038/NGEO1188.

Jakobsson, M. 1999. First high-resolution chirp sonar profiles from the central Arctic Ocean reveal erosion of the Lomonosov Ridge sediments. Marine Geology 158, 111–123. doi:10.1016/S0025-3227(98)00186-8.

Jakobsson, M., Gardner, J.V., Vogt, P., Mayer, L.A., Armstrong, A., Backman, J., Brennan, R., Calder, B., Hall, J.K., Kraft, B. 2005. Multibeam bathymetric and sediment profiler evidence for ice grounding on the Chukchi Borderland, Arctic Ocean. Quaternary Research 63, 150–160. doi:10.1016/j.yqres.2004.12.004.

Jakobsson, M., Polyak, L., Edwards, M., Kleman, J., Coakley, B. 2008. Glacial geomorphology of the Central Arctic Ocean: the Chukchi Borderland and the Lomonosove Ridge. Earth Surface Processes and Landforms 33, 526–545. doi:10.1002/esp.1667.

Jakobsson, M., Long, A., Ingólfsson, Ó., Kjær, K.H., Speilhagen, R.F. 2010a. New insights on Arctic Quaternary climate variability from paleo-records and numerical-modelling. Quaternary Science Reviews 29, 3349–3358. doi:10.1016/j.quascirev.2010.08.016.

Jakobsson, M., Nilsson, J., O'Regan, M., Backman, J., Löwemark, L., Dowdeswell, J.A., Mayer, L., Polyak, L., Colleoni, F., Anderson, L.G., Björk, G., Darby, D., Eriksson, B., Hanslik, D., Hell, B., Marcussen, C., Sellén, E., Wallin, A. 2010b. An Arctic Oean ice shelf during MIS 6 constrained by new geophysical and geological data. Quaternary Science Reviews 29, 3505–3517. doi:10.1016/j.quascirev.2010.03.015.

Jenness, J.L. 1952. Problem of glaciation in the western islands of Arctic Canada. Bulletin of the Geological Society of America 63, 939–952. doi:10.1130/0016-7606(1952)63[939:POGITW]2.0.CO;2.

Joughin, I., Alley, R.B. 2011. Stability of the West Antarctic ice sheet in a warming world. Nature Geoscience 4, 506–513. doi:10.1038/NGEO1194

Kaufman, D.S., Brigham-Grette, J. 1993. Aminostratigraphic correlations and paleotemperature implications, Pliocene-Pleistocene high-sea-level deposits, northwestern Alaska. Quaternary Science Reviews 12, 21–33. doi:10.1016/0277-3791(93).90046-O.

Kristoffersen, Y., Coakley, B., Jokat, W., Edwards, M., Brekke, H., Gjengedal, J. 2004. Seabed erosion on the Lomonosov Ridge, central Arctic Ocean: a tale of deep draft icebergs in the Eurasia Basin and the influence of Atlantic water inflow on iceberg motion? Paleoceanography 19: PA3006. doi:10.1029/2003PA000985.

Lamoureux, S.F., England, J. 2000. Late Wisconsinan of the central sector of the Canadian High Arctic. Quaternary Research 54, 182–188. doi:10.1006/qres.2000.2167.

Lisiecki, L.E., Raymo, M.E. 2007. Plio-Pleistocene climate evolution: trends and transitions in glacial cycle dynamics. Quaternary Science Reviews 26, 56–69. doi:10.1016/j.quascirev.2006.09.005.

Lunt, D.J., Haywood, A.M., Foster, G.L., Stone, E.J. 2009. The Arctic cryosphere in the Mid-Pliocene and the future. Philosophical Transactions of the Royal Society A 367, 49–67. doi:10.1098/rsta.2008.0218.

MacLean, B., Blasco, S., Bennett, R., Lakeman, T., Hughes-Clarke, J. 2012. Geological history of Amundsen Gulf over the last ~19,000 years: ameliorating climate transition from glacial to interglacial conditions. Abstract #650. International Polar Year 2012 Conference, Montreal, PQ, April 22–27, 2012.

MacPhee, R.D.E. 2007. Mammoths in the insular Nearctic? Some constraints on the existence of a Pleistocene megafaunal refugium in the Canadian Arctic Archipelago. Quaternary International 169-170, 29–38. doi:10.1016/j.quaint.2006.08.007.

Mangerud, J. 2004. Ice sheet limits on Norway and the Norwegian continental shelf. In: Ehlers, J. & Gibbard, P.L. (Eds.), Quaternary Glaciations - Extent and Chronology. Vol. 1 Europe. Elsevier, Amsterdam.

Maslin, M.A., Li, X.S., Loutre, M.-F., Berger, A. 1998. The contribution of orbital forcing to the progressive intensification of northern hemisphere glaciation. Quaternary Science Reviews 17, 411–426. doi:10.1016/S0277-3791(97)00047-4.

Miller, G.H., Andrews, J.T., Short, S.K. 1977. The last interglacial-glacial cycle, Clyde foreland, Baffin Island, N.W.T.: stratigraphy, biostratigraphy, and chronology. Canadian Journal of Earth Sciences 14, 2824–2857. doi:10.1139/e77-249.

Miller, G.H., Brigham-Grette, J., Alley, R.B., Anderson, L., Bauch, H.A., Douglas, M.S.V., Edwards, M.E., Elias, S.A., Finney, B.P., Fitzpatrick, J.J., Funder, S.V., Herbert, T.D., Hinzman, L.D., Kaufman, D.S., MacDonald, G.M., Polyak, L., Robock, A., Serreze, M.C., Smol, J.P., Speilhagen, R., White, J.W.C., Wolfe, A.P., Wolff, E.W. 2010. Temperature and precipitation history of the Arctic. Quaternary Science Reviews 29, 1679–1715. doi:10.1016/j.quascirev.2010.03.001.

Moran, K., Backman, J., Brinkhuis, H., Clemens, S.C., Cronin, T., Dickens, G.R., Eynaud, F., Gattacceca, J., Jakobsson, M., Jordan, R.W., Kaminski, M., King, J., Koc, N., Krylov, A., Martinez, N., Matthiessen, J., McInroy, D., Moore, T.C., Onodera, J., O'Regan, M., Pälike, H., Rea, B., Rio, D., Sakamoto, T., Smith, D.C., Stein, R., St John, K., Suto, I., Suzuki, N., Takahashi, K., Watanabe, M., Yamamoto, M., Farrell, J., Frank, M., Kubik, P., Jokat, W., Kristoffersen, Y. 2006. The Cenozoic palaeoenvironment of the Arctic Ocean. Nature 44, 601–605. doi:10.1038/nature04800.

Nixon, F.C. 2012. The glacial, sea level, and sea ice histories of Melville and Eglinton islands, western Canadian High Arctic: Last Glacial Maximum to present. Ph.D. thesis. University of Alberta, Edmonton, Alberta, Canada.

Ó Cofaigh, C. 1999. Holocene emergence and shoreline delevelling, southern Eureka Sound, High Arctic Canada. Géographie Physique et Quaternaire 53, 235–247.

Ó Cofaigh, C., Lemmen, D.S., Evans, D.J.A., Bednarski, J. 1999. Glacial sediment/landform assemblages in the Canadian High Arctic and their implications for Late Quaternary glaciation. Annals of Glaciology 28, 195–207.

Ó Cofaigh, C., England, J., Zreda, M. 2000. Late Wisconsinan glaciation of southern Eureka Sound: evidence for extensive Innuitian ice in the Canadian High Arctic during the Last Glacial Maximum. Quaternary Science Reviews 19, 1319–1341.

doi:10.1016/S0277-3791(99)00104-3.

Parrenin, F., Barnola, J.-M., Beer, J., Blunier, T., Castellano, E., Chappellaz, J., Dreyfus, G., Fischer, H., Fujita, S., Jouzel, J., Kawamura, K., Lemieux-Dudon, B., Loulergue, L., Masson-Delmotte, V., Narcisi, B., Petit, J.-R., Raisbeck, G., Raynaud, D., Ruth, U., Schwander, J., Severi, M., Spahni, R., Steffensen, J.P., Svensson, A., Udisti, R., Waelbroeck, C., Wolff, E. 2007. The EDC3 chronology for the EPICA Dome C ice core. Climate of the Past 3, 485–497. www.clim-past.net/3/485/2007/.

Peltier, W.R., Fairbanks, F.G. 2006. Global glacial ice volume and last glacial maximum duration from an extended Barbados sea level record. Quaternary Science Reviews 25, 3322–3337. doi: 10.1016/j.quascirev.2006.04.010.

Peltier, W.R., Drummond, R. 2008. Theological stratification of the lithosphere: a direct inference based upon the geodetically observed pattern of the glacial isostatic adjustment of the North American continent. Geophysical Research Letters 35, L16314. doi:10.1029/2008GL034586.

Péwé, T.L. 1975. Quaternary geology of Alaska. United States Geological Survey, Professional Paper 835.

Polyak, L., Edwards, M.H., Coakley, B.J., Jakobsson, M. 2001. Ice shelves in the Pleistocene Arctic Ocean inferred from glaciogenic deep-sea bedforms. Nature 410, 453–457. doi:10.1038/35068536.

Polyak, L., Darby, D., Bischof, J., Jakobsson, M. 2007. Stratigraphic constraints on late Pleistocene glacial erosion and deglaciation of the Chukchi margin, Arctic Ocean. Quaternary Research 67, 234–245. doi:10.1016/j.yqres.2006.08.001.

Polyak, L., Alley, R.B., Andrews, J.T., Brigham-Grette, J., Cronin, T.M., Darby, D.A., Dyke, A.S., Fitzpatrick, J.J., Funder, S., Holland, M., Jennings, A.E., Miller, G.H., O'Regan, M., Savelle, J., Serreze, M., St. John, K., White, J.W.C., Wolff, E. 2010. History of sea ice in the Arctic. Quaternary Science Reviews 29, 1757–1778. doi:10.1016/j.quascirev.2010.02.010.

Preece, S.J., Westgate, J.A., Froese, D.G., Pearce, N.J.G., Perkins, W.T. 2011. A catalogue of late Cenozoice tephra beds in the Klondike goldfields and adjacent areas, Yukon Territory. Canadian Journal of Earth Sciences 48, 1386–1418. doi:10.1139/E10-110.

Prest, V.K. 1969. Retreat of Wisconsin and Recent ice in North America. Geological Survey of Canada Map 1257A, scale 1:5,000,000.

Rignot, E. 2008. Changes in West Antarctic ice stream dynamics observed with ALOS PALSAR data. Geophysical Research Letters 35, L12505. doi:10.1029/2008GL033365.

Shapiro, B., Drummond, A.J., Rambaut, A., Wilson, M.C., Matheus, P.E., Sher, A.V., Pybus, O.G., Gilbert, M.T.P., Barnes, I., Binladen, J., Willerslev, E., Hansen, A.J., Baryshnikov, G.F., Burns, J.A., Davydov, S., Driver, J.C., Froese, D.G., Harington, C.R., Keddie, G., Kosintsev, P., Kunz, M.L., Martin, L.D., Stephenson, R.O., Storer, J., Tedford, R., Zimov, S., and Cooper, A. 2004. Rise and fall of the Beringian steppe bison. Science 306, 1561–1565. doi:10.1126/science.1101074.

Siddall, M., Milne, G.A. 2012. Understanding sea-level change is impossible without both insights from paleo studies and working across disciplines. Earth and Planetary Science Letters 315/316, 2–3. doi:10.1016/j.epsl.2011.10.023.

Smith, I.R. 1999. Late Quaternary glacial history of Lake Hazen Basin and eastern Hazen Plateau, northern Ellesmere Island, Nunavut, Canada. Canadian Journal of Earth Sciences 36, 1547–1565. doi:10.1139/e99-046.

Stokes, C.R., Clark, C.D., Darby, D.A., Hodgson, D.A. 2005. Late Pleistocene ice export events into the Arctic Ocean from the M'Clure Strait Ice Stream, Canadian Arctic Archipelago. Global and Planetary Change 49, 139-162. doi:10.1016/j.gloplacha.2005.06.001.

Stokes, C.R., Clark, C.D., Winsborrow, M.C.M. 2006. Subglacial bedform evidence for a major palaeo-ice stream and its retreat phases in Amundsen Gulf, Canadian Arctic Archipelago. Journal of Quaternary Science 21, 399–412. doi:10.1002/jqs.991.

Stokes, C.R., Clark, C.D., Storrar, R. 2009. Major changes in ice stream dynamics during deglaciation of the north-western margin of the Laurentide Ice Sheet. Quaternary Science Reviews 28, 721–738. doi:10.1016/j.quascirev.2008.07.019.

Svendsen, J.I., Gataullin, V., Mangerud, J., Polyak, L., 2004. The glacial history of the Barents and Kara Sea Region. In: Ehlers, J., Gibbard, P.L. (Eds.), Quaternary Glaciations - Extent and Chronology, Part I: Europe. Developments in Quaternary Science, Vol. 2a. Elsevier, Amsterdam.

Tarasov, L., Dyke, A.S., Neal, R.M., Peltier, W.R. 2011. A data-calibrated distribution of deglacial chronologies for the North American ice complex from glaciological modeling. Earth and Planetary Science Letters 315-316, 30–40. doi:10.1016/j.epsl.2011.09.010.

Thomas, R., Frederick, E., Li, J., Krabill, W., Manizade, W., Paden, J., Sonntag., Swift, R., Yungel, J. 2011. Accelerating ice loss from the fastest Greenland and Antarctic glaciers. Geophysical Research Letters 38, L10502. doi:10.1029/2011GL047304.

Thornalley, D.J.R., Barker, S., Broecker, W.S., Elderfield, H., McCave, I.N. 2011. The deglacial evolution of North Atlantic Deep Convection. Science 331, 202–205. doi:10.1126/science.1196812.

Trettin, H.P. (Ed.). 1991. Geology of the Innuitian Orogen and Arctic Platform of Canada and Greenland. Geology of Canada 3. Geological Survey of Canada, Ottawa.

Tushingham, A.M. 1991. On the extent and thickness of the Innuitian Ice Sheet: a postglacial adjustment approach. Canadian Journal of Earth Sciences 28, 231–239. doi:10.1139/e91-022.

Vincent, J.-S. 1982. The Quaternary history of Banks Island, NWT, Canada. Géographie physique et Quaternaire 36, 209–232.

Vincent, J.-S. 1983. La géologie du Quaternaire et la géomorphologie de l'Île Banks, Arctique Canadien. Geological Survey of Canada, Memoir 405.

Vincent, J.-S. 1984. Quaternary stratigraphy of the western Canadian Arctic Archipelago. In: Fulton, R.J. (Ed.), Quaternary Stratigraphy of Canada – A Canadian Contribution To IGCP Project 24. Geological Survey of Canada Paper, 84-10, pp. 87–100.

Vincent, J.-S., Morris, W.A., Occhietti, S. 1984. Glacial and nonglaical sediments of Matuyama paleomagnetic age on Banks Island, Canadian Arctic Archipelago. Geology 12, 139–142. doi:10.1130/0091-7613(1984)12<139:GANSOM>2.0.CO;2.

Vogt, P.R., Crane, K., Sundvor, E. 1994. Deep Pleistocene iceberg plowmarks on the Yermak Plateau: sidescan and 3.5 kHz evidence for thick calving ice fronts and a possible marine ice sheet in the Arctic Ocean. Geology 22, 403–406. doi:10.1130/0091-7613(1994)022<0403:DPIPOT>2.3.CO;2.

Weber, M.E., Clark, P.U., Ricken, W., Mitrovica, J.X., Hostetler, S.W., Kuhn, G. 2011. Interhemispheric ice-sheet synchronicity during the Last Glacial Maximum. Science 334, 1265–1269. doi:10.1126/science.1209299.

Wilson, J.T., Falconer, G., Mathews, W.H., Prest, V.K. 1958. Glacial Map of Canada. Geological Association of Canada, scale 1:5,000,000.

Zwally, H.J., Abdalati, W., Herring, T., Larson, K., Saba, J., Steffen, K. 2002. Surface melt-induced acceleration of Greenland Ice Sheet flow. Science 297, 218–222. doi:10.1126/science.1072708.

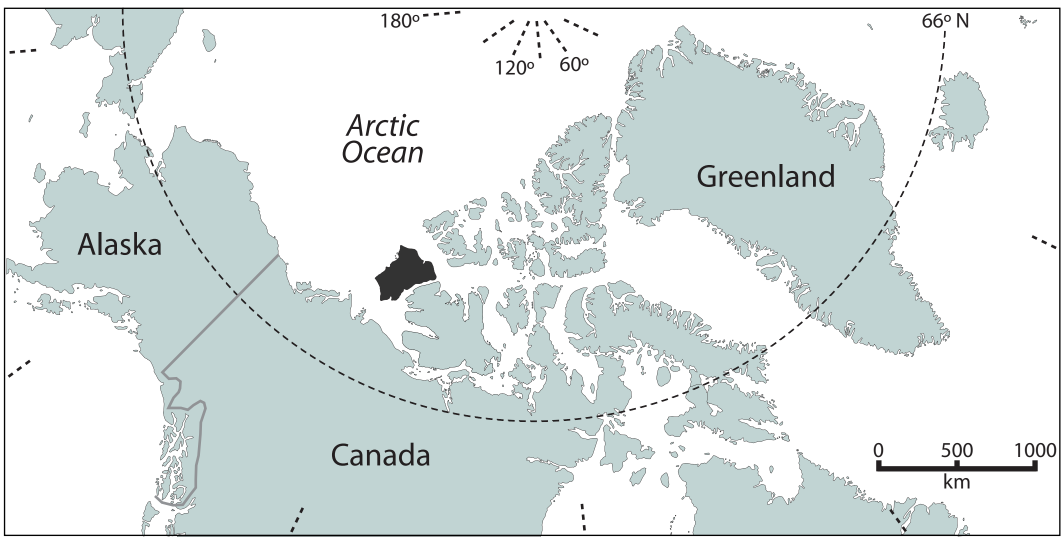

Figure 1.1. The location of Banks Island within the Canadian Arctic Archipelago.

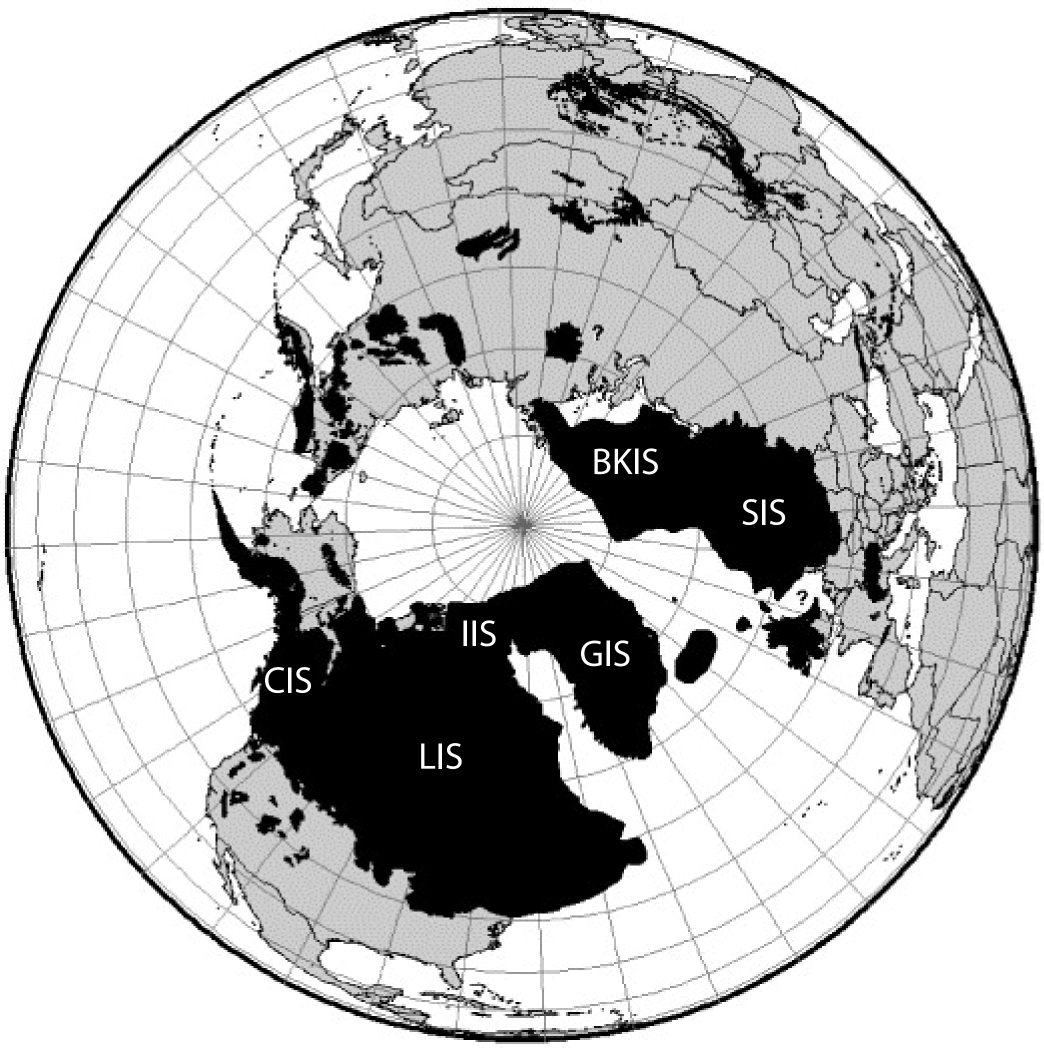

Figure 1.2. Extent of Northern Hemisphere ice cover during the Last Glacial Maximum. CIS-Cordilleran Ice Sheet; LIS-Laurentide Ice Sheet; IIS-Innuitian Ice Sheet; GIS-Greenland Ice Sheet; BKIS-Barents-Kara Ice Sheet; SIS-Scandinavian Ice Sheet. From Ehlers and Gibbard (2007).

Figure 1.3. Canadian Arctic Archipelago showing the extent of the Laurentide Ice Sheet (LIS), Innuitian Ice Sheet (IIS), and Greenland Ice Sheet (GIS) at the Last Glacial Maximum (LGM). The dashed blue line indicates the minimum extent of the LIS on Banks Island following England et al. (2009). Ice sheet limits elsewhere are modified from Dyke (2004), England et al. (2006, 2009), and Fritz et al. (2012).

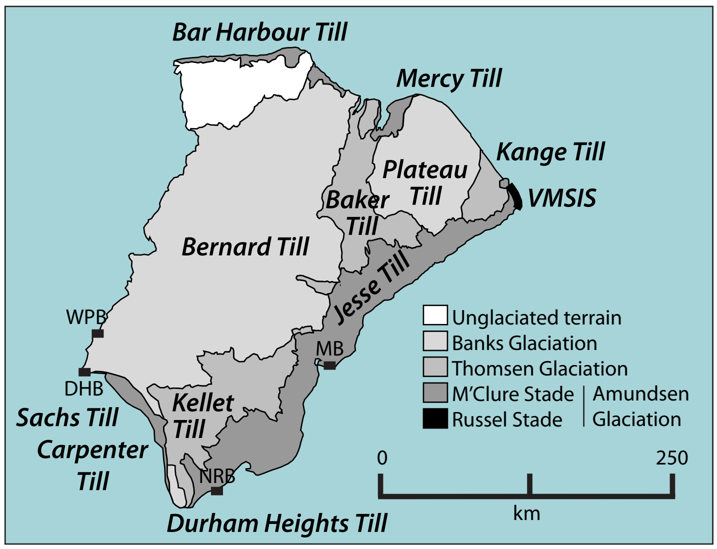

Figure 1.4. Generalized suficial geology of Banks Island as reported by Vincent (1982, 1983), which was considered to document at least three Quaternary glaciations. Note the purportedly unglaciated plateau in the northwest. VMSIS–Viscount Melville Sound Ice Shelf Moraine. The location of several prominent, Quaternary stratigraphic exposures ara also delineated; MB-Morgan Bluffs; NRB-Nelson River Bluffs, DWH-Duck Hawk Bluffs; WPB-Worth Point Bluffs.

CHAPTER 2

The Extent of Late Wisconsinan Glaciation and the Nature of Postglacial Relative Sea Level Change on Western Banks Island, Canadian Arctic Archipelago

INTRODUCTION

Banks Island is located in the western Canadian Arctic Archipelago (CAA) and is bounded by Amundsen Gulf to the south and M'Clure Strait to the north, two major outlets for expansive, former ice sheets that existed during Quaternary glaciations (England et al., 2009; Stokes et al., 2006, 2009; Fig. 2.1). Thus, the island is uniquely situated to record past ice sheet limits and glacier dynamics, which have implications for assessing former changes in paleoclimate and relative sea level, as well as the sedimentation history of the Arctic Ocean basin, where glacial bedforms at depths exceeding 1000 m have recently been identified (e.g. Polyak et al., 2001).

For more than 60 years, researchers investigating the Quaternary paleogeography of northern North America have hypothesized that Banks Island supported an unglaciated refugium during Late Wisconsinan glaciation (Hobbs, 1945; Jenness, 1952; Wilson et al., 1958; Fyles, 1962; Prest, 1969; Vincent, 1982, 1983; Dyke, 1987; Harington, 2005; MacPhee, 2007). This purportedly ice-free area contrasts markedly with adjacent islands and marine channels where thick, extensive ice sheets existed during the Last Glacial Maximum (LGM; Dyke and

Prest, 1987; Dyke et al., 2002; Dyke, 2003; England et al., 2006; Fig. 2.1). During the LGM the northwest Laurentide Ice Sheet (LIS), the southeast Innuitian Ice Sheet (IIS), and several small, local ice caps converged over the islands of the western CAA to form a complex, dynamic ice mass (Fig. 2.1) with multiple ice shelves and ice streams that operated for thousands of years (Dyke and Prest, 1987; Dyke et al., 2002; Dyke, 2003; Hanson, 2003; England et al., 2006, 2009; Stokes et al., 2006, 2009; Nixon and England, 2011).

Recent investigations by England et al. (2009) and Lakeman and England (2012), addressing the timing and extent of Late Wisconsinan glaciation on Banks Island, contradict previous ice sheet reconstructions by Vincent (1982, 1983). Vincent (1982, 1983) proposed that Banks Island was inundated by continental ice sheets on at least three separate occasions between >780,000 and 20,000 yr BP; acting as an ice-free refugium during the LGM (i.e. Harington, 2005; MacPhee, 2007; Fig. 2.1). However, the configuration, limits, and ages of these glaciations remained unconstrained. Furthermore, the pattern and magnitude of relative sea level change resulting from glacioisostatic crustal adjustments following ice sheet retreat were poorly documented. On the basis of new geomorphic evidence and a robust radiocarbon chronology, England et al. (2009) and Lakeman and England (2012) demonstrated that the northwest LIS inundated the northern interior of Banks Island, well beyond the LGM margin proposed by previous workers (Fyles, 1962; Vincent 1982, 1983; Dyke 1987; Fig. 2.1). For example, England et al. (2009) and Lakeman and England (2012) demonstrated that the LIS flowed northward across north-central Banks Island during the Late Wisconsinan and filled Castel and Mercy bays, and was confluent with an ice stream in M'Clure Strait (Stokes et al., 2005, 2009). The precise geometry, extent, and dynamics of the LIS across western Banks Island during the LGM remain to be clarified, however. This study is an extension of recent field investigations by England et al. (2009) and Lakeman and England (2012) and is aimed at further revising the conceptual model proposed by Vincent (1982, 1983) by revisiting the paleoenvironmental record of Quaternary landforms and sediments on west-central Banks Island (Fig. 2.1).

The objectives of this study are to: 1) determine the Late Wisconsinan limit of the LIS on Banks Island, 2) characterize local glacier dynamics during ice sheet retreat, and 3) document the history of postglacial sea level change resulting from glacioisostatic unloading of the crust following deglaciation. The study implicitly tests the commonly held hypothesis that the modern ecosystem of Banks Island evolved from its own Ice Age refugium. The synthesis also contributes to an improved understanding of long-term climatic variability in Arctic Canada and glacially-influenced sedimentary processes in the Arctic Ocean. Clarifying the natural history of Banks Island is also relevant to understanding modern sea level change, including the rate and magnitude of ongoing submergence impacting coastal communities in the western Canadian Arctic (e.g. Paulatuk, Tuktoyuktuk, Sachs Harbour; Fig. 2.1). Improved knowledge of past ice sheet extents and chronologies provides essential constraints for global geophysical modelling of modern sea level change (i.e. Siddall and Milne, 2012).

PREVIOUS WORK

The earliest studies to address the Quaternary history of Banks Island were limited in extent and reconnaissance in nature (Hobbs, 1945; Washburn, 1947;

Porsild, 1950; Jenness, 1952; Manning, 1956). Fyles (1962) completed the first detailed investigation of the physiography of Banks Island using aerial photographs and extensive field mapping. He recognized several distinct physiograhic regions on the island, including "extensive monotonous lowlands, massive hilly moraines… and dissected uplands", that he attributed to regional differences in bedrock geology and Pleistocene history. Fyles (1962) suggested that the Jesse till, a large moraine belt that rims the east coast of the island (Fig. 2.1), marked the limit of Late Wisconsinan glaciation on the island. This limit was adopted by subsequent compilations addressing the size and nature of the Late Wisconsinan LIS (i.e. Prest, 1969). The landscape west of the Jesse till was interpreted by Fyles (1962) to have been ice-free during the last glaciation based on the apparent absence of "fresh" glacial landforms and the striking dominance of fluvial erosion and deposition in many catchments. However, he acknowledged the presence of glacial landforms and deposits originating from one or more earlier continental glaciations on western Banks Island, of unknown age.

Vincent (1982, 1983) and Vincent et al. (1984) revisited the Quaternary geomorphic and sedimentary records on Banks Island and applied several new correlation techniques not employed by previous researchers (i.e. paleomagnetism, amino acid geochronology). Vincent (1982, 1983) identified several formal climatostratigraphic units on Banks Island and interpreted them as a conformable succession of Quaternary glacial-interglacial environments. The oldest, most extensive glaciation was termed the Banks Glaciation and was estimated to be more than 780,000 years old (Vincent et al., 1984; Fig. 2.1). This was followed by two successively less extensive glaciations, the Thomsen Glaciation and finally the

Amundsen Glaciation, which was further subdivided into the M'Clure and Russel Stades, corresponding to the Early and Late Wisconsinan, respectively (Fig. 2.1).

The till sheets associated with these glaciations include the Bernard, Baker, Kellet, and Jesse tills (Fig. 2.1), which were distinguished primarily on the basis of their lithology, their relationship to inferred ice sheet margins, and their presumed relative ages. Vincent (1982, 1983) assigned the Jesse till to the Early Wisconsinan based on amino acid ratios from shell fragments collected from the surface of a marine delta overlying the till. The tills west of the Jesse till, were assigned to older Quaternary glaciations following Fyles' (1962) earlier observations. The northwest plateau was purported to have never been glaciated (Fig. 2.1) based on an apparent absence of till and glacial erratics. The only glacial landform on the island regarded by Vincent (1982, 1983) to be of Late Wisconsinan age was a prominent moraine on the northeast coast (Fig. 2.1), which was subsequently ascribed to an LGM ice shelf (the Viscount Melville Sound Ice Shelf) in M'Clure Strait (Hodgson and Vincent, 1984; Hodgson, 1994). The till sheets identified by Vincent (1982, 1983) were also formally associated with a series of proglacial lakes and postglacial marine transgressions and regressions.

Vincent's (1982, 1983) reconstruction sought to correlate the geomorphic record, expressed as multiple surficial tills and marine deposits, with various stratigraphic units in several exposures on the island. These correlations were made using primarily lithostratigraphy; aminostratigraphy was also used but only where fossil molluscs were identified. The final reconstruction of Quaternary events proposed by Vincent (1982, 1983, 1984) represents a remarkably complete history of Quaternary environmental change, one in which the subsurface record perfectly mirrors the surficial geology, regardless of a general lack of absolute ages for the identified deposits.

In the first major challenge to Vincent's (1982, 1983) reconstruction, Dyke (1987) reinterpreted the age of the Jesse till, reassigning it to the Late Wisconsinan on the basis of an associated marine deposit dating to 11,355–12,410 cal yr BP (GSC-1437). Thus, Dyke (1987) reverted the Late Wisconsinan ice margin back to that of Fyles (1962) and Prest et al. (1968), and attributed the Viscount Melville Sound Ice Shelf moraine to a deglacial ice shelf. Consequently, Dyke and Prest (1987) and later compliations (Dyke et al. 2002; Dyke, 2003) portrayed the Jesse till as the maximum extent of the northwest LIS during the LGM (Fig. 2.1). Furthermore, England and Furze (2011) confirmed a deglacial age for the Viscount Melville Sound Ice Shelf moraine on northeast Banks Island.

England et al. (2009) and Lakeman and England (2012) reinvestigated the surficial geology and geomophology of northern and eastern Banks Island. They observed previously unreported glacial and marine deposits, many of which contradict the conceptual model proposed by Vincent (1982, 1983). For example, new observations indicate northward ice-flow from the northern interior of Banks Island into M'Clure Strait and not the opposite as proposed by Vincent (1982, 1983). Furthermore, newly identified ice-contact deltas at the heads of Mercy and Castel bays on the north coast of Banks Island yielded multiple radiocarbon ages of approximately 13.75 cal yr BP (England and Furze, 2008; England et al., 2009; Lakeman and England, 2012) . These ages, combined with new geomorphic mapping, indicate that the northwest LIS occupied the interior of Banks Island during the final stages of the Late Wisconsinan. As a result, glacial deposits farther east (i.e. up-ice), such as the Jesse till, must postdate ice sheet withdrawal from the interior and relate to the final phase of deglaciation on Banks Island (Lakeman and England., 2012). These data also suggest that the as yet unidentified LGM limit of the northwest LIS is situated west of Castel Bay, perhaps lying offshore on the Beaufort Sea shelf (England et al., 2009; Fig. 2.1).

Throughout eastern and northern Banks Island, England et al. (2009) and Lakeman and England (2012) did not observe any of the raised marine deposits and shorelines reported by Vincent (1982, 1983), despite exhaustive field surveys. For example, on the east coast, sediments and landforms associated with the *Big Sea* (120–215 m asl), the *East Coast Sea* (120 m asl), and the *Schuyter Point Sea* (<25 m asl), which purportedly span multiple glaciations (Vincent, 1982, 1983), are all absent. Similarly, sedimentary evidence for *Lake Ivitaruk* in the Thomsen River valley and the *Investigator Sea* (<30 m asl) in Mercy and Castel bays is not present. In contrast, England et al. (2009) and Lakeman and England (2012) observed marine limit shorelines in Mercy and Castel bays at 41 and 37 m asl, respectively. These data document a previously unrecognized amount of glacioisostatic unloading by the northwest LIS on northern Banks Island following Late Wisconsinan glaciation, which is consistent with new geomorphic observations indicating a thicker and more expansive northwest LIS (England et al., 2009).

METHODS

Detailed mapping of surficial landforms and sediments across central Banks Island permits a high-resolution reconstruction of ice sheet retreat following the LGM. Glacial and marine landforms and sediments were mapped and investigated in the field using aerial photography, satellite imagery, and widespread surveys by foot, ATV, canoe, and helicopter in the summers of 2008, 2009, and 2010. The extent and pattern of retreat for the LIS was determined using cross-cutting relationships among mapped glacial landforms. The elevation of deglacial, raised marine deltas and beaches was measured by digital altimetry and corrected for temperature and atmospheric pressure.

The chronology of Late Wisconsinan glaciation was established by Accelerator Mass Spectrometry (AMS) radiocarbon dating of marine molluscs collected from glacial and marine sediments. A total of 11 radiocarbon ages are reported from 9 samples across the field area and 10 additional ages are reported from the Jesse till (Table 2.1). Radiocarbon ages were obtained from the W. M. Keck Carbon Cycle Accelerator Mass Spectrometry Laboratory (UCIAMS), University of California at Irvine and the National Ocean Sciences Accelerator Mass Spectromety Facility (NOSAMS), Woods Hole Oceanographic Institute. Unless otherwise stated, all radiocarbon ages are reported in ^{14}C years Before Present (1950) and are not corrected for marine reservoir effects because they commonly exceed 30,000 ^{14}C yr BP.

In addition, two optically stimulated luminescence (OSL) ages were obtained from a raised marine deposit on Phillips Island off the west coast of Banks Island. These ages were obtained fom quartz sand (90–180 um) at the Sheffield Centre for International Drylands Research (SCIDR) Luminescence Laboratory. The dose rate for the samples was determined by thick source beta counting using a Riso Multi-channel beta counter and by inductively coupled plasma mass spectrometry at SGS Laboratories, Ontario, Canada. Elemental concentrations were converted to annual dose rates using data from Aitken (1998), Adamiec and Aitken (1998), and Marsh et al. (2002). Samples underwent quartz extraction and cleaning following the procedure of Bateman and Catt (1996) and were preheated to 260°C for 10 seconds. The palaeodose determinations were derived using the single aliquot regenerative (SAR) approach (Murray and Wintle, 2000) and measurements made on a Riso TL DA-20 luminescence reader with radiation doses administered using a calibrated ^{90}Sr beta source. The sample data imply that the ages are reproducible and that the samples were reset prior to burial.

GLACIAL LANDFORMS AND SEDIMENTS

West-central Banks Island is an extensive, low plain with gently rolling hills dissected by broad, shallow, west-draining valleys. It is underlain by poorly lithified sandstone and shale of the Palaeocene Eureka Sound Formation and unlithified sand and gravel of the Pliocene Beaufort Formation (Miall, 1979). The region is mantled by discontinuous thin till that is commonly composed of reworked sand and gravel of local origin with rare erratic boulders. Postglacial valleys are occupied by modern alluvium, postglacial peat, and relict glaciofluvial sand and gravel. Proglacial and ice-lateral meltwater channels developed during former glaciation(s) are the most widespread glacial landforms. They are distinguished on the basis of their morphology and location, often nested or paired and situated on valley sides oriented oblique to slope. Morphologically, they are characterized by steep valley sides and gradients, are nested, and are currently occupied by misfit streams. They are inscribed over the primary drainage network, which is characterized by a series of long, west-flowing rivers that begin near the east coast, adjacent to the Jesse till, and occupy broad, shallow valleys floored by alluvium and swampy tundra with myriad, ice wedge polygons and shallow ponds.

The pattern of glacial meltwater channels on west-central Banks Island is summarized in Figure 2.2. On the west coast, ice-lateral meltwater channels terminate at marine limit, adjacent to the Beaufort Sea. These channels also delineate a formerly digitate, terrestrial ice margin that was characterized by several glacier lobes occupying the primary river valleys (Fig. 2.2). Similarly, younger ice-lateral meltwater channels lying farther inland, delineate a multi-lobate ice margin, indicating that ice sheet retreat proceeded eastward up the major river valleys (Fig. 2.2). However, in the central interior, meltwater channels outline a large curvilinear ice front, which contrasts markedly with the highly digitate ice margin farther west (Fig. 2.2). This curvilinear ice margin dates to ~14 cal ka BP and, therefore, delineates the position and geometry of a deglacial ice margin of the northwest LIS (Lakeman and England, 2012). Importantly, the pattern of ice sheet retreat in the study area, which is recorded by these widespread ice-lateral meltwater channels, has no discontinuities in the form of cross-cutting ice margins.

Several, prominent proglacial meltwater channels, which emanate from various mapped ice margins, are present in the study area (Fig. 2.2). These channels, as well as the ice-lateral meltwater channels delineating the evolution of the retreating ice front, commonly descend into the primary river valleys where they are graded to expansive terraces, which are up to several kilometres wide and traceable to the Beaufort Sea as accordant surfaces (Fig 2.2). These terraces constitute sand and gravel outwash, confirming that the valleys were sandurs during deglaciation, transporting high volumes of glaciofluvial sediment to the Beaufort Sea from the retreating ice sheet margin (Fig. 2.2). Many of these large, west-draining catchments have headwaters near the east coast of the island, indicating that these sandurs remained active up until the northwest LIS retreated fully from the island's east coast. The outwash surfaces were not reworked or incised to any great extent following their abandonment.

Few moraines occur in the study area. Those that are present are narrow, discontinuous, ice-thrust moraines. Several kames and kettles also occur on the broad, sloping plain of western Banks Island, especially along the Beaufort Sea coast. Kames are primarily composed of reworked sand and gravel from the underlying Beaufort Fm. These deposits often occur as nested concentrations of flat-topped mounds and conical hills situated on the lowlands, although isolated kames occur as well. Kettles are widespread, occurring in greatest concentration in the low-lying areas of western Banks Island. Higher surfaces within the study area, including the northwest plateau, generally lack kettles but are nonetheless covered by a veneer of till and sparse large erratics of varying lithology. Of those that are present, basalts and gabbros are most abundant, likely sourced from the Shaler Mountains, Victoria Island. Sandstones and granites are present but less abundant compared to mafic erratics in the study area and compared to the concentration of sandstones and granites in the Jesse till (Lakeman and England, 2012).

RAISED MARINE DEPOSITS

Well-preserved, raised beaches and ice-contact deltas comprise the only identifiable raised shoreline on western Banks Island (Fig. 2.3). The beaches discontinuously rim the coastline (Fig. 2.3) and trim till lying upslope. They, therefore, clearly mark marine limit and can be attributed to deglaciation of the west coast. Ice-contact deltas are also accordant with the beaches and emanate from broad, proglacial and ice-lateral meltwater channels (Fig. 2.3). Below the shoreline, in low-lying areas adjacent to the coast, inorganic sand and silt occur with rare mollusc fragments. Available stratigraphic exposures in these deposits expose 0.5 to 2 m of stony sand and silt overlying clayey diamict (Fig. 2.4). The stony sand and silt has a sharp contact with underlying clayey diamict and is dominantly planar-laminated. The uppermost ~0.5 m of stony sand and silt is massive, likely a product of reworking during sea level regression.

The elevation of marine limit varies on the west coast from 22 to 40 m asl (Fig. 2.3). In Storkerson Bay, marine limit is marked by a prominent beach terrace at 30 m asl, which is traceable for more than 30 km. Between Liot Point and First Point (Fig. 2.3), the elevation of the same beach terrace with accompanying deltas falls from 28 to 22 m asl. North of First Point, the beach terrace rises in elevation and is accordant with a well-preserved ice-contact delta at 25 m asl near the mouth of the Adam River (Fig. 2.3). Farther north, in the Bernard River valley, several proglacial and ice-lateral meltwater channels terminate at small fan deltas, which are composed of gravelly sand and attain a maximum elevation of ~30 m asl (Fig. 2.3). Between Burnett Bay and the Davies River (Fig. 2.3), multiple, well-preserved beaches and ice-contact deltas mark marine limit at 38–40 m asl.

On the small islands just offshore from western Banks Island (Fig. 2.3), raised marine landforms are present but sparse, probably the result of evident, widespread Holocene coastal erosion. On Norway Island an ice-contact delta remnant composed of sandy gravel foresets, rises to 32 m asl, marking a former relative sea level to at least this elevation (Fig. 2.3). Similarly, raised beaches on Robilliard Island and Phillips Island attain elevations of 22–29 m asl (Fig. 2.3).

In addition to well-preserved shorelines, the study area includes a few coastal exposures of fossiliferious littoral and deltaic sediments. In section, these sediments commonly contain abundant organic matter (including locally high concentrations of woody detritus derived from the Beaufort Fm.) and a diverse molluscan fauna. For example, two bluffs at the head of Burnett Bay are composed of deltaic to littoral sediments with abundant valves of *Hiatella arctica*, *Astarte borealis*, and *Portlandia arctica* (Fig. 2.5). The *North Bluff* consists primarily of finely-laminated and rippled, fossiliferous stony sand, whereas the *South Bluff* is composed of interbedded stony sand and fossiliferous, organic-rich mud. The uppermost 0.5–1 m of sediment at both bluffs consists of fossiliferous, massive stony sand that has a gradual contact with the underlying stratified sediment (Fig. 2.5). In addition, these upper sediments extend laterally across the top of the bluffs to adjacent, low-lying areas. Given their stratigraphy and sedimentology, these massive upper sediments are interpreted to be reworked from the underlying stratified sediments, likely during sea level regression. A glaciotectonized exposure on Phillips Island, ~35 km to the northwest, reveals interbedded sand and muds with abundant valves of *H. arctica* and *A. borealis*. This deposit is similar to the bluffs in Burnett Bay, however, glaciogenic faults and overturned folds disrupt the stratigraphy.

Observations of the modern coastline include widespread drowned tundra, commonly polygonized by ice-wedges that are undergoing thermal and mechanical erosion; coastal microcliffs; submerged deltas; estuaries; barrier beaches; washover fans; and extensive sea ice-push ridges. These features unequivocally document a modern transgression of the coast that is of unknown duration.

CHRONOLOGY

Eleven radiocarbon ages were obtained for 9 samples of fossil marine molluscs collected from raised marine sediments across the study area (Table 1). Paired, whole valves of *A. borealis* collected at 5–6 m asl in growth position from coastal bluffs in Burnett Bay provided ages of 45,600 ± 480 (NOSAMS-79612) and 45,500 ± 600 (NOSAMS-79614) ^{14}C yr BP (Table 1; Fig. 2.5). Despite the nearly identical ages from two separate deposits, there is uncertainty whether these ages are truly finite. Therefore, the age of the deposits cannot be confidently resolved. Overlying surface collections of whole valves and fragments of *A. borealis* from the reworked massive sediment capping the bluffs, provided younger ages of 33,600 ± 240 (NOSAMS-79613), 35,100 ± 220 (NOSAMS-79615), and 38,540 ± 330 (UCI-77838) ^{14}C yr BP (Table 1; Fig. 2.5). These dated mollusc samples may have been winnowed from the underlying deposit that yielded the ~46 ka BP ages. If so, they would require a higher than modern relative sea level during the Mid Wisconsinan (MIS 3). Alternatively, these mollusc samples may have been redeposited from till in a high deglacial relative sea level that permitted reworking and erosion of marine sediments pre-dating the ice advance.

The exposure on Phillips Island composed of glaciotectonized and fossiliferous littoral sand contains whole valves of *H. arctica* and *A. borealis* that yeilded non-finite radiocarbon ages (Table 1). Two OSL ages of 118 ± 5.7 ka BP (Shfd11043) and 110 ± 4.2 ka BP (Shfd11071; Table 2) from a single stratigraphic horizon, which immediately overlies the radiocarbon-dated stratum, provide a maximum-limiting age for the subsequent phase of glaciation. The sedimentological and biostratigraphic affinity between this deposit and the bluffs in Burnett Bay raises further uncertainty regarding whether the ~46 ka BP radiocarbon ages are indeed finite (i.e. whether they accurately represent the age of the Burnett Bay bluffs).

Rare, surface collections of whole valves and fragments of *A. borealis* and *H. arctica* (2–5 m asl) were obtained from inorganic stony sand and silt in low-lying areas along the coast (i.e. Fig. 2.4). These samples yielded ages of 30,700 ± 140 (NOSAMS-79536), 34,700 ± 200 (NOSAMS-79539), and 49,900 ± 550 (NOSAMS-79535) ^{14}C yr BP (Table 1 and Fig. 2.4). As these mollusc samples are exceedingly rare and the accompanying stony sand and silt has little to no interbedded organic matter, they are interpreted to have been redeposited. Indeed, their stratigraphic relationship to underlying till indicates that they were redeposited during deglaciation of the coast and deposition of marine limit. A genetic relationship between the inorganic stony sand and silt and marine limit is inferred, because the sediments rises in elevation to the marine limit shoreline (22–40 m asl, Fig. 2.3) and comprises the dominant outcrop in low-lying, coastal areas. Consequently, the ages of 30,700 ± 140 (NOSAMS-79536) and 34,700 ± 200 (NOSAMS-79539) provide a maximum-limiting age for the widespread and generally unfossiliferous stony sand and silt, and for the surveyed marine limit. A Late Wisconsinan age for the marine limit is perhaps additionally supported by a maximum-limiting age of 44,800 ± 770 (NOSAMS-79616) ^{14}C yr BP (Table 1) from a redeposited shell fragment in an ice-contact delta on Norway Island (32 m asl).

There are currently no samples of molluscs of deglacial age (i.e. younger than the LGM) available from the west coast. Similarly, no reliable, closely-limiting deglacial ages from marine molluscs have been reported from western Prince Patrick Island and the Arctic Mainland west of Baillie Island (Hodgson et al., 1994; Dyke et al., 1996; Dyke, 2003; Dyke et al., 2003; Fig. 2.1). The absence of marine molluscs older than ~14 cal ka BP from the southwestern CAA is attributed to the full dissappearance of a marine molluscan fauna from the continental shelves of the western CAA during the LGM (Kaufman et al., 2004; England and Furze, 2008). Thus, the earliest phase of deglaciation along terrestrial margins of the northwest LIS and southwest IIS, predated the restablishment of a marine molluscan fauna from the north Pacific, which coincided with the resubmergence of Bering Strait (Kaufman et al., 2004; England and Furze, 2008).

DISCUSSION

TIMING AND EXTENT OF LATE WISCONSINAN GLACIATION

The available stratigraphy and chronology across west-central Banks Island indicates one or more intervals of non-glacial marine sedimentation during the period MIS 3–5 (Fig. 2.6). The prevalence of *A. borealis* in these deposits implies that local nearshore marine conditions resembled those of the southwest Canadian Arctic during the Holocene (Dyke et al., 1996). Additional ages, spanning 32 to 55 ^{14}C yr BP, for redeposited mollusc fragments collected from the Jesse till on the east coast, which was deposited between ~13.75 and 12.9 cal ka BP (Lakeman and England, 2012), indicate that similar ice-free conditions may have extended at least as far east as Prince of Wales Strait. Indeed, two ages of ~32 ^{14}C ka BP from the Jesse till support the MIS 3 (Mid Wisconsinan) LIS reconstruction by Dyke et al. (2002), in which the ice sheet margin in the western Canadian Arctic is confined to Victoria Island in the CAA and areas east of the Mackenzie River on mainland Canada.

As the marine limit on western Banks Island has a clear geomorphic association with adjacent glacial landforms and sediments, it must relate to glacioisostaic unloading of western Banks Island following glaciation (Fig. 2.6). The age of marine limt is constrained to some time after ~31 ^{14}C ka BP, based on the youngest maximum-limiting age for redeposited marine molluscs collected from sand and silt situated seaward of marine limit shorelines. This chronology, therefore, indicates that the study area was inundated by the northwest LIS during the Late Wisconsinan (Fig. 2.6). This is consistent with results from England et al. (2009), which proposed the amalgamation of all till sheets and associated raised marine deposits across northern Banks Island into a single Late Wisconsinan deglacial sequence. The maximum limit achieved by the LIS cannot be ascertained in the study area. However, the distribution of ice-lateral meltwater channels (i.e. extending as far west as marine limit) and widespread evidence for glaciotectonism on many of the small islands west of Banks Island, imply that the ice sheet terminated on the Beaufort Sea shelf during the Late Wisconsinan. Due to the lack of deglacial molluscs from the study area, the precise age of deglaciation along the west coast of Banks Island cannot be determined and the degree to which marine limit is diachronous is not known. Consquently, the best minimum-limiting age for deglaciation of the west coast is approximately 14 cal ka BP, the timing of ice sheet retreat from Castel and Mercy bays (England and Furze, 2008; England et al., 2009; Lakeman and England, 2012).

A MIS 3 or 5 age for the marine limit is untenable as fossiliferous marine sediments are rare from the west coast. Those that are present (i.e. Burnett Bay and Phillips Island bluffs) have no clear geomorphic or stratigraphic relationship to the marine limit shoreline. Furthermore, the ice-contact deltas that are accordant with the widespread beaches indicate that marine limit is deglacial in origin.

These results reject the longstanding hypothesis purporting the existence of an ice-free refugium on Banks Island during the LGM (Fyles, 1962; French, 1972; Vincent, 1982, 1983; Dyke, 1987; Harington, 2005). Additionally, these new results falsify previous correlations proposed by Vincent (1982, 1983, 1984) and Vincent et al. (1984) between the stratigraphic record and the surficial geology. For example, Vincent (1982, 1983, 1984) and Vincent et al. (1984) correlated magnetically reversed tills (i.e. >780,000 yrs old) exposed in multiple stratigraphic exposures with the Bernard till (Fig. 2.1), which is now ascribed to the Late Wisconsinan on the basis of multiple maximum- and minimum-limiting radiocarbon ages of ~31 ^{14}C ka BP and ~14 cal ka BP, respectively.

LATE WISCONSINAN ICE SHEET DYNAMICS

The glacial geomorphology of west-central Banks Island permits the development of a detailed reconstruction of the behaviour of the northwest LIS during the last deglaciation. The absence of any deglacial ages on marine molluscs from the west coast leaves the timing of ice sheet retreat loosely constrained to an interval prior to 14 cal ka BP (England and Furze, 2008; England et al., 2009; Lakeman and England, 2012). Despite this uncertainty, the pattern of ice sheet retreat is well-recorded by widespread ice-marginal meltwater channels (Fig. 2.2). For example, the westernmost (i.e. oldest) ice-lateral meltwater channels delineate a multilobate ice front conforming to the major river valleys (Fig. 2.7). This pattern demonstrates that the geometry of the retreating ice front was topographically-controlled and confirms that the ice sheet was locallly thin (Fig. 2.7). This contrasts with evidence from M'Clure Strait, where grounded ice was at least 635 m thick (England et al., 2009; Lakeman and England, 2012). The evidence for thin ice cover during deglaciation possibly reflects diminished westward ice-flow across Banks Island from an LGM ice divide located on Victoria Island (Dyke, 1983, 1984; Dyke et al., 1992; England et al., 2009), which formerly supplied ice terminating on the Beaufort Sea shelf. Thus, it is possible that ice divides within the northern LIS were beginning to thin at this time or that dynamical changes within the ice sheet (i.e. greater ice-flux to calving margins in the adjacent marine channels) reduced ice-flow to western Banks Island.

Following initial withdrawal of the northwest LIS from the Beaufort Sea shelf, ice sheet retreat proceeded eastward across the study area (Fig. 2.7). Widespread ice-lateral meltwater channels and the general paucity of moraines indicate that the ice sheet margin remained cold-based and proceeded without any regionally significant readvances or stillstands. Where rare moraines occur, these are likely the product of ice-thrusting of frozen sediments along the ice margin where convergent ice-flow generated sufficient strain or where minor, local readvances occurred. By ~14 cal ka BP, the ice sheet margin was situated in the central interior and was still dominantly cold-based (Fig. 2.7). The position of the ice margin at ~14 cal ka BP is supported by widespread evidence that the ice sheet in the central interior supplied two outlet glaciers in Castel and Mercy bays up until ~13.75 cal ka BP, when the ice margin began to retreat southward and eastward to Prince of Wales Strait (England et al., 2009; Lakeman and England, 2012). The nature of ice sheet retreat following ~14 cal ka BP is presented in Lakeman and England (2012) and in England et al. (2009).

Perhaps the oldest evidence for deglaciation of the west coast is recorded by beaches and ice-contact deltas north of the Bernard River (Fig. 2.3). These deposits rise in elevation from 30 m asl near the Bernard River to 40 m asl in Burnett Bay, well above the 13 m asl marine limit at Cape Prince Alfred (J. England and M. Furze pers. comm., 2010; Fig. 2.3). If this shoreline is indeed of Late Wisconsinan age, as indicated by the available chronology, then it records a difference in marine limit of 27 m across ~50 km. This suggests that there was a significant difference in the timing of deglaciation between Burnett Bay/Bernard River and Cape Prince Alfred. The LIS was thicker and faster-flowing in M'Clure Strait relative to western Banks Island and, as such, was characterized by a major ice stream that likely terminated at a floating ice shelf for much of the last deglaciation (Stokes et al., 2005, 2009; England et al., 2009). This dynamical distinction could have resulted in a significant offset in the timing of final deglaciation of the north and west coasts; with the west coast becoming ice-free earlier as regional ice divides accommodated greater mass loss via calving in the marine channels by undergoing drawdown and diminished ice-flow to distal terrestrial margins on western Banks Island. A regression from ~40 to 13 m asl could be achieved by glacioisostatic unloading over the course of several thousand years, assuming conservative estimates of relative sea level half-lives for postglacial emergence curves across the

CAA (Dyke and Peltier, 2000). However, this remains speculative because the chronology is insufficient to determine the precise age of marine limit in the study area.

POSTGLACIAL RELATIVE SEA LEVEL CHANGE

The prominent shoreline on the west coast is deglacial in age because it constitutes multiple ice-contact deltas and concordant beaches. Therefore, the shoreline constitutes marine limit and estimates the magnitude of glacioisostatic unloading of western Banks Island following the last glaciation. A component of eustatic relative sea level change during the early postglacial interval cannot be negated or estimated because the timing of relative sea level change following deglaciation is only loosely constrained. Furthermore, the timing of deglaciation within study area may have been variable. Nevertheless, the documented marine limit along the west coast significantly exceeds geophysical model estimates by Tarasov and Peltier (2004), which were derived using ice sheet reconstructions with no LGM glaciation of western Banks Island (Dyke et al., 2002; Dyke, 2003). This divergence indicates greater glacioisostatic unloading following the LGM than previously considered. The new geomorphological and relative sea level observations, therefore, indicate the presence of an extensive LIS in the southwest CAA during the LGM, which was hypothesized by Tarasov and Peltier (2004) to account for the divergence of geophysical model estimates from regional field observations. Similarly, on Melville and Prince Patrick islands, where recent geomorphological mapping indicates more extensive Late Wisconsinan glaciation than previously recognized, new relative sea level data (England et al., 2009; Nixon and England, 2011; Coulthard, pers. comm., 2011) does not match model-derived estimates of marine limit and postglacial relative sea level change (Tarasov and Peltier, 2004).

Other relative sea level data from Banks Island is summarized in Figure 2.8. Marine limit rises in elevation from west to east along the north coast (England et al., 2009) and from southwest to northeast along the east coast (Lakeman and England, 2012). The age of marine limt on the north coast varies from greater than 14 cal ka BP west of Cape M'Clure to ~14 cal ka BP in Castel Bay, Mercy Bay, and Parker Point (England et al., 2009; Lakeman and England, 2012). On the east coast, marine limit is isochronous, ~12.75 cal ka old (Lakeman and England, 2012). This dataset constitutes an important constraint on current and future geophysical models of the last glaciation in northern North America (i.e. Tarasov et al., 2012).

Outwash in several major west-draining valleys on western Banks Island (e.g. adjacent to the Bernard and Storkerson rivers; Fig. 2.2) is graded to a base level that is similar to modern sea level. These valleys carried outwash throughout deglaciation as glacier ice occupied their catchments until ~13 cal ka BP, when the northwest LIS retreated fully from the island (Lakeman and England, 2012; Figs. 2.7 and 2.8). As a result, it is provisionally inferred that the ~13 cal ka BP shoreline on the west coast of Banks Island was similar to modern.

It is clear from observations of the modern shoreline that the coast is currently submerging, following a transgression from a lowstand of unknown age and depth. Similar observations from elsewhere on Banks Island (Lakeman and England, 2012) indicate that modern coastal submergence characterizes its entire coastline. Indeed, Andrews and Peltier (1989) as well as recent relative sea level reconstructions from Melville and Eglinton islands (Nixon and England, 2011) place

Banks Island on the submergence side of the zero isobase (a theoretical line separating submergent from emergent coastlines). It is possible that the lowstand on the west coast was achieved in the latest Pleistocene or early Holocene if deglaciation of western Banks Island can be considered analogous to deglaciation of the southwest margin of the LIS in Atlantic Canada (e.g. Shaw and Forbes, 1995; Stea et al., 2001; Bell et al., 2003). The lowstand elsewhere, such as on the east coast, was perhaps achieved later because deglaciation there was delayed until ~12.75 cal ka BP (Lakeman and England, 2012). Relative sea level rise across Banks Island from the time of the lowstand to present can be attributed to eustatic sea level rise (i.e. Peltier and Fairbanks, 2006), the eastward migration and collapse of a glacioisostatic forebulge (i.e. Dyke and Peltier, 2000), and steric sea level rise (i.e. Antonov et al., 2005). Similar conclusions regarding Holocene relative sea level lowstands on Eglinton and Melville islands have been made by Nixon and England (2011).

ARCTIC OCEAN BATHYMETRY

Over the past decade, substantial advances in the acquisition of multibeam bathymetric echo sounder data and chirp sonar sub-bottom profiler data have facilitated multiple, high-resolution surveys of the Arctic Ocean sea floor (Vogt et al., 1994; Jakobsson, 1999; Polyak et al., 2001, 2007; Kristoffersen et al, 2004; Jakobsson et al., 2005, 2008; Engels et al., 2008). These data reveal conspicuous glacial bedforms occurring to depths of approximately 1000 m on the Lomonosov Ridge (Polyak et al., 2001), 900 m on the Chukchi Borderland (Jakobsson et al., 2005, 2008), and 850 m on the Yermak Plateau (Vogt et al., 1994; Fig. 2.9).

Glacial bedforms are most abundant on the Chukchi Borderland (Jakobsson et al., 2008b; Fig. 2.9) where multiple episodes of ice grounding are recognized and provisionally attributed to MIS 6, 4, and 2 (Darby et al., 2005; Polyak et al., 2007). On the Northwind Ridge, one of several north-trending ridges comprising the Chukchi Borderland, glacial bedforms oriented east-west and occurring to depths of approximately 450 m (Fig. 2.9) have been firmly radiocarbon dated to the Late Wisconsinan (Polyak et al., 2007). These bedforms constitute multiple parallel, low-relief lineations reaching tens of kilometres in length. At shallower depths (<300–400 m) lineations and ridges are crosscut and obscured by abundant, randomly oriented iceberg plowmarks. Lineations are interpreted as flutes, recording the grounding of glacier ice shelves or the grounding of coalescent iceberg armadas (Polyak et al., 2001, 2007; Jakobsson et al., 2005). Subbottom sonar records confirm that the flutes are composed of unstratified, glaciogenic diamictons and are capped by postglacial mud (Polyak et al., 2007). These records also document an erosional unconformity beneath the flutes (Jakobsson et al., 2005; Polyak et al., 2007). This knowledge confirms that the flutes were produced beneath grounded glacier ice, whether in the form of an ice shelf or a coalescent iceberg armada. Whatever the exact mode of deposition, these flutes record the existence of glacier ice thick enough to ground in the Arctic Ocean during the last glaciation. This may have been augmented by thick and likely permanent sea ice cover across the Arctic Ocean during the LGM (i.e. Bradley and England, 2008), the evidence for which lies in sedimentary records containing abiotic intervals with very low sedimentation rates, including a possible hiatus between approximately 13 and 20 ^{14}C ka BP (Poore et al., 1999; Polyak et al., 2004).

The extent of the northwest LIS on Banks Island serves as a proxy for the thickness and extent of grounded ice in Amundsen Gulf and M'Clure Strait, where the existence of large ice streams during the LGM is hypothesized (Stokes et al., 2005, 2006, 2009; England et al., 2009). Recognition that the northwest LIS inundated western Banks Island, terminating on the Beaufort Sea shelf, confirms the former existence of a more expansive northwest LIS during the Late Wisconsinan. This sector of the LIS has been tentatively invoked as the source of a glacier ice shelf or a coalescent iceberg armada that produced the bedforms on the Chukchi Borderland at depths of ≤450 m (Polyak et al., 2001, 2007; Jakobsson et al., 2005). Indeed, England et al. (2009) demonstrated a minimum LGM ice thickness of 635 m in M'Clure Strait. Furthermore, two piston cores (750 and 124, respectively) from western Amundsen Gulf record several episodes of significant ice-rafting between 14 and 11 cal ka BP (Scott et al., 2009), demonstrating that the marine channels of the western CAA likely served as major iceberg sources for the Arctic Ocean during the LGM. The results of this study are consistent with such a hypothesis but demonstrate the need for additional offshore mapping on the Beaufort Sea shelf.

Surveyed glacial bedforms occurring at depth greater than 450 m are more widespread on the Chukchi Borderland than those of Late Wisconsinan age and have been dated to MIS 4 or greater (Polyak et al., 2007). The bedforms are primarily composed of flutes but also occur in association with nested, transverse, arcuate ridges, which parallel bathymetric contours (Polyak et al., 2001). These ridges are interpreted as grounding line deposits, which presumably record the evolution of ice rises that anchored extensive grounded ice shelves composed of a mélange of thick glacier and sea ice. Additional flutes occur at similar depths on the

Beaufort Sea margin north of Alaska and are attributed to the same phase of ice grounding (Engels et al., 2008). If these bedforms serve as a proxy for the severity of contemporaneous glaciation in the western Canadian Arctic, then they would suggest a thicker, more extensive ice sheet during MIS Stage 4 or greater. However, an accurate regional chronology for the pre-LGM bedforms on the Chukchi Borderland and the Beaufort Sea margin, as well as a comprehensive understanding of their genesis, is lacking, and as a result a common age and specific source have yet to be demonstrated. This uncertainty also characterizes the lineations on the Lomonosov Ridge that achieve depths exceeding 1000 m (Polyak et al., 2001).

CONCLUSIONS

This study provides new constraints on the Late Wisconsinan extent of the northwest LIS on Banks Island. During the LGM the ice margin was likely situated offshore at an undesignated limit on the Beaufort Sea shelf, west of Banks Island. Former grounding lines and other submarine ice-marginal deposits have yet to be identified. These results complement those of England et al. (2009) from northern Banks Island, and contradict the hypothesis that the modern ecosystem on Banks Island evolved from an Ice Age refugium. Additionally, the recognition of a thicker and more expansive ice sheet during the LGM verifies the suitability of the regional paleoclimate to ice sheet buildup during the late Pleistocene. The LGM extent of the LIS west of Banks Island further elaborates on the thickness and extent of former ice streams that exited Amundsen Gulf and M'Clure Strait (England et al., 2009; Stokes et al., 2006, 2009). Thus, these results bear on the sedimentary history of the adjacent Arctic Ocean basin and support recent evidence for LGM scouring of the sea floor by glacier ice at depths of up to ~450 m (Polyak et al., 2001, 2007; Jakobsson et al., 2005).

Ice sheet withdrawal across western Banks Island following the LGM was characterized by a predominantly cold-based ice margin that deposited few moraines. Abundant ice-lateral and proglacial meltwater channels, however, allow the pattern of ice sheet retreat to be reconstructed. These landforms delinate a thin, multilobate ice margin, the geometry of which was predominantly defined by preexisting fluvial valleys. No significant readvances or pauses in ice sheet retreat are recognized. The timing of initial deglaciation of the west coast of Banks Island cannot be constrained by the existing chronology, however, the ice sheet margin was situated in the interior of Banks Island by ~14 cal ka BP (England et al., 2009; Lakeman and England, 2012).

The elevation of the deglacial marine limit on western Banks Island is greater than previous model estimates and, thus, documents greater glacioisostatic depression of the crust by a thicker, more extensive ice sheet than formerly recognized. These shoreline observations constitute important new data for regional geophysical models of former and ongoing relative sea level change in the western CAA. Thus, this study will help improve estimates of future coastal submergence, which is already impacting several coastal communities in the western CAA, such as Paulatuk, Tuktoyuktuk, and Sachs Harbour.

REFERENCES

Adamiec, G., Aitken, M.J. 1998. Dose-rate conversion factors update. Ancient TL 16, 37–50.

Aitken, M.J. 1998. An Introduction to Optical Dating: The dating of Quaternary sediments by the use of Photo-Stimulated Luminescence. Oxford Science Publication.

Andrews, J.T., Peltier, W.R. 1989. Quaternary geodynamics in Canada. In: Fulton, R.J. (Ed.), Quaternary Geology of Greenland and Canada. Geological Survey of Canada, Ottawa, Canada. pp. 541–572.

Antonov, J., Levitus, S., Boyer, T.P. 2005. Thermosteric sea-level rise, 1955–2003. Geophysical Research Letters 32, L12601. doi:10.1029/2005GL023112.

Bateman, M.D., Catt, J.A. 1996. An Absolute chronology for the raised beach deposits at Sewerby, E. Yorkshire, UK. Journal of Quaternary Science 11, 389–395. doi:10.1002/(SICI)1099-1417(199609/10)11:5<389::AID-JQS260>3.0.CO;2-K.

Bell, T., Batterson, M.J., Liverman, D.G.E., Shaw, J. 2003. A new late-glacial sea-level record for St. George's Bay, Newfoundland. Canadian Journal of Earth Sciences 40, 1053–1070. doi:10.1139/e03-024.

Bradley, R.S., England, J.H. 2008. The Younger Dryas and the sea of ancient ice. Quaternary Research 70, 1–10. doi:10.1016/j.yqres.2008.03.002.

Darby, D., Jakobsson, M., Polyak, L. 2005. Icebreaker expedition collects key Arctic sea floor and ice data. EOS Transactions, American Geophysical Union 86, 549–556.

Dyke, A.S. 1983. Quaternary geology of Somerset Island, District of Franklin. Geological Survey of Canada, Memoir 404.

Dyke, A.S. 1984. Quaternary geology of Boothia Peninsula and northern District of Keewatin, Central Canadian Arctic. Geological Survey of Canada, Memoir 407.

Dyke, A.S. 1987. A reinterpretation of glacial and marine limits around the northwestern Laurentide Ice Sheet. Canadian Journal of Earth Sciences 24, 591–601. doi:10.1139/e87-058.

Dyke, A.S. 2003. An outline of North American deglaciation with emphasis on central and northern Canada. In: Ehlers, J. (Ed.), Extent and Chronology of Quaternary Glaciation. Elsevier.

Dyke, A.S., Prest, V.K. 1987. Late Wisconsinan and Holocene history of the Laurentide Ice Sheet. Géographie physique et Quaternaire 41, 237–263.

Dyke, A.S., Peltier, W.R. 2000. Forms, response times and variability of relative sea-level curves, glaciated North America. Geomorphology 32, 315–333. doi:10.1016/S0169-555X(99)00102-6.

Dyke, A.S., Morris, T.S., Green, D.E.C., England, J. 1992. Quaternary geology of Prince of Wales Island, Arctic Canada. Geological Survey of Canada, Memoir 433.

Dyke, A.S., Dale, J.E., McNeely, R.N. 1996. Marine molluscs as indicators of environmental change in glaciated North America and Greenland during the last 18,000 years. Géographie physique et Quaternaire, 50, 125–184.

Dyke, A.S., Andrews, J.T., Clark, P.U., England, J.H., Miller, G.H., Shaw, J., Veillette, J.J. 2002. The Laurentide and Innuitian ice sheets during the Last Glacial Maximum. Quaternary Science Reviews 21, 9–31. doi:10.1016/S0277-3791(01)00095-6.

Dyke, A.S., Moore, A., Robertson, L. 2003. Deglaciation of North America. Geological Survey of Canada, Open File 1574.

Engels, J.L., Edwards, M.H., Polyak, L., Johnson, P.D. 2008. Seafloor evidence for ice shelf flow across the Alaska–Beaufort margin of the Arctic Ocean. Earth Surface Processes and Landforms 33, 1047–1063. doi:10.1002/esp1601.

England, J.H., Furze, M.F.A. 2008. New evidence from the western Canadian Arctic Archipelago for the resubmergence of Bering Strait. Quaternary Research 70, 60–67. doi:10.1016/j.yqres.2008.03.001.

England, J.H., Furze, M.F.A. 2011. The Viscount Melville Sound Ice Shelf of the NW Laurentide Ice Sheet: a story befitting the seminal contributions of Art Dyke. 41st International Arctic Workshop, Université du Québec à Montreal, Montréal, Canada, March 2–4, 2011.

England, J.H., Atkinson, H., Bednarski, J., Dyke, A.S., Hodgson, D.A., O'Cofaigh, C. 2006. The Innuitian Ice Sheet: configuration, dynamics and chronology. Quaternary Science Reviews 25, 689–703. doi:10.1016/j.quascirev.2005.08.007.

England, J.H., Furze, M.F.A, Doupé, J.P. 2009. Revision of the NW Laurentide Ice Sheet: implications for paleoclimate, the northeast extremity of Beringia, and Arctic Ocean sedimentation. Quaternary Science Reviews 28, 1573–1596. doi:10.1016/j.quascirev.2009.04.006.

French, H.M. 1972. The proglacial drainage of northwest Banks Island. The Musk-Ox 10, 26–31.

Fyles, J.G. 1962. Physiography. In: Thorsteinsson, R., Tozer, E.T., Banks, Victoria, and Stefansson Island, Arctic Archipelago. Geological Survey of Canada, Memoir 330, pp. 8–17.

Hanson, M. 2003. Late Quaternary Glaciation, Relative Sea Level History and Recent Coastal Submergence of Northeast Melville Island, Nunavut. M.Sc. thesis. University of Alberta, Edmonton, Alberta, Canada.

Harington, C.R. 2005. The eastern limit of Beringia: mammoth remains from Banks and Melville islands, Northwest Territories. Arctic 58, 361–369.

Hobbs, W.H. 1945. The boundary of the latest glaciation in Arctic Canada. Science 101, 549–551. doi:10.1126/science.101.2631.549.

Hodgson, D.A. 1994. Episodic ice streams and ice shelves during retreat of the northwesternmost sector of the late Wisconsinan Laurentide Ice Sheet over the central Canadian Arctic Archipelago. Boreas 23, 14–28. doi:10.1111/j.1502-3885.1994.tb00582.x.

Hodgson, D.A., Vincent, J.-S. 1984. A 10,000 yr B.P. extensive ice shelf over Viscount Melville Sound, Arctic Canada. Quaternary Research 22, 18–30. doi:10.1016/0033-5894(84)90003-6.

Hodgson, D.A., Taylor, R.B., Fyles, J.G. 1994. Late Quaternary sea level changes on Brock and Prince Patrick islands, western Canadian Arctic Archipelago. Géographie physique et Quaternaire 48, 69–84.

Jakobsson, M. 1999. First high-resolution chirp sonar profiles from the central Arctic Ocean reveal erosion of the Lomonosov Ridge sediments. Marine Geology 158, 111–123. doi:10.1016/S0025-3227(98)00186-8.

Jakobsson, M., Gardner, J.V., Vogt, P., Mayer, L.A., Armstrong, A., Backman, J., Brennan, R., Calder, B., Hall, J.K., Kraft, B. 2005. Multibeam bathymetric and sediment profiler evidence for ice grounding on the Chukchi Borderland, Arctic Ocean. Quaternary Research 63, 150–160. doi:10.1016/j.yqres.2004.12.004.

Jakobsson, M., Macnab, R., Mayer, L., Anderson, R., Edwards, M., Hatzky, J., Schenke, H.W., Johnson, P. 2008a. An improved bathymetric portrayal of the Arctic Ocean: implications for ocean modeling and geological, geophysical and oceanographic analyses. Geophysical Research Letters 35, L07602. doi:10.1029/2008GL033520.

Jakobsson, M., Polyak, L., Edwards, M., Kleman, J., Coakley, B. 2008b. Glacial geomorphology of the Central Arctic Ocean: the Chukchi Borderland and the Lomonosov Ridge. Earth Surface Processes and Landforms 33, 526–545. doi:10.1002/esp.1667.

Jenness, J.L. 1952. Problem of glaciation in the western islands of Arctic Canada. Bulletin of the Geological Society of America 63, 939–952. doi:10.1130/0016-7606(1952)63[939:POGITW]2.0.CO;2.

Kaufman, D.S., and 29 others. 2004. Holocene thermal maximum in the western Arctic (0–180°W). Quaternary Science Reviews 23, 529–560. doi:10.1016j.quascirev.2003.09.007.

Kristoffersen, Y., Coakley, B., Jokat, W., Edwards, M., Brekke, H., Gjengedal, J. 2004. Seabed erosion on the Lomonosov Ridge, central Arctic Ocean: a tale of deep draft icebergs in the Eurasia Basin and the influence of Atlantic water inflow on iceberg motion? Paleoceanography 19, PA3006. doi:10.1029/2003PA000985.

Lakeman, T.R., England, J.H. 2012. Paleoglaciological insights from the age and morphology of the Jesse till and adjacent deposits, western Canadian Arctic. Quaternary Science Reviews 47, 82–100. doi:10.1016/j.quascirev.2012.04.018.

MacPhee, R.D.E. 2007. Mammoths in the insular Nearctic? Some constraints on the existence of a Pleistocene megafaunal refugium in the Canadian Arctic

Archipelago. Quaternary International 169–170, 29–38. doi:10.1016/j.quaint.2006.08.007.

Manning, T.H. 1956. Narrative of a second Defence Research Board expedition to Banks Island, with notes on the country and its history. Arctic 9, 2–77.

Marsh, R.E., Prestwich, W.V., Rink, W.J., Brennan, B.J. 2002. Monte Carlo determinations of the beta dose rate to tooth enamel. Radiation Measurements 35, 609–616. doi:10.1016/S1350-4487(02)00065-3.

Miall, A.D. 1979. Mesozoic and Tertiary geology of Banks Island, Arctic Canada: the history of an unstable craton margin. Geological Survey of Canada, Memoir 387.

Murray, A.S., Wintle, A.G. 2000. Luminescence dating of quartz using an improved single-aliquot regenerative-dose protocol. Radiation Measurements 32, 57–73. doi:10.1016/S1350-4487(99)00253-X.

Nixon, F.C., England, J.H. 2011. Holocene relative sea-level fluctuations in the western Canadian High Arctic: last deglaciation to present. XVIII International Union for Quaternary Research (INQUA) Congress, Bern, Switzerland, July 21–27, 2011.

Peltier, W.R., Fairbanks, R.G. 2006. Global glacial ice volume and Last Glacial Maximum duration from an extended Barbados sea level record. Quaternary Science Reviews 25, 3322–3337. doi:10.1016/j.quascirev.2006.04.010.

Polyak, L., Edwards, M.H., Coakley, B.J., Jakobsson, M. 2001. Ice shelves in the Pleistocene Arctic Ocean inferred from glaciogenic deep-sea bedforms. Nature 410, 453–457. doi:10.1038/35068536.

Polyak, L., Curry, W.B., Darby, D.A., Bischof, J., Cronin, T.M. 2004. Contrasting glacial/interglacial regimes in the western Arctic Ocean as exemplified by a sedimentary record from the Mendeleev Ridge. Palaeogeography, Palaeoclimatology, Palaeoecology 203, 73–93. doi:10.1016/S0031-0182(03)00661-8.

Polyak, L., Darby, D., Bischof, J., Jakobsson, M. 2007. Stratigraphic constraints on late Pleistocene glacial erosion and deglaciation of the Chukchi margin, Arctic Ocean. Quaternary Research 67, 234–245. doi:10.1016/j.yqres.2006.08.001.

Poore, R.Z., Osterman, L., Curry, W.B., Phillips, R.L. 1999. Late Pleistocene and Holocene meltwater events in the western Arctic Ocean. Geology 27, 759–762. doi:10.1130/0091-7613(1999)027<0759:LPAHME>2.3.CO;2.

Porsild, A.E. 1950. A biological exploration of Banks and Victoria Islands. Arctic 3, 45–54.

Prest, V.K. 1969. Retreat of Wisconsin and Recent ice in North America. Geological Survey of Canada Map 1257A, scale 1:5,000,000.

Scott, D.B., Schell, T., St.-Onge, G., Rochon, A., Blasco, S. 2009. Foraminiferal assemblage changes over the last 15,000 years on the Mackenzie-Beaufort sea slope and Amundsen Gulf, Canada: implications for past sea ice conditions. Paleoceanography 24, PA2219. doi:10.1029/2007PA001575.

Shaw, J., Forbes, D.L. 1995. The postglacial relative sea-level lowstand in Newfoundland. Canadian Journal of Earth Sciences 32, 1308–1330. doi:10.1139/e95-107.

Siddall, M., Milne, G.A. 2012. Understanding sea-level change is impossible without both insights from paleo studies and working across disciplines. Earth and Planetary Science Letters 315/316, 2–3. doi:10.1016/j.epsl.2011.10.023.

Stea, R.R., Fader, G., Scott, D.B., Wu, P. 2001. Glaciation and relative sea-level change in Maritime Canada. In: Retelle, M.J., Weddle, T.K. (Eds.), Deglacial history and relative sea-level changes, northern New England and adjacent Canada. Geological Society of America, Special Paper 351, pp. 35–50.

Stokes, C.R., Clark, C.D., Darby, D.A., Hodgson, D.A. 2005. Late Pleistocene ice export events into the Arctic Ocean from the M'Clure Strait Ice Stream, Canadian Arctic Archipelago. Global and Planetary Change 49, 139–162. doi:10.1016/j.gloplacha.2005.06.001.

Stokes, C.R., Clark, C.D., Winsborrow, M.C.M. 2006. Subglacial bedform evidence for a major palaeo-ice stream and its retreat phases in Amundsen Gulf, Canadian Arctic Archipelago. Journal of Quaternary Science 21, 399–412. doi:10.1002/jqs.991.

Stokes, C.R., Clark, C.D., Storrar, R. 2009. Major changes in ice stream dynamics during deglaciation of the north-western margin of the Laurentide Ice Sheet. Quaternary Science Reviews 28, 721–738. doi:10.1016/j.quascirev.2008.07.019.

Tarasov, L., Dyke, A.S., Neal, R.M., Peltier, W.R. 2012. A data-calibrated distribution of deglacial chronologies for the North American ice complex from glaciological modeling. Earth and Planetary Science Letters 315–316, 30–40. doi:10.1016/j.epsl.2011.09.010.

Vincent, J.-S. 1982. The Quaternary history of Banks Island, NWT, Canada. Géographie physique et Quaternaire 36, 209–232.

Vincent, J.-S. 1983. La géologie du Quaternaire et la géomorphologie de l'Île Banks, Arctique Canadien. Geological Survey of Canada, Memoir 405.

Vincent, J.-S. 1984. Quaternary stratigraphy of the western Canadian Arctic Archipelago. In: Fulton, R.J. (Ed.), Quaternary Stratigraphy of Canada – A Canadian Contribution To IGCP Project 24. Geological Survey of Canada Paper, 84-10, pp. 87–100.

Vincent, J.-S., Morris, W.A., Occhietti, S. 1984. Glacial and nonglaical sediments of Matuyama paleomagnetic age on Banks Island, Canadian Arctic Archipelago. Geology 12, 139–142. doi:10.1130/0091-7613(1984)12<139:GANSOM>2.0.CO;2.

Vogt, P.R., Crane, K., Sundvor, E. 1994. Deep Pleistocene iceberg plowmarks on the Yermak Plateau: sidescan and 3.5 kHz evidence for thick calving ice fronts and a possible marine ice sheet in the Arctic Ocean. Geology 22, 403–406. doi:10.1130/0091-7613(1994)022<0403:DPIPOT>2.3.CO;2.

Washburn, A.L. 1947. Reconnaissance geology of portions of Victoria Island and adjacent regions, Arctic Canada. Geological Society of America, Memoir 22.

Wilson, J.T., Falconer, G., Mathews, W.H., Prest, V.K. 1958. Glacial Map of Canada. Geological Association of Canada, scale 1:5,000,000.

Table 2.1 Radiocarbon ages cited in this chapter.

	Laboratory number[a]	^{14}C age[b] (yr BP)	Lab Error[c] (yr BP)	Dated Material	Location	Coordinates	Sample Elevation (m asl)	Site Description	Reference
West coast, Banks Island	NOSAMS-79535	49900	550	*A. borealis* (fragment)	First Point	73° 17' 14.8'' N 124° 32' 58.7'' W	5	Surface: stony sand and silt	This study
	NOSAMS-79536	30700	140	*A. borealis* (whole valve)	Adam River	73° 25' 12.2" N 124° 23' 11.2" W	2	Surface: stony sand and silt	This study
	NOSAMS-79539	34700	200	*H. arctica* (fragment)	Liot Point	73° 05' 16.4" N 124° 51' 24.4" W	3	Surface: stony sand and silt	This study
	NOSAMS-79612	45600	480	*A. borealis* (whole valve)	*South Bluff* Burnett Bay	73° 49' 54.3" N 123° 52' 13.5" W	6	Stratigraphic section: organic-rich, stony mud	This study
	NOSAMS-79613	33600	240	*A. borealis* (fragment)	*North Bluff* Burnett Bay	73° 50' 12.1" N 123° 53' 24.2" W	4	Surface: sandy gravel on top of the bluff	This study
	NOSAMS-79614	45500	600	*A. borealis* (whole valve)	*North Bluff* Burnett Bay	73° 50' 17.7" N 123° 53' 56.4" W	5	Stratigraphic section: stony sand	This study
	NOSAMS-79615*	35100	220	*A. borealis* (whole valve)	*North Bluff* Burnett Bay	73° 50' 29.8" N 123° 54' 09.4" W	6	Surface: sandy gravel on top of the bluff	This study
	UCI-77838*	38540	330	*A. borealis* (whole valve)	*North Bluff* Burnett Bay	73° 50' 29.8" N 123° 54' 09.4" W	6	Surface: sandy gravel on top of the bluff	This study
Norway Island	NOSAMS-79616	44800	770	*A. borealis* (fragment)	Norway Island	73° 42' 11.2" N 124° 35' 51.5" W	5-30	Stratigraphic section: sandy gravel delta foresets	This study
Phillips Island	NOSAMS-79617*	>52000		*H. arctica* (whole valve)	Phillips Island	74° 05.101' N 124° 33.275' W	7	Stratigraphic section: glaciotectonized stony sand	This study
	UCI-77839*	>57300		*H. arctica* (whole valve)	Phillips Island	74° 05.101' N 124° 33.275' W	7	Stratigraphic section: glaciotectonized stony sand	This study

Table 2.1 (cont.) Radiocarbon ages cited in this chapter.

	Laboratory number[a]	^{14}C age[b] (yr BP)	Lab Error[c] (yr BP)	Dated Material	Location	Coordinates	Sample Elevation (m asl)	Site Description	Reference
East coast, Banks Island	UCI-50741	49500	1210	*H. arctica* (fragment)	Jesse till	72.86513° N 118.21583° W	36-38	Surface: marine limit delta	This study
	UCI-50748	41490	460	Unidentified (fragment)	Jesse till	72° 55' 40.9" N 118° 23' 35.1" W	145	Surface: outwash terrace	This study
	UCI-50749	46100	790	*H. arctica* (?) (fragment)	Jesse till	73° 05' 27.6" N 118° 56' 35.7" W	~98	Surface: gully cut into till	This study
	UCI-60258	44000	1000	*H. arctica* (?) (fragment)	Jesse till	72° 16' 32.7" N 120° 19' 25.2" W	45	Surface: glaciolac. delta	This study
	UCI-60261	49700	2100	*H. arctica* (?) (fragment)	Jesse till	72° 13' 03.3" N 120° 11' 39.9" W	21	Stratigraphic section; sandy gravel foresets of marine limit delta	This study
	UCI-60264	48000	1700	*H. arctica* (?) (fragment)	Jesse till	72° 14' 49.3" N 120° 00' 07.8" W	24	Surface: till	This study
	UCI-60269	32530	250	*H. arctica* (?) (fragment)	Jesse till	72° 14' 04.2" N 120° 00' 49.4" W	38	Surface: wave-washed till	This study
	UCI-60271	39610	600	*H. arctica* (?) (fragment)	Jesse till	72° 06' 32.9" N 120° 12' 00.3" W	37	Surface: wave-washed till	This study
	UCI-60272	55200	4000	*H. arctica* (?) (fragment)	Jesse till	72° 11' 31.9" N 120° 09' 41.7" W	17	Stratigraphic section: sandy gravel foresets of marine limit delta	This study
	UCI-60273	32640	260	*H. arctica* (?) (fragment)	Jesse till	72° 03' 56.8" N 120° 14' 58.1" W	26	Surface: glaciolac. terrace	This study

Notes: [a] - NOSAMS (National Ocean Sciences Accelerator Mass Spectrometry Facility, Woods Hole Oceanographic Institute); UCI (University of California at Irvine). [b] - no marine reservoir correction. [c] - 1-sigma. * - indicates redate on the same valve.

Table 2.2 Optically stimulated luminescence ages from Phillips Island.

Laboratory number[a]	Elevation (m asl)	Depth (cm)	Palaeodose (De) (Gy)	Dose rate (µGy/a)	Age (ka BP)	Material	Coordinates	Reference
Shfd11043	7	150	92.1 ± 1.93	784 ± 34	118 ± 5.7	Glaciotectonized gravelly sand	74° 05' 05.5" N 124° 33' 13.7"W	This study
Shfd11071	7	150	88.8 ± 2.40	810 ± 22	110 ± 4.2	Glaciotectonized gravelly sand	74° 05' 05.5" N 124° 33' 13.7"W	This study

Notes: [a] - Shfd (Sheffield Centre for International Drylands Research).

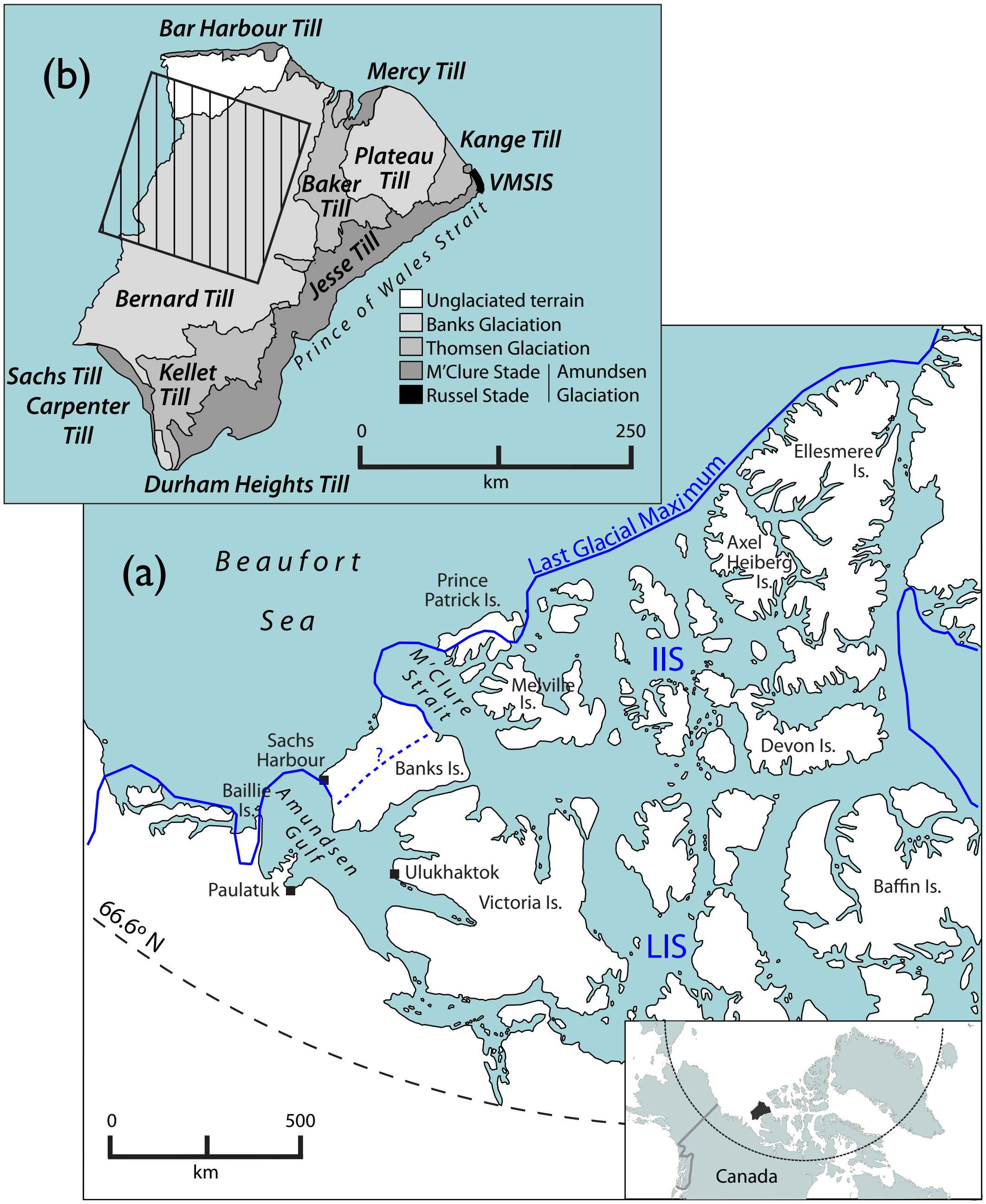

Figure 2.1. (a) Canadian Arctic Archipelago showing the extent of the Innuitian Ice Sheet (IIS) and Laurentide (LIS) Ice Sheet at the Last Glacial Maximum. The dashed blue line indicates the minimum extent of the LIS on Banks Island following England et al. (2009) and Lakeman and England (In Press; see Chapter 3). Ice sheet limits elsewhere are modified from Dyke (2004) and England et al. (2006, 2009). (b) Generalized surficial geology of Banks Island as reported by Vincent (1982, 1983), which was considered to document at least three Quaternary glaciations. Note the purportedly unglaciated plateau in the northwest. The study area is denoted by the shaded box. VMSIS–Viscount Melville Sound Ice Shelf Moraine.

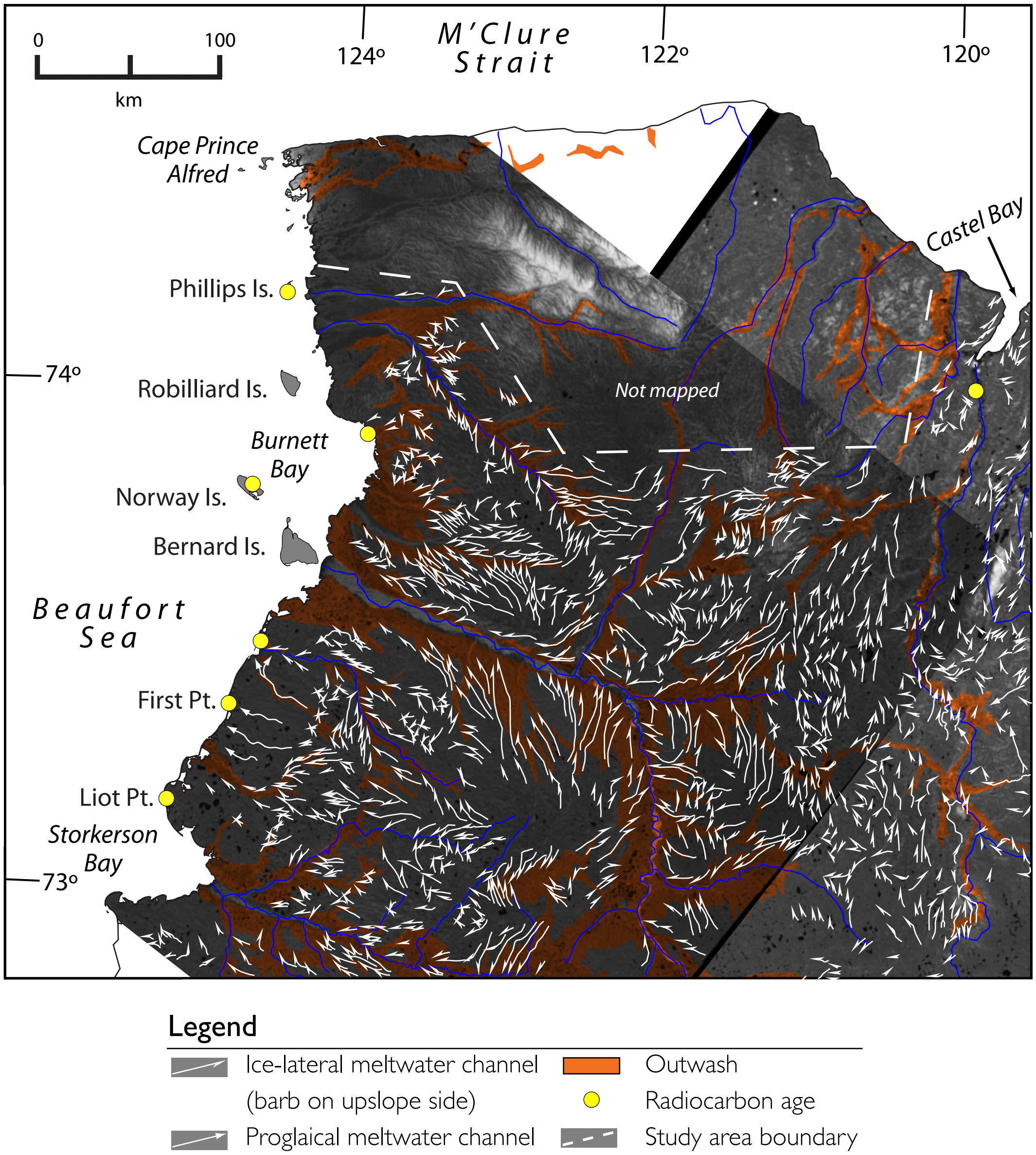

Figure 2.2. The distribution of meltwater channels, outwash, and radiocarbon ages in the study area, shown on a composite Landsat 7 orthoimage (band 8) of west-central Banks Island.

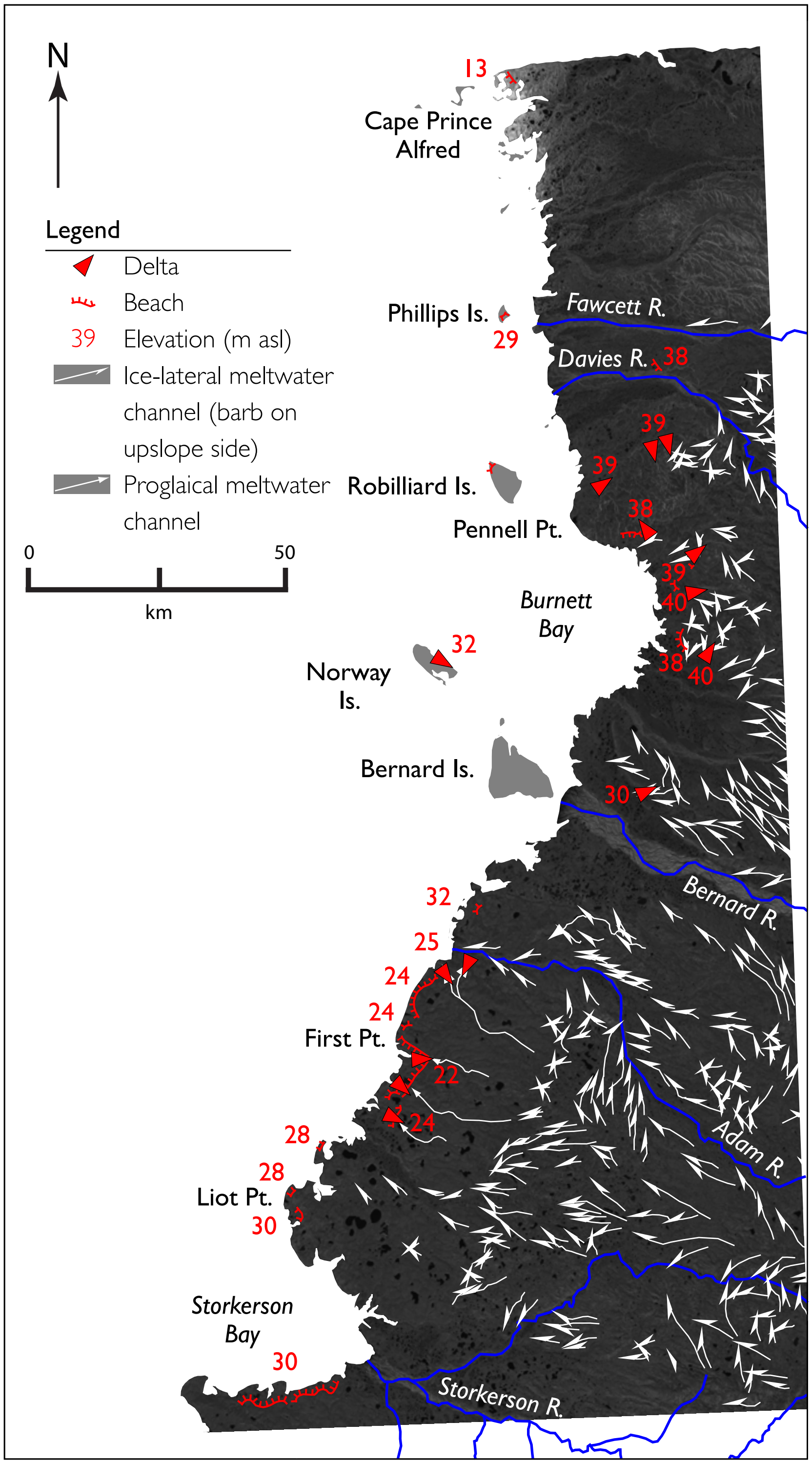

Figure 2.3. The location and elevation of raised marine beaches and ice-contact deltas on west-central Banks Island. These landforms comprise a single, prominent shoreline that is traceable from Storkerson Bay to the Davies River. Note the 13m marine limit shoreline at Cape Prince Alfred (J. England and M. Furze, pers. comm., 2010).

Figure 2.4. Coastal exposure at First Point showing massive and planar-laminated stony sand and silt overlying clayey till. Rare shell fragments from the massive stony sand, capping this exposure, yielded a radiocarbon age of 49,900 ± 550 ^{14}C yr BP (NOSAMS-79535; Table 2.1). Additional mollusc samples from the same deposit elsewhere yielded ages of 34,700 ± 200 ^{14}C yr BP (NOSAMS-79539) and 30,700 ± 140 ^{14}C yr BP (NOSAMS-79536; Table 2.1).

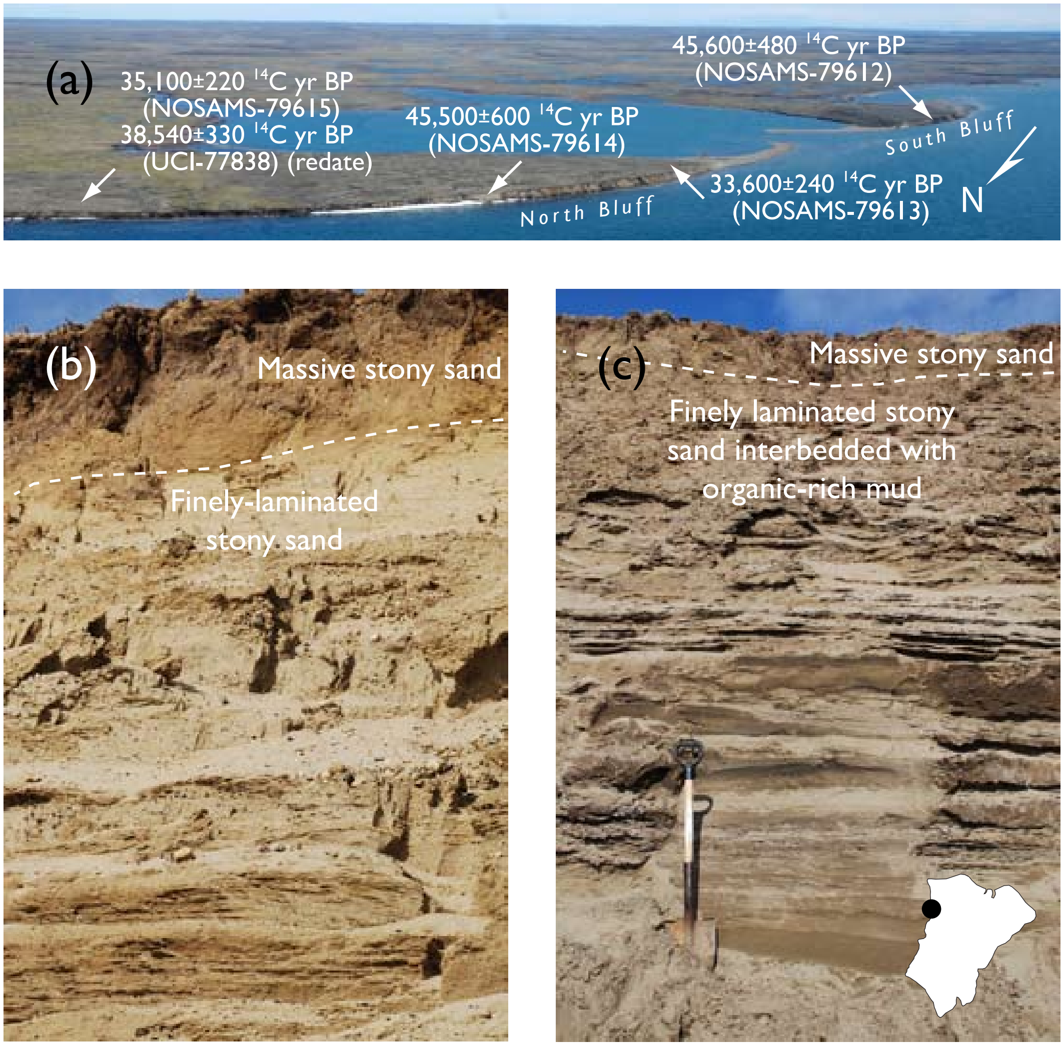

Figure 2.5. (a) Oblique photograph of two bluffs at the head of Burnett Bay (Fig. 2.3), looking southeast. Locations of radiocarbon ages are shown. NOSAMS-79615, UCI-77838, and NOSAMS-79613 are surface collections of whole valves and fragments of *A. borealis*, ranging in age from 33-39 ^{14}C ka BP (Table 2.1). NOSAMS-79612 and NOSAMS-79614 are collections of abundant, paired, whole valves of *A. borealis* from the *South* and *North* bluffs, respectively. (b) The *North Bluff*: fossiliferous, finely-laminated and rippled stony sand, overlain by massive stony sand. (c) The *South Bluff*: finely laminated and rippled stony sand interbedded with fossiliferous, stony, organic-rich mud, overlain by massive stony sand.

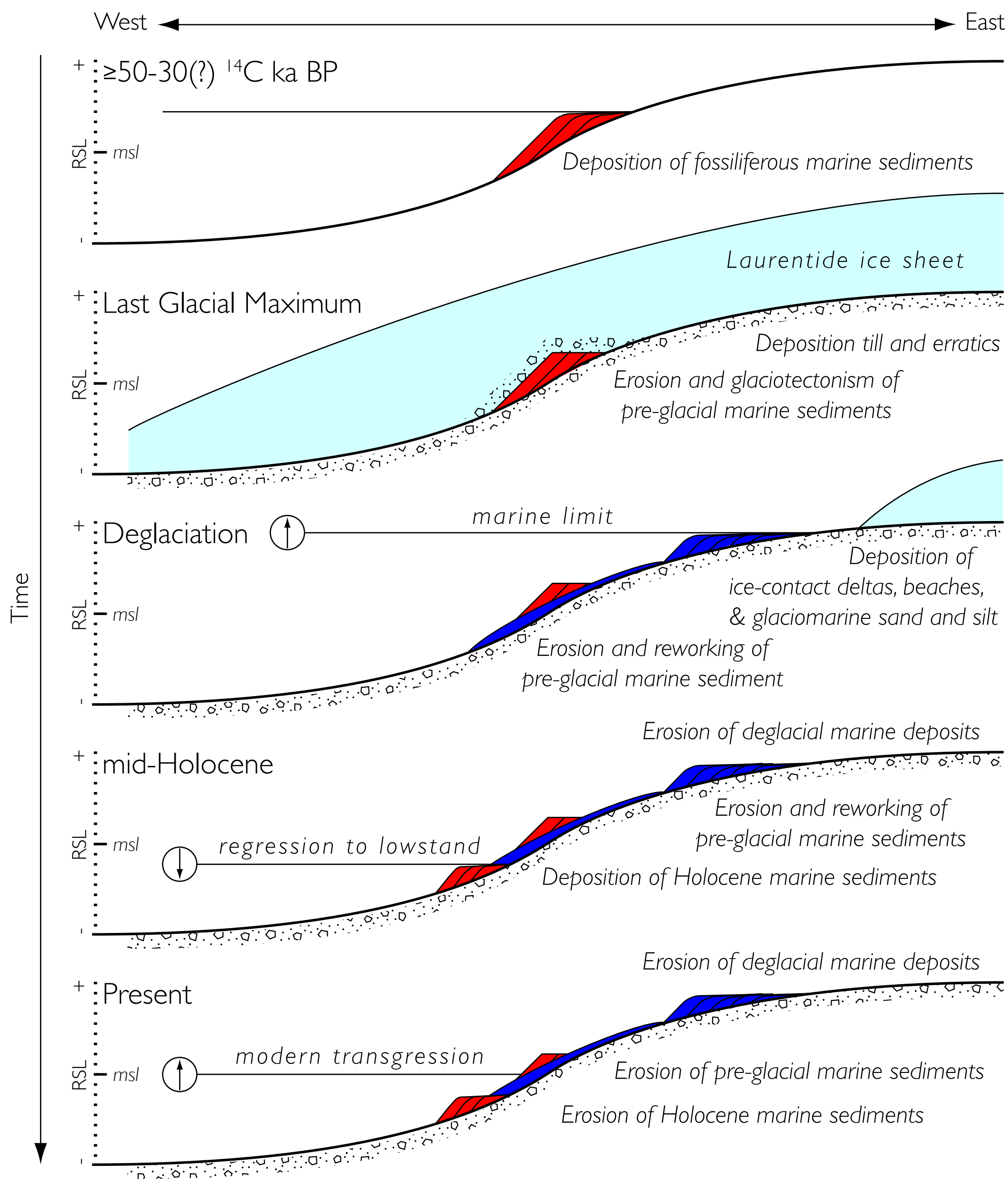

Figure 2.6. Conceptual model of late Pleistocene environments on western Banks Island.

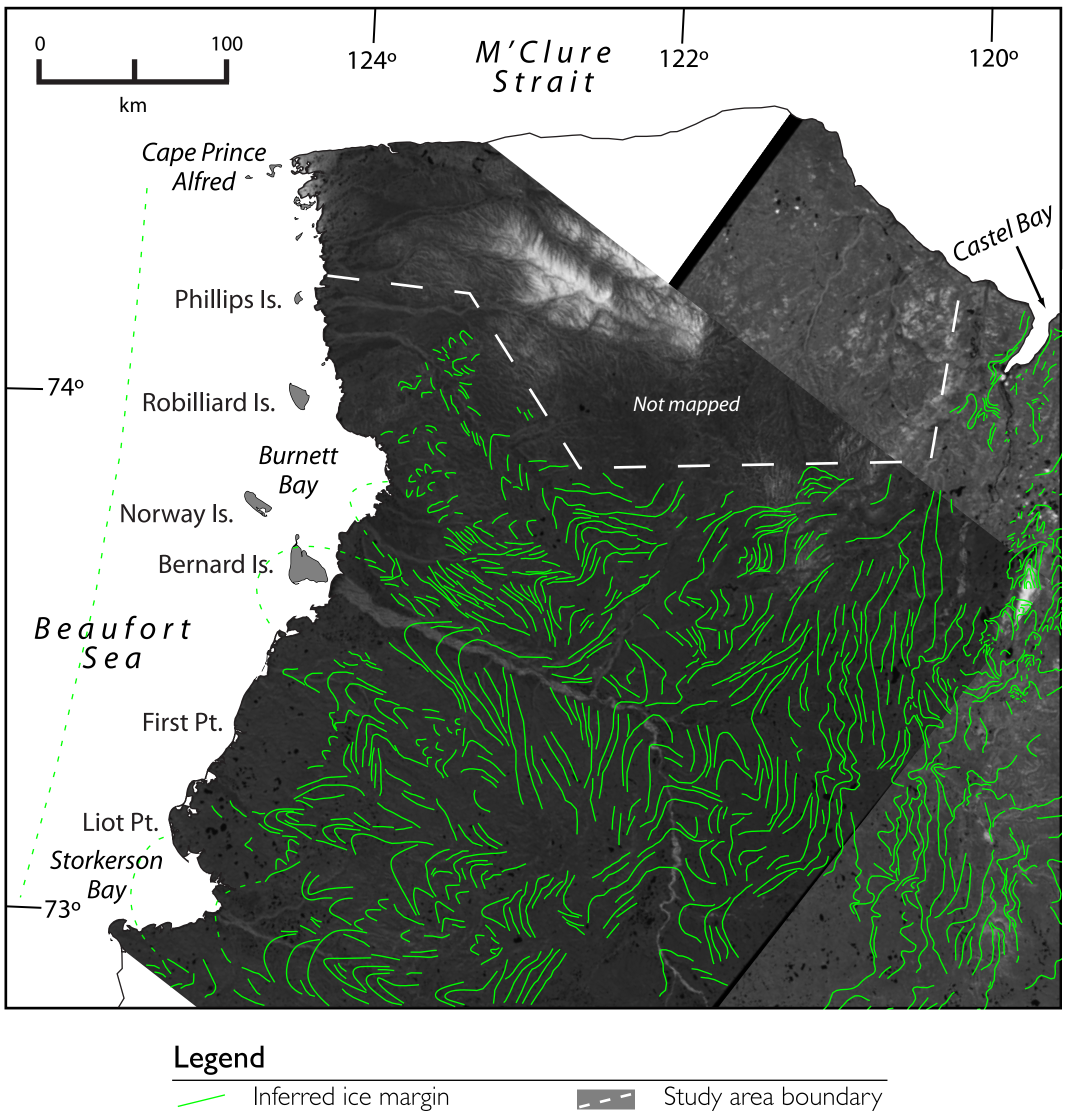

Figure 2.7. Inferred deglacial ice margins shown on a composite Landsat 7 orthoimage (band 8) of westcentral Banks Island.

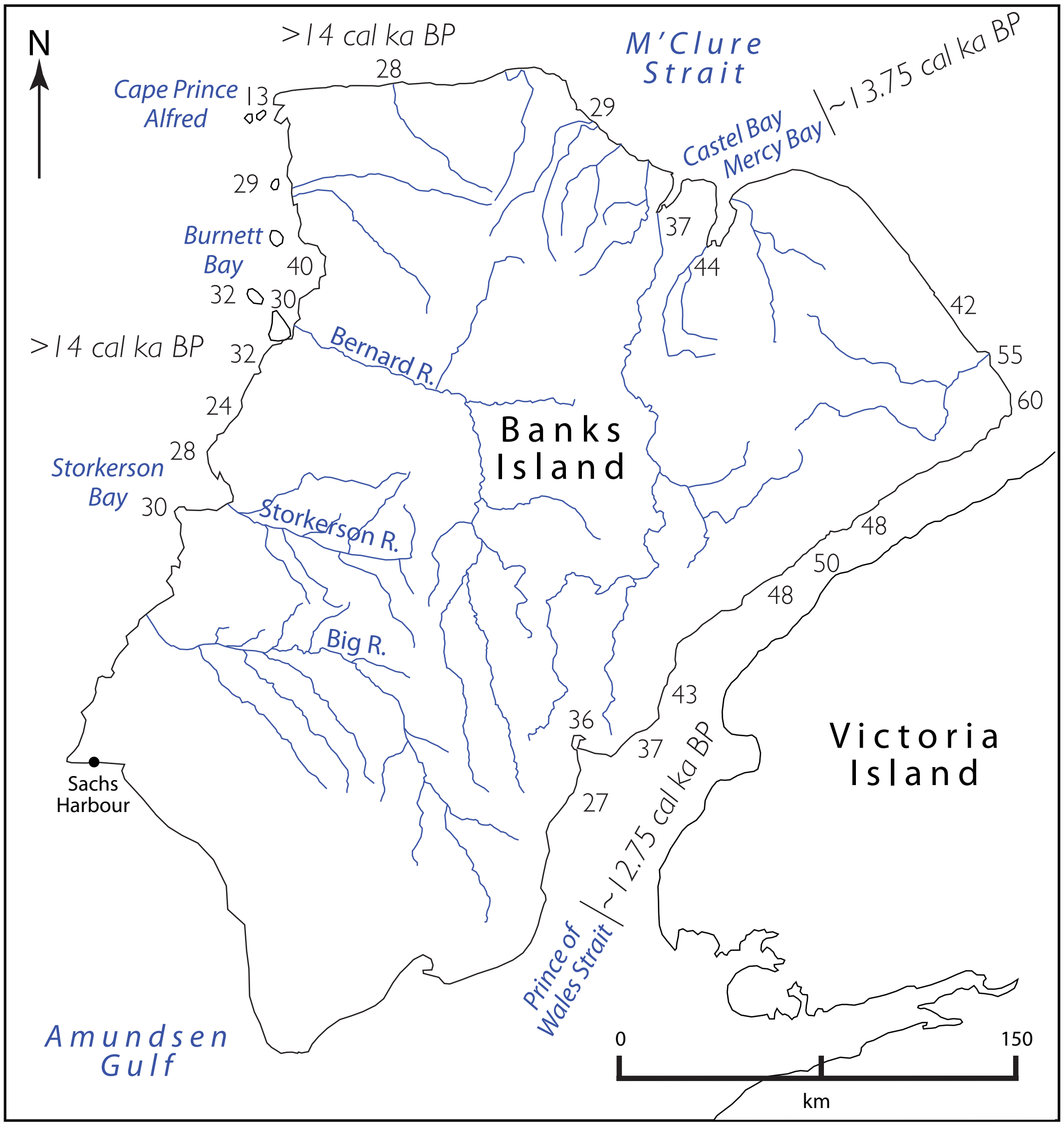

Figure 2.8. The age and elevation (m asl) of marine limit on Banks Island. The age of marine limit on the west coast is unknown. Data from the north coast of Banks Island is from England et al. (2009). Data from Castel Bay and the east coast of Banks Island is from Lakeman and England (2012).

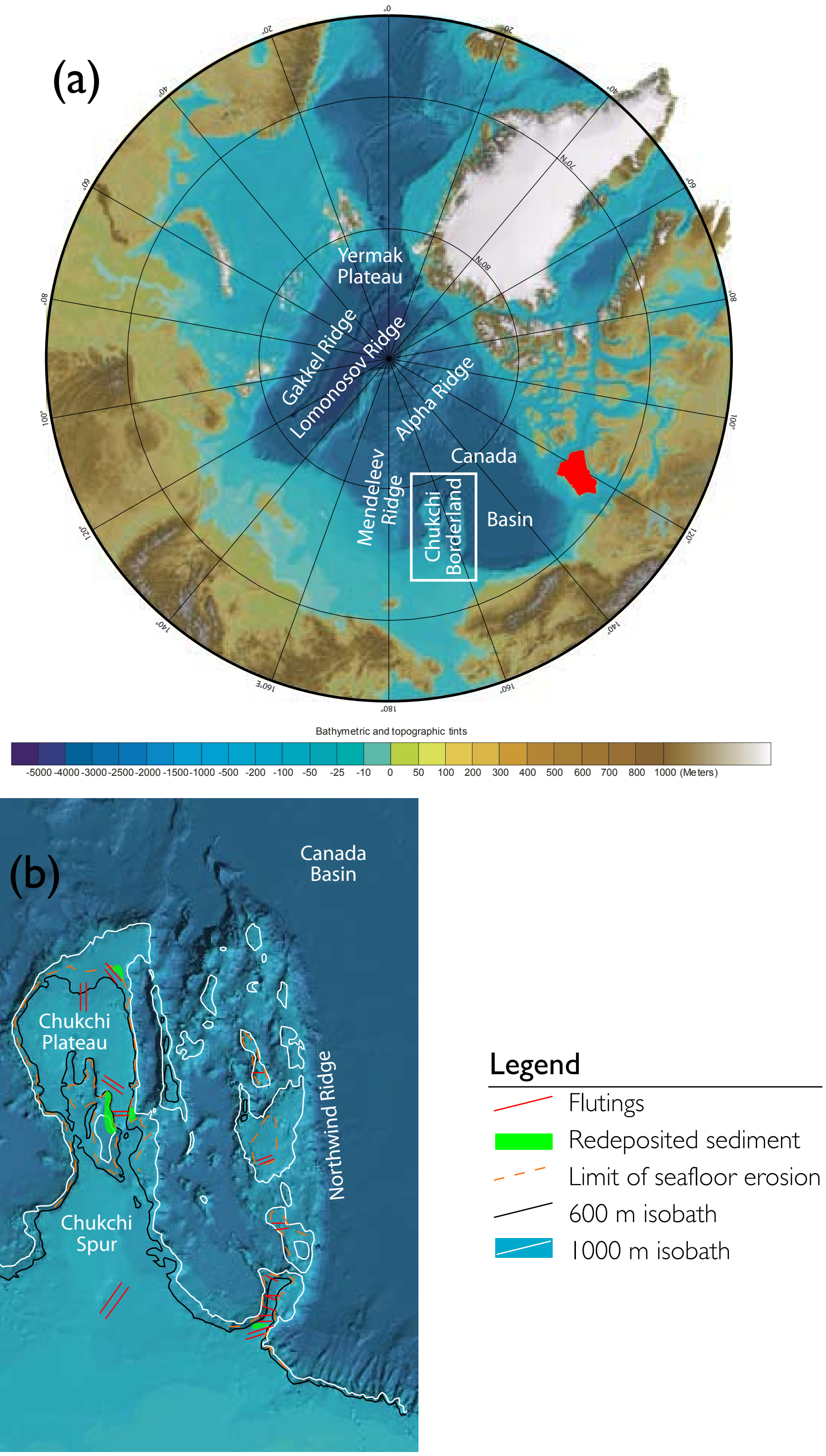

Figure 2.9. (a) International Bathymetric Chart of the Arctic Ocean (IBCAO) showing the location of the Chukchi Borderland and other selected features on the Arctic Ocean seafloor (Jakobsson et al. (2008a). Banks Island is shown in red. Box marks the location of (b). (b) Glacial bedforms on the Chukchi Borderland. From Jakobsson et al (2008b).

CHAPTER 3

Paleoglaciological Insights from the Age and Morphology of the Jesse Moraine Belt, Western Canadian Arctic

INTRODUCTION

Late Wisconsinan deglaciation of the Canadian Arctic Archipelago (CAA) involved ice sheet withdrawal along predominantly cold-based, terrestrial margins and faster-flowing, marine-based margins in the interisland channels, where multiple, former ice streams are hypothesized (Dyke and Prest, 1987; Hodgson, 1994; Dyke, 1999, 2004; Dyke et al., 2002; Atkinson, 2003; De Angelis and Kleman, 2005; Stokes et al., 2005, 2006, 2009; England et al., 2006, 2009; De Angelis and Kleman, 2007). Importantly, ice sheet mass loss during deglaciation was dominated by calving along tidewater margins, a configuration very similar to that of the present West Antarctic Ice Sheet, which has long been recognized as potentially unstable (Weertman, 1974; Mercer, 1978). In this respect, inferences of former terrestrial, ice-marginal processes in the CAA, as well as the timing and nature of adjacent marine-based ice sheet retreat, constitute important constraints on our understanding of the dynamical response of high latitude ice sheets to such variables as paleoclimate and sea level change. Furthermore, the Late Wisconsinan history of ice dynamics and ice-marginal processes in the CAA comprises a valuable analogue for models addressing future ice sheet stability (i.e. Bentley, 2010).

Banks Island (70,028 km^2) is situated in the western CAA (Fig. 3.1) and has a long history of geomorphological investigations aimed at characterizing the history of Quaternary glaciation (Hobbs, 1945; Jenness, 1952; Wilson et al., 1958; Fyles, 1962; Prest, 1969; Vincent, 1982, 1983; Dyke, 1987). Until recently, much of the island was regarded as an ice-free refugium during the last glaciation, and eleven till sheets purported to be of different geomorphic or lithologic character, lying beyond the inferred Late Wisconsinan ice limit (Fig. 3.2), were ascribed to three to four glaciations of vastly different ages (Fyles, 1962; Prest, 1969; Vincent, 1982, 1983; Dyke, 1987, 2004; Dyke and Prest, 1987; Dyke et al., 2002). A new, robust chronology presented in Lakeman and England (submitted for publication) and in England et al. (2009) demonstrates that the northwest Laurentide Ice Sheet (LIS) inundated Banks Island during the Last Glacial Maximum (LGM), terminating on the Beaufort Sea shelf. As a result, the purported till sheets that span the island are now considered to be part of a single depositional sequence of Late Wisconsinan age that left the bedrock predominantly unobscured (England et al., 2009; Fig. 3.2). Hence, Vincent's (1982, 1983) formal recognition of discrete till sheets of climatostratigraphic importance (Fig. 3.2, inset) has been abandoned. Here we elaborate on the nature of Late Wisconsinan glaciation on Banks Island, using the glacial geomorphology to reconstruct past ice sheet dynamics of the northwest LIS.

The focus of this study is the 350 km-long Jesse moraine belt, which includes the formerly recognized Jesse till on eastern Banks Island and an unnamed, correlative deposit on adjacent Prince Albert Peninsula, Victoria Island (Fig. 3.2).

Originally identified by Fyles (1962), the thickness, continuity, and geomorphology of the Jesse till make it unique among the eleven formerly recognized till sheets on Banks Island (Vincent, 1982, 1983). Consequently, the study aims to characterize the age and significance of the Jesse moraine belt (Fig. 3.2) in relation to distal glaciogenic landforms and sediments, deposited during preceding ice sheet retreat (Fig. 3.2). The objectives are to: i) describe the geomorphology and sedimentology of the Jesse till in relation to distal glaciogenic deposits in order to characterize former ice-marginal processes, ii) evaluate spatial and temporal variations in ice-marginal depositional environments to inform estimates of past ice sheet dynamics, and iii) consider potential causal linkages between former ice sheet dynamics and past fluctuations in climate, sea level, and the timing and pattern of regional deglaciation. To address these objectives a robust radiocarbon chronology is combined with detailed glacial geomorphological observations. The resulting, conceptual model of deglaciation documents the nature of the final phase of ice sheet retreat from Banks Island and northwest Victoria Island. The timing and pattern of penecontemporaneous deglaciation in M'Clure Strait and elsewhere are summarized and their impacts on ice-marginal processes on Banks Island and Victoria Island are considered. Similarly, the importance of late-glacial relative sea level changes and climatic perturbations of varying magnitude and regional significance, such as those during the Bølling–Allerød and Younger Dryas chronozones (Rasmussen et al., 2006), are scrutinized. This new reconstruction of the deglacial environments of eastern Banks Island and northwestern Victoria Island improves our understanding of the last glacial-interglacial transition in Arctic Canada and serves as a proxy for Late Pleistocene environmental change.

METHODS

Glacial and marine landforms and sediments on north-central and eastern Banks Island were mapped over the course of widespread field surveys spanning two summers, using available aerial photography and satellite imagery. The extent and pattern of retreat for the LIS was determined using cross-cutting relationships among mapped glacial landforms. Observations from Banks Island were collated with those from Prince Albert Peninsula, Victoria Island, which are available in Fyles (1962, 1963), Stokes et al. (2005), and Storrar and Stokes (2007). The chronology of Late Wisconsinan ice sheet retreat was established using radiocarbon ages of fossil marine molluscs collected from glacial and marine sediments along more than ~900 km of coastline. This suite of ages, consisting of 50 from Banks Island, 33 from western Victoria Island, and 3 from the Canadian Arctic Mainland, is summarized in Table 3.1. The total from Banks Island includes 34 new Accelerator Mass Spectrometry (AMS) radiocarbon ages that were obtained from the W. M. Keck Carbon Cycle Accelerator Mass Spectrometry Laboratory, University of California (Irvine). All radiocarbon ages were calibrated using a ΔR value of 335 ± 85 years (Coulthard et al., 2010) in Calib v.6.0, which uses the Marine09 calibration curve (Reimer et al., 2009).

GEOMORPHIC OBSERVATIONS

The study area includes many of Vincent's (1982, 1983) proposed till sheets that were partly based on early physiographic divisions by Fyles (1962; Fig. 3.2).

The oldest till sheets recognized by Vincent (1982, 1983) were the Bernard, Plateau, and Durham Heights tills (Fig. 3.2), which Vincent (1982, 1983) and Vincent et al. (1984) surmised were correlative and deposited during the Banks Glaciation, more than 780,000 years ago (i.e. during the Matuyama Chron). However, their lithologies essentially mimic the underlying bedrock, thereby precluding their utility (Figs. 3.1 and 3.2). Furthermore, recent mapping has demonstrated that these surfaces contain only sparse igneous and metamorphic erratics, and are dissected by a complex pattern of glacial meltwater channels. Till flanking the Thomsen River valley was termed the Baker till by Vincent (1982, 1983; Figs. 3.2 and 3.3) and postulated to be younger than the Bernard and Plateau tills but nonetheless deposited during a pre-Wisconsinan glaciation. Baker till is predominantly a mixture of sand, silt, and clay derived from the underlying Cretaceous bedrock with a low concentration of erratic clasts of primarily quartzite, granite and limestone that range in size from pebbles to small cobbles with rare boulders. Finally, Vincent (1982, 1983) proposed that the northern limit of the Baker till was cross-cut by the Mercy till, however this proposal was dismissed by England et al. (2009). As stated, the purported till sheets of Vincent (1982, 1983) are now considered to be part of a discontinuous deposit of Late Wisconsinan age (England et al., 2009; Lakeman and England, submitted for publication). It is emphasized that subsequent references to these formerly recognized till sheets are meant to facilitate comparisons with previous literature but do not constitute a desire to perpetuate this former terminology.

NORTH-CENTRAL BANKS ISLAND AND THE THOMSEN RIVER VALLEY

In the northwest part of the study area (Fig. 3.3) the limit of the Baker till is generally inconspicuous. However, a contemporaneous ice margin is delineated by a series of nested lateral moraines in Castel Bay, deposited by a north-flowing glacier (Figs. 3.3 and 3.4a). On the distal flank of the outermost left-lateral moraine, above the Desert River valley, glaciolacustrine deltas emanating from the moraines reach elevations of 65 m asl (Fig. 3.4b). These deltas contrast with lower, ice-contact deltas at 33 m asl that demarcate marine limit (the highest elevation achieved by the sea prior to glacioisostatic emergence). Additional lateral moraines are present in Mercy Bay, where they record similar northward-flowing ice, and are situated adjacent to ice-contact deltas and beaches marking marine limit at 41 m asl (England and Furze, 2008; England et al., 2009; Fig. 3.3). In the Thomsen River valley, marine limit is recorded by a series of ice-contact deltas and beaches at 37 m asl, 15 km south of the head of Castel Bay (Figs. 3.3 and 3.5). The lower Thomsen River valley is characterized by few moraines and abundant ice-lateral and proglacial meltwater channels, indicating a general pattern of ice retreat to the south and east, into the island's interior (Fig. 3.3). In contrast, the lowland south of the head of Mercy Bay is characterized by abundant recessional moraines and hummocky terrain, documenting a similar direction of ice retreat into the interior (England et al., 2009).

The western limit of the Baker till is marked by a discontinuous series of moraines near Shoran Lake (Fig. 3.6). These moraines are composed of silty to sandy, well-sorted medium gravels with rare cobbles and boulders, likely derived from outwash or from remnant exposures of the Beaufort Fm. They are interpreted as ice-thrust moraines because they comprise multiple, sharp-crested, parallel ridges and commonly exhibit conspicuous shear planes that rise in the direction of ice-flow (Fig. 3.6). Mapped ice-lateral meltwater channels parallel the moraines, both to the north and south. Some of these ice-lateral meltwater channels merge with contemporaneous ice-lateral meltwater channels traversing the Bernard till. These geomorphic relationships between two proposed till sheets indicate that the purported boundary does not represent a former ice margin. Rather, moraine deposition was both intermittent and spatially variable, and coeval with landscape incision by adjacent ice-lateral meltwater channels. This interpretation is further confirmed by additional areas of concentrated moraines to the south and east, including the Thomsen River valley, that are flanked by ice-lateral meltwater channels (Fig. 3.3). As a result, the Bernard and Baker tills, previously defined on predominantly lithological criteria by Vincent (1982, 1983), are synchronous, as was also recognized by England et al. (2009).

A similar geomorphic relationship occurs along the northeast boundary of the Baker till where it contacts the Plateau till. Here, hummocky terrain abutting the Devonian sandstone plateau approximates the limit of the Baker till, and adjacent ice-lateral meltwater channels incised into the sandstone bedrock appear to document contemporaneous ice sheet retreat across the plateau (Fig. 3.3). In this area, however, the precise relationship between the hummocky terrain (i.e. the limit of the till) and the adjacent ice-lateral meltwater channels is not as clear. Therefore, it remains possible that the limit of the till represents a former ice margin. Furthermore, it cannot be discounted that some of the meltwater channels on the plateau relate to one or more preceding glaciations. Throughout the

Thomsen River valley, widespread ice-lateral meltwater channels, their associated outwash fans, and sporadic moraines delineate various glacier termini, which record ice sheet withdrawal to the south and east. Multiple glaciolacustrine deposits of rhythmically-bedded silt with dropstones occupy the upper Thomsen River valley; the largest of which covers >50 km^2. Numerous, sandy, outwash terraces flank the Thomsen River valley, for about 125 km, from approximately 73° N to Castel Bay, indicating that it served as a major conduit for meltwater during deglaciation as ice retreated to the southeast (Fig. 3.3).

EASTERN BANKS ISLAND

The Jesse till comprises a 350 km-long moraine belt, up to 40 km wide, that rims the east coast (Fig. 3.7). The till is generally sandy in texture and has a high concentration of basalt and gabbro boulder erratics, commonly >4 m in diameter. It overlies poorly consolidated Cretaceous to Eocene clastic sedimentary bedrock for much of its length; on northeastern Banks Island it overlies well-lithified, Devonian sandstone (Figs. 3.1 and 3.2). Widespread retrogressive thaw flow slides occur in the Jesse till, both above and below marine limit. They expose foliated, clean, ground ice as well as foliated, sediment-rich ground ice that is sharply overlain by 1–2 m of till (Fig. 3.8). The sediment-rich ice contains clasts, including boulders, many of which are striated, confirming its glacial origin. Widespread hummocky terrain, sinuous end moraines, sharp-crested (ice-thrust?) moraines, kettle lakes, and kames delineate the western margin of the Jesse till (Fig. 3.7), which contrasts markedly with the Baker till to the west (Fig. 3.9). Another contrasting feature is the myriad proglacial and ice-lateral meltwater channels, floored by coarse gravel outwash, up to 4 km in width, that descend west and north from inside the limit of the Jesse till (Fig. 3.9). These channels generally constitute the upper reaches of the major fluvial catchments draining west and north across the island today, such as the Big, Storkerson, Bernard, and Thomsen rivers (Fig. 3.2).

The central axis of the moraine belt is composed of broad, low moraines, commonly up to 500 m wide, interspersed with widespread kettle lakes (Fig. 3.10). Rare occurrences of fluted till comprise four small flow-sets (Flow-sets 13–16 on Figs. 3.2 and 3.7). Observations of foliated, sediment-rich ice, many >3 m thick, clearly indicate that many of the moraines are ice-cored (Fig. 3.8). Furthermore, the complex distribution of abundant, large kettle lakes on the surface of the till is the product of postglacial degradation of buried glacier ice, which is further recorded by deglacial kame deltas and shorelines at higher elevations surrounding their basins. Other kettles have drained completely, exposing areas of stony (glacio?) lacustrine silt.

The eastern flank of the Jesse till is characterized by a wide array of sediment-landform assemblages distinct from the rest of the moraine belt. For example, several east-draining valleys contain large areas of rhythmically-bedded, stony silt exhibiting abundant soft-sediment deformation. Previously mapped as till (Vincent, 1982, 1983), these glaciolacustrine exposures also contain poorly consolidated diamicts, interpreted as sub-aquatic debris flows. Adjacent interfluves lack glaciolacustrine sediment but are covered by till and large, sub-horizontal kame terraces. These deposits are composed of coarse gravel and boulders, and are commonly traceable for more than 10 km (Figs. 3.7 and 3.11). Some kame terraces grade to coarse gravel kame deltas, marking the extent and elevation of proglacial lakes dammed by glaciers occupying the valleys. At the heads of some valleys, narrow spillways traverse the Jesse till, recording meltwater routing to the west from these former lakes. Younger kame terraces at lower elevations are generally restricted to the outer coast where they trend northeast and occur in association with similarly oriented moraines, as well as kame deltas and beaches (Fig. 3.7).

The northernmost 50 km of the Jesse till, terminating at Parker Point, is marked by a thinner till blanket, the general absence of kettle lakes, several ice-lateral meltwater channels, and coast-parallel moraines (Fig. 3.7). The moraines are sharp-crested and extend to Russel Point, where they are inset by a younger moraine deposited by the Viscount Melville Sound Ice Shelf (Hodgson and Vincent, 1984; Hodgson, 1994; England et al., 2009). These moraines are flanked by prominent meltwater channels incised into the underlying Devonian bedrock. Throughout its coastal extent, the Jesse till is onlapped by fossiliferous deglacial marine sediments, deposited as ice-contact deltas and beaches during ice sheet withdrawal from Prince of Wales Strait (Fig. 3.7). The highest of these deposits mark marine limit, which rises from 27 m asl south of Jesse Bay to 50 m asl north of Johnson Point, and to 60 m asl near Russell Point (England et al., 2009; Fig. 3.7). At several localities, ice-contact deltas and beaches occur in association with nested coast-parallel moraines below marine limit, which are likely the product of deglacial ice shelves.

PRINCE ALBERT PENINSULA, VICTORIA ISLAND

In the northern interior of Prince Albert Peninsula, Fyles (1963) reported tilted fluvial and/or lacustrine sand and silt comprising multiple ice-thrust moraine ridges (Fig. 3.7). These ridges lack a continuous till cover but display boulder erratics. Nearby, faint flutings and drumlinoid landforms comprise a northwest-trending flow-set (Flow-set 5 on Figs. 3.2 and 3.7), which is at right angles to the moraines. Additional, similarly oriented flow-sets, comprising streamlined subglacial bedforms of varying morphology, occur near Walker Bay (Flow-sets 4 and 6 on Figs. 3.2 and 3.7) and Richard Collinson Inlet (Flow-sets 1, 2, and 3 on Fig. 3.2). Apart from the few moraines and mapped flow-sets, proglacial and ice-lateral meltwater channels dominate the interior of Prince Albert Peninsula.

A contiguous moraine belt, similar in character to the Jesse till, is situated on the west coast of Prince Albert Peninsula (Fig. 3.7), overlying Ordovician-Silurian carbonate bedrock (Fig. 3.1). Originally described by Fyles (1962, 1963), the moraine belt constitutes large areas of broad, ice-cored moraines, with widespread coast-parallel ridges traceable for up to 130 km. Between Walker Bay and Armstrong Point (Fig. 3.7) nested moraines at elevations of up to 250–300 m asl are composed of loamy till and occur in close association with numerous, steep-walled kettle lakes. Along the coast at lower elevations, a single, prominent moraine of stony till, approximately 5–10 m high and 300 m wide, can be traced continuously for about 130 km. North of Deans Dundas Bay, subglacial streamlined bedforms comprise a flow-set trending northeast (Flow-set 7; Figs. 3.2 and 3.7), which is bounded to the northeast by ice-cored moraines and hummocky terrain. Between Armstrong Point and Peel Point the moraine belt is characterized by a single, broad moraine at 50–100 m asl, which is separated from adjacent higher terrain by a deeply-incised, ice-lateral meltwater channel. This moraine and its associated meltwater channels clearly resemble landforms on adjacent northeast Banks Island. The coastal moraine belt is associated with a series of ice-lateral meltwater channels that terminate at ice-contact deltas. These deltas mark marine limit and reach elevations of about 85 m asl near Peel Point in the north (Hodgson, 1994) and 56 m asl near Berkeley Point in the south (A.S. Dyke, pers. comm., 2011; Fig. 3.7).

Distal to the coastal moraine belt are several proglacial meltwater channels that traverse the interior of Prince Albert Peninsula, crosscutting older moraines and drumlins (Fig. 3.7). These channels, together with mapped ice-lateral meltwater channels document ice-free terrain in the interior upland of the peninsula. Importantly, these landforms allow the identification of correlative deposits on the peninsula. For example, a prominent, proglacial channel draining inland from the coastal moraine belt near Deans Dundas Bay flows to the northeast, where it becomes an ice-lateral meltwater channel constrained by nested lateral moraines on the west side of Richard Collinson Inlet that continue along the coast to Peel Point (Fig. 3.7). The moraines occur in association with high abundances of basaltic erratics south and east of Richard Collinson Inlet (Fyles, 1963). In addition, the moraines lie adjacent to two large flow-sets near the head of the inlet (Flow-sets 8 and 9; Figs. 3.2 and 3.7). Previously mapped and characterized in detail by Fyles (1963) and Stokes et al. (2009), these flow-sets constitute assemblages of highly elongated flutings and drumlins with convergent onset zones, and similarly oriented eskers near their termini. Although the flow-sets demonstrably differ in age (i.e. flow-set 8 is truncated by flow-set 9 and is, thus, older) they record similar ice-flow trajectories.

CHRONOLOGY

Maximum-limiting ages are currently unavailable to constrain the timing of ice sheet retreat from north-central Banks Island. For example, no fossil molluscs have been collected west of Castel Bay, possibly because ice retreat there predated the reestablishment of molluscan fauna following the late-glacial submergence of Bering Strait (Kaufman et al., 2004; England and Furze, 2008; England et al., 2009). Widespread minimum-limiting radiocarbon ages are available, however, which also closely approximate the timing of subsequent ice sheet withdrawal from the north-central interior. Large, thin-walled fragments of *Hiatella arctica* collected from an ice-contact delta near the mouth of the Thomsen River are 13,425–13,845 cal yrs old (UCI-60257; Fig. 3.12 and Table 3.1) and provide a minimum-limiting age for deglaciation of Castel Bay. Eight similar ages, including two dates of 13,250–13,795 cal yr BP from *Cyrtodaria kurriana* (TO-12496) and 13,275–13,695 cal yr BP from *H. arctica* (UCI-24794), are available from Mercy Bay (England and Furze, 2008; England et al., 2009; Fig. 3.12 and Table 3.1). Collectively, the ages indicate ice sheet retreat from the north-central coast as early as about 13.75 cal ka BP (Fig. 3.12).

Maximum-limiting radiocarbon ages for the Jesse till are provided by fossil mollusc fragments collected from the surface of the till and by fragments redeposited from glacier ice or till in glaciofluvial, glaciolacustrine, and glaciomarine sediments, including foresets and gravel surface lags of marine limit deltas (Table 3.1). The ages of all these redeposited fragments span approximately 36 to >50 cal ka BP (Table 3.2). The most closely-limiting maximum age for the Jesse till, however, comes from Castel and Mercy bays, which, based on observations of the pattern of ice sheet retreat, became ice-free prior to deposition of the Jesse till. Thus, the Jesse till was deposited after 13.75 cal ka BP.

Fossil-bearing, ice-contact deltas and postglacial marine sediments on the east and west shores of Prince of Wales Strait provide consistent minimum-limiting ages for deposition of the Jesse till and the coastal moraine belt on Prince Albert Peninsula. Dated samples, including both *H. arctica* and *C. kurriana*, were collected from sites distributed along the full length of the strait (Fig. 3.12). On Banks Island, a suite of older ages have calibrated 2-sigma probability distributions between 12.5 and 13.0 cal ka BP, indicating isochronous ice sheet withdrawal from eastern Banks Island into Prince of Wales Strait by about 12.75 cal ka BP (Fig. 3.12). Two ages of 13,145–13,520 cal yr BP (UCI-50753) and 12,705–13,190 cal ka BP (UCI-60268) from *C. kurriana* and *Portlandia arctica*, respectively, are anomalously old (Fig. 3.12 and Table 3.1). If correct, they may record an early ice-free interval prior to or during deposition of the Jesse till. However, the validity of these two outliers is doubtful as they contradict the large number of consistent ages. *P. arctica* has been demonstrated to provide exaggerated ages due to the uptake of old carbon in carbonate terrains (Dyke et al., 2002; England et al., 2004, 2012). No similar problem has been demonstrated for *C. kurriana* (England and Furze, 2008; England et al., 2009).

On northern Prince Albert Peninsula, three radiocarbon ages for samples of *H. arctica* collected from raised marine sediments on the proximal side of the left-lateral moraines exiting Richard Collinson Inlet, span 12,675–13,150 cal ka BP (GSC-3366, GSC-4224, and GSC-4248; Figs. 3.7 and 3.13 and Table 3.1). The moraines in Richard Collinson Inlet clearly relate to the formation of Flow-set 8 and thus the ages not only provide a minimum-limiting age for the moraines but Flow-sets 8 to 12 as well (Fig. 3.2). As a result, deglaciation of Richard Collinson Inlet was underway by about 12.9 cal ka BP (Fig. 3.13), making it coeval with ice retreat from Prince of Wales Strait. Farther southwest, three previously published radiocarbon ages are available from the west coast of Prince Albert Peninsula (Fig. 3.13 and Table 3.1; McNeely and Brennan, 2005). Two ages from Deans Dundas Bay and Armstrong Point on *H. arctica* range from 12,250 to 12,785 cal yr BP (GSC-4288 and GSC-3529; Fig. 3.13 and Table 3.1). An older age of 12,605–13,120 cal yr BP (GSC-3376) from unidentified marine shells (*H. arctica*?) is also available from Deans Dundas Bay (Fig. 3.13 and Table 3.1). Three unpublished ages for samples of *H. arctica*, collected by A.S. Dyke (GSC-Ottawa) near Berkeley Point, range from 12,085 to 13,150 cal yr BP and include an age of 12,645–13,150 cal ka BP (Fig. 3.13 and Table 3.1). All six samples from the west coast of Prince Albert Peninsula were collected from marine sediments lying on the proximal (i.e. west) side of the prominent coastal moraine belt and thus, provide minimum-limiting ages for its abandonment. These ages are coeval with the suite of ages from the east coast of Banks Island, which postdate deposition of the Jesse till (Figs. 3.12 and 3.13) and confirm that the full length of Prince of Wales Strait was deglaciated abruptly about 12.75 cal ka BP.

DEGLACIATION OF BANKS ISLAND AND PRINCE OF WALES STRAIT

The geomorphic record and radiocarbon chronology allow the pattern and nature of ice sheet retreat from Banks Island and adjacent Prince Albert Peninsula to be elucidated. Two phases of ice recession are recognized and summarized below.

THOMSEN PHASE

The Thomsen Phase was characterized by the general southeastward retreat of the LIS from north-central to eastern Banks Island (Fig. 3.14). In the Desert River valley, widespread glaciolacustrine sediments (to 65 m asl; Figs. 3.3 and 3.4) require grounded glacier ice in M'Clure Strait, which impounded meltwater from ice margins retreating inland from Castel Bay. Thus, the minimum-limiting age of ~13.75 cal ka BP from the head of Castel Bay not only closely constrains the timing of ice sheet retreat from Castel Bay, but the withdrawal of glacier ice in M'Clure Strait as well. Fluted till near the head of Castel Bay indicates episodes of basal-sliding during the final phase of local deglaciation, which was characterized by the retreat of a tidewater terminus. Basal-sliding was likely initiated and/or sustained by the glacier's calving margin, which helped facilitate ice sheet drawdown, until it retreated south into the Thomsen River valley, depositing the marine limit delta (37 m asl) ~13.75 cal ka BP.

In Mercy Bay, several lateral moraines are correlative to those in Castel Bay and document an adjacent northward-flowing trunk glacier (England et al., 2009; Fig. 3.3). Following its withdrawal from the head of the bay, this glacier deposited abundant recessional moraines south of Mercy Bay, which contrast markedly with the scant till and moraines in the lowermost Thomsen River valley (Fig. 3.3). This may imply polythermal bed conditions inland of Mercy Bay, while the adjacent glacier terminating in the Thomsen River valley remained cold-based following ~13.75 cal ka BP.

Farther south, glacial landforms imply that ice sheet retreat after ~13.75 cal ka BP was characterized by the general southward recession of a cold-based ice margin (Figs. 3.3 and 3.14). Abundant ice-lateral meltwater channels, incised into the underlying bedrock, document initial eastward recession of a thin, arcuate, cold-based ice margin. Ice-thrust moraines near Shoran Lake postdate ice sheet withdrawal from Castel and Mercy bays, and indicate westward flow of a polythermal glacier occupying the central Thomsen River valley, which punctuated widespread recession of a more pervasive cold-based ice margin elsewhere. Similar moraines lying adjacent to the Thomsen River valley farther south and east indicate that this polythermal outlet glacier remained an active component of the retreating northwest LIS across the north-central interior of Banks Island (Figs. 3.3 and 3.14).

Where moraines were not deposited, the pattern of ice sheet retreat along the Thomsen River valley is marked by abundant ice-lateral and proglacial meltwater channels, outwash fans, kame terraces, and glaciolacustrine deposits (Figs. 3.3 and 3.14). The final phase of ice retreat from the Thomsen River valley is documented by extensive, rhythmically-bedded silt 20 km south of Green Cabin. These sediments were previously noted by Vincent (1982, 1983), who used them to justify the former existence of a large (~100 km), proglacial lake (Lake Ivitaruk) inundating the Thomsen River valley. Despite exhaustive field surveys, we found no sedimentary or geomorphic evidence for a former proglacial lake of this size. Instead, we infer that these sediments accumulated in a deglacial lake dammed by ice flowing into the Thomsen valley via several eastern tributaries. These small, cold-based lobes were the last glaciers to occupy the Thomsen River valley (Fig.

3.14). Following deglaciation of the valley, the extensive, sandy, outwash terraces, deposited during previous glacier retreat, were abandoned and incised as relative sea level fell, due to glacioisostatic emergence of the island. At the same time, the valleys draining west to the Beaufort Sea served as conduits for meltwater and outwash, as the ice sheet retreated farther east.

In the upland interior of Prince Albert Peninsula, the deformation of fluvial/lacustrine sediments and the formation of a faint, northwest-trending flow-set (Flow-set 5 on Figs. 3.2 and 3.7) are clear examples of glaciotectonism and basal-sliding, respectively. Flow-set 5, despite its faint geomorphic character, is unique on Prince Albert Peninsula and, therefore, may result from local surging, ice streaming, or simply fast-flow. The flow-set, as noted by Fyles (1963), predates deposition of the coastal moraine belt on Prince Albert Peninsula and, thus, records the final phase of westward ice-flow over the peninsula. As such, it relates to the general southeastward recession of the LIS from north-central Banks Island (Fig. 3.14). Flow-sets farther east (Flow-sets 1, 2, and 3; Fig. 3.2) may record a correlative phase of ice-flow, possibly initiated or sustained by the loss of grounded ice in M'Clure Strait. Hypotheses regarding their age, however, remain essentially untestable because they are not clearly related to dateable (i.e. fossiliferous) deglacial sediments.

PRINCE OF WALES PHASE

The Prince of Wales Phase was characterized by a regional readvance or stillstand of the northwest LIS, resulting in the deposition of the Jesse till on eastern Banks Island and the coastal moraine belt on Prince Albert Peninsula. The nearly identical geomorphic character of these moraine belts clearly demonstrates that they share a common origin. This is further demonstrated by their concordant minimum-limiting radiocarbon ages, indicating a preceding interval of widespread moraine deposition (Fig. 3.14). As a result, we propose that the deposit be referred to, hereafter, as *the Jesse moraine belt*.

The Jesse moraine belt outlines a late-glacial ice lobe that occupied Prince of Wales Strait, terminating in M'Clure Strait as a tidewater trunk glacier (Fig. 3.14). The thick drift (~1–2m) and the greater abundance of erratics and moraines compared to immediately distal sites document a substantial change in the dynamics of the northwest LIS. The conspicuous increase in the concentration of mafic erratics compared to distal glacial sediments requires an ice-flow trajectory across the Shaler Mountains, where Neoproterozoic basalt and gabbro comprises the Minto Inlier on Victoria Island (Fig. 3.1). This trajectory was arcuate in shape, flowing initially to the northwest across the Shaler Mountains and then northeast along the axis of Prince of Wales Strait. Components of onshore flow onto Banks and Victoria islands were also present in Prince of Wales Strait. For example, the moraines marking the limits of the Jesse moraine belt on eastern Banks Island and western Prince Albert Strait, between the southern boundary of the study area and approximately 73° N, record northwestward and southeastward ice-flow from the lobe, respectively (Fig. 3.7).

There are no clear examples of crosscutting relationships along the margin of the Jesse moraine belt (Fig. 3.9). Instead, their contact is commonly obscured by outwash emanating from proglacial and ice-lateral meltwater channels relating to deposition of the moraine belt. Similarly, the eastern boundary of the Jesse moraine belt on Prince Albert Peninsula is poorly characterized. Consequently, it remains equivocal whether the moraine belt is the product of a regional readvance or stillstand.

Kettle lakes, debris-rich ground ice, and sub-parallel, arcuate end moraines, all occurring in association with widespread ice-lateral meltwater channels (Fig. 3.10) suggest that the Jesse moraine belt is the product of controlled moraine deposition by a polythermal glacier in Prince of Wales Strait (Dyke and Evans, 2003; Evans, 2009). Controlled moraines originated as debris bands, produced by debris entrainment processes (i.e. net adfreezing) associated with ice-flow from areas of extensive warm-based bed conditions to narrow marginal zones that were frozen to the bed, in contact with permafrost (Evans, 2009). Ice-thrusting of frozen sediments in the cold-based marginal zone may have also delivered debris to the surface. In this case, it seems likely that ice-thrusting was augmented by ice-flow against the reverse slopes of the northwest and southeast shores of Prince of Wales Strait. Downwasting of the ice sheet margin concentrated debris on the glacier surface, masking underlying glacier ice that was subsequently abandoned by ice sheet retreat via differential ablation. Ice-lateral meltwater channels provide widespread evidence for a cold-based ice margin, whereas isolated occurrences of subglacial streamlined bedforms within the limits of the Jesse moraine belt (Flow-sets 6 (?), 7, 13–16; Figs. 3.2 and 3.7) indicate warm basal thermal regimes farther up-ice. Furthermore, the thick drift comprising the moraine belt attests to the magnitude of debris delivery to the cold-based ice margin from adjacent warm-based zones (Dyke and Evans, 2003). Thus, abandonment of the debris-covered ice cores and deposition of moraines followed incremental retreat of a polythermal glacier (Fig. 3.14).

In the northern part of the study area, the character of the Jesse moraine belt adjacent to the northeast Devonian Plateau on Banks Island records a distinct mode of deposition. Here, linear, ice-lateral meltwater channels abutting the plateau are the dominant landform and record northward meltwater drainage to M'Clure Strait (Fig. 3.7). Few moraines are present and the absence of kettle lakes, suggests little buried ice. Similarly, the Jesse moraine belt on Prince Albert Peninsula is characterized by fewer kettle lakes and end moraines and by more landscape dissection by ice-lateral meltwater channels (Fig. 3.7). Thus, northern Prince of Wales Strait was likely characterized by landscape incision along the edges of a stable, cold-based ice margin that likely comprised part of the terminus of the trunk glacier in Prince of Wales Strait (Fig. 3.14). This contrasts with controlled moraine deposition that was the dominant ice-marginal process farther south (Fig. 3.7).

The Jesse moraine belt on Prince Albert Peninsula occurs in association with flow-sets 8 and 9 at the head of Richard Collinson Inlet (Fig. 3.7). These flow-sets are composed of highly elongated lineations with convergent onset zones, indicating the presence of two former ice streams that exited Richard Collinson Inlet, as recognized by Stokes et al. (2005, 2009). Mapped geomorphic relationships between the flow-sets and adjacent moraines and meltwater channels across the peninsula confirm that ice streaming in Richard Collinson Inlet was coeval with ice-free conditions in the upland areas of Prince Albert Peninsula and controlled moraine deposition along Prince of Wales Strait (Fig. 3.14).

Along the northern third of Prince of Wales Strait, the lowest and youngest coast-parallel moraines record a readvance or stillstand prior to final ice retreat (Fig. 3.7). Ice-contact channels and deltas crosscutting the moraines demonstrate that ice sheet retreat proceeded from northeast to southwest, along the axis of Prince of Wales Strait (Fig. 3.14). The rate of retreat was rapid, perhaps occurring in less than a century, as it cannot be resolved in the radiocarbon chronology (Figs. 3.12 and 3.13).

South of approximately 73° N, following deposition of the controlled moraines, the ice lobe in Prince of Wales Strait thinned and narrowed, causing ice margins on eastern Banks Island and western Prince Albert Peninsula to retreat eastwards and westwards, respectively (Fig. 3.14). On Banks Island, this withdrawal dammed proglacial lakes in many east coast valleys (Fig. 3.7). Abundant high-elevation kame terraces (Fig. 3.7) document meltwater drainage into these lakes and delineate a digitate, cold-based ice margin (Fig. 3.14). Discontinuous kame terraces at lower elevations (Fig. 3.7) outline the wastage of the ice margin as it thinned and retreated downslope to the southeast in contact with multiple ice-dammed lakes, recorded by beaches, deltas and kame deltas (Fig. 3.14). The expanse and continuity of the kame terraces suggests that the ice margins remained stable for years to decades, implying that recession of the ice front was intermittent. However, few moraines occur in association with the kames suggesting that ice sheet retreat was not punctuated by intervals of positive net mass balance, perhaps a result of significant ice loss via calving into proglacial lakes and northern Prince of Wales Strait. The final stages of ice withdrawal are recorded by small, sinuous moraines, ice-lateral meltwater channels, and kames that occur discontinuously along the coast (Fig. 3.7), delineating multiple, sub-linear ice margins (Fig. 3.14). These landforms are likely the product of small-scale readvances by thin or floating ice that responded to rapid changes in its margin and concomitant reorganizations of ice-flow prior to final collapse of the glacier in Prince of Wales Strait at about 12.75 cal ka BP.

Controlled moraine deposition along the axis of Prince of Wales Strait and ice streaming in Richard Collinson Inlet occurred between ~13.75 and 12.75 cal ka BP. The cessation of ice streaming in Richard Collinson Inlet, recorded by Flow-sets 8 and 9, was occurring, if not complete, by about 12.9 cal ka BP (Fig. 3.13) when ice streams, represented by younger flow-sets (Flow-sets 11 and 12) were active farther south. By approximately 12.75 cal ka BP, all of Prince of Wales Strait was ice-free (Figs. 3.12 and 3.13). Geomorphic relationships confirm that ice retreat in Prince of Wales Strait proceeded from north to south; however, the rate of this retreat is currently unresolvable because the calibrated radiocarbon ages overlap significantly (Figs. 3.12 and 3.13). Nevertheless, calibrated age ranges do not normally exceed 500 years, suggesting that final deglaciaton of Prince of Wales Strait occurred within that timespan. Furthermore, geomorphic observations indicating the former presence of one or more deglacial ice shelves, may suggest that final deglaciation occurred over an even shorter interval if they collapsed catastrophically. This scenario demonstrates the utility of detailed geomorphic mapping in characterizing ice-marginal fluctuations that occurred over decadel- to centennial-timescales and are, hence, unresolvable by current radiocarbon dating applied to latest Pleistocene deposits.

DISCUSSION

ICE SHEET DYNAMICS

This new reconstruction constrains the age of the formerly proposed Baker and Jesse tills to an approximately thousand-year interval, between 13.75 and 12.75 cal ka BP. As a result, the thin drift designated as *the Baker Till* and the moraine belt designated as *the Jesse Till* were each deposited over several centuries at most. This contrasts markedly with previous interpretations that attributed them to separate glaciations (Fyles, 1962, 1963; Vincent, 1982, 1983; Dyke, 1987).

Changes in the geometry and dynamics of the northwest LIS on northern Banks Island and northwestern Victoria Island are well documented for the period 13.75 to 12.75 cal ka BP (Fig. 3.14). During the Thomsen Phase, following initial withdrawal from Castel and Mercy bays ~13.75 cal ka BP, the northwest LIS was characterized by eastward recession of a predominantly cold-based margin to the east coast of Banks Island (Fig. 3.15). Deposition of ice-thrust moraines was limited in extent but, nonetheless, occurred, likely as a result of polythermal bed conditions where topography favoured sustained, convergent ice-flow. The termination of the Thomsen Phase was marked by the continued ablation of thin, cold-based ice and the cessation of westward ice-flow across Prince of Wales Strait as the interior upland of Prince Albert Peninsula became ice-free (Fig. 3.15).

The Prince of Wales Phase records the oldest documented, regional readvance or stillstand of the northwest LIS during the late-glacial. Examining the age and morphology of the Jesse moraine belt and its relationship to adjacent glacial landforms provides important insights into the dynamic behavior of the northwest

LIS. Most notably, widespread controlled moraines record the expansion of warm-based ice in Prince of Wales Strait after 13.75 cal ka BP and its interaction with adjacent cold-based ice margins. A deglacial age of ~12.9 cal ka BP from Richard Collinson Inlet implies that thinning over the Shaler Mountains by this time was sufficient to cause a significant reduction in northward ice-flow and thus the deglaciation of Richard Collinson Inlet (Fig. 3.15). Consequently, it is inferred that deglaciation of northern Prince of Wales Strait began around this time. Therefore, the dynamical parameters, which occasioned deposition of the Jesse moraine belt, coincided with the Bølling–Allerød chronozone, clearly predating the Younger Dryas (Figs. 3.12, 3.13, and 3.15).

Changes in the dynamics of the northwest LIS recorded by the deposition of the Jesse moraine belt coincided with a reorganization of regional ice-flow trajectories. This reorganization was characterized by the cessation of westward ice-flow across Prince of Wales Strait and the initiation of northward ice-flow along the strait, which was coeval with ice streaming in Richard Collinson Inlet. These changes in the pattern and nature of ice-flow unequivocally postdate the evacuation of grounded ice in M'Clure Strait, which is documented by several radiocarbon ages older than ~13.5 cal ka BP from southwest Melville, northern Banks, and northern Victoria islands (Fig. 3.15; McNeely and Brennan, 2005; England et al., 2009).

The withdrawal of the northwest LIS from M'Clure Strait was rapid, retreating ~350 km in less than 400 calibrated years (England et al., 2009; Figs. 3.12, 3.13, and 3.15a, b). This retreat involved an enormous calving margin that proceeded eastwards into Viscount Melville Sound. Enhanced ice sheet mass loss via this calving would have increased the topographic channeling of ice-flow in the northwest sector of the LIS, leading to the rapid drawdown of ice over Victoria Island. Indeed, this drawdown likely resulted in the development of a deglacial ice divide over the Shaler Mountains, which sustained ice-flow through nearby marine channels and bays during this interval. A late-glacial ice divide in the Shaler Mountains was originally proposed by Stokes et al. (2006, 2009) based on the geometry of ice stream flow-sets on western Victoria Island, including those at the head of Richard Collinson Inlet. The relative abundance of mafic erratics within the Jesse moraine belt provides direct evidence for an ice-flow trajectory from the Shaler Mountains where permanent or intermittent warm-based bed conditions must have existed. Northward ice-flow through Prince of Wales Strait also may have been augmented by thick, grounded ice in northeast Amundsen Gulf, which had yet to become ice-free (Fig. 3.15; Dyke et al., 2003b). Thus, in addition to an ameliorating climate, topographic channeling and associated strain heating, perhaps triggered by enhanced mass loss via calving, may account for the expansion of a warm-based thermal regime in the northwest LIS following ~13.75 cal ka BP.

On the adjacent Arctic mainland, near Bluenose Lake on the eastern flank of the Brock Plateau (Fig. 3.1), widespread areas of ice-cored, controlled moraine record a period of slow retreat by grounded ice in Amundsen Gulf, punctuated by small readvances (St.-Onge and McMartin, 1995, 1999). These deposits occur in association with ice stream flow-sets situated immediately to the east (i.e. up-ice; St.-Onge and McMartin, 1995; Dyke et al., 2003b) and are tentatively correlated to the Jesse moraine belt based on the available chronology. A basal radiocarbon age of 13,050–13,480 cal yr BP (AA50868; Figs. 3.13 and 3.15; Table 3.1) from a sediment core from "South Lake", immediately west (i.e. distal) of the Bluenose

Lake moraines, provides a closely-limiting age for the deposit (Rühland et al., 2009). An additional age of 12,570–12,965 cal yr BP (GSC-4757; Figs. 3.13 and 3.15; Table 3.1) near Paulatuk delimits the timing of ice retreat from Darnley Bay and, thus, moraine deposition near Bluenose Lake (Kerr, 1996; Dyke et al., 2003a; McNeely and Brennan, 2005). GSC-4757 is a reanalysis of a previous age determination of 12,615–13,250 cal yr BP (AECV-643Cc; Table 3.1), which is slightly older but nonetheless overlaps significantly with GSC-4757. Should this tentative correlation between the Jesse moraine belt and the Bluenose Lake moraines prove to be correct, it would indicate a period of regional controlled moraine deposition along the terrestrial margin of the northwest LIS.

Rapid ice sheet withdrawal from Prince of Wales Strait coincided with deglaciation of eastern Amundsen Gulf approximately 12.75 cal ka BP (Fig. 3.15). The oldest deglacial radiocarbon age from southwest Victoria Island is 12,540–12,915 cal yr BP (AA-46720; Figs. 3.13; Table 3.1) from outer Diamond Jenness Peninsula and is similar to two ages from outer Wollaston Peninsula of 12,525–12,920 cal yr BP (GSC-6286) and 12,530–12,910 cal yr BP (GSC-6288; Dyke and Savelle, 2000; Dyke et al., 2003b; Figs. 3.13; Table 3.1). These ages overlap with those from Prince of Wales Strait and Darnley Bay (Fig. 3.13), rendering the rate of ice sheet retreat from eastern Amundsen Gulf unresolvable in the existing chronology. Nevertheless, the ice sheet margin reached western Victoria Island shortly after ~12.75 cal ka BP. The abrupt, regional abandonment of the Jesse moraine belt at ~12.75 cal ka BP and the contemporaneous withdrawal of the northwest LIS from eastern Amundsen Gulf involved the loss of at least 45,000 km^2 of ice. This rapid retreat was likely facilitated by widespread calving in eastern

Amundsen Gulf, which widens eastward. This geometry would have forced the calving margin to widen as it moved eastwards, inducing a positive feedback that ultimately augmented ice sheet retreat to Victoria Island (Stokes et al., 2006).

Following ~12.75 cal ka BP, the northwest LIS persisted in bays and channels along southwestern Victoria Island for the duration of the Younger Dryas chronozone (Dyke and Savelle, 2000; Dyke et al., 2003b; Hodgson and Dyke, 2005). Stabilization of the ice sheet margin is manifested in the form of widespread controlled moraines as well as numerous lateral moraines displaying abundant cross-cutting relationships. In addition, the local deglacial chronology spans approximately 1000 years, from ~12.5 cal ka BP to ~11.7 cal ka BP. On this basis, Dyke and Savelle (2000), Dyke et al. (2003b), and Hodgson and Dyke (2005) proposed a diminished rate of ice retreat for this interval, compared to relatively rapid retreat during the preceding Bølling–Allerød chronozone. Widespread field mapping and a significantly expanded deglacial chronology throughout the western CAA (England et al., 2009; Nixon, 2012; this paper) strengthens their conclusion, which, until recently suffered from a paucity of detailed geomorphological data and sparse deglacial chronologies from the region.

IMPLICATIONS OF CONTROLLED MORAINE DEPOSITION

Like the Jesse moraine belt, controlled moraine deposition on Wollaston Peninsula and at Bluenose Lake followed rapid, ice sheet withdrawal from adjacent marine channels. This commonality suggests that changing ice dynamics, induced by a preceding interval of rapid retreat, favoured widespread controlled moraine deposition. Because, controlled moraines are an indicator of polythermal bed conditions, their widespread occurrence in the western Canadian Arctic indicates the general expansion of a warm-based thermal regime in the northwest LIS during the last deglaciation (Dyke and Evans, 2003). If this hypothesis is correct, then the paleoclimatic significance of these moraine belts is diminished, especially in the absence of local, independent paleoclimatic archives. For example, the Jesse moraine belt and the Bluenose Lake moraine complex were deposited during the Bølling–Allerød chronozone, when local climate may have been in phase with general warming of the northern hemisphere. In contrast, the controlled moraines on Wollaston Peninsula coincide with the Younger Dryas chronozone when the climate of the northern hemisphere deteriorated into full-glacial conditions. This apparent discrepancy suggests that paleoclimate was not the primary mechanism triggering the deposition of these controlled moraines. However, given that the Jesse moraine belt was deposited over the course of a few centuries and the moraines on Wollaston Peninsula over a thousand years, it could be reasoned that a cooler climate, of sufficient duration to overcome inherent ice sheet lag times, was conducive to ongoing controlled moraine deposition.

Future attempts to evaluate the relative importance of paleoclimate to the deposition of controlled moraines in the western Canadian Arctic must necessarily involve new, independent paleoclimatic records. Presently, no independent paleoclimatic archives extending back to 14–12 cal ka BP are available from the western CAA. For example, a lacustrine-derived pollen record from southern Melville Island approaching this interval terminates at ~12 cal ka BP (Peros et al., 2010). This record suggests cool, dry environmental conditions during the latest Pleistocene; however, the quality and chronological resolution of their archive is insufficient to test hypotheses regarding environmental change during the Bølling–

Allerød and Younger Dryas chronozones (Peros et al., 2010). In the absence of suitable paleoclimatic archives, the local nature of late-glacial climate changes and their efficacy in effecting rates of ice sheet retreat in the Canadian Arctic remains speculative.

A consideration of the primary mechanisms responsible for instigating widespread deposition of controlled moraines along terrestrial margins of the northwest LIS must also include latest Pleistocene relative sea level change. For example, expansion of warm-based thermal regimes and deposition of controlled moraines may also have been occasioned by intervals of relative sea level rise, capable of instigating short episodes of significant marine-based glacier retreat. Associated, rapid retreat of ice sheet grounding lines, potentially augmented by the loss of buttressing ice shelves and/or sea ice, would have triggered faster ice velocities, increased strain heating, and topographic channeling as a means to re-equilibrate regional ice divides with rapidly changing ice sheet margins and surface gradients (i.e. Rignot, 1998; Shepherd et al., 2002; De Angelis and Skvarca, 2003; Payne et al., 2004; Thomas et al., 2004; Stokes et al., 2009; Wingham et al., 2009). These processes appear to be the most effective mechanisms for initiating the expansion of a warm-based thermal regime throughout the northwest LIS and, thus, abrupt deposition of controlled moraines from the Arctic Mainland to northern Banks Island. Perhaps most intriguing is meltwater pulse 1a (ca. 14.6 cal ka BP; Fairbanks, 1989; Clark et al., 2002; Peltier, 2005; Deschamps et al., 2012), which, although a feature of the latest Pleistocene eustatic sea level curve, may have been regionally manifested in such a way as to initiate the broad-scale ice sheet retreat in M'Clure Strait and western Amundsen Gulf. Alternatively, this phase of ice sheet retreat may have contributed to that period of enhanced eustatic sea level rise. These correlations, however, remain speculative and warrant future investigations.

TIMING OF ICE STREAM ACTIVITY

This is the first study to closely constrain the ages of several former ice streams in the western CAA. Previous attempts by Stokes et al. (2009) to estimate the timing of multiple ice streaming events in the northwest LIS remain partly speculative as their chronology is based on regional ice sheet reconstructions by Dyke (2004) and Dyke et al. (2003a), which have little to no chronological basis in the western CAA beyond ~12.5 cal ka BP. Furthermore, as Dyke et al. (1992) noted, ice stream flow-sets are generally not dateable because they remained covered by ice when they were active. The abundant new ages presented in this study extend the regional deglacial chronology to 13.75 cal ka BP and, together, with new geomorphic mapping constitute a unique opportunity to determine the age of ice streaming events for the northwest LIS. For example, observed geomorphic relationships among controlled moraines, meltwater channels, lateral moraines, and drumlins and flutings on Prince Albert Peninsula demonstrate that this assemblage of subglacial and ice-lateral landforms is contemporaneous. Therefore, age determinations for ice-lateral landforms (i.e. lateral moraines and ice-lateral meltwater channels) necessarily closely constrain the age of adjacent subglacial bedforms (i.e. ice stream flow-sets). The available chronology provides a minimum-limiting age of 12.9 cal ka BP for the cessation of ice streaming in Richard Collinson Inlet and, thus, ice stream flow-sets 8 and 9 (Figs. 3.7 and 3.14). As a corollary, adjacent flow-sets 10, 11, and 12; Figs. 3.7 and 3.14) must relate to phases of deglaciation following 12.9 cal ka BP.

CONCLUSIONS

New radiocarbon dates bearing on the age of mapped deglacial landforms on Banks Island and western Victoria Island outline the geometry and dynamics of the northwest LIS from approximately 13.75 cal ka BP to 12.75 cal ka BP. This new, regional reconstruction documents changes in ice-marginal depositional processes, providing new perspectives on ice sheet responses to late-glacial climate, relative sea level, and rapidly changing ice sheet geometry (among other variables). Results of this study confirm that the Jesse moraine belt is the product of a regional change in ice-marginal processes along the retreating northwest LIS. This involved the transition from a predominantly cold-based thermal regime, where landscape modification was dominated by short-lived, glacial meltwater streams, to polythermal bed conditions, conducive to widespread deposition of controlled moraines, sharp-crested lateral moraines, and ice stream bedforms. Initial abandonment of the Jesse moraine belt occurred approximately 12.9 cal ka BP, making its deposition coeval with the end of the Bølling–Allerød chronozone. The role of paleoclimate in triggering the documented changes in ice dynamics remains uncertain because independent and quantifiable paleoclimatic archives for this period are currently unavailable from the western CAA. Ice sheet withdrawal from M'Clure Strait and western Amundsen Gulf preceded deposition of the Jesse moraine belt and correlative controlled moraines on the Arctic Mainland (Bluenose Lake), as well as younger moraines on southwest Victoria Island (Wollaston Peninsula). This coincidence strongly suggests a causal relationship, whereby rapid ice sheet withdrawal from the major marine channels of the western CAA induced an expansion of warm-based thermal regimes in the northwest LIS. Such hypotheses will likely be advanced further through regional numerical modeling studies of the dynamics of the late-glacial northwest LIS and its sensitivity to climate, sea level change and changing ice sheet geometries.

REFERENCES

Atkinson, N., 2003. Late Wisconsinan glaciation of Amund and Ellef Ringnes islands, Nunavut: evidence for the configuration, dynamics and deglacial chronology of the northwest sector of the Innuitian Ice Sheet. Canadian Journal of Earth Sciences 40, 351–363. doi:10.1139/e02-106.

Bentley, M.J., 2010. The Antarctic palaeo record and its role in improving predictions of future Antarctic Ice Sheet change. Journal of Quaternary Science 25, 5–18. doi:10.1002/jqs.1287.

Clark, P.U., Mitrovica, J.X., Milne, G.A., Tamisiea, M.E., 2002. Sea level finger printing as a direct test for the source of global melwater pulse 1a. Science 295, 2438–2441. doi:10.1126/science.1068797.

Coulthard, R.D., Furze, M.F.A., Pienkowski, A.J., Nixon, F.C., England, J.H., 2010. New marine DR values for Arctic Canada. Quaternary Geochronology 5, 419–434. doi:10.1016/j.quageo.2010.03.002.

De Angelis, H., Kleman, J., 2005. Palaeo-ice streams in the northern Keewatin sector of the Laurentide Ice Sheet. Annals of Glaciology 42, 135–144. doi:10.3189/172756405781812925.

De Angelis, H., Kleman, J., 2007. Palaeo-ice streams in the Foxe/Baffin sector of the Laurentide Ice Sheet. Quaternary Science Reviews 26, 1313–1331. doi:10.1016/j.quascirev.2007.02.010.

De Angelis, H., Skvarca, P., 2003. Glacier surge after ice shelf collapse. Science 299, 1560–1562. doi:10.1126/science.1077987.

Deschamps, P., Durand, N., Bard, E., Hamelin, B., Camoin, G., Thomas, A.L., Henderson, G.M., Okuno, J., Yokoyama, Y., 2012. Ice-sheet collapse and sea-level rise at the Bolling warming 14,600 years ago. Nature 483, 559–564. doi:10.1038/nature10902.

Dyke, A.S., Evans, D.J.A., 2003. Ice-marginal terrestrial landsystems: northern Laurentide and Innuitian ice sheet margins. In: Evans, D.J.A. (Ed.), Glacial Landsystems. Arnold, London, pp. 143–165.

Dyke, A.S., Prest, V.K., 1987. Late Wisconsinan and Holocene history of the Laurentide Ice Sheet. Géographie physique et Quaternaire 41, 237–263.

Dyke, A.S., Savelle, J.M., 2000. Major end moraines of Younger Dryas age on Wollaston Peninsula, Victoria Island, Canadian Arctic: implications for paleoclimate and for formation of hummocky moraine. Canadian Journal of Earth Sciences 37, 601–619. doi:10.1139/e99-118.

Dyke, A.S., Morris, T.F., Green, D.E.C., England, J., 1992. Quaternary Geology of Prince of Wales Island, Arctic Canada. In: Geological Survey of Canada, Memoir 433.

Dyke, A.S., Andrews, J.T., Clark, P.U., England, J.H., Miller, G.H., Shaw, J., Veillette, J.J., 2002. The Laurentide and Innuitian Ice Sheets during the Last Glacial Maximum. Quaternary Science Reviews 21, 9–31. doi:10.1016/S0277-3791(01)00095-6.

Dyke, A.S., Moore, A., Robertson, L., 2003a. Deglaciation of North America. Geological Survey of Canada. Open File 1574.

Dyke, A.S., St.-Onge, D.A., Savelle, J.M., 2003b. Deglaciation of Southwestern Victoria Island and Adjacent Arctic Mainland, Nunavut-Northwest Territories. Geological Survey of Canada. Map 2027A, scale 1:500,000.

Dyke, A.S., 1987. A reinterpretation of glacial and marine limits around the northwestern Laurentide Ice Sheet. Canadian Journal of Earth Sciences 24, 591–601. doi:10.1139/e87-058.

Dyke, A.S., 1999. The Last Glacial Maximum and the deglaciation of Devon Island: support for an Innuitian Ice Sheet. Quaternary Science Reviews 18, 393–420. doi:10.1016/S0277-3791(98)00005-5.

Dyke, A.S., 2004. An outline of North American deglaciation with emphasis on central and northern Canada. In: Ehlers, J. (Ed.), Extent and Chronology of Quaternary Glaciation. Elsevier.

England, J.H., Furze, M.F.A., 2008. New evidence from the western Canadian Arctic Archipelago for the resubmergence of Bering Strait. Quaternary Research 70, 60–67. doi:10.1016/j.yqres.2008.03.001.

England, J.H., Atkinson, N., Dyke, A.S., Evans, D.J.A., Zreda, M., 2004. Late Wisconsinan buildup and wastage of the Innuitian Ice Sheet across southern Ellesmere Island, Nunavut. Canadian Journal of Earth Sciences 41, 39–61. doi:10.1139/E03-082.

England, J.H., Atkinson, H., Bednarski, J., Dyke, A.S., Hodgson, D.A., O Cofaigh, C., 2006. The Innuitian Ice Sheet: configuration, dynamics and chronology. Quaternary Science Reviews 25, 689–703. doi:10.1016/j.quascirev.2005.08.007.

England, J.H., Furze, M.F.A., Doupé, J.P., 2009. Revision of the NW Laurentide Ice Sheet: implications for the paleoclimate, the northeast extremity of Beringia, and Arctic Ocean sedimentation. Quaternary Science Reviews 28, 1573–1596. doi:10.1016/j.quascirev.2009.04.006.

England, J.H., Dyke, A.S., Coulthard, R.D., McNeely, R., Aitken, A. 2012. The exaggerated radiometric age of deposit-feeding molluscs in calcareous environments. Boreas. doi:10.1111/j.1502-3885.2012.00256.x.

Evans, D.J.A., 2009. Controlled moraines: origins, characteristics and palaeoglaciological implications. Quaternary Science Reviews 28, 183–208. doi:10.1016/j.quascirev.2008.10.024.

Fairbanks, R.G., 1989. A 17,000-year glacio-eustatic sea level record; influence of glacial melting rates on the Younger Dryas event and deep-ocean circulation. Nature 342, 637–642. doi:10.1038/342637a0.

Fyles, J.G., 1962. Physiography. In: Thorsteinsson, R., Tozer, E.T. (Eds.), Banks, Victoria and Stefansson Islands, Arctic Archipelago. Geological Survey of Canada, Memoir 330, pp. 8–17.

Fyles, J.G., 1963. Surficial Geology of Victoria and Stefansson Islands, District of Franklin. In: Geological Survey of Canada, Bulletin 101.

Hobbs, W.H., 1945. The boundary of the latest glaciation in Arctic Canada. Science 101, 549–551. doi:10.1126/science.101.2631.549.

Hodgson, D.A., Dyke, A.S., 2005. Rapid Allerød and Slow Younger Dryas Deglaciation at the Northwest Margin of the Laurentide Ice Sheet (NW Victoria Island) and Contrasting Ice Regimes. Abstracts. Canadian Quaternary Association, Winnipeg. A35 p.

Hodgson, D.A., Vincent, J.-S., 1984. A 10,000 yr B.P. extensive ice shelf over Viscount Melville Sound, Arctic Canada. Quaternary Research 22, 18–30. doi:10.1016/0033-5894(84)90003-6.

Hodgson, D.A., 1994. Episodic ice streams and ice shelves during retreat of the northwesternmost sector of the late Wisconsinan Laurentide Ice Sheet over the central Canadian Arctic Archipelago. Boreas 23, 14–28. doi:10.1111/j.1502-3885.1994.tb00582.x.

Jenness, J.L., 1952. Problem of glaciation in the western islands of Arctic Canada. Bulletin of the Geological Society of America 63, 939–952. doi:10.1130/0016-7606(1952)63[939:POGITW]2.0.CO;2.

Kaufman, D.S., et al., 2004. Holocene thermal maximum in the western Arctic (0–180°W). Quaternary Science Reviews 23, 529–560. doi:10.1016/j.quascirev.2003.09.007.

Kerr, D.E., 1996. Late Quaternary sea level history in the Paulatuk to Bathurst Inlet area, Northwest Territories. Canadian Journal of Earth Sciences 33, 389–403. doi:10.1139/e96-029.

Lakeman, T.R., England, J.H. The Extent of Late Wisconsinan Ice Cover and the Nature of Postglacial Relative Sea Level Change on Western Banks Island, Canadian Arctic Archipelago, submitted for publication.

Lowdon, J.A., Blake, W., Jr. 1973. Geological Survey of Canada radiocarbon dates XIII. Geological Survey of Canada, Paper 73–7.

Lowdon, J.A., Blake, W., Jr. 1980. Geological Survey of Canada radiocarbon dates XX. Geological Survey of Canada, Paper 80–7.

McNeely, R., McCuaig, S., 1991. Geological Survey of Canada radiocarbon dates XXIX. Geological Survey of Canada, Paper 89–7.

McNeely, R., Jorgensen, P.K., 1992. Geological Survey of Canada radiocarbon dates XXX. Geological Survey of Canada, Paper 90–7.

McNeely, R., Brennan, J., 2005. Geological Survey of Canada Revised Shell Dates. Geological Survey of Canada. doi:10.4095/221215. Open File 5019.

Mercer, J.H., 1978. West Antarctic ice sheet and CO_2 greenhouse effect: a threat of disaster. Nature 271, 321–325. doi:10.1038/271321a0.

Nixon, F.C., 2012. The glacial, sea level, and sea ice histories of Melville and Eglinton islands, western Canadian High Arctic: Last Glacial Maximum to present. Ph.D. thesis, University of Alberta, Edmonton, Canada.

Payne, A.J., Vieli, A., Shepherd, A.P., Wingham, D.J., Rignot, E., 2004. Recent dramatic thinning of largest West Antarctic ice stream triggered by oceans. Geophysical Research Letters 31, L23401. doi:10.1029/2004GL021284.

Peros, M., Gajewski, K., Paull, T., Ravindra, R., Podritske, B., 2010. Multi-proxy record of postglacial environmental change, south-central Melville Island, Northwest Territories, Canada. Quaternary Research 73, 247–258. doi:10.1016/j.y.qres.2009.11.010.

Peltier, W.R., 2005. On the hemispheric origins of meltwater pulse 1a. Quaternary Science Reviews 24, 1655–1671. doi:10.1016/j.quascirev.2004.06.023.

Prest, V.K., 1969. Retreat of Wisconsin and Recent Ice in North America. Geological Survey of Canada. Map 1257A, Scale 1:5,000,000.

Rasmussen, S.O., Andersen, K.K., Svensson, A.M., Steffensen, J.P., Vinther, B.M., Clausen, H.B., Siggaard-Andersen, M.-L., Johnsen, S.J., Larsen, L.B., Dahl-Jensen, D., Bigler, M., Rothlisberger, R., Fischer, H., Goto-Azuma, K., Hansson, M.E., Ruth, U., 2006. A new Greenland ice core chronology for the last glacial termination. Journal of Geophysical Research 111, D06102. doi:10.1029/2005JD006079.

Reimer, P.J., Baillie, M.G.L., Bard, E., Bayliss, A., Beck, J.W., Blackwell, P.G., Bronk-Ramsey, C., Buck, C.E., Burr, G.S., Edwards, R.L., Friederich, M., Grootes, P.M., Guilderson, T.P., Hajdas, I., Heaton, T.J., Hogg, A.G., Hughen, K.A., Kaiser, K.F., Kromer, B., McCormac, F.G., Manning, S., Reimer, R.W., Richards, D.A., Southon, J.R., Talamo, S., Turney, C.S.M., van der Plicht, J., Weyhenmeyer, C.E., 2009. IntCal09 and Marine09 radiocarbon age calibration curves, 0–50,000 years cal BP. Radiocarbon 51, 1111–1150.

Rignot, E.J., 1998. Fast recession of a West Antarctic glacier. Science 281, 549–551. doi:10.1126/science.281.5376.549.

Rühland, K., St. Jacques, J.-M., Beierle, B.D., Lamoureux, S.F., Dyke, A.S., Smol, J.P., 2009. Lateglacial and Holocene paleoenvironmental changes recorded in lake sediments, Brock Plateau (Melville Hills), Northwest Territories, Canada. The Holocene 19, 1005–1016. doi:10.1177/0959683609340999.

Shepherd, A., Wingham, D.J., Mansley, J.A.D., 2002. Inland thinning of the Amundsen Sea sector, West Antarctica. Geophysical Research Letters 29, 1364. doi:10.1029/2001GL014183.

St.-Onge, D.A., McMartin, I., 1995. Quaternary Geology of the Inman River Area, Northwest Territories. In: Geological Survey of Canada, Bulletin 446.

St.-Onge, D.A., McMartin, I., 1999. La moraine du Lac Bluenose (Territoires du nordouest), une moraine à noyau de glace de glacier. Géographie physique et Quaternaire 53, 287–295.

Stokes, C.R., Clark, C.D., Darby, D.A., Hodgson, D., 2005. Late Pleistocene ice export events into the Arctic Ocean from the M'Clure Strait Ice Stream, Canadian Arctic Archipelago. Global and Planetary Change 49, 139–162.

Stokes, C.R., Clark, C.D., Winsborrow, M.C.M., 2006. Subglacial bedform evidence for a major palaeo-ice stream and its retreat phases in Amundsen Gulf, Canadian Arctic Archipelago. Journal of Quaternary Science 21, 399–412. doi:10.1002/jqs.991.

Stokes, C.R., Clark, C.D., Storrar, R., 2009. Major changes in ice stream dynamics during deglaciation of the north-western margin of the Laurentide Ice Sheet. Quaternary Science Reviews 28, 721–738. doi:10.1016/j.quascirev.2008.07.019.

Storrar, R., Stokes, C.R., 2007. A glacial geomorphological map of Victoria Island, Canadian Arctic. Journal of Maps 2007, 191–210. doi:10.4113/jom.2007.78.

Thomas, R., Rignot, E., Kanagaratnam, P., Krabill, W., Casassa, G., 2004. Force perturbation analysis of Pine Island Glacier, Antarctica, suggests cause for recent acceleration. Annals of Glaciology 39, 133–138.

Vincent, J.-S., 1982. The Quaternary history of Banks Island, NWT, Canada. Géographie physique et Quaternaire 36, 209–232.

Vincent, J.-S., 1983. La géologie du Quaternaire et la géomorphologie de l'Île Banks, Arctique Canadien. Geological Survey of Canada, Memoir 405.

Vincent, J.-S., Morris, W.A., Occhietti, S., 1984. Glacial and nonglaical sediments of Matuyama paleomagnetic age on Banks Island, Canadian Arctic Archipelago. Geology 12, 139–142. doi:10.1130/0091-7613(1984)12<139:GANSOM>2.0.CO;2.

Weertman, J., 1974. Stability of the junction between an ice sheet and an ice shelf. Journal of Glaciology 13, 3–13.

Wilson, J.T., Falconer, G., Mathews, W.H., Prest, V.K., 1958. Glacial Map of Canada. Geological Association of Canada. Scale 1:5,000,000.

Wingham, D.J., Wallis, D.W., Shepherd, A., 2009. Spatial and temporal evolution of Pine Island Glacier thinning, 1995–2006. Geophysical Research Letters 36, L17501. doi:10.1029/2009GL039126.

Table 3.1 Deglacial radiocarbon ages cited in this study.

	Laboratory number[a]	^{14}C age[b] (yr BP)	Lab Error[c] (yr BP)	Calibrated age range[d] (yr BP)	Dated Material	Location	Coordinates	Sample Elevation (m asl)	Relative sea level (m asl)	Reference
Banks Island	UCI-60257	12550	30	13425 – 13845	*H. arctica*	Castel Bay	73° 58' 28.6'' N 119° 43' 00.3'' W	7	37	This study
	TO-12496	12380	110	13250 – 13795	*C. kurriana*	Mercy Bay	73° 00' 07.6" N 119° 11' 49.6" W	0.5-1.5	41	England et al. (2009)
	TO-12497	11970	100	12765 – 13355	*H. arctica*	Mercy Bay	73° 00' 07.6" N 119° 11' 49.6" W	0.5-1.6	41	England et al. (2009)
	UCI-24793	12170	25	13120 – 13455	*C. kurriana*	Mercy Bay	73° 00' 07.6" N 119° 11' 49.6" W	0.5-1.7	41	England et al. (2009)
	TO-12841	11800	70	12670 – 13165	*C. kurriana*	Mercy Bay	73° 00' 07.6" N 119° 11' 49.6" W	0.5-1.8	41	England et al. (2009)
	UCI-24794	12345	30	13275 – 13695	*H. arctica*	Mercy Bay	73° 00' 07.6" N 119° 11' 49.6" W	0.5-1.9	41	England et al. (2009)
	TO-12842	11910	100	12720 – 13295	*H. arctica*	Mercy Bay	73° 00' 07.6" N 119° 11' 49.6" W	0.5-1.10	41	England et al. (2009)
	TO-12499	12220	100	13105 – 13645	*H. arctica*	Mercy Bay	73° 00' 07.6" N 119° 11' 49.6" W	0	41	England et al. (2009)
	GSC-5096	11700	95	12615 – 13110	*H. arctica*	Mercy Bay	74° 09' 24" N 119° 04' 24" W	1.75	20?	McNeely & Jorgensen (1992); McNeely & Brennan (2005)
	GSC-1437	11000	135	11355 – 12410	*H. arctica*	Parker Point	73° 46' N 116° 02' W	85-88	?	Lowdon & Blake (1973); McNeely & Brennan (2005)
	UCI-24770	12915	25	13780 – 14270	*H. arctica*	Russel Point	73° 35' 04.9" N 115° 31' 13.4" W	41	46-60	England et al. (2009)
	TO-12840	12690	70	13485 – 14040	*H. arctica*	Russel Point	73° 35' 04.9" N 115° 31' 13.4" W	41	46-60	England et al. (2009)
	TO-12491	12200	90	13100 – 13610	*H. arctica*	Russel Point	73° 35' 04.9" N 115° 31' 13.4" W	41	46-60	England et al. (2009)
	TO-12492	11730	80	12640 – 13120	*H. arctica*	East coast of Banks Island	73° 13' 30" N 116° 37' 09.8" W	4	4-46	England et al. (2009)
	GSC-2413	11400	200	11915 – 13090	*H. arctica*	East coast of Banks Island	73° 13' 30" N 116° 37' 12" W	16	16-46	Lowdon & Blake (1980); McNeely & Brennan (2005)
	GSC-4245	11200	65	12000 – 12605	*H. arctica*	East coast of Banks Island	73° 13' 06" N 116° 40' W	5.5-9	≤46	McNeely & Jorgensen (1992); McNeely & Brennan (2005)

Table 3.1 (cont.) Deglacial radiocarbon ages cited in this study.

	Laboratory number[a]	^{14}C age[b] (yr BP)	Lab Error[c] (yr BP)	Calibrated age range[d] (yr BP)	Dated Material	Location	Coordinates	Sample Elevation (m asl)	Relative sea level (m asl)	Reference
Banks Island	UCI-50750	11565	25	12570 – 12920	*H. arctica*	East coast of Banks Island	73° 03' 51.9" N 117° 16' 01.5" W	~20	50	This study
	UCI-50883	11240	25	12110 – 12610	*H. arctica*	East coast of Banks Island	72° 56' 27.6" N 117° 50' 27.2" W	10-15	52	This study
	UCI-50881	11495	25	12540 – 12890	*H. arctica*	East coast of Banks Island	72° 53' 48.8" N 118° 01' 19.3" W	15-17	17-52	This study
	UCI-50743	11715	25	12660 – 13090	*H. arctica*	East coast of Banks Island	72° 52' 17.0" N 118° 09' 24.3" W	5	50	This study
	UCI-50892	11565	25	12570 – 12920	*C. kurriana*	East coast of Banks Island	72° 52' 17.0" N 118° 09' 24.3" W	5	50	This study
	UCI-50745	11475	20	12525 – 12870	*H. arctica*	East coast of Banks Island	72° 52' 17.0" N 118° 09' 24.3" W	11	50	This study
	UCI-50746	11265	20	12175 – 12625	*C. kurriana*	East coast of Banks Island	72° 52' 17.0" N 118° 09' 24.3" W	11	50	This study
	UCI-50742	11285	20	12185 – 12645	*H. arctica*	East coast of Banks Island	72° 51' 36.7" N 118° 10' 18.7" W	4	50	This study
	UCI-50747	11305	25	12200 – 12660	*H. arctica*	East coast of Banks Island	72° 48' 57.0" N 118° 23' 22.0" W	3-4.5	≤50	This study
	UCI-50752	11515	20	12550 – 12895	*H. arctica*	East coast of Banks Island	72° 40' 47.7" N 118° 57' 30.9" W	5	40	This study
	UCI-50753	12225	20	13145 – 13520	*C. kurriana*	East coast of Banks Island	72° 40' 47.7" N 118° 57' 30.9" W	1.5-2	40	This study
	UCI-60277	11415	30	12355 – 12765	*C. kurriana*	East coast of Banks Island	72° 40' 47.7'' N 118° 57' 30.9'' W	1.5-2	40	This study
	UCI-60278	11635	35	12595 – 12980	*H. arctica*	East coast of Banks Island	72° 40' 47.7'' N 118° 57' 30.9'' W	1.5-2	40	This study
	UCI-50754	11450	20	12515 – 12825	*H. arctica*	East coast of Banks Island	72° 40' 47.7" N 118° 57' 30.9" W	13	40	This study
	UCI-60280	11340	30	12245 – 12690	*C. kurriana*	East coast of Banks Island	72° 40' 47.7'' N 118° 57' 30.9'' W	13	40	This study
	UCI-50891	11205	25	12060 – 12595	*H. arctica*	East coast of Banks Island	72° 39' 32.1" N 119° 15' 24.4" W	>5	43	This study

Table 3.1 (cont.) Deglacial radiocarbon ages cited in this study.

	Laboratory number[a]	^{14}C age[b] (yr BP)	Lab Error[c] (yr BP)	Calibrated age range[d] (yr BP)	Dated Material	Location	Coordinates	Sample Elevation (m asl)	Relative sea level (m asl)	Reference
Banks Island	UCI-50888	11290	25	12185 – 12650	*H. arctica*	East coast of Banks Island	72° 39' 07.7" N 119° 09' 11.2" W	3	43	This study
	UCI-50889	11360	25	12290 – 12715	*H. arctica*	East coast of Banks Island	72° 39' 07.4" N 119° 09' 18.6" W	8-10	43	This study
	UCI-50890	11445	25	12510 – 12805	*C. kurriana*	East coast of Banks Island	72° 39' 07.4" N 119° 09' 18.6" W	10	43	This study
	UCI-50887	11470	25	12525 – 12870	*H. arctica*	East coast of Banks Island	72° 39' 06.8" N 119° 08' 56.8" W	2.5-3	43	This study
	UCI-50886	11485	25	12530 – 12885	*H. arctica*	East coast of Banks Island	72° 34' 25.1" N 119° 10' 12.0" W	13	~40	This study
	UCI-50885	11580	25	12575 – 12930	*H. arctica*	East coast of Banks Island	72° 34' 04.1" N 119° 09' 39.6" W	~10	40	This study
	UCI-50884	11605	25	12575 – 12965	*H. arctica*	East coast of Banks Island	72° 18' 25.4" N 119° 37' 54.2" W	~17	33	This study
	UCI-60259	11275	30	12175 – 12635	*H. arctica*	East coast of Banks Island	72° 15' 45.6" N 120° 16' 33.5" W	4	≤44	This study
	UCI-60266	11270	30	12175 – 12635	*H. arctica*	East coast of Banks Island	72° 13' 57.1" N 119° 58' 54.4" W	4	≤45	This study
	UCI-60267	11160	35	11985 – 12575	*C. kurriana*	East coast of Banks Island	72° 13' 57.1" N 119° 58' 54.4" W	4	≤46	This study
	UCI-60260	11490	35	12530 – 12890	*H. arctica*	East coast of Banks Island	72° 12' 59.8" N 120° 11' 00.6" W	6	36	This study
	UCI-60262	11360	35	12270 – 12715	*H. arctica*	East coast of Banks Island	72° 12' 58.6" N 120° 11' 16.6" W	9	36	This study
	UCI-60263	11445	35	12380 – 12815	*C. kurriana*	East coast of Banks Island	72° 12' 58.6" N 120° 11' 16.6" W	12	36	This study
	UCI-60270	11500	30	12540 – 12895	*H. arctica*	East coast of Banks Island	72° 06' 42.2" N 120° 11' 59.5" W	11-15	≥21	This study
	UCI-60276	11420	40	12350 – 12785	*C. kurriana*	East coast of Banks Island	72° 02' 56.0" N 120° 14' 46.8" W	6	30	This study
	UCI-60274	11645	30	12605 – 12980	*H. arctica*	East coast of Banks Island	72° 02' 22.3" N 120° 16' 23.8" W	19	30	This study

Table 3.1 (cont.) Deglacial radiocarbon ages cited in this study.

	Laboratory number[a]	^{14}C age[b] (yr BP)	Lab Error[c] (yr BP)	Calibrated age range[d] (yr BP)	Dated Material	Location	Coordinates	Sample Elevation (m asl)	Relative sea level (m asl)	Reference
Banks Island	UCI-60275	11560	40	12565 – 12930	*H. arctica*	East coast of Banks Island	72° 02' 13.5'' N 120° 16' 14.4'' W	19	30	This study
Banks Island	GSC-2545	11600	50	12575 – 12970	*H. arctica*	East coast of Banks Island	72° 02' 13" N 120° 15' 43" W	21	30	Lowdon and Blake (1980); McNeely & Brennan (2005)
Victoria Island	GSC-6840	12500	60	13380 – 13825	*H. arctica*	Natkusiak Peninsula	72° 52' 12" N 110° 19' 49.2" W	105-111	135	McNeely & Brennan (2005)
Victoria Island	GSC-3511	12200	50	13115 – 13520	*H. arctica*	Natkusiak Peninsula	72° 52' 12" N 110° 19' 49.2" W	105-110	135	McNeely & Brennan (2005)
Victoria Island	GSC-3519	11300	50	12180 – 12665	*H. arctica*	Wynniatt Bay	72° 22' N 110° 05' W	~90	130	McNeely & Brennan (2005)
Victoria Island	GSC-48	11310	75	12635 – 13105	*H. arctica*	Richard Collinson Inlet	72° 34' N 113° 53' W	67	85	Dyck and Fyles (1966); McNeely & Brennan (2005)
Victoria Island	GSC-403	11000	160	12225 – 12825	*H. arctica*	Loch Point	73° 02' N 114° 02' W	?	>55	McNeely and Brennan (2005)
Victoria Island	GSC-3409	11700	260	12585 – 13155	*H. arctica*	Loch Point	73° 01' 54" N 114° 02' 30" W	43	>55	McNeely and Brennan (2005)
Victoria Island	GSC-4257	11600	160	12570 – 12985	*H. arctica*	Loch Point	73° 09' N 114° 08' W	46	>55	McNeely and Brennan (2005)
Victoria Island	GSC-3366	11800	100	12680 – 13145	*H. arctica*	Loch Point	73° 10' 48" N 114° 05' 48" W	55	>55	McNeely and Brennan (2005)
Victoria Island	GSC-4224	11800	110	12675 – 13150	*H. arctica*	Loch Point	73° 11' 12" N 114° 09' W	54	>55	McNeely and Brennan (2005)
Victoria Island	GSC-4248	11800	110	12675 – 13150	*H. arctica*	Peel Point	73° 17' 30" N 114° 26' W	20-30	85	McNeely and Brennan (2005)
Victoria Island	GSC-3529	11400	45	12320 – 12770	*H. arctica*	Prince Albert Peninsula	73° 00' N 116° 04' 12" W	2-4	?	McNeely & Brennan (2005)
Victoria Island	GSC-3376	11700	105	12605 – 13120	marine shells	Prince Albert Peninsula	72° 15' 36" N 118° 01' 42" W	2	>18	McNeely & Brennan (2005)
Victoria Island	GSC-4288	11400	65	12250 – 12785	*H. arctica*	Prince Albert Peninsula	72° 14' 36" N 118° 04' W	32	>32	McNeely & Brennan (2005)

Table 3.1 (cont.) Deglacial radiocarbon ages cited in this study.

	Laboratory number[a]	^{14}C age[b] (yr BP)	Lab Error[c] (yr BP)	Calibrated age range[d] (yr BP)	Dated Material	Location	Coordinates	Sample Elevation (m asl)	Relative sea level (m asl)	Reference
Victoria Island	GSC-6583	11500	50	12345 – 12960	*H. arctica*	Prince Albert Peninsula	71° 54' 25.7" N 118° 58' 33.5" W	<29	55	Dyke (Unpublished)
	AA-46725	11770	90	12645 – 13150	*H. arctica*	Prince Albert Peninsula	71° 54' 25.6" N 118° 58' 33.5" W	29	54	Dyke (Unpublished)
	AA-46722	11265	65	12085 – 12645	*H. arctica*	Prince Albert Peninsula	71° 37' 51.4" N 118° 59' 10.7" W	41	54	Dyke (Unpublished)
	GSC-4300	11000	55	11585 – 12380	*H. arctica*	Diamond Jenness Peninsula	71° 08' 06" N 117° 53' W	65	65-72	McNeely & Brennan (2005)
	GSC-3533	11400	50	12305 – 12780	*H. arctica*	Diamond Jenness Peninsula	71° 05' 24" N 118° 01' 30" W	61	72	McNeely & Brennan (2005)
	GSC-6582	11060	60	11715 – 12410	*H. arctica*	Diamond Jenness Peninsula	70° 59' 01.1" N 118° 20' 15.7" W	48-50	50-75	Dyke et al. (2003b)
	AA-46720	11515	90	12540 – 12915	*H. arctica*	Diamond Jenness Peninsula	70° 58' 25.8" N 118° 21' 42.4" W	4-6	75	Dyke et al. (2003b)
	GSC-3558	11400	50	12305 – 12780	*H. arctica*	Diamond Jenness Peninsula	70° 48' 24" N 117° 55' 48" W	76	~81	Dyke et al. (2003b); McNeely & Brennan (2005)
	GSC-3843	11300	50	12180 – 12665	*H. arctica*	Diamond Jenness Peninsula	70° 47' 24" N 117° 52' W	47	~81	Dyke et al. (2003b); McNeely & Brennan (2005)
	GSC-3566	11100	50	11855 – 12565	*H. arctica*	Wollaston Peninsula	70° 02' N 117° 17' W	91	~105	Dyke et al. (2003b); McNeely & Brennan (2005)
	GSC-4203	11000	45	11605 – 12375	*H. arctica*	Wollaston Peninsula	70° 02' N 117° 17' W	80	80-105	Dyke et al. (2003b); McNeely & Brennan (2005)
	GSC-6320	11170	110	12020 – 12600	*H. arctica*	Wollaston Peninsula	69° 56' 05" N 117° 12' 45" W	84	106	Dyke and Savelle (2000)
	GSC-6296-1	11130	120	11575 – 12380	*H. arctica*	Wollaston Peninsula	69° 55' 52" N 117° 11' 35" W	94	120	Dyke and Savelle (2000)
	GSC-6296-2	11300	160	12095 – 12685	*H. arctica*	Wollaston Peninsula	69° 55' 52" N 117° 11' 35" W	94	106	Dyke and Savelle (2000)
	GSC-3727	11000	100	11595 – 12380	*H. arctica*	Cape Baring	69° 55' N 117° 09' W	105	120	McNeely & McCuaig (1991); Dyke et al. (2003b)
	GSC-6286	11470	120	12525 – 12920	*H. arctica*	Wollaston Peninsula	69° 54' 45" N 117° 10' 30" W	87-89	120	Dyke and Savelle (2000)

Table 3.1 (cont.) Deglacial radiocarbon ages cited in this study.

	Laboratory number[a]	^{14}C age[b] (yr BP)	Lab Error[c] (yr BP)	Calibrated age range[d] (yr BP)	Dated Material	Location	Coordinates	Sample Elevation (m asl)	Relative sea level (m asl)	Reference
Victoria Island	GSC-6288	11460	100	12530 – 12910	*H. arctica*	Wollaston Peninsula	69° 54' 10" N 117° 09' 00" W	96	120	Dyke and Savelle (2000)
	GSC-6279	11070	50	11855 – 12565	*H. arctica*	Wollaston Peninsula	69° 53' 43" N 117° 06' 30" W	106	120	Dyke et al. (2003b)
	GSC-6319	11220	60	12010 – 12605	*H. arctica*	Wollaston Peninsula	69° 53' 45" N 117° 05' 50" W	106	120	Dyke et al. (2003b)
	GSC-6277	11080	60	11845 – 12565	*H. arctica*	Wollaston Peninsula	69° 40' 20" N 116° 33' 30" W	95	120	Dyke et al. (2003b)
Arctic mainland	GSC-4757	11600	50	12575 – 12970	*H. arctica*	Darnley Bay	69° 35' N 123° 08' W	5	~30	McNeely & Brennan (2005)
	AECV-643Cc	11790	160	12615 – 13250	*H. arctica*	Darnley Bay	69° 35' N 123° 08' W	6	~30	Kerr (1996)
	AA50868	12120	80	13050 – 13480	Moss	"South Lake"	69° 04' 49.2" N 121° 25' 32.5" W	n/a	n/a	Rühland et al. (2009)

Notes: [a] - GSC (Geological Survey of Canada); TO (Isotrace Laboratory, University of Toronto); UCI (University of California at Irvine). [b] - no reservoir correction. [c] - 1-sigma. [d] - 2-sigma.

Table 3.2 Radiocarbon ages of redeposited molluscs from the Jesse till.

	Laboratory number[a]	^{14}C age[b] (yr BP)	Lab Error[c] (yr BP)	Calibrated age range[d] (yr BP)	Dated Material	Site Description	Coordinates	Sample Elevation (m asl)	Reference
Jesse till	UCI-50741	49500	1210	/ – /	*H. arctica* (fragment)	Rare fragments from surface of marine limit delta	72.86513° N 118.21583° W	36-38	This study
	UCI-50748	41490	460	43754 – 45337	Unidentified (fragment)	Rare fragments from surface of outwash terrace	72° 55' 40.9" N 118° 23' 35.1" W	145	This study
	UCI-50749	46100	790	46792 – 50000	*H. arctica* (?) (fragment)	Rare fragments from gully cut into till	73° 05' 27.6" N 118° 56' 35.7" W	~98	This study
	UCI-60258	44000	1000	44811 – 48882	*H. arctica* (?) (fragment)	Rare fragments from surface of glaciolac. delta	72° 16' 32.7'' N 120° 19' 25.2'' W	45	This study
	UCI-60261	49700	2100	/ – /	*H. arctica* (?) (fragment)	Rare fragments from foresets of marine limit delta	72° 13' 03.3'' N 120° 11' 39.9'' W	21	This study
	UCI-60264	48000	1700	/ – /	*H. arctica* (?) (fragment)	Rare fragments from surface of till	72° 14' 49.3'' N 120° 00' 07.8'' W	24	This study
	UCI-60269	32530	250	35326 – 36806	*H. arctica* (?) (fragment)	Rare fragments from surface of wave-washed till	72° 14' 04.2'' N 120° 00' 49.4'' W	38	This study
	UCI-60271	39610	600	42252 – 44169	*H. arctica* (?) (fragment)	Rare fragments from surface of wave-washed till	72° 06' 32.9'' N 120° 12' 00.3'' W	37	This study
	UCI-60272	55200	4000	/ – /	*H. arctica* (?) (fragment)	Rare fragments from foresets of marine limit delta	72° 11' 31.9'' N 120° 09' 41.7'' W	17	This study
	UCI-60273	32640	260	35381 – 36964	*H. arctica* (?) (fragment)	Rare fragments from surface of glaciolac. terrace	72° 03' 56.8'' N 120° 14' 58.1'' W	26	This study

Notes: [a] - UCI (University of California at Irvine). [b] - no reservoir correction. [c] - 1-sigma. [d] - 2-sigma.

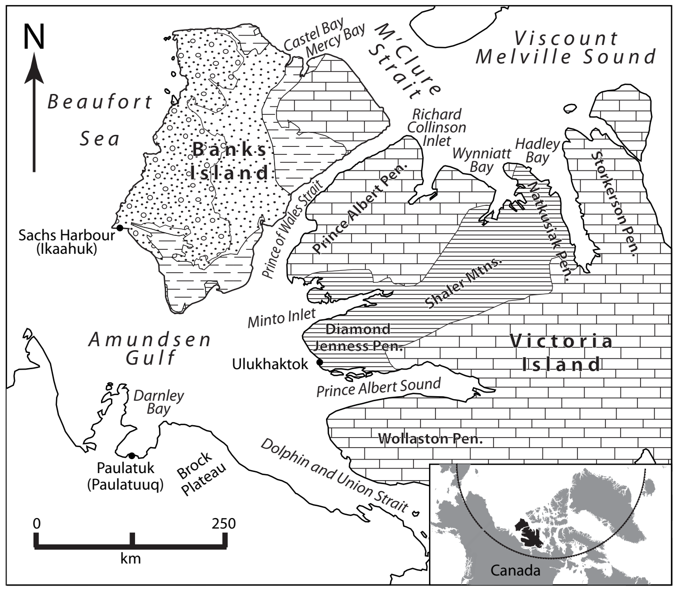

Legend

Miocene-Pliocene
Unconsolidated sand and gravel (Beaufort Fm.)

Paleocene-Eocene
Poorly lithified sand (Eureka Sound Fm.)

Cretaceous
Poorly lithified clay and silt; minor sandstone (Kanguk, Hassel, Christopher, Isachsen Fms.)

Cambrian-Devonian
Carbonate (Weatherall, Parry Island, Cass Fiord, Cape Clay Fms.)

Neoproterozoic
Metasediments, sandstone, siltstone, shale, carbonate, and capping basalt and gabbro (Shaler Sgp., Rae Gp., Natkusiak Fm., Kuujjua Fm., Glenelg Fm.)

Figure 3.1. Place names and generalized bedrock geology of Banks Island and Victoria Island, western Canadian Arctic Archipelago.

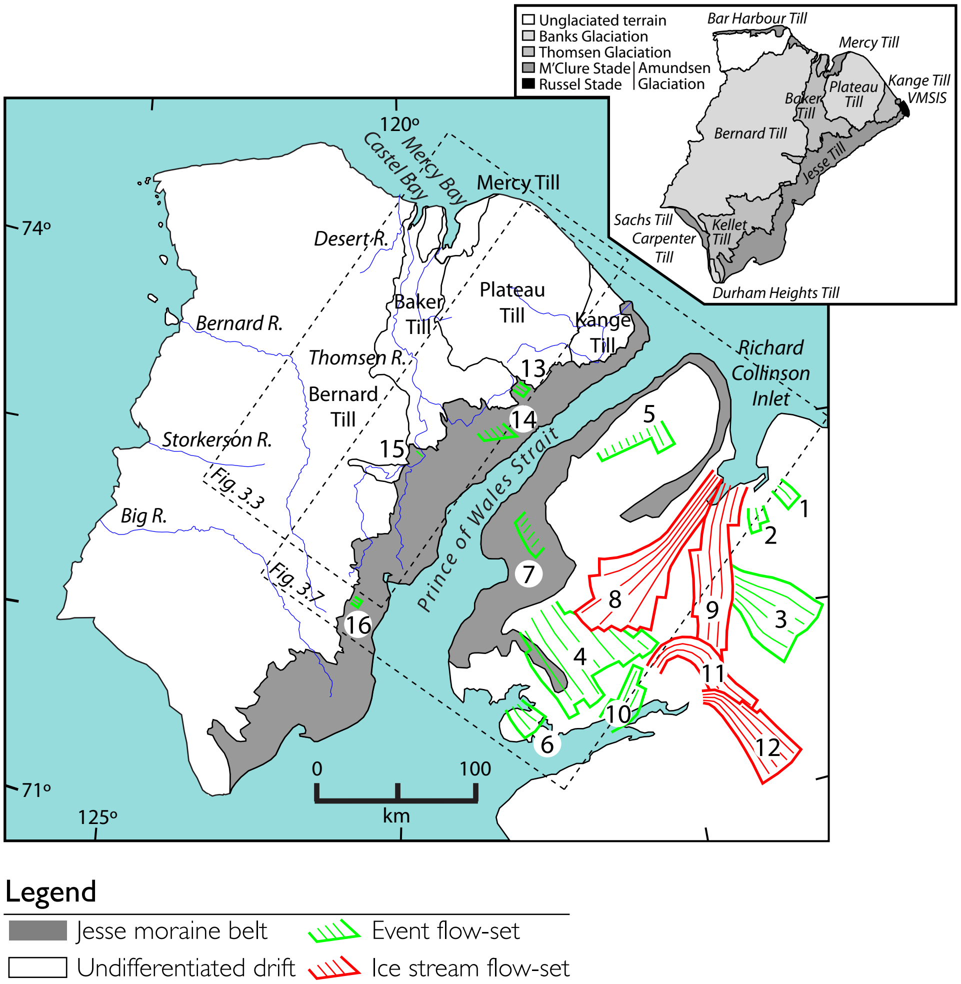

Legend

Figure. 3.2. The Jesse moraine belt on eastern Banks Island and northwest Prince Albert Peninsula, Victoria Island. The limits of the moraine belt correspond to those of the Jesse till on Banks Island (Fyles, 1963; Vincent, 1982, 1983) and to those of a coastal moraine belt on Prince Albert Peninsula (Fyles, 1963; Storrar and Stokes, 2007). Numbered red and green patterns show the location and orientation of ice stream flow-sets and event flow-sets, respectively (after Stokes et al., 2005, 2009). Dashed boxes delineate the locations of Figs. 3.3 and 3.7. The limits of Vincent's (1982, 1983) Bernard, Baker, Mercy, Plateau, and Kange tills are also shown. The inset shows all the surficial till sheets on Banks Island as reported by Vincent (1982, 1983). The matching shades denote correlative till sheets, which were interpreted to record three to four separate Quaternary glaciations. These deposits are now considered to be a single depositional sequence relating to Late Wisconsinan glaciation, which inundated the island and terminated on the Beaufort Sea shelf (England et al., 2009; Lakeman and England, submitted for publication). VMSIS – Viscount Melville Sound Ice Shelf moraine.

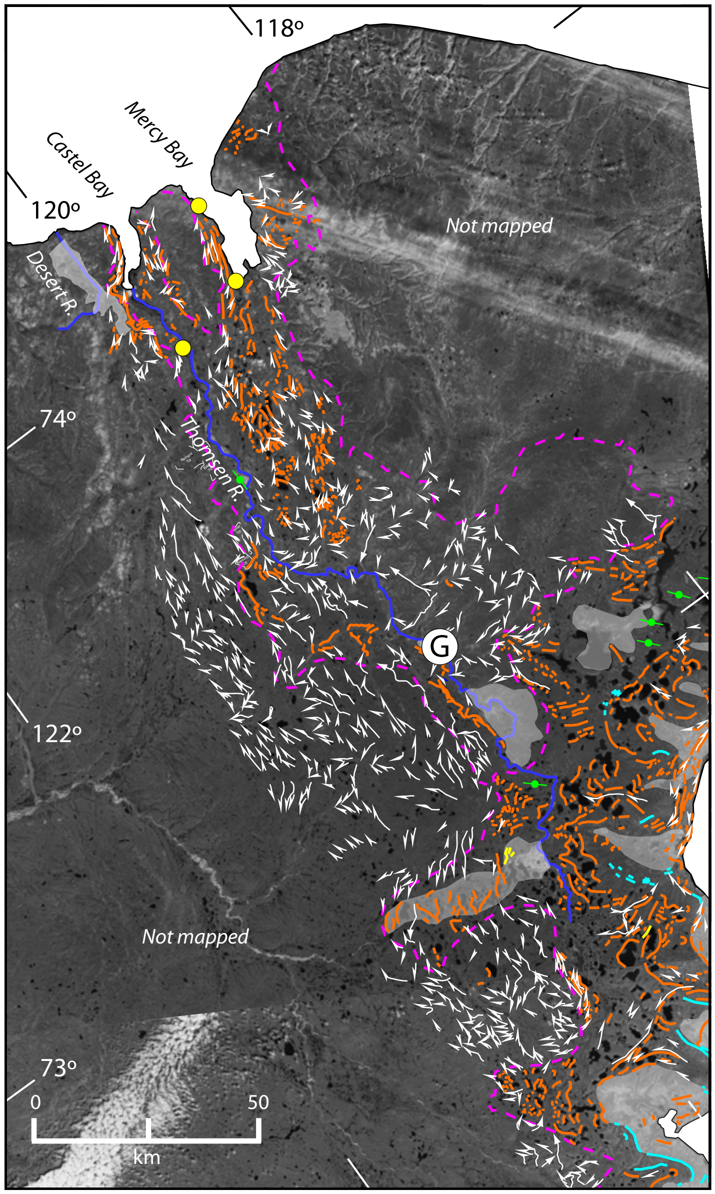

Legend

	Moraine		Fluting
	Kame terrace		Glaciolacustrine sediment
	Esker		Radiocarbon age
	Ice-lateral meltwater channel (barb on upslope side)	G	Green Cabin
	Proglaical meltwater channel		Purported till boundary from Vincent (1982, 1983)

Figure 3.3. Glacial landforms and sediments of north-central Banks Island, shown on a composite Landsat 7 orthoimage (band 8). The map area includes the Bernard, Plateau, Baker, Mercy, and Jesse tills of Vincent (1982, 1983; see Fig. 3.2). Mapped landforms in Mercy Bay follow those in England et al. (2009).

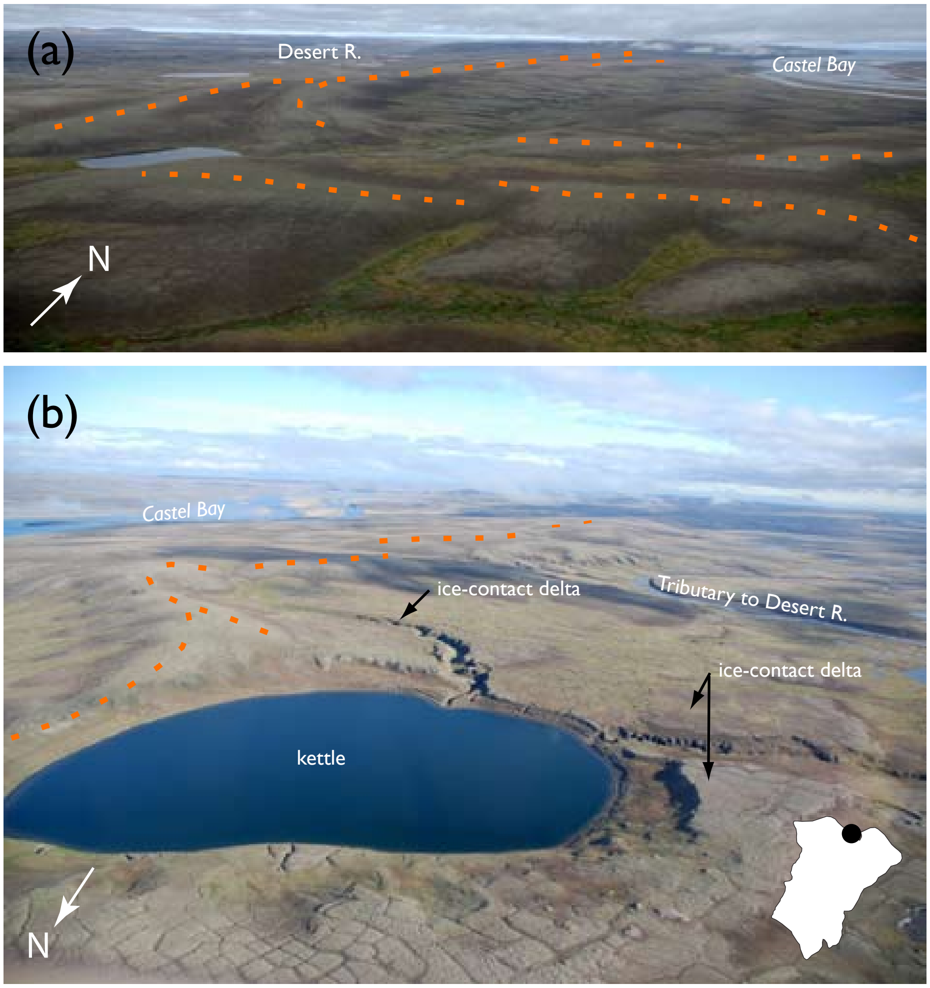

Figure. 3.4. (a) Left-lateral moraines (dashed orange lines) in Castel Bay. View is to the northwest, in the direction of former ice-flow. (b) Ice-contact, glaciolacustrine deltas (arrowed) abutting the distal flank of a left-lateral moraine (dashed orange line) in Castel Bay. View is to the southeast, in the opposite direction of former ice-flow. These deltas are situated at 65 m asl and contrast with a suite of lower glaciomarine deltas at 33 m asl, which mark the local marine limit. As a result, the pictured, glaciolacustrine deltas must record a former ice-dam at the head of the Desert River valley (i.e. grounded or floating ice in M'Clure Strait).

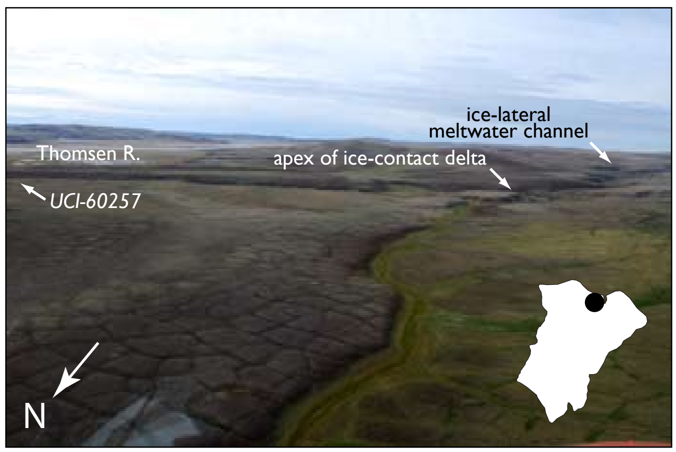

Figure. 3.5. Ice-contact, marine limit delta at 37 m asl, approximately 15 km south of the head of Castel Bay, northern Banks Island. The location of radiocarbon sample UCI-60257 (13,425–13,845 cal ka BP), among the distal bottomsets of the delta, is also shown. View is to the southeast, up the Thomsen River valley.

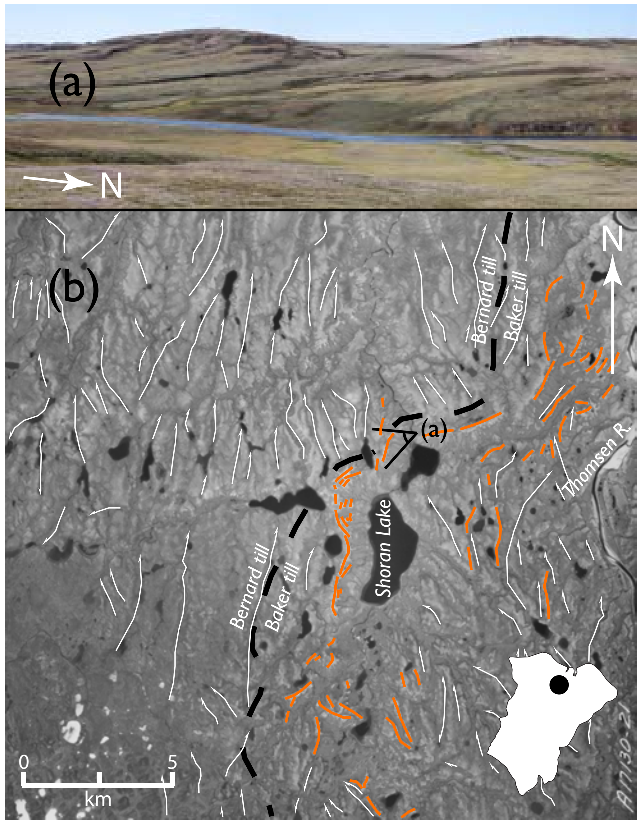

Legend

Ice-lateral meltwater channel (barb on upslope side)   Moraine

Figure. 3.6. (a) Ice-thrust moraines near Shoran Lake marking the western limit of Vincent's (1982, 1983) Baker till. The moraines are sharp-crested and exhibit conspicuous shear planes that rise in the direction of ice-flow. View is to the west. (b) Aerial photograph of Shoran Lake showing the purported contact between the Baker and Bernard till (Vincent, 1982, 1983). Ice-lateral meltwater channels parallel the moraines marking the limit of the Baker till, and some merge with contemporaneous ice-lateral meltwater channels traversing the Bernard till. This demonstrates that the purported till sheet boundary does not represent a former ice margin and is not isochronous. Aerial photograph A17130-21.

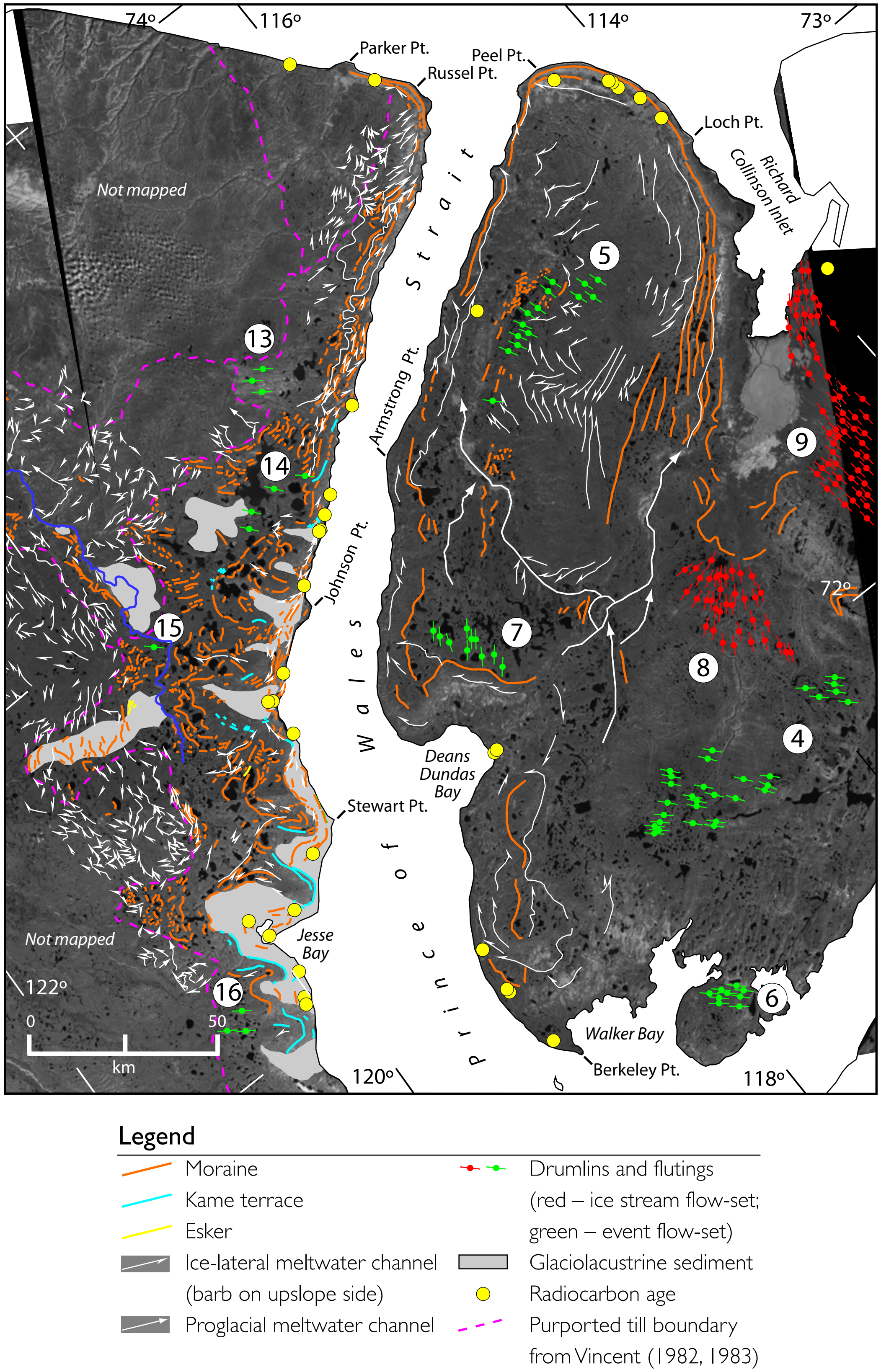

Figure 3.7. Glacial landforms and sediments of eastern Banks Island and Prince Albert Peninsula, shown on a composite Landsat 7 orthoimage (band 8).

Figure 3.8. Foliated, clast-rich ground ice >3 m thick underlying the Jesse till, north of Johnson Point. Ice is interpreted to be of glacial origin.

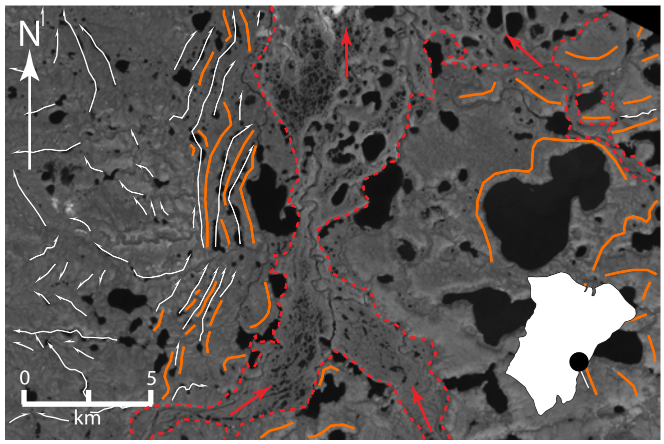

Legend

Moraine

Ice-lateral meltwater channel (barb on upslope side)

Proglacial meltwater channel

Outwash

Figure 3.9. Landsat 7 orthoimage (band 8) showing contact between controlled moraines of the Jesse till (right) and the meltwater channel-dominated Baker till (left). Multiple proglacial and ice-lateral meltwater channels, as well as widespread outwash, demarcate patterns of ice-marginal drainage.

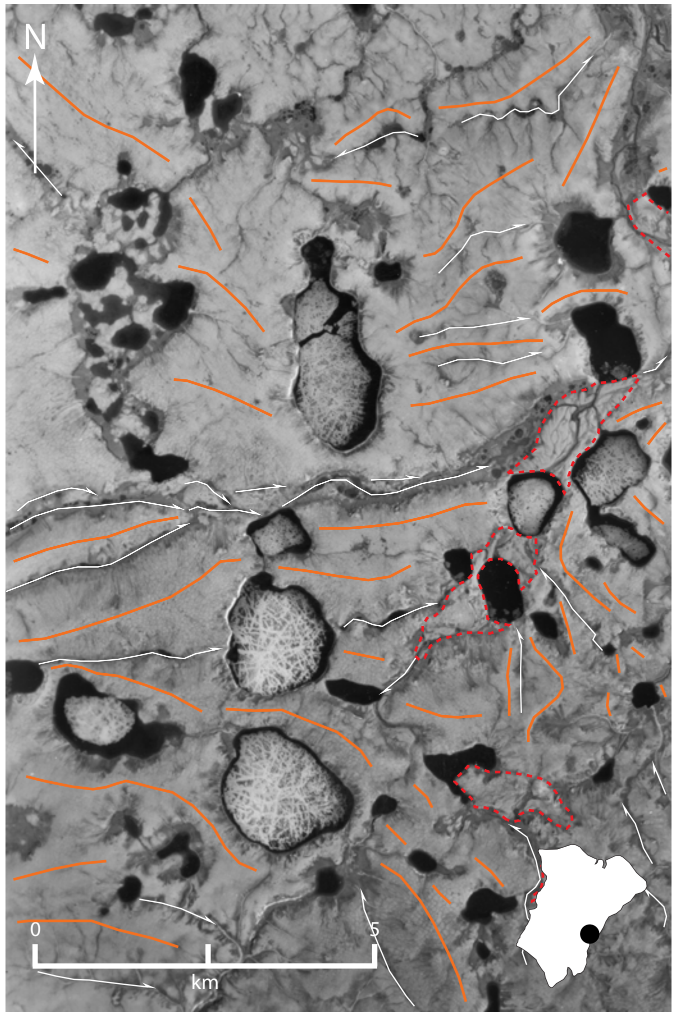

Legend

Moraine — In-wash kame delta — Ice-lateral meltwater channel (barb on upslope side)

Figure 3.10. Aerial photograph showing controlled-moraines among kettled terrain on the Jesse till. Multiple ice-lateral meltwater channels and in-wash kame deltas demarcate patterns of ice-marginal drainage. Aerial photograph A17379-5.

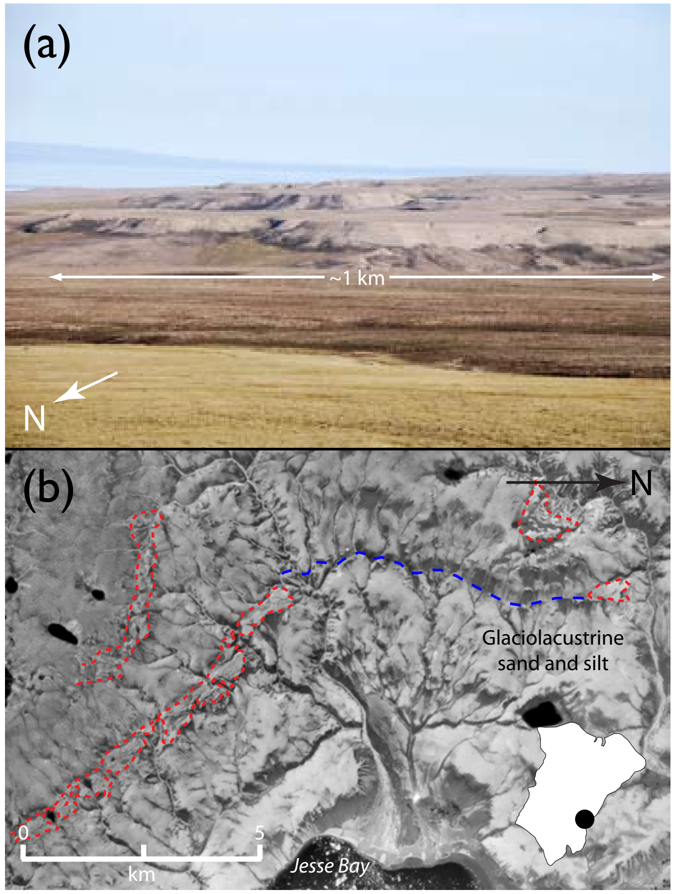

Legend

Kame terrace/delta

Former proglacial lake shoreline

Figure. 3.11. (a) Kame terraces and deltas above the south shore of Jesse Bay on the east coast of Banks Island. The terraces abut the Jesse till and descend toward the foreground (i.e. west). View is to the southeast; Victoria Island is visible on the horizon. (b) Aerial photograph showing the continuity and spatial extent of kame terraces south of Jesse Bay. Aerial photograph A17130-51.

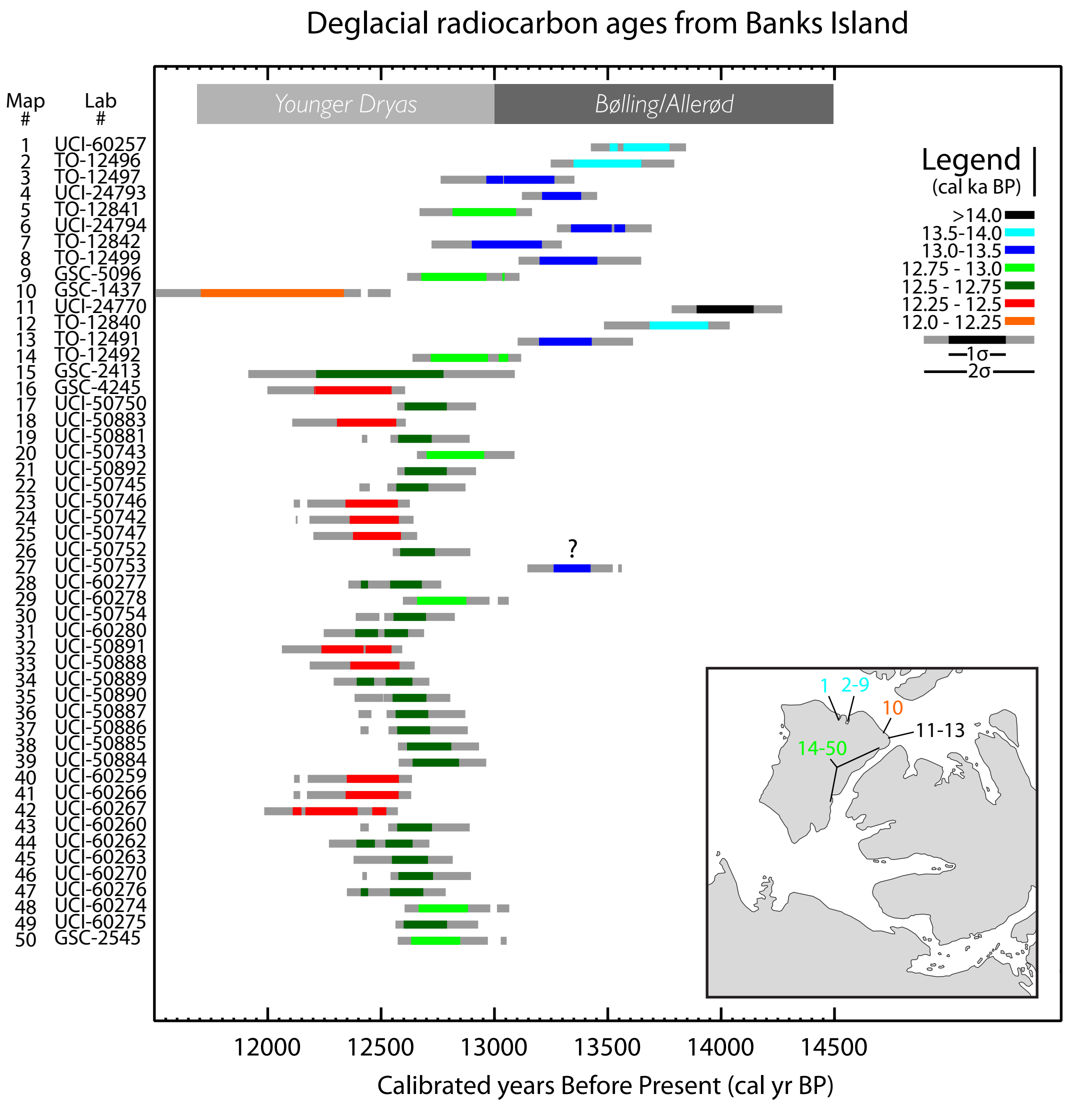

Figure 3.12. Calibrated deglacial radiocarbon ages from Banks Island. Ages are grouped into 250-500 year intervals according to their peak probabilities.

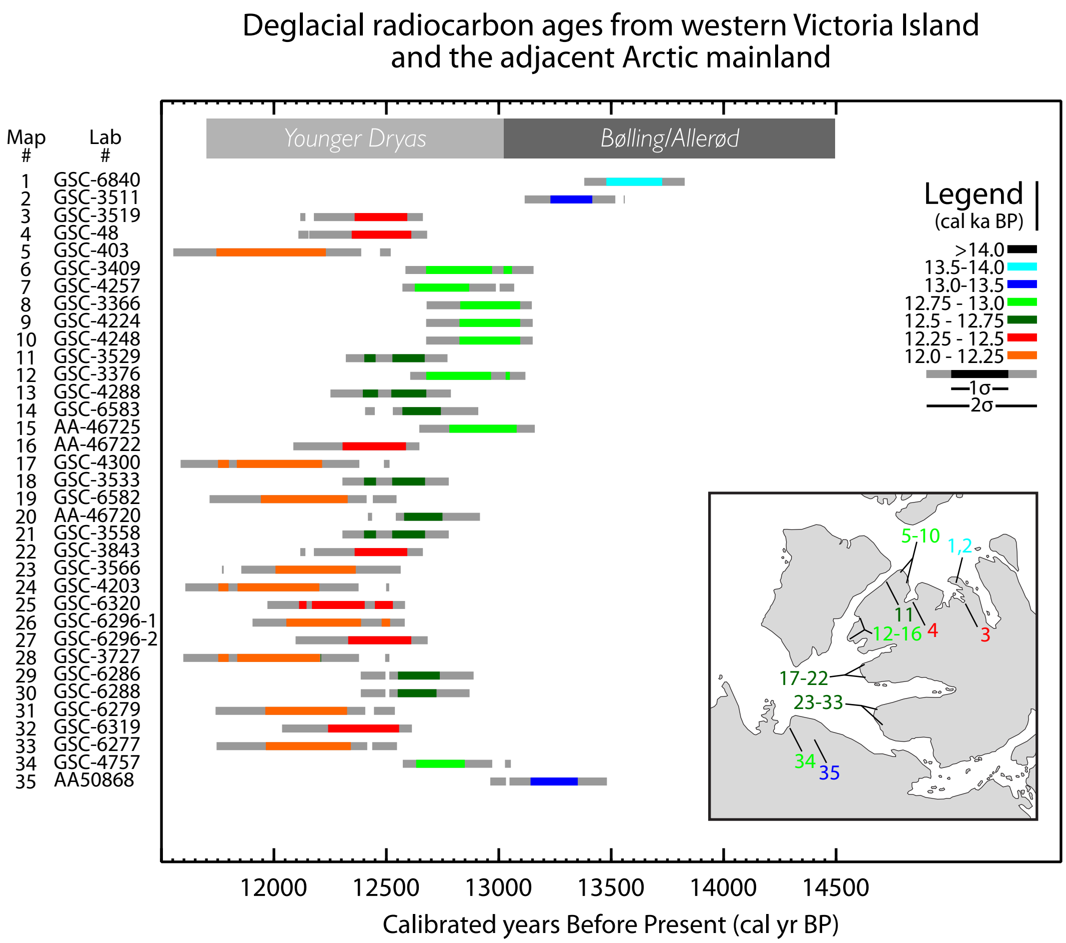

Figure 3.13. Calibrated deglacial radiocarbon ages from western Victoria Island and the adjacent Arctic mainland. Ages are grouped into 250-500 year intervals according to their peak probabilities.

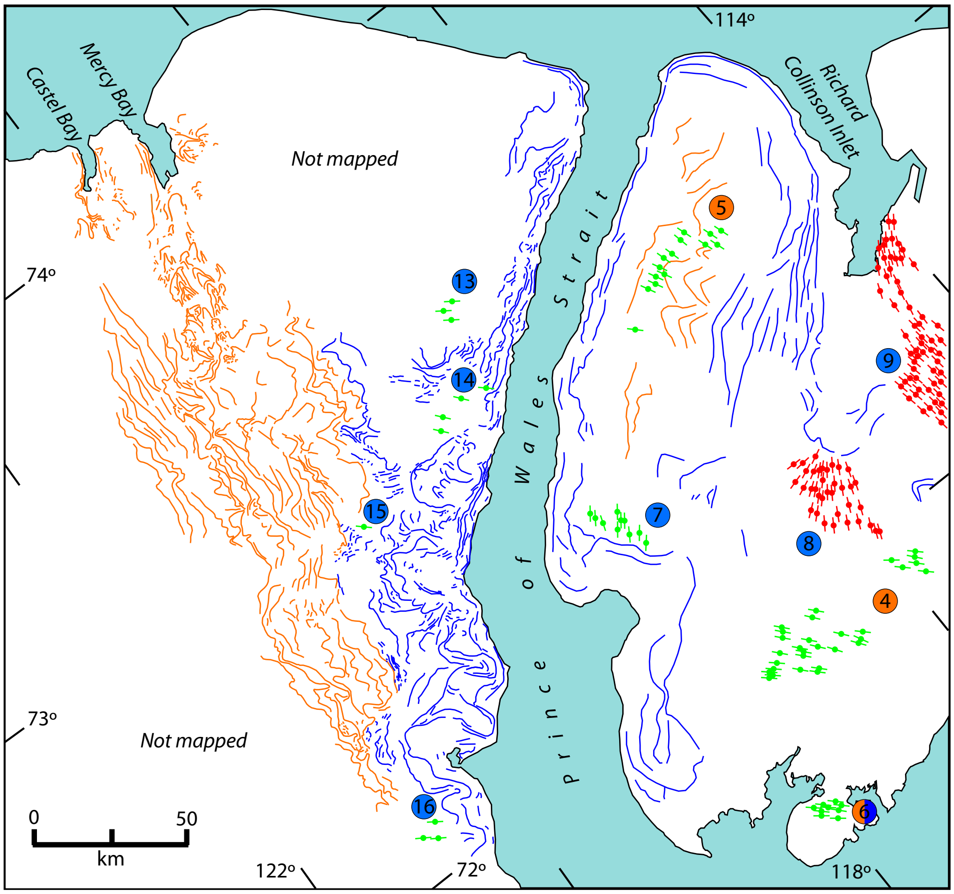

Legend

	Inferred ice margin (Thomsen Phase)		Drumlins and flutings (red – ice stream flow-set; green – event flow-set)
	Inferred ice margin (Prince of Wales Phase)	4	Flow-set (Thomsen Phase)
		8	Flow-set (Prince of Wales Phase)

Figure 3.14. Inferred former ice margins for the Thomsen and the Prince of Wales phases of ice sheet retreat.

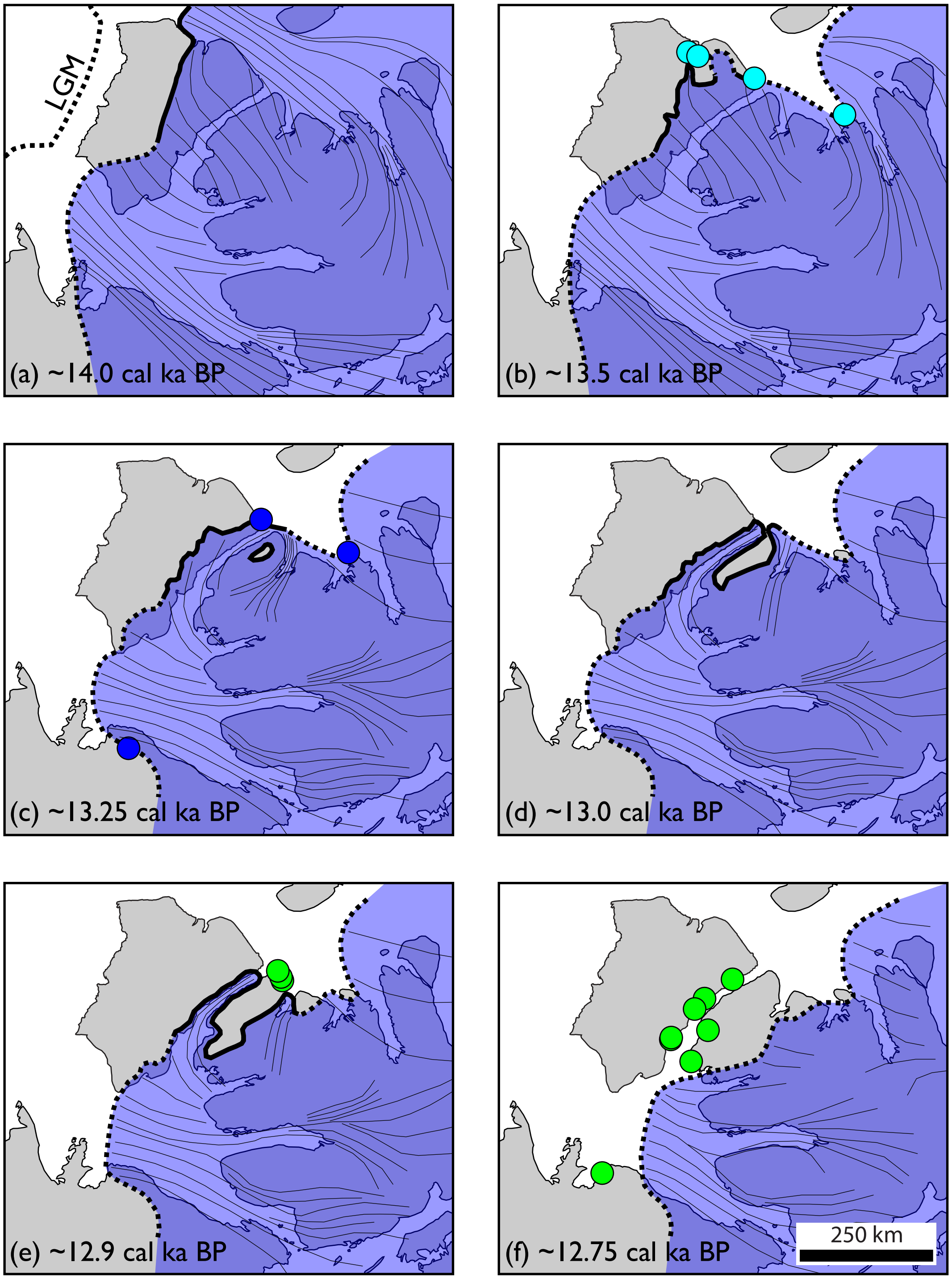

Figure 3.15. (see following page for caption)

Figure 3.15. Reconstructed ice margins and generalized ice-flow from ~14.0 to ~12.75 cal ka BP for Banks Island, western Victoria Island, and the adjacent Canadian Arctic Mainland. (a) and (b) depict the Thomsen Phase when ice sheet retreat on Banks Island was generally cold-based. (a) also shows the postulated LGM extent of the northwest LIS on the Beaufort Sea Shelf. (c), (d), and (e) depict the Prince of Wales Phase when polythermal bed conditions resulted in an ice sheet readavance or stillstand and the deposition of the Jesse moraine belt. (f) illustrates the rapid withdrawal of the northwest LIS from Prince of Wales Strait and eastern Amundsen Gulf following deposition of the Jesse moraine belt. Ice margins for western Victoria Island and the Canadian Arctic Mainland are modified from Dyke (2004) and Dyke et al. (2003b).

CHAPTER 4

REVISION OF THE EARLY QUATERNARY STRATIGRAPHY AT MORGAN BLUFFS, BANKS ISLAND, WESTERN CANADIAN ARCTIC

INTRODUCTION

Multiple Quaternary stratigraphic exposures on Banks Island (Figs. 4.1a and 4.1b) comprise a unique paleoenvironmental archive in the Canadian Arctic Archipelago (CAA). Initially surveyed and correlated by Vincent (1982, 1983) and Vincent et al. (1983), these sediments purportedly constitute the most complete record of Quaternary environmental change in the Canadian Arctic outside the Yukon, and include fossiliferous preglacial fluvial gravel, till, outwash, and glaciomarine rhythmites, among others. The stratigraphic framework developed by Vincent (1982, 1983) and Vincent et al. (1983) comprised numerous climatostratigrahic units, purportedly recording various glaciations and interglaciations, which were recognized as Formations and assigned representative type sections at various localities on the island. This stratigraphic framework was then correlated to widespread sites in the circum-Arctic, including Alaska (Matthews and Ovenden, 1990) and the Arctic Ocean basin (Clark et al., 1984). Later investigations by Vincent et al. (1984), Vincent (1990), and Barendregt et al. (1998) modified the stratigraphic framework through the application of paleoecology and magnetostratigraphy (Tables 4.1 and 4.2).

The objective of this study is to reexamine the purported stratigraphy and sedimentology at Morgan Bluffs, a ~ 6 km long exposure on the north shore of Jesse Bay on eastern Banks Island (Fig. 4.1c). The bluffs constitute a discontinuous exposure of non-glacial and glaciogenic sediments, some of which are more than 780,000 years old, based on their paleomagnetic polarity (Barendregt et al., 1998). A new examination of the stratigraphy is warranted because advances in glacial sedimentology permit new insights into past depositional environments and their precise relationships with climate, which were not considered in former studies. Specifically, previous assumptions regarding the climatostratigraphic importance of the sedimentary units comprising the bluffs took no account of rapid vertical and lateral facies changes, which are a hallmark of most Quaternary sedimentary successions (i.e. Eyles et al., 1983; Evans, 2003). Furthermore, the surficial geological record of Quaternary glaciation on Banks Island, which was interpreted by Vincent (1982, 1983, 1990) to be identical to the stratigraphic record, has been fundamentally revised (England and Furze, 2008; England et al., 2009; Lakeman and England, submitted; see Chapters 2; Lakeman and England, 2012; see Chapter 3).

A reinvestigation of the sedimentology and stratigraphy at Morgan Bluffs will place previously compiled paleoecological data, bearing on the nature, scale and rapidity of past environmental changes, into an improved geological context. Furthermore, a revised stratigraphic framework will allow future geochronological and paleoecological studies to make accurate stratigraphic correlations to both terrestrial successions in the circum-Arctic and marine sediments retrieved from the Arctic Ocean basin. Documented terrestrial archives of early to mid Quaternary and Late Pliocene paleoenvironments are especially rare in the North American

Arctic (Vincent, 1982, 1983, 1990; Vincent et al., 1983; 1984; Bennike and Böcher, 1990; Fyles, 1990; Matthews and Ovenden, 1990; Brigham-Grette and Carter, 1992; Kaufman and Brigham-Grette, 1993; Fyles et al., 1994, 1998; Barendregt et al., 1998; Funder et al., 2001). Thus, this study adds important new terrestrial observations to a sparse and fragmentary dataset of Arctic environmental change from ~3 to 1 Ma. New paleoenvironmental data for geophysical model reconstructions of Arctic environmental change augments that from marine sedimentary proxies and terrestrial ice-core proxies, which may have indirect relationships with contemporaneous, adjacent terrestrial environments.

STUDY AREA

Vincent (1982, 1983) described 12 sedimentary exposures at Morgan Bluffs (A to L; Fig. 4.1c) and correlated various geological units into a single, composite lithostratigraphy (Fig. 4.2). This composite stratigraphy was then correlated to other composite lithostratigraphies from other bluffs on the island, such as Worth Point Bluffs, Duck Hawk Bluffs, and Nelson River Bluffs (Figs. 4.1b and 4.2). When compiled, this broad stratigraphic framework was purported to be more or less complete, spanning at least two early Quaternary glaciations with intervening interglaciations (Table 4.1). Vincent's (1982, 1983) lithostratigraphic correlations between the multiple exposures at Morgan Bluffs and between the various bluffs on the island were reaffirmed in Vincent et al. (1984) and Vincent (1984, 1990).

Barendregt et al. (1998) was the first study to test the reported stratigraphy of Morgan, Worth Point, Duck Hawk, and Worth Point bluffs. Using magnetostratigraphy, they illustrated that the sediments comprising Morgan Bluffs are predominantly magnetically-reversed, dating to the Matuyama Chron (i.e. more than 780,000 years old). Furthermore, their results falsified previous lithostratigraphic correlations proposed for similar sedimentary units at Morgan Bluffs and other sites across Banks Island. For example, Barendregt et al. (1998) demonstrated that marine sediments, glaciofluvial gravels, and a till, previously identified by Vincent (1982, 1983, 1984, 1990) and Vincent et al. (1984) as the Nelson River Fm. deposited during the Thomsen Glaciation (Fig. 4.2 and Table 4.1), are magnetically-reversed, likely deposited during the Matuyama Chron (Table 4.2). However, similar sediments at Nelson River Bluffs, the type section for the Nelson River Fm., were measured to be magnetically-normal, likely deposited during the Brunhes Chron. Thus, the previous lithostratigraphic correlation made by Vincent (1982, 1983, 1984, 1990) and Vincent et al. (1984) was dismissed and the magnetically-reversed sediments at Morgan Bluffs, although similar in lithology, were attributed to an older, unnamed glaciation during the Matuyama Chron (Table 4.2).

Similarly, Barendregt et al. (1998) clarified the distribution and age of the Morgan Bluffs Fm., originally identified at Morgan Bluffs by Vincent (1982, 1983). They demonstrated that the formation is predominantly magnetically-reversed but noted a normal-polarity ice-wedge cast near its upper contact. They also considered the flora, fauna, and relict permafrost structures within the Morgan Bluffs Fm. to be more typical of the Mid to Late Pleistocene, as opposed to the Late Pliocene-Early Pleistocene, which was assumed to be generally warmer. On this basis, Barendregt et al. (1998) correlated the Morgan Bluffs Fm. to the Jaramillo Subchron (0.99-1.07 Ma). Furthermore, the documented magnetostratigraphy of other bluffs on the island revealed the absence of the Morgan Bluffs Fm., thereby falsifying earlier lithostratigraphic correlations made by Vincent (1982, 1983, 1984, 1990) and Vincent et al. (1984; Tables 4.1 and 4.2).

Clearly, the paleomagnetic data compiled by Barendregt et al. (1998) was fundamental in refining Vincent's (1982, 1983) preliminary stratigraphic framework for the various Quaternary exposures on Banks Island. However, Barendregt et al. (1998) did not systematically reassess the sedimentology of the Quaternary sediments. For example, they did not use detailed sedimentological observations to test Vincent's (1982, 1983) previous stratigraphic correlations between the multiple exposures comprising Morgan Bluffs. As a result, the composite stratigraphy presented by Barendregt et al. (1998) was only refined in terms of its magnetostratigraphy but otherwise remained identical to that of Vincent (1982, 1983, 1984, 1990) and Vincent et al. (1984; Fig. 4.2 and Tables 4.1 and 4.2). Furthermore, a comprehensive understanding of the facies changes recorded by the sediments at Morgan Bluffs, and their utility for reconstructing past environmental changes, has yet to be developed.

METHODS

This study investigates ten stratigraphic exposures (sections 1 to 10; Fig. 4.1) that generally correspond to sections C to I in Vincent (1982, 1983) and Barendregt et al. (1998; Fig. 4.1). The sediments comprising these exposures are characterized in terms of their grain sizes, depositional structures, deformational structures, fossils, bed thicknesses, bed geometries, and contacts. Bodies of sediment with distinct characteristics, distinguishing them from neighbouring sediments, are termed lithofacies (Reading, 1986; Walker, 1992). Multiple lithofacies are organized into lithofacies associations, based on their sedimentological similarities, the nature of their contacts, and their inferred genetic relationships. Lithofacies associations record a combination of depositional processes, which enable former depositional environments to be inferred. Section logs, presented in Figure 4.3, are used to summarize lithofacies (LF), lithofacies associations (LFA), and new lithostratigraphic correlations.

LITHOFACIES AND LITHOFACIES ASSOCIATIONS

LFA 1

DESCRIPTION

LFA 1 is composed of two lithofacies, LF1.1 and LF1.2, visible in sections 1 and 2 (Fig. 4.3a). LF1.1 constitutes 4 to 5 m of rhythmically bedded silty clay and fine to medium sand (Fig. 4.4a). The silty clay beds are up to 20 cm thick, are dominantly horizontally-laminated, and have gradational to rippled upper contacts with overlying sand beds. Sand beds are up to 10 cm thick and horizontally- and cross-laminated, and are frequently rippled along their upper contacts with silty clay beds. In addition, Vincent (1983) reported brittle, articulated valves of *Astarte* as well as marine diatoms from his section C, which is near section 1 in the present study (Fig. 1c). LF1.2 overlies LF1.1 and is composed of 3 to 4 m of interbedded: massive mud with widespread flame structures; normally-graded, horizontally- and cross-laminated sandy mud; horizontally-laminated, medium to coarse sand beds with fine to medium pebble lenses and stringers; and cross-laminated coarse sand and gravel lenses (Fig. 4.4b). Several of the beds comprising LF1.2 dip at angles up to 30º (Fig. 4.4c). Collectively, LFA 1 is up to 8 m thick and dips 5 to 10º to the east and northeast.

INTERPRETATION

LFA 1 constitutes marine delta bottomsets (LF1.1) and foresets (LF1.2). The rhythmites at the base of LFA 1 give way to alternating thick sand beds and clay beds, recording progradation of the delta front and lateral migration of distributary channels on the delta slope. Current indicators within the unit as well as the observed inclination of the bedding planes suggest eastward progradation into the sea, likely sustained by fluvial transport and deposition, as the grain size of LFA 1 is not indicative of a glacially-fed delta.

LFA 2

DESCRIPTION

LFA 2 contains two lithofacies (LF2.1 and 2.2) and reaches a maximum thickness of 8 m. LF2.1 comprises the base of LFA 2 and is visible in sections 1, 2 and 3 (Figs. 4.3a and 4.5). It is primarily composed of clast-supported, sandy, medium to coarse pebble gravel beds that are generally massive to weakly-stratified, with rare cross-bedding (Figs. 4.6a and 4.6c). The gravel beds contain minor cobbles, are 50 –100 cm thick, and commonly have detrital organic matter interspersed throughout. The organic matter includes twigs, moss, seeds, and is occasionally concentrated at the base of individual gravel beds. The gravel is interbedded with stony medium sand lenses that are up to 10 cm thick (Figs. 4.6a and 4.6c). These sand lenses are horizontally-laminated, cross-laminated, and rarely planar crossbedded, and increase in abundance towards the top of the facies. Also interbedded with the sand and gravel are discontinuous, 1-3 cm thick, organic horizons containing twigs, woody detritus, peat, seeds, and other unidentifiable organic material. The lower contact of LF2.1 with LF1.2 is erosional, marked by the incision of broad channels into LF1.2 (Figs. 4.4c and 4.4d).

LF2.2 is composed of dark grey, sandy and stony clay horizons that are up to 20 cm thick (Fig. 4.6d). It is visible in Section 2 where it is interbedded with LF2.1. Horizons of LF2.2 are traceable laterally for up to 30 m and occur in association with widespread relict periglacial features (Fig. 4.7). For example, one horizon in Section 2 is associated with prominent ice wedge casts and has been cryoturbated into multiple involutions within the bounding sandy gravel (Fig. 4.7). Some ice wedge casts are vertically nested in a chevron pattern indicating that they were syngentic. Other observed horizons of LF2.2 have not been as extensively cryoturbated or as well preserved.

INTERPRETATION

LFA 2 comprises the Morgan Bluffs Fm. of Vincent (1982, 1983) that he interpreted as interglacial fluvial sediments. LF2.1 records clastic aggradation in a braided river system, where channel migration and/or hiatuses in aggradation resulted in periods of subaerial exposure, marked by the presence of occasional paleosols (LF2.2) and permafrost structures. The documented syngenetic ice wedge casts demonstrate the vertical growth of permafrost and ice wedges as sediment aggraded (French, 1976). The lower contact of LFA 2 is erosional and documents the fluvial overstepping of the preceding delta (LFA 1), instigated by sea level regression.

LFA 3

DESCRIPTION

LFA 3 is composed of three lithofacies (LF3.1, 3.2, and 3.3) and is up to 17 m thick. LF3.1 is exposed in sections 1, 2, and 3 (Figs. 4.3a and 4.5). It comprises stony and well-sorted medium to coarse sand beds that are commonly interbedded with sandy fine to medium pebble gravel (Figs. 4.8a and 4.8c). Sand beds are 10-15 cm thick and dominantly horizontally-laminated; however, ripple cross-laminations and planar cross-bedding are also present (Figs. 4.8a and 4.8c). Gravel beds are 10-15 cm thick and massive to weakly stratified (Figs. 4.8a, 4.8b, and 4.8c). Sedimentary evidence for former ice wedges is also present throughout LF3.1; one example in Section 1 was measured to be over 2 m in height (Fig. 4.8a). These sand and gravel beds commonly have sharp lower contacts and contain mud and peat rip-up clasts (Fig. 4.8a).

LF3.2 is composed of stony clay and peat horizons up to 10 cm thick (Fig. 4.8b). These horizons are commonly truncated by overlying sand and gravel beds and, thus, are not traceable laterally for more than a few metres.

LF3.3 is composed of rhythmically bedded silty mud and fine to medium sand, up to 1 m thick (Fig. 4.8d). Individual mud and sand beds are 1-2 cm thick and are occasionally stony (Fig. 4.8d). One exposure of LF3.3 forms a prominent, characteristic break in slope along the western part of the bluffs. At several locations the bedding of LF3.3 has been deformed by the subsequent deposition of overlying sand and gravel.

INTERPRETATION

LFA 3 conformably overlies LFA 2 and documents a similar phase of aggradation by a braided fluvial system. Pauses or hiatuses in aggradation are marked by paleosol fragments (LF3.2), peat accumulations (LF3.2), permafrost structures, and floodplain or overbank deposits (LF3.3). Taken together, LFA 2 and LFA 3 fine upward from dominantly gravel to sand, possibly recording a trend towards decreasing stream competency or an increase in the supply of sand in the catchment.

LFA 4

DESCRIPTION

LFA 4 is composed of 8 lithofacies (LF4.1 to 4.8), and comprises a wedge that thickens and fines eastward, where it reaches a thickness of ~15 m. The lower contact with LFA 3 is irregular and undulose and, thus, likely unconformable.

LF4.1 is exposed in Sections 1 through 4 (Fig. 4.3a) and is composed of well-sorted, stony medium sand with rare massive to weakly stratified medium to coarse pebble gravel lenses (Figs. 4.9a, 4.9b, and 4.9c). The sand beds are horizontally- and ripple cross-laminated as well as planar crossbedded, and commonly exhibit convolute bedding where they occur in close proximity to gravel lenses (Figs. 4.9a, 4.9b, and 4.9c). The sand beds are 15-30 cm thick, dip at varying angles (up to 30º), and commonly form broad, shallow channels.

LF4.2 is exposed in Sections 4 through 8 (Figs. 4.3b and 4.3c) and is dominantly composed of interbedded fine to medium sand and silt couplets, which are frequently contorted, and generally fine in texture eastward (Figs. 4.9d and

4.9e). Pebbly sand beds are also present but they are minor and decrease in abundance towards the east. The sand comprising the couplets is generally massive to horizontally-laminated and the silt beds are massive and marked by widespread flame and loading structures (Fig. 4.9e). Commonly the bedding within LF4.2 is deformed where it is overlain by a diamict of LF4.3. LF4.2 contains widespread syndepositional deformation structures, including overturned folds and minor faults with measureable displacement on the order of 1-2 cm (Fig. 4.9e).

A single, well-consolidated diamict traceable from Section 3 to 7 comprises LF4.3 (Fig. 4.10a). The diamict is matrix-supported and clay-rich, with thicknesses of 0.3 to 1.5 m. Pebbles are the most abundant clasts, however, faceted and striated cobbles and small boulders are also present, often situated at the base of the diamict (Fig. 4.10c). Sand intraclasts, which have been plastically-deformed into boudins, also occur within the diamict (Figs. 4.10c). The diamict is massive except where boudins give the beds weak stratification. The diamict truncates bedding in underlying sediments and in several instances deformed but weakly-stratified sequences (<0.5 m thick) of silty sand from underlying sediment were observed along its lower contact (Fig. 4.10d). LF4.3 is overlain by interbedded sequences of LF4.4 and LF4.5.

Matrix-supported, clay-rich diamicts also comprise LF4.4, which is visible in Sections 3 through 8 (Fig. 4.3). These deposits, however, are generally thinner than LF4.3 (<0.5 m), have weak stratification, and are not traceable laterally for more than ~100 m, as they form lenses tens of metres wide, which commonly interfinger with bounding sediment comprising LF4.5 (Fig. 4.10b). Indeed, the diamicts comprising LF4.4 vary significantly in their lateral continuity and degree of consolidation. The diamicts comprising LF4.4 also contain fewer clasts than LF4.3 and cobbles and boulders are generally absent.

LF4.5 is a complex, coarse clastic sequence made up of admixed sandy gravel, stony medium sand, and silt beds of varying thicknesses (Figs. 4.11a and 4.11b). Sandy medium to coarse gravel is moderately- to well-sorted and stratified, sometimes at high angles (Fig. 4.11a). Where this lithofacies is situated beneath LF4.3, it forms normally-graded lenses up to 2 m thick with erosional lower contacts (Figs. 4.10d and 4.11a). Where this lithofacies overlies LF4.3, it forms a laterally continuous, massive to horizontally-bedded unit, 1-3 m thick, and traceable from Section 3 to 7 (Figs. 4.3 and 4.12). LF4.5 is commonly interbedded with lenses of diamict belonging to LF4.4, and also contains stony clay rip-up clasts, likely derived from these associated diamicts (Fig. 4.10b).

LF4.6 is a diamict composed of poorly-sorted, sandy, fine to coarse gravel (containing cobbles) that constitute massive, irregularly shaped lenses, 1 to 2 m wide and up to 1 m in height (Figs. 4.9d and 4.11b). These lenses are situated within sediments belonging to LF4.2, LF4.5, and LF4.7, and are associated with syndepositional deformation (folds and faults) of the underlying and adjacent strata. In some instances, these gravelly diamict lenses are found at the centre of broad synclines within LF4.5 (Fig. 4.11b).

LF4.7 is exposed in Sections 4 through 8 (Figs. 4.3b and 4.3c) and consists of massive, stony and sandy mud beds that are up to 3 m thick (Figs. 4.11a, 4.11b, 4.11c, and 4.12). This facies increases in abundance and thickness to the east, where it overlies LF4.3, LF4.4, LF4.5, and LF4.6 (Figs. 4.11a, 4.11b, and 4.12). In several exposures these stony mud beds have an upper contact that is gradational with LF4.8 (Fig. 4.11c). In addition, while no fossils were identified during this study, Vincent (1983) reported the presence of molluscs (unknown species) from clayey silt resembling LF4.7 in section 5.

LF4.8 is visible in sections 2 and 4 through 8 (Fig. 4.3), and was observed to be up to 25 m thick. It is made up of generally uninterrupted sequences of rhythmites, which fine upward and to the east, from horizontal- and ripple-laminated fine to medium sand with capping massive silt and rare sandy gravel lenses (Figs. 4.11c and 4.11d), to horizontally-laminated to massive silt with capping mud and rare horizontally-laminated fine to medium sand beds (Figs. 4.11e). The couplets commonly contain dropstones (Fig. 4.11c), are up to 10 cm thick, and often exhibit minor syndepositional faults with up to 1 cm of displacement. In addition, Vincent (1983) reported multiple marine mollusc species, including *Portlandia arctica (gray)*, *Astarte borealis (Schumacher)*, and *Astarte (Nicania)*, from sediments similar to LF4.8 in his sections J, K and L, which lie to the northeast of section 10 in the present study.

INTERPRETATION

LFA 4 is a generally conformable sequence recording the onset of glacially influenced, subaqueous sedimentation in a marine basin. LF4.1 and 4.2 record delta foreset deposition and attendant turbidite deposition, respectively. The steeply-dipping, channelized, stony sand and gravel comprising LF4.1 documents deposition by former distributary channels on a delta slope. The fine sand and silt couplets, which fine to the east and comprise LF4.2, have widespread loading structures and contorted bedding. These sediments indicate rapid sedimentation from turbidites originating on the delta slope, likely resulting from high rates of glacially influenced sediment delivery to the delta.

LF4.3 is interpreted as a till because it is laterally continuous and contains faceted and striated cobbles of probable glacial origin, which are absent from the underlying LF4.1 or 4.2. Furthermore, the deformed but weakly-stratified sequences of silty sand observed along the lower contact of LF4.3 are interpreted as glacitectonites. Thus, LF4.3 records a glacier advance across a former delta. The sandy gravel lenses and stony medium sand and silt beds with mud rip-up clasts, which comprise LF4.5, are interpreted to record high-energy sedimentation of sand and gravel by turbid plumes emanating from the grounding line of a former glacier. Where LF4.5 occurs below LF4.3 as sandy gravel lenses, these sediments likely record intermittent sedimentation in front of the advancing ice margin or sporadic preservation of a pre-existing deposit that was largely eroded by the glacier advance. The laterally continuous exposure of LF4.5 above the till (LF4.3; Fig. 4.12), on the other hand, is interpreted as a grounding line fan that was deposited upon glacier retreat. Unlike the diamict comprising LF4.3, the diamicts comprising LF4.4 are weakly stratified and are not laterally continuous. They are, thus, interpreted to record widespread subaqueous debris flow deposition, either originating from the former glacier margin or from the remobilization of sediments belonging to LF4.5. Additional evidence for the proximity of a glacier is LF4.6, which is composed of the massive, irregularly shaped coarse gravel lenses that are interpreted as iceberg dump structures and grounding structures. Furthermore, the massive stony silt and clay beds, which comprise LF4.7 and reach thicknesses of up to 4-5 m, likely record sedimentation beneath a floating ice shelf or widespread iceberg armadas. Finally, LF4.8 records the deposition of glaciomarine rhythmites with minor iceberg sedimentation, in the form of dropstones and dump structures. This documents the conformable transition from an ice-proximal environment to an ice-distal environment, during which sedimentation from icebergs continued but was less frequent. The glacier advance recorded by LF4.3 to 4.8 presumably originated to the west of Morgan Bluffs, as suggested by the overall eastward fining of LFA 4.

LFA 5

DESCRIPTION

LFA 5 consists of stratified sand and gravel, LF5.1, that is exposed in Sections 3, 9, and 10. LF5.1 is up to 65 m thick and rests unconformably on LFA 4, as seen in Sections 3 and 9 (Figs. 4.3a and 4.3c). The base of LF5.1 comprises a massive to weakly-stratified sandy coarse gravel bed that is up to 2 m thick (Fig. 4.13a). Above this is interbedded sand and gravel (Fig. 4.13a). Sandy fine gravel beds are normally-graded (Fig. 4.13b) and capped by stony medium to coarse sand beds that are horizontally-, cross-, and trough cross-laminated (Fig. 4.13b). Additional, well-sorted, medium to coarse sand beds commonly exhibit cross-laminations, cross-bedding, and climbing ripples (Fig. 4.13c). LF5.1 also contains many large cobbles and rare boulders up to 1 m in diameter, which are commonly striated and faceted. The bedding planes within LF5.1 dip at angles up to 10° towards the southeast (Figs. 4.13a and 4.13d).

INTERPRETATION

The contact between LFA 4 and LFA 5 constitutes a major unconformity. A significant amount of erosion is implied by the absence of LF4.8 (rhythmites) from

LFA 4 in Section 3, which is up to 25 m thick elsewhere (Fig. 4.3). As well, LFA 5 appears to be inset within LFA 4 (Fig. 4.14). This erosion was likely concomitant with the deposition of LFA 5, which comprises ice-contact delta foresets. Although generally coarse in texture, LFA 5 contains abundant sedimentary structures such as climbing ripples and graded beds that are characteristic of aggradation on a prograding ice-contact delta front. The larger clasts, including those up to 1 m in diameter, are commonly striated and faceted, which attests to their glacial origin and proximity to a retreating glacier margin.

LFA 6

DESCRIPTION

LFA 6 is composed of two lithofacies (LF6.1 and LF6.2), which outcrop in Section 9 and 10 where they are up to 10 m thick, collectively (Fig. 4.3c). LF6.1 was only observed in Section 10 where it conformably overlies LFA 5. It is composed of poorly-sorted, coarse gravel beds, massive clayey diamicts with many faceted and striated cobbles, horizontally-laminated and ripple cross-laminated sand, and horizontally-laminated stony silt and mud (Figs. 4.15a and 4.15b). The gravel beds are up to 1.5 m thick and are clast-supported with a sand matrix. The diamict beds are up to 1 m thick, have a sand and silt-rich clay matrix, and are matrix-supported (Fig. 4.15a). The upper 10-20 cm of the diamicts commonly exhibit crude normal-grading at their upper contacts with overlying sediments (Fig. 4.15a). This normal grading is characterized by a decreasing concentration of gravel and cobble clasts and an increasing concentration of clay. The sand, silt, and mud beds are generally less than 20 cm thick.

LF6.2 is made up of sandy rhythymites with dropstones (Fig. 4.15b). In Section 9, these sediments conformably overlie LFA 5 (Fig. 4.13d). In Section 10, these sediments conformably overlie LF6.1, which together comprise an overturned fold (Fig. 4.15c). Horizontal- and ripple cross-laminated fine to medium sand with capping silt comprise the rhythmites, which are up to 5 cm thick (Fig. 4.15b). The deformation within LF6.1 and LF6.2 is both syn- and postdepositional, as it includes the aforementioned overturned folds and minor faults with up to several cm of displacement.

INTERPRETATION

LFA 6 records subaqueous debris flow, turbidite, and rhythmite deposition in a glacial lake. These sediments closely resemble other local exposures of glaciolacustrine sediment dating to the last deglaciation (Fig. 4.15d; Lakeman and England, 2012; see Chapter 3). The deformation of the rhythmites likely records rapid sedimentation and subsequent instability of the lake floor induced by its drainage. In addition, some of this deformation may be the result of glaciotectonism induced by oscillations of the former ice margin.

SYNTHESIS

The Quaternary sedimentary record at Morgan Bluffs records a variety of glacial and non-glacial environments. The stratigraphy can be placed into three separate successions, recording three distinct phases of apparently conformable sedimentation.

SUCCESSION 1

The first comprises LFA 1, 2 and 3 and documents the progradation of a marine delta (LFA 1), followed by the aggradation of gravel-dominated (LFA 2) and then sand-dominated (LFA 3) braided river valleys. The fluvial overstepping of the delta by LFA 2, resulting in deposition of fluvial gravel, records an interval of sea level regression, possibly occasioned by glacioisostasy, tectonics, or eustatic sea level.

LFA 2 is equivalent to the Morgan Bluffs Formation, first identified by Vincent (1982, 1983) and preliminarily dated by Barendregt et al (1998) to around 0.99-1.07 Ma (the Jaramillo Subchron) on the basis of a normal polarity ice wedge cast near its upper contact that is amongst strata having reversed polarity. Although the Jaramillo Subchron may well be recorded in LFA 2, the precise interval of time recorded by LFA 2 has yet to be demonstrated. Existing pollen and macrofossil records from the proposed formation record a climate that was warmer than present, supporting a low arctic ecosystem with widespread shrub birch, and hence interpreted as an interglacial (Matthews et al., 1986; Vincent, 1990). Detailed inventories of pollen as well as floral and faunal macrofossils collected from the Morgan Bluffs Fm. at Morgan Bluffs are available in Matthews et al. (1986) and Vincent (1990). However, the precise stratigraphic locations that these records were collected from remain unclear. Therefore, the degree of paleoclimatological and paleoecological variation within the formation also remains undocumented. Finally, no systematic study has been made on small mammal remains that were first reported by Matthews et al. (1986). As a result, significant improvements could still be added to our understanding of the early Quaternary environment recorded by LFA 2.

The subsequent trend to an aggrading, sand-dominated braided river valley (LFA 3) signals a significant change in sediment supply within the catchment, possibly instigated by climate, as well as the continued growth of accommodation space in the adjoining basin (i.e. the ancestral Prince of Wales Strait). The widespread occurrence of former ice wedges throughout LFA 3 indicates that climate may have been generally similar to that recorded by LFA 2. Alternatively, the transition to a sand-dominated braided river valley may record the beginning of a cooler climate coincident with the onset of a former interstadial or glaciation. These hypotheses warrant the collection of new paleoecological data and an improved geochronological framework for the stratigraphy.

SUCCESSION 2

The second is composed of LFA 4, which marks the first occurrence of glacially influenced sedimentation in the stratigraphy at Morgan Bluffs. LFA 4 documents the progradation of a glacier-fed delta with deposition of turbidites (LF4.1, 4.2), and a subsequent glacier advance resulting in deposition of till (LF4.3). This was followed by glacier retreat and the deposition of a grounding line fan (LF4.5) and widespread diamicts resulting from subaqueous debris flows (LF4.4). This was contemporaneous with sedimentation by floating and grounded icebergs (LF4.6) and sedimentation beneath an ice shelf or large iceberg armadas (LF4.7). The subsequent deposition of thick rhythmites (LF4.8) indicates the prevalence of glacially-sourced turbid plumes originating from a former ice margin that was more distal to Morgan Bluffs following local glacier retreat and ice shelf collapse.

All the diamicts (LF4.3 and LF4.4) within LFA 4 were previously interpreted as tills by Vincent (1982, 1983, 1990) and Barendregt et al. (1998) and, thus, attributed to at least two separate continental glaciations, each with an intervening interglaciation recorded by sediments belonging to LF4.5. Given new observations of the sedimentology and of the lateral and vertical relationships between different lithofacies across various exposures comprising Morgan Bluffs, this interpretation is deemed untenable. For example, if true, it would require astonishingly little sedimentation of minimal facies variety in a marine basin by multiple ice sheets, which is at odds with known rates and modes of sedimentation at present submarine glacier margins (i.e. Dowdeswell, 1987; Powell, 1990, 2003; Powell and Domack, 1995).

The base of LFA 4 constitutes an unconformity and, thus, its relationship to LFA 3 is unclear (Fig. 4.5). The magnetic polarity of LFA 4 is reversed, indicating that it is likely older than 780,000 years old (i.e. within the Matuyama Chron; Barendregt et al., 1998). Further, if the upper part of the underlying LFA 2 records the Jaramillo Subchron, as proposed by Barendregt et al. (1998), then LFA 4 would date to 0.99–0.78 Ma.

SUCCESSION 3

The third is composed of LFA 5 and 6, which document the progradation of ice-contact delta foresets into an ice-dammed lake (LF5.1), followed by localized deposition of subaqueous debris flow diamicts and turbidites (LF6.1), followed by the accumulation of rhythmically-bedded sand and silt deposited by turbid plumes originating from a distal ice margin (LF6.2). Formerly interpreted as glacial outwash by Vincent (1982, 1983), LFA 5, as well as LFA 6, show close affinity to previously mapped deposits recording a large proglacial lake that inundated Jesse Bay and adjacent valleys during the last deglaciation (Lakeman and England, 2012; see Chapter 3; (Fig. 4.15d)). The lake was dammed by the northwest Laurentide Ice Sheet ~12,750 calibrated years Before Present, as it impinged the east coast of Banks Island from Prince of Wales Strait. The stratigraphic and geographic location of LFA 5 and 6 also displays a genetic relationship with adjacent, large ice-lateral meltwater channels on the hillslope above Morgan Bluffs. These meltwater channels are firmly correlated with the widespread sedimentary and geomorphic evidence for the former ice-dammed lake in Jesse Bay (Lakeman and England, 2012; see Chapter 3). As a result, LFA 5 and 6 are interpreted to be Late Wisconsinan and related to the withdrawal of the northwest Laurentide Ice Sheet from Banks Island to Prince of Wales Strait. No paleomagnetic data from Barendregt et al. (1998) are available for LFA 5 to negate a postulated Late Wisconsinan age. Indeed, paleomagnetic data from LFA 6, which conformably overlies LFA 5, has a normal polarity (Barendregt et al., 1998), consistent with this interpretation.

Alternatively, LFA 5 and 6 may have been deposited during the advance phase of the last glaciation, when a similar ice-dammed lake likely formed along the Laurentide Ice Sheet margin as it inundated Banks Island from Victoria Island sometime after ~30 ka BP (Lakeman and England, 2012; see Chapter 3). However, till was not observed overlying LFA 5 or 6 and the inferred genetic relationship with between LFA 5 and 6 and adjacent meltwater channels would seem to preclude this interpretation.

CONCLUSIONS

The observed lithofacies and lithofacies associations within this study negate several lithostratigraphic units proposed previously; including purported multiple tills (Vincent, 1982, 1983, 1990; Barendregt et al., 1998). Hence, the reinterpretation also rejects the elaborate climatostratigraphic interpretations and correlations that followed and that are widespread in the literature (Vincent, 1982, 1983, 1990; Vincent et al., 1984; Clark et al., 1984; Matthews et al., 1986; Barendregt et al., 1998). The reconstruction presented here documents a wide array of facies of both glacial and interglacial/interstadial affinity that can be amalgamated into three distinct intervals of sedimentation (i.e. successions). The first records the progradation of a delta, followed by fluvial aggradation of a braided river valley perhaps ~ 1 Ma ago. The second documents a glacier advance across a former marine delta more than 780,000 years ago. The third succession is interpreted to record sedimentation by an ice-contact delta into an ice-dammed lake during the last deglaciation, ~12,750 cal yr BP (Lakeman and England, 2012; see Chapter 3.

Given the absence of a robust chronology for much of the stratigraphy at Morgan Bluffs, it is premature to consider potential correlations across Banks Island, let alone more distant sites in the Canadian Arctic, as well as to Plio-Pleistocene deposits in Alaska or to marine sediment cores from the Arctic Ocean basin (Clark et al., 1984; Vincent et al., 1984). We emphasize the dismissal of previous correlations proposed for the Quaternary stratigraphic exposures across Banks Island, which were widely published (Vincent, 1982, 1983, 1990; Barendregt et al., 1998). A robust synthesis would require renewed sedimentological analyses of the diverse sediments reported at these sites, and their propensity in many areas to have been significantly glaciotectonized (Vaughan, 2012). More widespread mapping would allow the range of depositional environments to be precisely characterized, and the broad stratigraphic framework of the exposures to be clarified. A comprehensive perspective regarding the origin of Quaternary sediments on Banks Island will facilitate the identification of sediments with climatostratigraphic importance. These can then be strategically investigated and correlated to provide insights into the Quaternary paleoenvironmental evolution of the western Canadian Arctic and adjacent Arctic Ocean.

REFERENCES

Barendregt, R.W., Vincent, J.-S., Irving, E., Baker, J. 1998. Magnetostratigraphy of Quaternary and late Tertiary sediments on Banks Island, Canadian Arctic Archipelago. Canadian Journal of Earth Sciences 35, 147–161. doi:10.1139/e97-094.

Bennike, O., Böcher, J. 1990. Forest-tundra neighbouring the North Pole: plant and insect remains from the Plio-Pleistocene Kap København Formation, north Greenland. Arctic 43, 331–338.

Brigham-Grette, J., Carter, L.D. 1992. Pliocene marine transgressions of northern Alaska: circumarctic correlations and paleoclimatic interpretations. Arctic 45, 74–89.

CAPE – Last Interglacial Project Members. 2006. Last Interglacial Arctic warmth confirms polar amplification of climate change. Quaternary Science Reviews 25, 1383–1400. doi:10.1016/j.quascirev.2006.01.033.

Clark, D.L., Vincent, J.-S., Jones, G.A., Morris, W.A. 1984. Correlation of marine and continental glacial and interglacial events, Arctic Ocean and Banks Island. Nature 311, 147–149. doi:10.1038/311147a0.

Dowdeswell, J.A. 1987. Processes of glacimarine sedimentation. Progress in Physical Geography 11, 52–90. doi:10.1177/030913338701100103.

Evans, D.J.A. (Ed.) 2003. Glacial Landsystems. Arnold, London.

Evans, D.J.A., Benn, D.I. 2004. Facies description and the logging of sedimentary exposures. In Evans, D.J.A. and Benn, D.I. (Eds), A Practical Guide to the Study of Glacial Sediments. Arnold, London, 5–51.

Eyles, N., Eyles, C.H., Miall, A.D. 1983. Lithofacies types and vertical profile models; an alternative approach to the description and environmental interpretation of glacial diamict and diamictite sequences. Sedimentology 30, 393–410. doi:10.1111/j.1365-3091.1983.tb00679.x.

French, H.M. 1976. The Periglacial Environment. Longman, London, 309 pp.

Funder, S., Bennike, O., Bocher, J., Israelson, C., Strand Petersen, K., Simonarson, L..A. 2001. Bulletin of the Geological Society of Denmark 48, 117–134.

Fyles, J.G. 1990. Beaufort Formation (Late Tertiary) as seen from Prince Patrick Island, Arctic Canada. Arctic 43, 393–403.

Fyles, J.G., Hills, L.V., Matthews, J.V., Jr., Barendregt, R., Baker, J., Irving, E., Jetté, H. 1994. Ballast Brook and Beaufort Formations (Late Tertiary) on northern Banks Island, Arctic Canada. Quaternary International 22/23, 141–171. doi:10.1016/1040-6182(94)90010-8.

Fyles, J.G., McNeil, D.H., Matthews, J.V., Barendregt, R.W., Marincovich, L., Brouwers, E., Bednarski, J., Brigham-Grette, J., Ovenden, L.W., Miller, K.G., Baker, J., Irving, E.

1998. Geology of Hvitland beds (Late Pliocene), White Point lowland, Ellesmere Island, Northwest Territories. Geological Survey of Canada Bulletin 512, 35pp.

Kaufman, D.S., Brigham-Grette, J. 1993. Aminostratigraphic correlations and paleotemperature implications, Pliocene-Pleistocene high-sea-level deposits, northwestern Alaska. Quaternary Science Reviews 12, 21–33. doi:10.1016/0277-3791(93)90046-O.

Kaufman, D.S., Ager, T.A., Anderson, N.J., Anderson, P.M., Andrews, J.T., Bartlein, P.J., Brubaker, L.B., Coats, L.L., Cwynar, L.C., Duvall, M.L., Dyke, A.S., Edwards, M.E., Eisner, W.R., Gajewski, K., Geirsdottir, A., Hu, F.S., Jennings, A.E., Kaplan, M.R., Kerwin, M.W., Lozhkin, A.V., MacDonald, G.M., Miller, G.H., Mock, C.J., Oswald, W.W., Otto-Bleisner, B.L., Porinchu, D.F., Ruhland, K., Smol, J.P., Steig, E.J., Wolfe, B.B., 2004. Holocene thermal maximum in the western Arctic (0-180°W). Quaternary Science Review 23, 529–560. doi:10.1016/j.quascirev.2003.09.007.

Lakeman, T.R., England, J.H. 2012. Paleoglaciological insights from the age and morphology of the Jesse till and adjacent deposits, western Canadian Arctic. Quaternary Science Reviews 47, 82–100. doi:10.1016/j.quascirev.2012.04.018.

Lakeman, T.R., England, J.H. The extent of Late Wisconsinan ice cover and the nature of postglacial relative sea level change on western Banks Island, Canadian Arctic Archipelago, submitted for publication.

Matthews, J.V., Jr., Ovenden, L.E. 1990. Late Tertiary plant macrofossils from localities in Arctic/Subarctic North America: a review of the data. Arctic 43, 364–392.

Matthews, J.V., Jr., Mott, R.J., Vincent, J.-S. 1986. Preglacial and interglacial environments of Banks Island: pollen and macrofossils from Duck Hawk Bluffs and related sites. Géographie physique et Quaternaire 40, 279–298.

Peltier, W.R., Fairbanks, R.G. 2006. Global glacial ice volume and Last Glacial Maximum duration from an extended Barbados sea level record. Quaternary Science Reviews 25, 3322–3337. doi:10.1016/j.quascirev.2006.04.010.

Powell, R.D. 1990. Glacimarine processes and grounding-line fans and their growth to ice their growth to ice-contact deltas. In: Dowdeswell, J.A., Scourse, J.D. (Eds.), Glacimarine Environments: Processes and Sediments. Geological Society, London, Special Publication 53, 53–73.

Powell, R.D. 2003. Subaquatic landsystems; fiords. In Evans, D.J.A. (Ed.), Glacial Landsystems, London, 313–347.

Powell, R.D., Domack, 1995. Modern glaciomarine environments. In: Menzies, J. (Ed.), Glacial Environments. Volume 1: Modern Glacial Environments: Processes, Dynamics and Sediments. Butterworth-Heinemann, Oxford, 445–486.

Reading, H.G. (Ed.) 1986. Sedimentary Environments and Facies. Oxford, Blackwell.

Vaughan, J.M. 2012. Quaternary glacial and sea level history of south Banks Island, NT, Canada. Abstract #247. XVIII International Union of Quaternary Research (INQUA) Congress, Bern, Switzerland, July 21–27, 2011.

Vincent, J.-S. 1982. The Quaternary history of Banks Island, NWT, Canada. Géographie physique et Quaternaire 36, 209–232.

Vincent, J.-S. 1983. La géologie du Quaternaire et la géomorphologie de l'Île Banks, Arctique Canadien. Geological Survey of Canada, Memoir 405.

Vincent, J.-S. 1984. Quaternary stratigraphy of the western Canadian Arctic Archipelago. In: Fulton, R.J. (Ed.), Quaternary Stratigraphy of Canada – A Canadian Contribution To IGCP Project 24. Geological Survey of Canada Paper, 84-10, pp. 87–100.

Vincent, J.-S. 1990. Late Tertiary and Early Pleistocene deposits and history of Banks Island, southwestern Canadian Arctic Archipelago. Arctic 43, 339–363.

Vincent, J.-S., Occhietti, S., Rutter, N., Lortie, G., Guilbault, J.-P., de Boutray, B. 1983. The late-Tertiary – Quaternary stratigraphic record of the Duck Hawk Bluffs, Banks Island, Canadian Arctic Archipelago. Canadian Journal of Earth Sciences 20, 1694–1712. doi:10.1139/e83-160.

Vincent, J.-S., Morris, W.A., Occhietti, S. 1984. Glacial and nonglaical sediments of Matuyama paleomagnetic age on Banks Island, Canadian Arctic Archipelago. Geology 12, 139–142. doi:10.1130/0091-7613(1984)12<139:GANSOM>2.0.CO;2.

Walker, R.G. 1992. Facies, facies models and modern stratigraphic concepts. In: Walker, R.G. and James, N.P. (Eds.), Facies Models: Response to Sea-level Change. Geological Association of Canada, Toronto, pp. 1–14.

Table. 4.1 Stratigraphic framework for Quaternary sediments on Banks Island, after Vincent (1990).

Chronlogy		Ma	Geological Events			Lithostratigraphy: North Zone (surficial geology)	East Zone (Morgan & Nelson River bluffs)	West Zone (Worth Point & Duck Hawk bluffs)
Holocene			Postglacial			Organic, eolian, alluvial, marine, and colluvial sediments		
Late Pleistocene	Late Wisconsinan	0.01	Amundsen Glaciation	Russell Stade	Prince of Wales Fm.		Schuyter Point Sea sediments Viscount Mellive Sound Ice Shelf moraine	
	Early Wisconsinan			M'Clure Stade		Investigator Sea and Meek Point Sea sediments Bar Harbour and Mercy till	East Coast Sea sediments Jesse till	Carpenter till Meek Point Sea sediments Sachs till
						Pre Amundsen Sea sediments		
	Sangamonian		Cape Collinson Interglaciation			Cape Collinson Fm.		
Middle Pleistocene		0.13	Thomsen Glaciation		Nelson River Fm.	Big Sea sediments Baker till	Big Sea sediments Kellett, Baker, and Kange till Pre Thomsen Sea sediments	Big Sea sediments Kellett till
Early Pleistocene	*Bruhnes* *Matuyama*	0.78	Morgan Bluffs Interglaciation			Morgan Bluffs Fm.		
			Banks Glaciation		Duck Hawk Bluffs Fm.	Bernard and Plateau till	Post Banks Sea sediments Bernard and Plateau till Pre Banks Sea sediments	Post Banks Sea sediments Bernard and Durham Heights till Pre Banks Sea sediments
			Interglaciation or Preglacial					Worth Point Fm.

Table. 4.2 Stratigraphic framework for Quaternary sediments on Banks Island, after Barendregt (1998).

Chronology		Ma	Geological Event		Worth Point Bluffs	Duck Hawk Bluffs	Nelson River Bluffs	Morgan Bluffs
					Stratigraphic Exposure			
Holocene			Postglacial		Colluvium	Colluvium	Colluvium	Colluvium
Late Pleistocene	Late Wisconsinan	0.01	Amundsen Glaciation	Russell Stade				
Late Pleistocene	Early Wisconsinan		Amundsen Glaciation	M'Clure Stade		*Prince of Wales Fm.* Sachs till Pre-Amundsen Sea sediments	*Prince of Wales Fm.* Jesse till Pre-Amundsen Sea sediments	*Prince of Wales Fm.* Jesse till
Late Pleistocene	Sangamonian		Cape Collinson Interglaciation			*Cape Collinson Fm.* Organics	*Cape Collinson Fm.* Organics	
Middle Pleistocene		0.13	Thomsen Glaciation		*Nelson River Fm.* Big Sea sediments	*Nelson River Fm.* Big Sea sediments	*Nelson River Fm.* Big Sea sediments Kellet till	*Nelson River Fm.* Kellet till Pre-Thomsen Sea sediments
Middle Pleistocene			Unnamed Interglaciation			Organics	Organics	
Middle Pleistocene			Unnamed Glaciation				Unnamed till and marine sediments	
Middle Pleistocene / Early Pleistocene	*BRUNHES* *MATUYAMA*	0.78	Unnamed Interglaciation			Colluvium		
Early Pleistocene			Unnamed Glaciation					Marine sediments Glaciofluvial gravels Till Marine sediments
Early Pleistocene	*Jaramillo*	0.99	Morgan Bluffs Interglaciation					Organic sands and gravels
Early Pleistocene		1.07	Up to 4 Glaciations, including the Banks Glaciation		*Duck Hawk Bluffs Fm.* Colluviated Bernard till	*Duck Hawk Bluffs Fm.* Post-Banks Sea sediments Bernard till Pre-Banks Sea sediments	*Duck Hawk Bluffs Fm.* Bernard till and 3 other tills	*Duck Hawk Bluffs Fm.* Post-Banks Sea sediments Bernard till and glaciomarine sed. Pre-Banks Sea sediments
Early Pleistocene	*Olduvai*	1.61 1.77 1.95	Interglaciation or Preglacial		*Worth Point Fm.* Organic Silt Colluvium	*Worth Point Fm.* Eolian sediments		

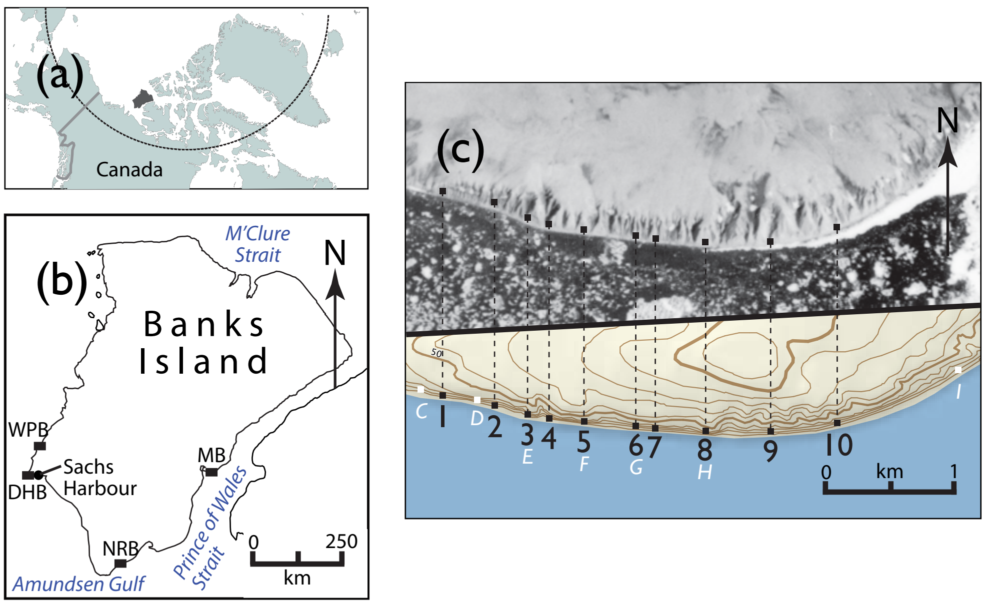

Figure 4.1. (a) The location of Banks Island (shaded) within the Canadian Arctic Archipelago. (b) The location of Morgan Bluffs (MB), Nelson River Bluffs (NRB), Worth Point Bluffs (WPB) and Duck Hawk Bluffs (DHB) across southern Banks Island. (c) Stratigraphic exposures at Morgan Bluffs shown on an aerial photograph (above) and a topographic map (below). Black numbers and boxes correspond to stratigraphic exposures described in text. Those identified and characterized by Vincent (1982, 1983) and Barendregt et al. (1998) are denoted by the white letters and boxes.

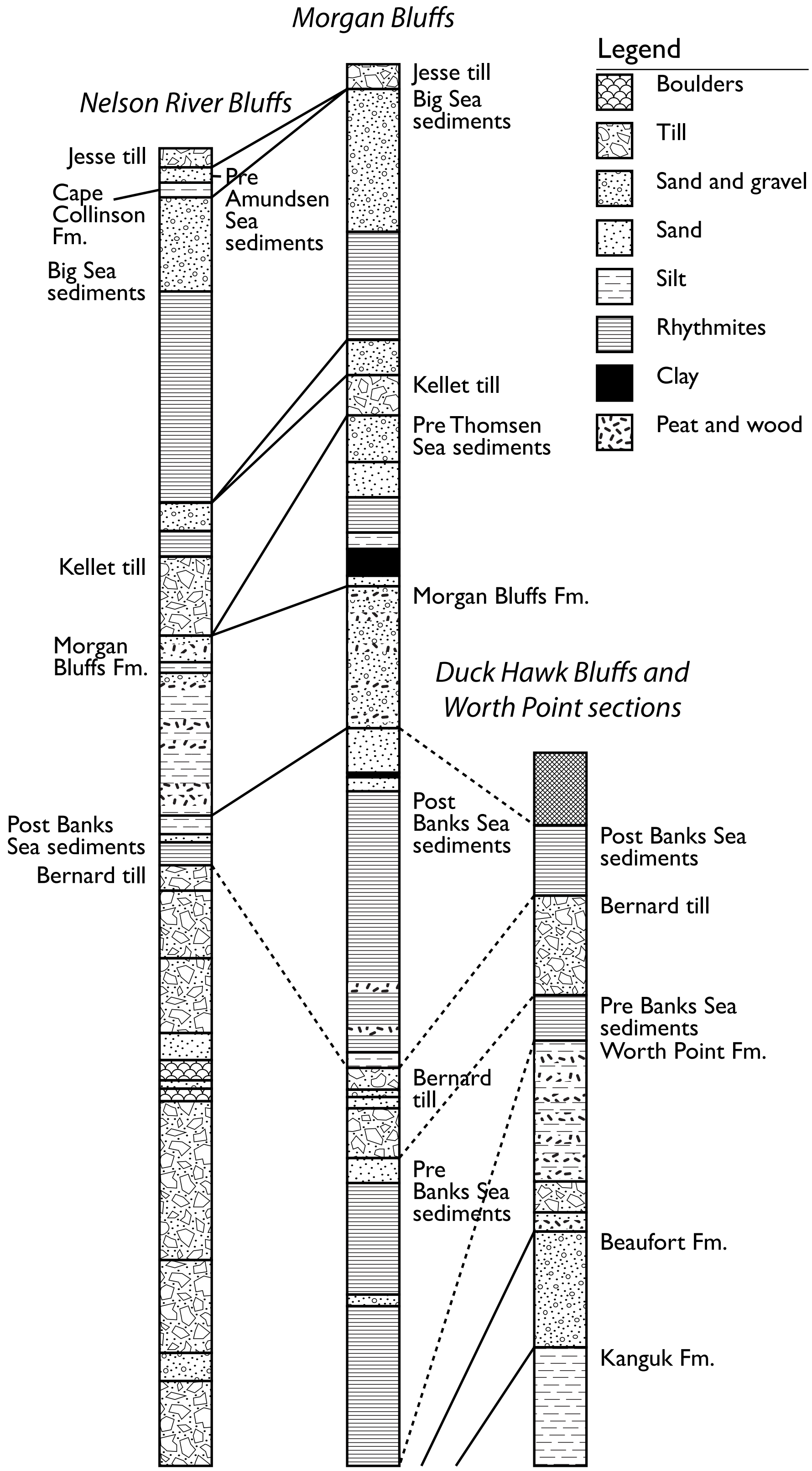

Figure 4.2. Composite stratigraphy for Nelson Bluffs, Morgan Bluffs, Duck Hawk Bluffs, and Worth Point Sections, after Vincent (1982).

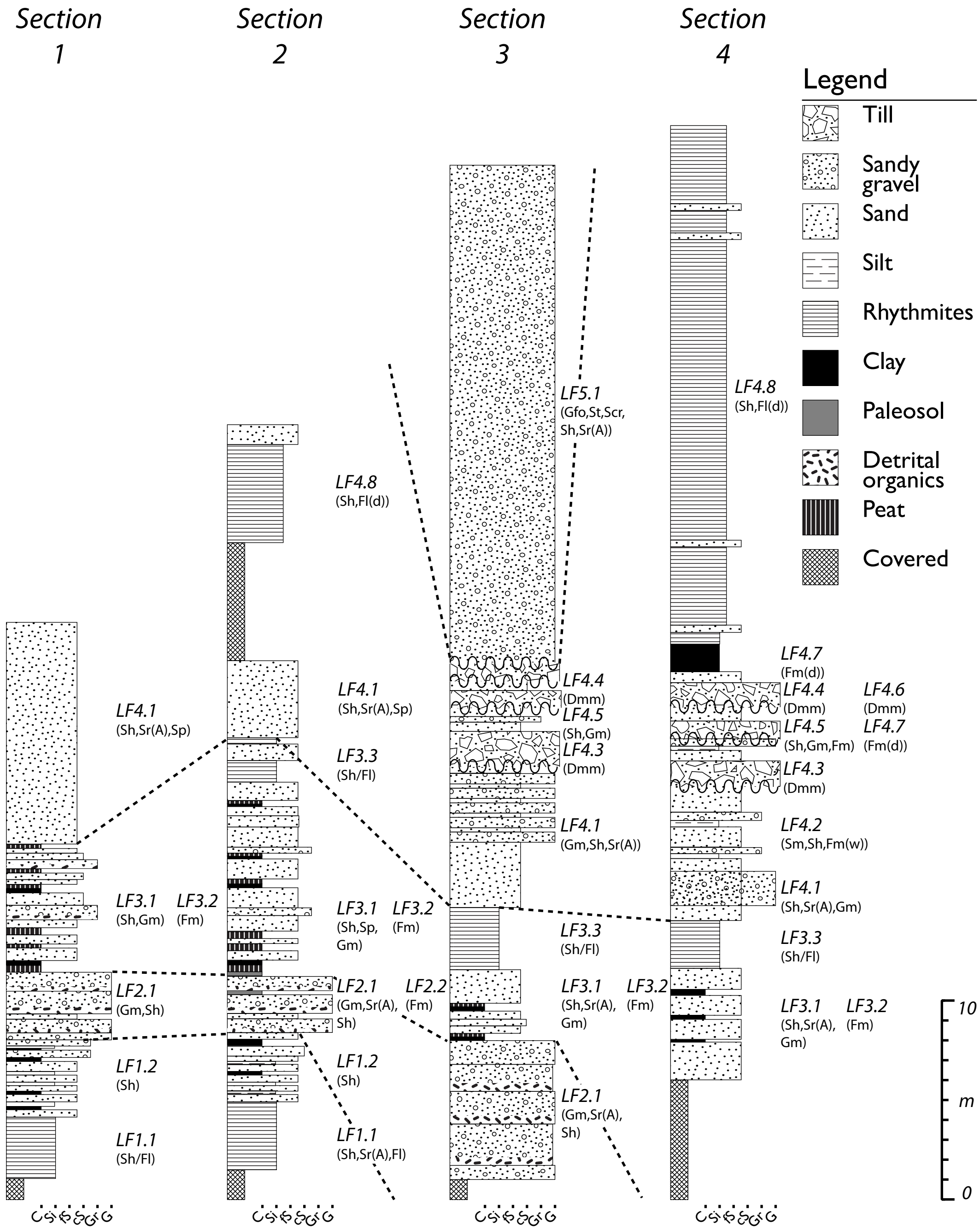

Figure 4.3a. Lithofacies (LF) and lithofacies associations (LFA) comprising the stratigraphy of Sections 1 to 4 at Morgan Bluffs. Locations of Sections 1 to 4 are shown on Figure 4.1. Lithofacies codes follow those in Evans and Benn (2004).

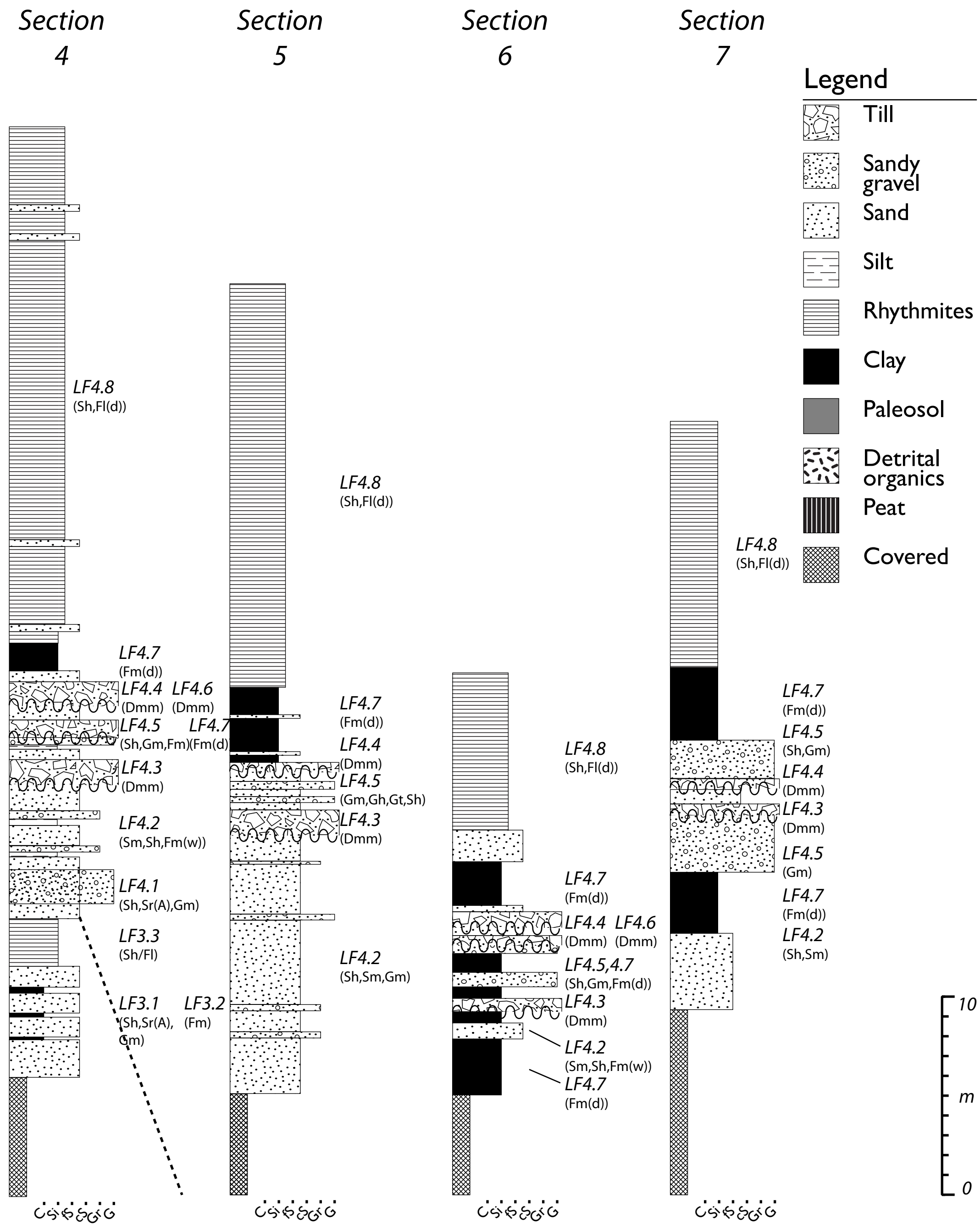

Figure 4.3b. Lithofacies (LF) and lithofacies associations (LFA) comprising the stratigraphy of Sections 4 to 7 at Morgan Bluffs. Locations of Sections 4 to 7 are shown on Figure 4.1. Lithofacies codes follow those in Evans and Benn (2004).

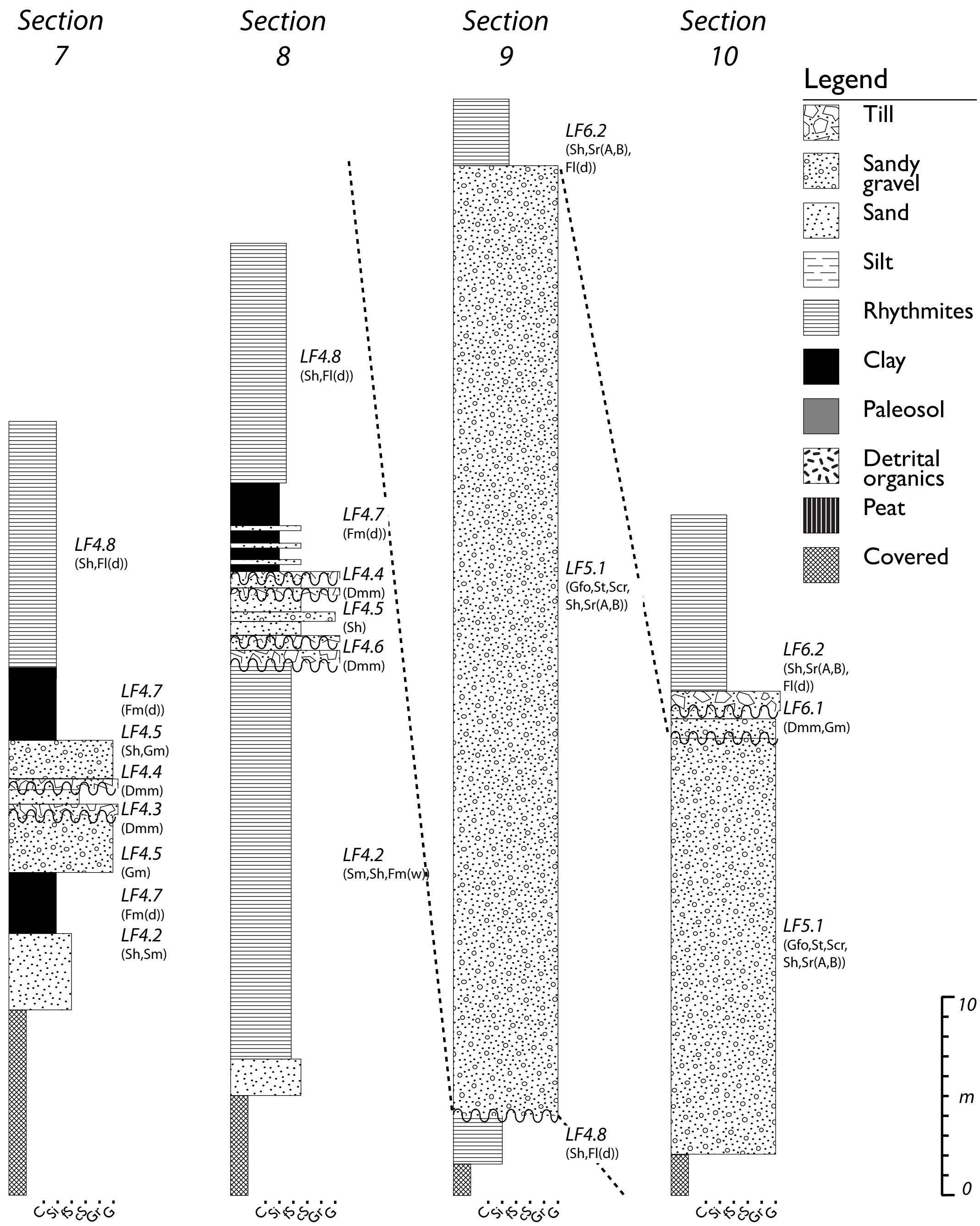

Figure 4.3c. Lithofacies (LF) and lithofacies associations (LFA) comprising the stratigraphy of Sections 7 to 10 at Morgan Bluffs. Locations of Sections 7 to 10 are shown on Figure 4.1. Lithofacies codes follow those in Evans and Benn (2004).

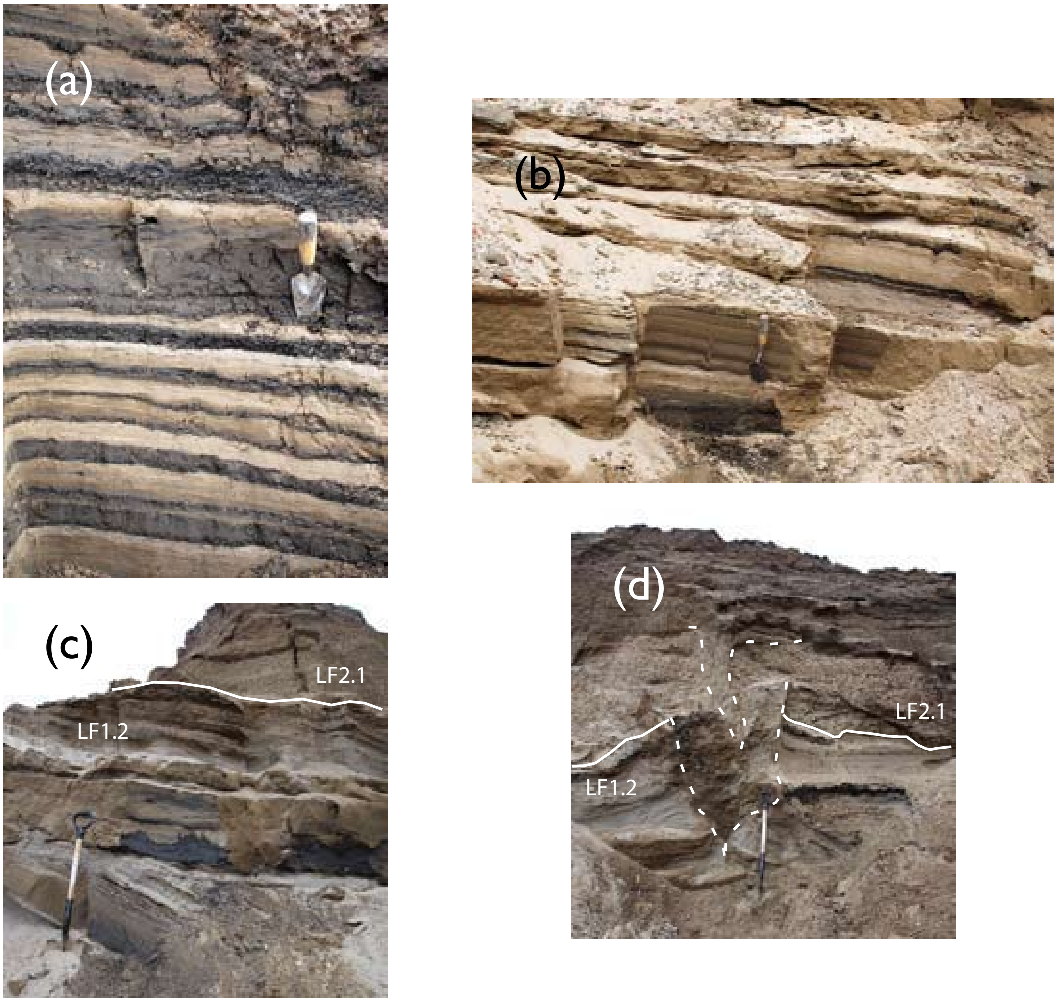

Figure 4.4. **(a)** Lithofacies 1.1 (LF1.1); rhythmically-bedded horizontally- and cross-laminated sand and horizontally-laminated silty clay. **(b)** Lithofacies 1.2 (LF1.2); interbedded massive mud with widespread flame structures; normally-graded, horizontally- and cross-laminated sandy mud; horizontally-laminated, medium to coarse sand beds with fine to medium pebble lenses and stringers; and cross-laminated coarse sand and gravel lenses. **(c)** Sharp, erosional contact (marked by solid white line) between LF1.2 and LF2.1 at Section 2. Note the high angle of dip of some beds comprising LF1.2. **(d)** Two ice wedge casts (delineated by dashed white line) obscuring the deformed contact between LF1.2 and LF2.1 at Section 2.

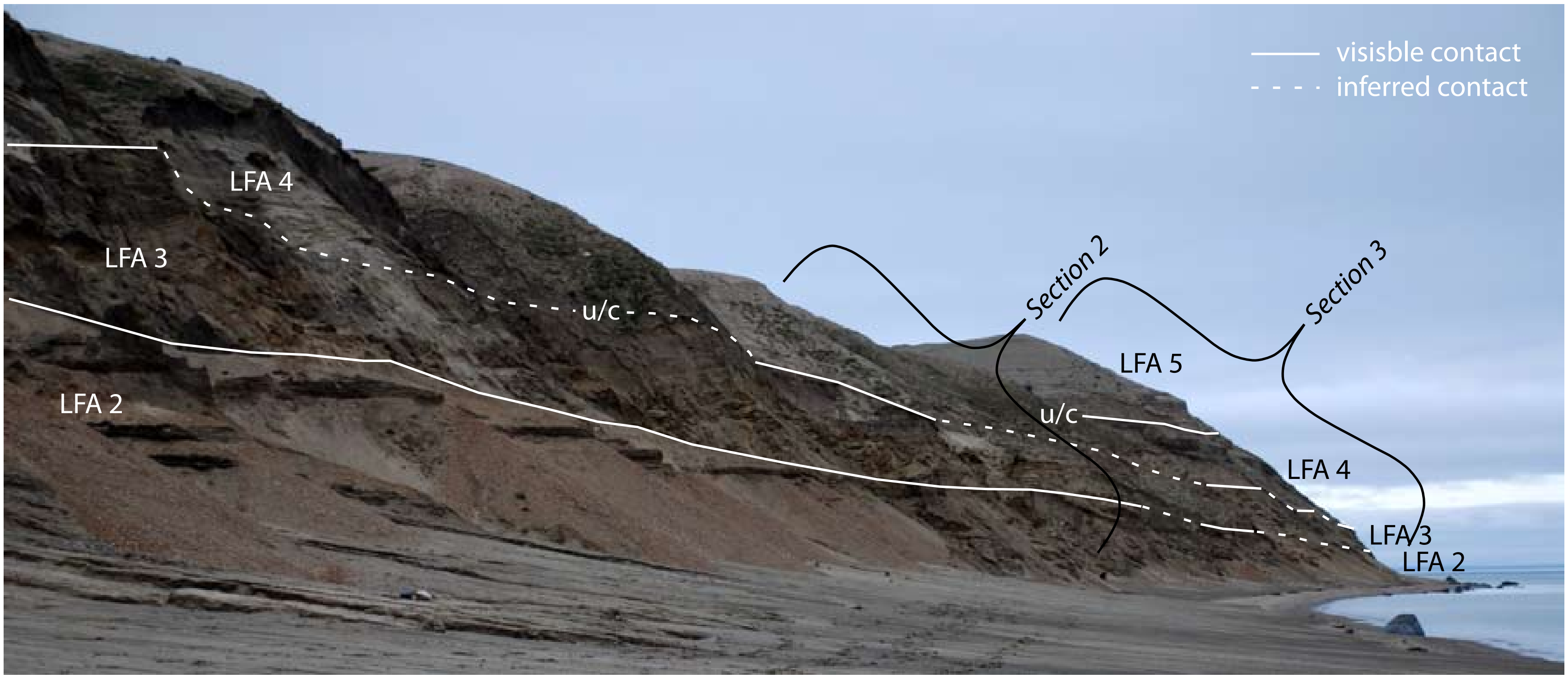

Figure 4.5. Photograph of Morgan Bluffs showing the geometry of LFA 2 to 5 in the vicinity of Sections 2 and 3. The contact between LFA 2 and 3 is conformable. The contact between LFA 3 and 4 is erosional, displaying an irregular, undulose geometry, and thus unconformable (u/c). Similarly, the erosional contact between LFA 4 and 5 represents an unconformity, as demonstrated in Section 3 where LF 4.8 is absent.

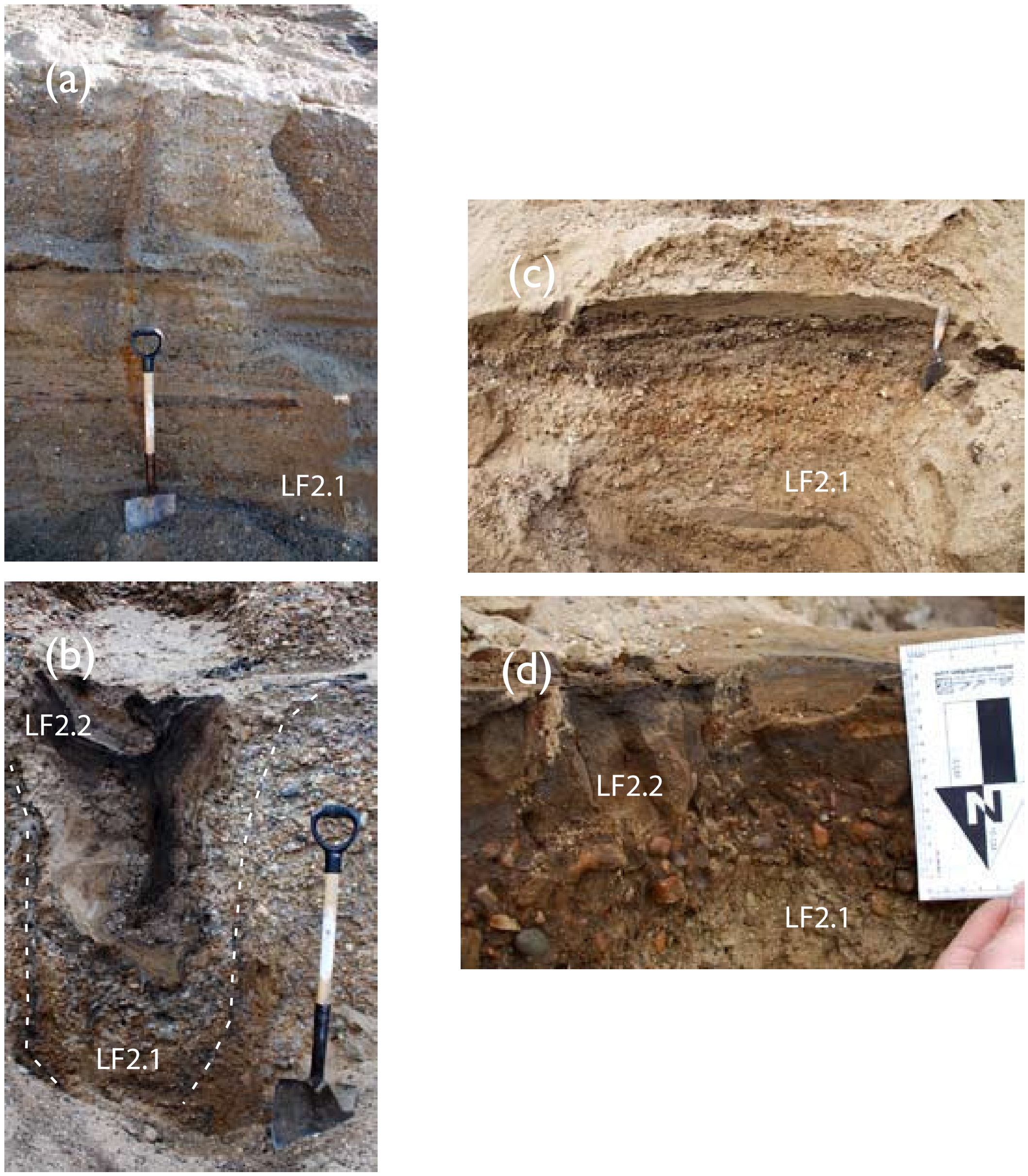

Figure 4.6. **(a)** Lithofacies 2.1 (LF2.1); massive to weakly-stratified, clast-supported, sandy gravel interbedded with horizontally-laminated, cross-laminated, and rarely planar crossbedded stony medium sand lenses. **(b)** Ice wedge cast within LF2.1, which is outlined by deformed sand, gravel, and peat. The boundary of the ice wedge is delineated by the dashed white line. **(c)** Rare cross-bedding within the sandy gravel comprising LF2.1. **(d)** Lithofacies 2.2 (LF2.2); dark grey, sandy and stony clay horizons.

Figure 4.7. Photograph of Section 2 showing an involuted paleosol (LF2.2) within fluvial gravel (LF2.1). Also visible are two ice wedge casts (delineated by the dashed white line). The right-most ice wedge cast is vertically nested in a chevron pattern and is, thus, likely syngenetic.

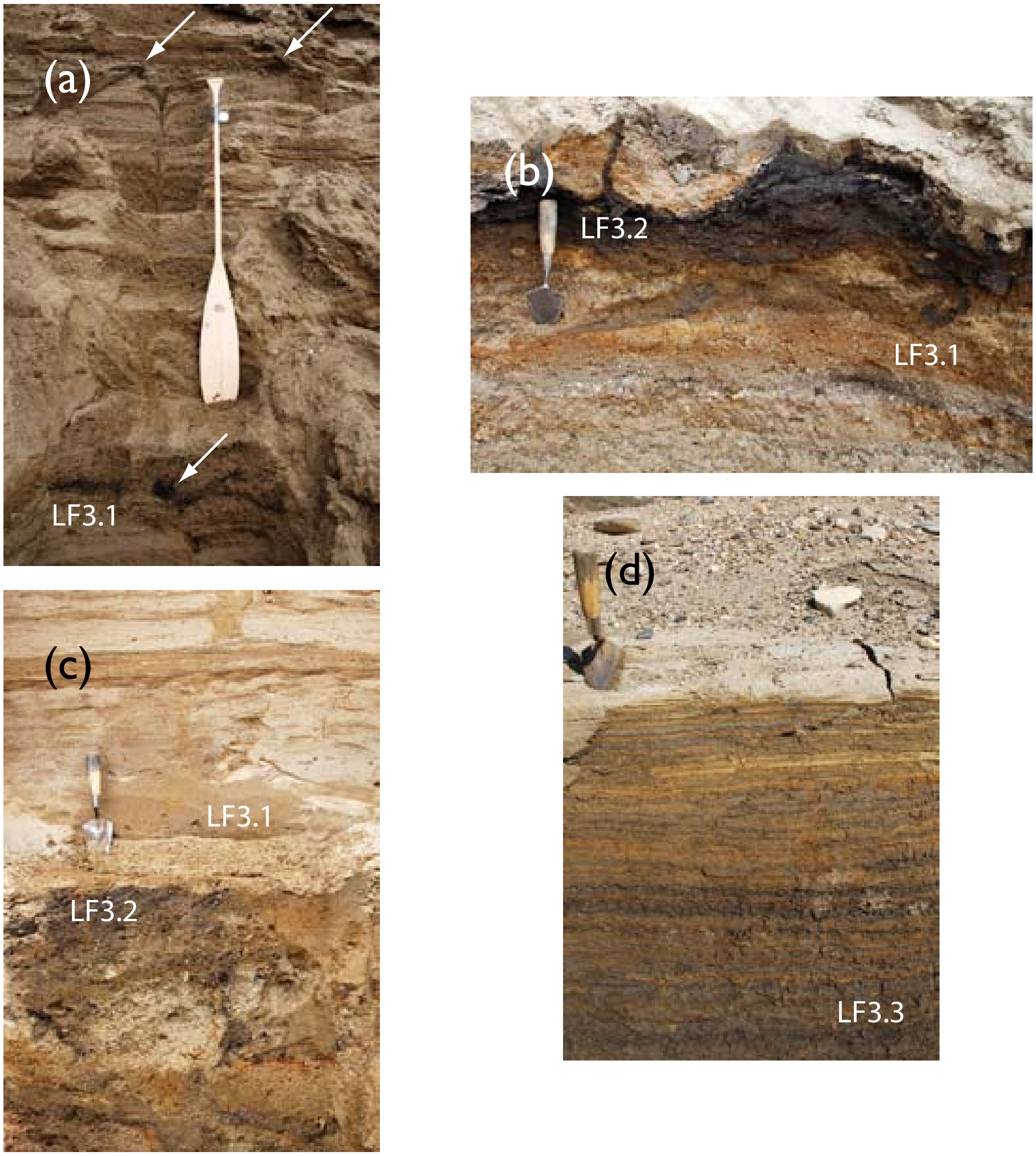

Figure 4.8. **(a)** Lithofacies 3.1 (LF3.1); horizontally- and cross-laminated, stony and well-sorted medium to coarse sand beds interbedded with massive to weakly-stratified sandy fine to medium pebble gravel. Note the peat rip-up clasts (arrows) and truncated ice wedge (left of paddle) that is over 2 m long. **(b)** Lithofacies 3.2 (LF3.2); peat horizon deformed by overlying sand and gravel. **(c)** LF3.2; stony clay horizon overlain by LF3.1. **(d)** Lithofacies 3.3 (LF3.3); rhythmically bedded silty mud and fine to medium sand.

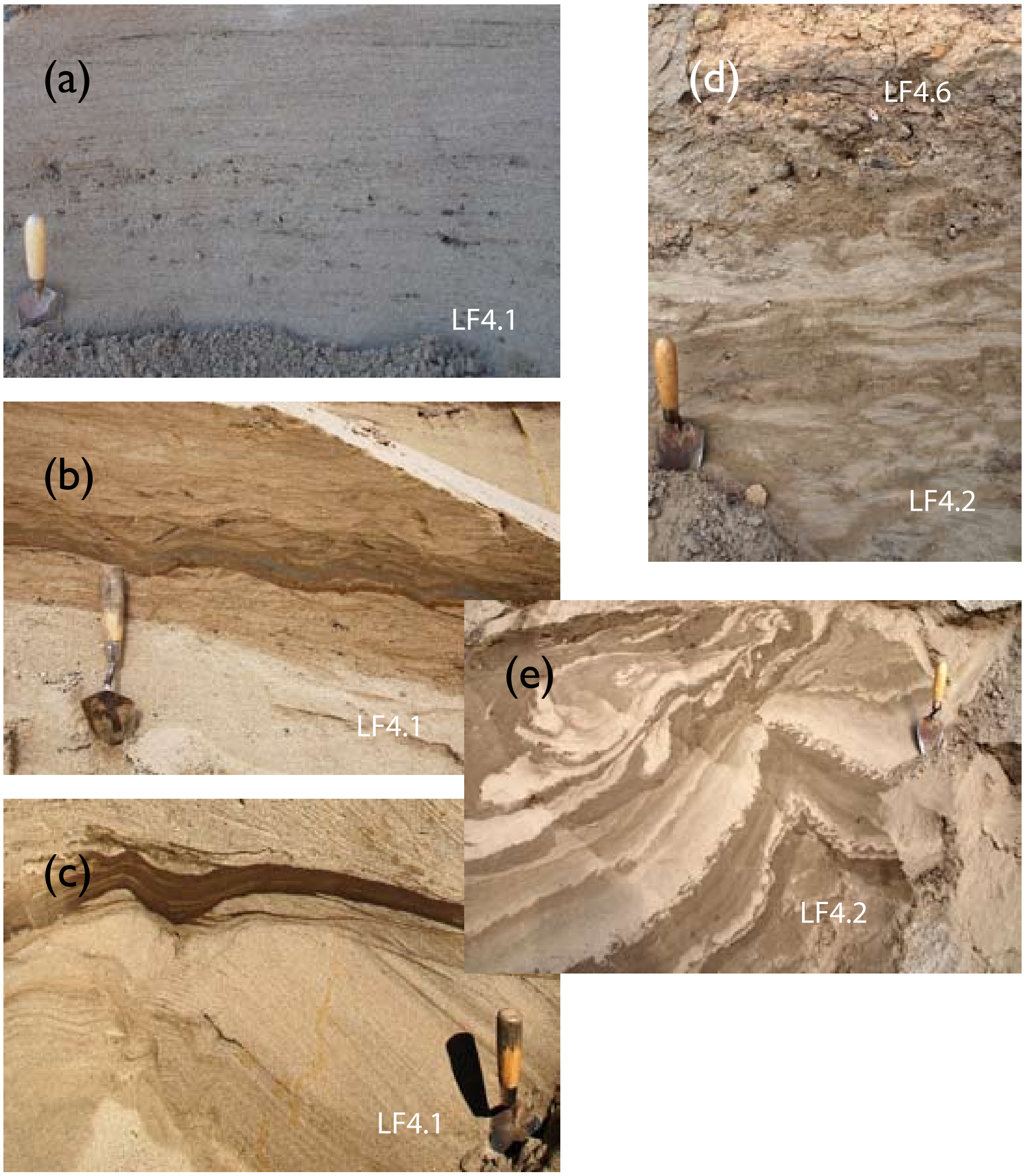

Figure 4.9. **(a-c)** Lithofacies 4.1 (LF4.1); well-sorted, stony medium sand beds displaying a wide range of current structures, including horizontal-, cross-, and trough cross-laminations and convolute bedding. Sand beds are occasionally interbedded with massive to weakly stratified sandy medium to coarse pebble gravel lenses. **(d)** Lithofacies 4.2 (LF4.2); interbedded fine to medium sand and silt couplets. The bedding in this exposure has been deformed by the subsequent deposition of the overlying, poorly-sorted gravel lense comprising Lithofacies 4.6 (LF4.6). **(e)** Interbedded fine to medium sand and silt couplets, comprising LF4.2, which exhibits widespread flame and loading structures.

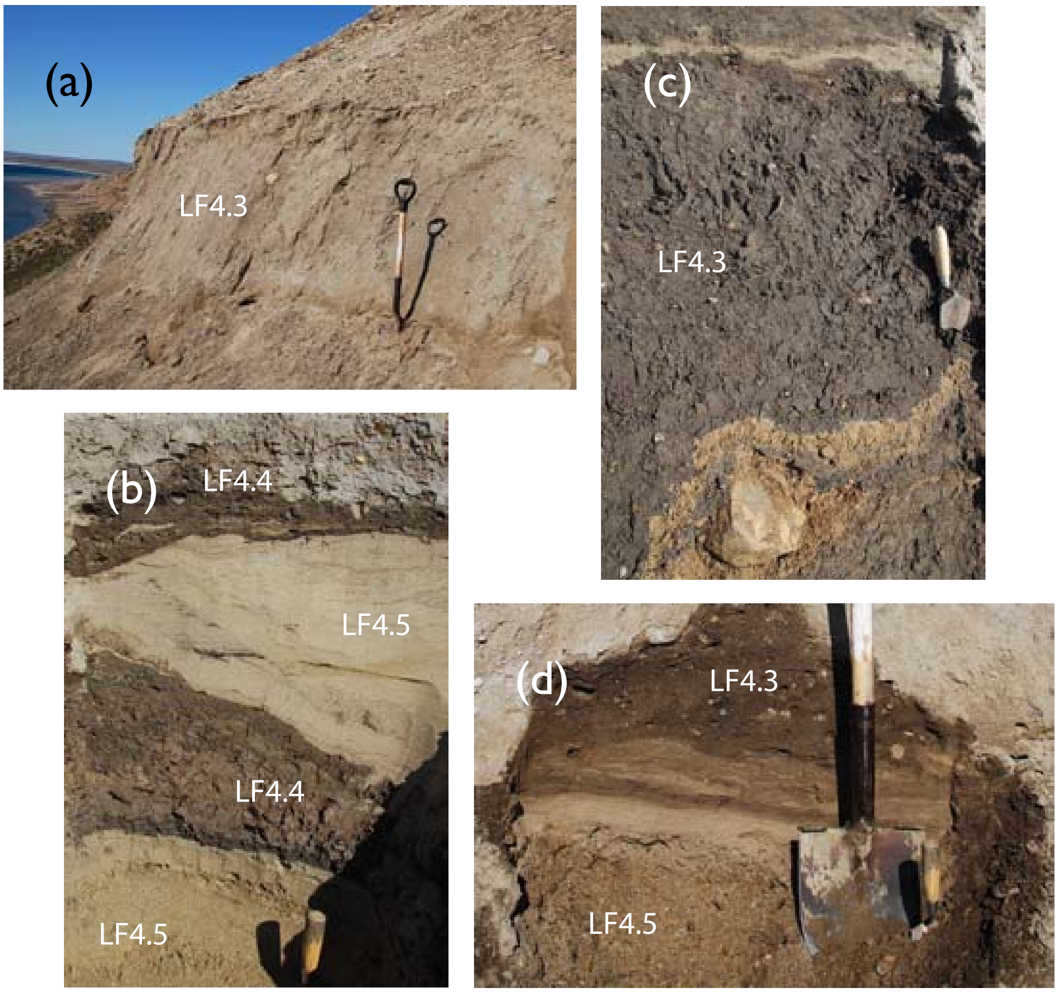

Figure 4.10. **(a)** Lithofacies 4.3 (LF4.3); matrix-supported, clay-rich diamict. **(b)** Diamict lenses of LF4.4 interfingering with sand beds of Lithofacies 4.5 (LF4.5). Note the crude stratification in the diamicts and the dark grey clay rip-up clasts within the uppermost exposure of LF4.5. **(c)** A deformed sand intraclast and boulder within a diamict of LF4.3. **(d)** LF4.3 overlying massive sandy gravel and horizontally-laminated medium sand and silt of LF4.5 The lower contact of LF4.3 is marked by a glacitectonite made up of deformed sands originating from LF4.5.

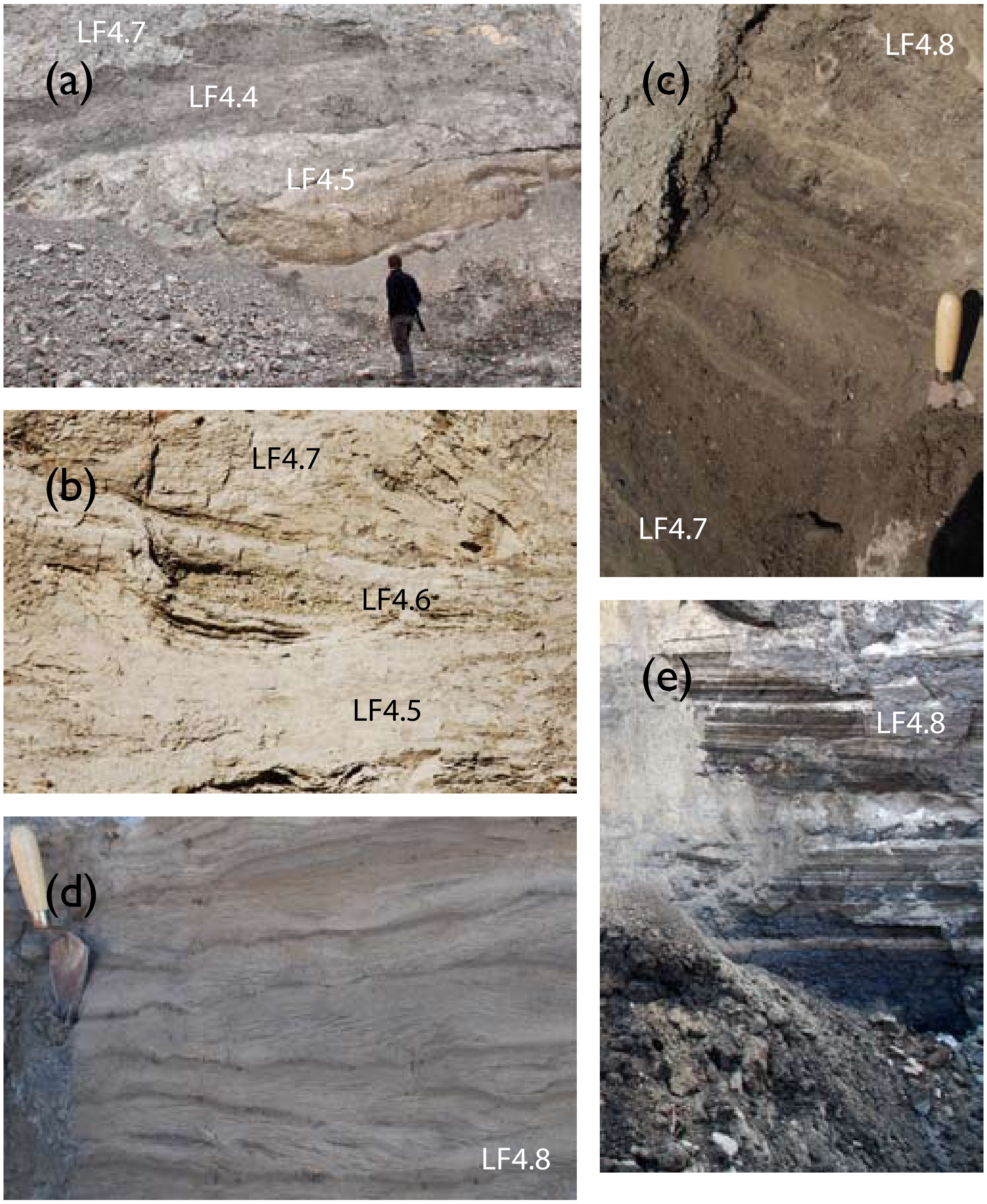

Figure 4.11. **(a)** Lithofacies 4.5 (LF4.5), stratified, sandy gravel lense overlain by stony medium sand and silt. LF4.4 (clayey diamict) overlies the sand and gravel and has been deformed. Stony mud (LF4.7) overlies LF4.4. **(b)** Poorly sorted, massive sandy gravel lense (LF4.6) within stony sand (LF4.5), and overlain by stony mud (LF4.7). **(c)** Lithofacies 4.7 and 4.8 (LF4.7 and LF4.8); massive, stony and sandy mud (LF4.7) overlain by weakly-stratified sandy silt with dropstones (LF4.8). **(d)** Lithofacies 4.8 (LF4.8); ripple cross-laminated medium sand and massive to horizontall-laminated fine sand to silt couplets. **(e)** LF4.8; rhythmites composed of massive to horizontally-laminated silt interbedded with mud. Note the occurance of a rare, thick, horizontally-laminated sand bed at the top of the photo.

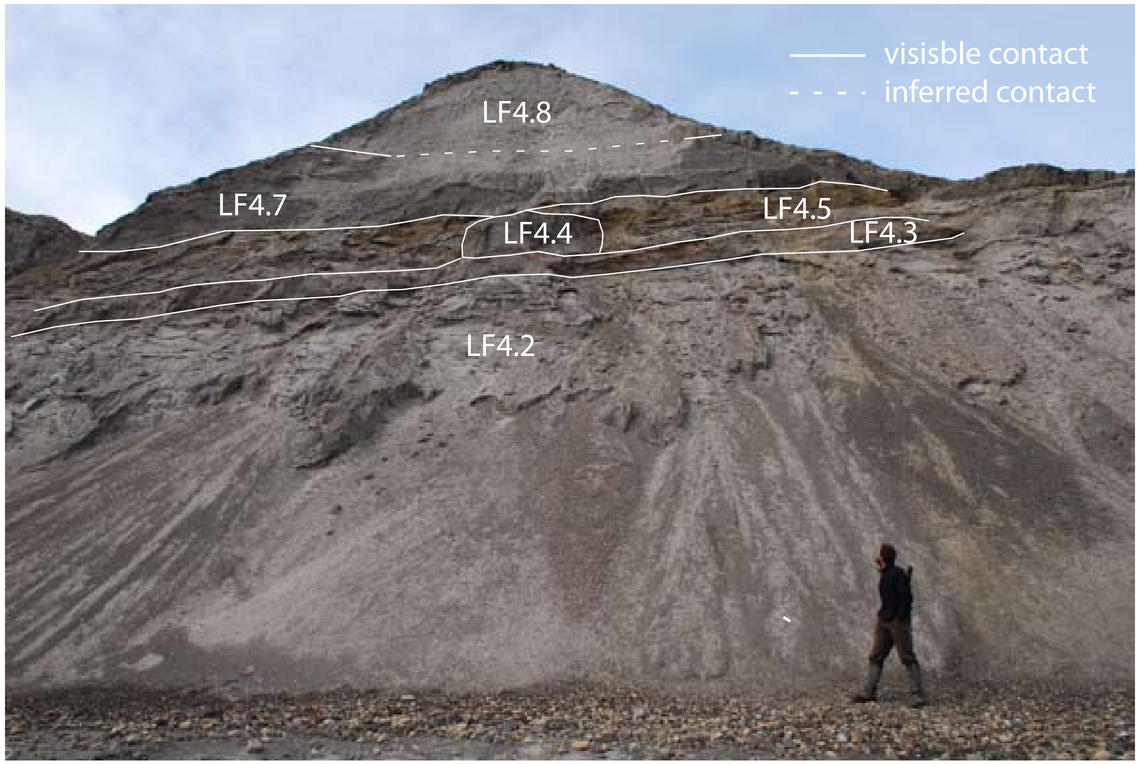

Figure 4.12. Photograph of Section 7 showing the stratigraphic distribution of Lithofacies (LF) 4.2, 4.3, 4.4, 4.5, 4.7, and 4.8. LF4.3 and LF4.5 are traceable laterally from Section 3 to 8 (see Fig. 4.3).

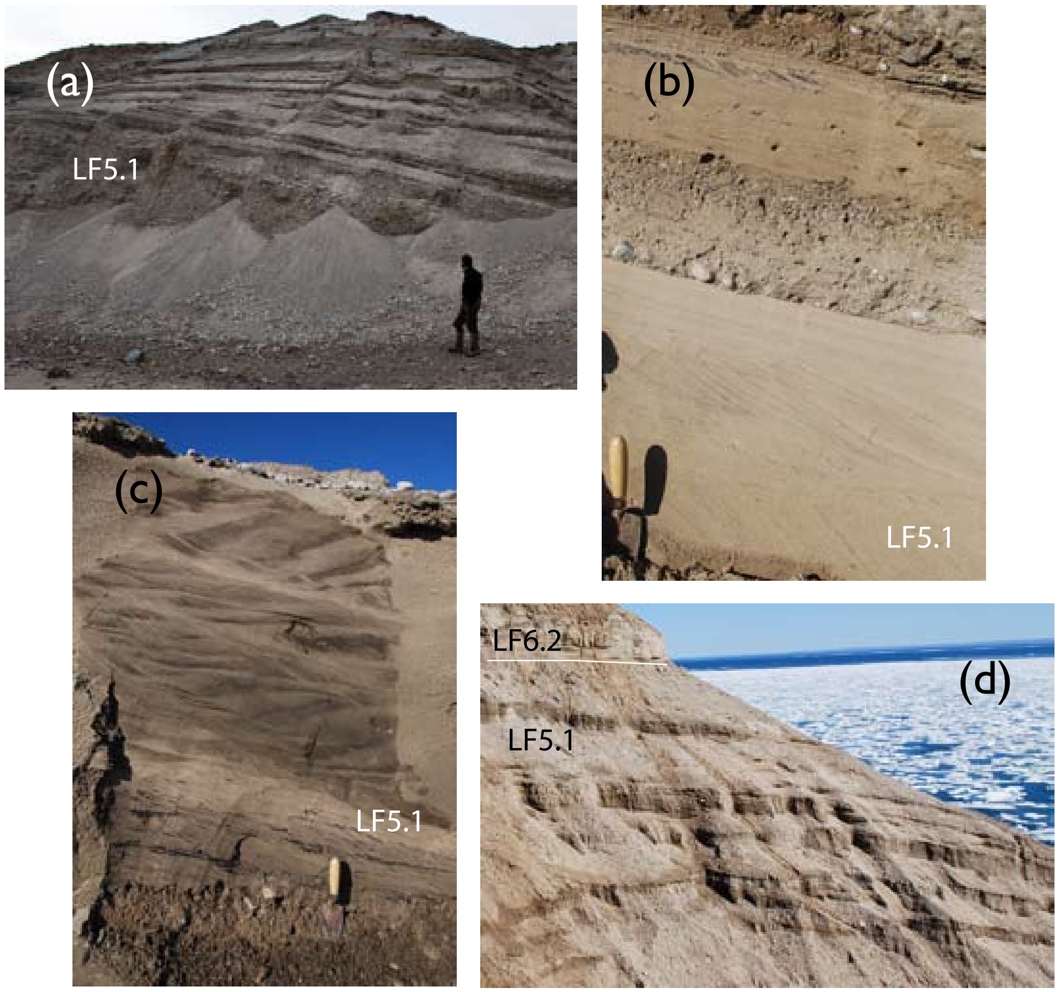

Figure 4.13. **(a)** Stratified sand and gravel comprising Lithofacies 5.1 (LF5.1). Note the ~2 m thick, massive to weakly-stratified, sandy gravel bed at the base of LF5.1. **(b)** A cross-lamintated, medium sand bed overlain by a normally-graded sandy fine gravel bed, which is overlain by a stony, medium to coarse sand bed that is horizontally-, cross-, and trough cross-laminated **(c)** Climbing ripples within LF5.1. **(d)** Stratified sand and gravel of LF5.1, which dips to the southeast at about 10º, conformably overlain by rhythmically-bedded sand and silt of Lithofacies 6.2 (LF6.2). Contact is delineated by the white line.

Figure 4.14. Photograph of LFA 5 and LFA 6 in Section 9 (to the left) unconformably (u/c) overlying LFA 4 in Section 8 (to the right). View is to the south.

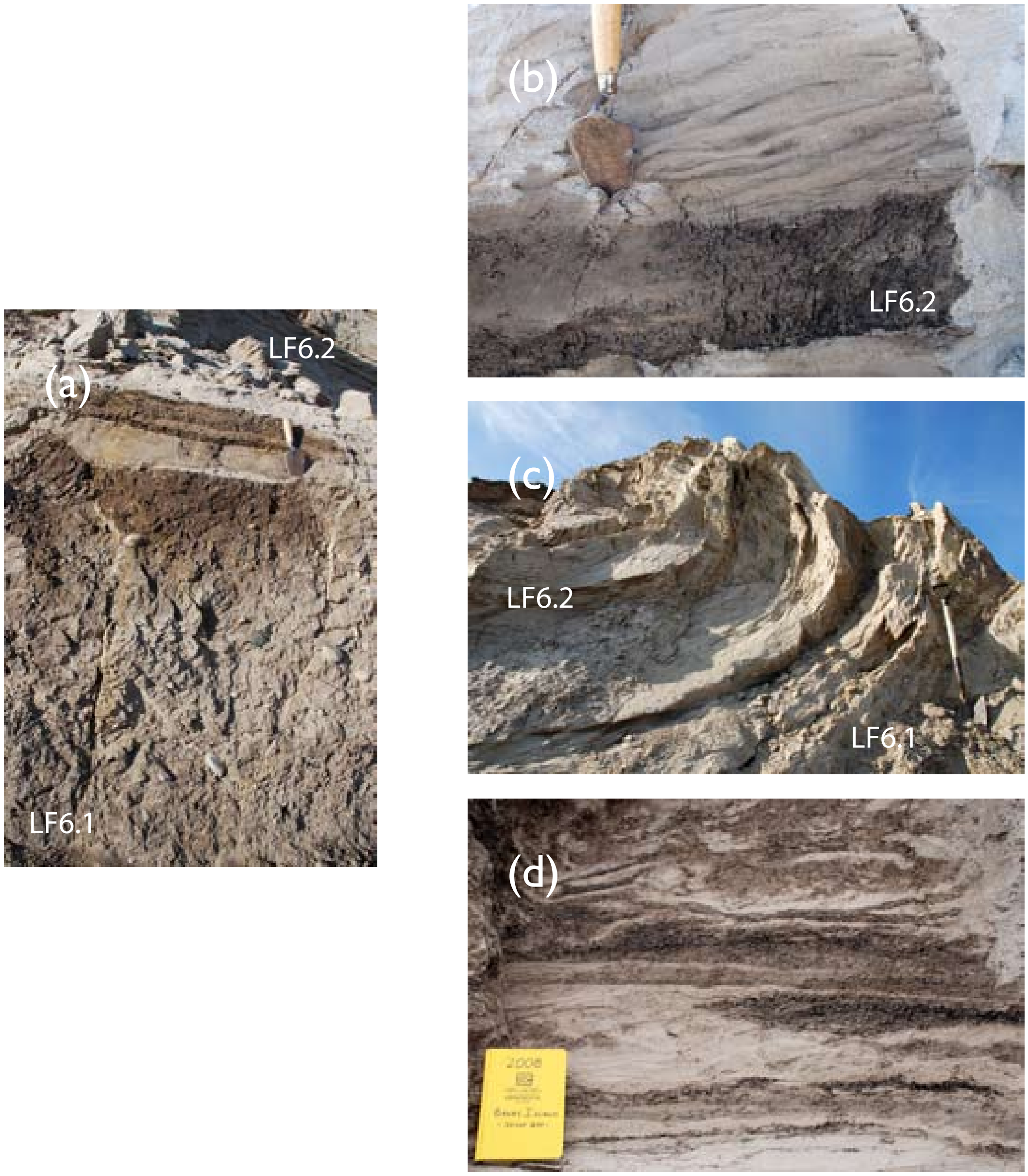

Figure 4.15. **(a)** Lithofacies 6.1 (LF6.1); a massive clayey diamict that is crudely normally-graded, overlain by a horizontally-laminated medium sand bed and inter-bedded, horizontally-laminated silt and mud. Lithofacies 6.2 (LF6.2), composed of sandy rhythmites with rare mud beds, overlies LF6.1. **(b)** A massive mud bed overlain by ripple cross-laminated fine sand within LF6.2. **(c)** An example of an overturned fold within LF6.1 and LF6.2. **(d)** An outcrop of deglacial glaciolacustrine sediment approximately 5 km east of Morgan Bluffs that has been dated to ~12,750 calibrated years Before Present (Lakeman and England, 2012).

CHAPTER 5

CONCLUSIONS

SIGNIFICANT CONTRIBUTIONS

This dissertation tests and refines geological hypotheses in order to contextualize and inform forecasts of future environmental change. Major contributions from this research include new data for assessing the dynamics of high-latitude ice sheets, future relative sea level change in the western Canadian Arctic Archipelago, Arctic paleoenvironmental change, the depositional history of the Arctic Ocean basin, and the Quaternary landscape evolution of the Canadian Arctic.

An improved understanding of ice sheets and sea level is of particular international concern (i.e. Joughin and Alley, 2011) because of uncertainties regarding their relationship to the documented, rapid rise in global temperatures beginning in the 19th century (IPCC, 2007). Research of both former and ongoing ice sheet dynamics and sea level change clarifies important constraints on geophysical models charged with assessing future responses of the cryosphere and the oceans to historically unprecedented rates and magnitudes of global climate change (i.e., Bentley, 2010; Long et al., 2011; Price et al., 2011; Deschamps et al., 2012; Tarasov et al., 2012).

The Jesse moraine belt comprises one of the largest moraine belts in Arctic Canada and signals the regional expansion of warm-based thermal regimes in the northwest LIS, which subsequently occasioned an interval of rapid, extensive ice sheet retreat and thinning during the last deglaciation. Deposition of the Jesse moraine belt involved a regional stillstand or advance of the ice sheet margin on eastern Banks Island and on northwest Victoria Island. The timing of this resurgence is confined to 13.75-12.75 cal ka BP and followed an interval of significant ice stream retreat in M'Clure Strait ~13.75 cal ka BP, when the ice margin retreated >300 km, from north-central Banks Island to northwest Victoria Island, in less than 500 years. The Jesse moraine belt comprises widespread controlled moraines, indicating that the basal thermal regime of the ice sheet became polythermal. The onset of widespread warm-based conditions in the northwest LIS, with attendant cold-based conditions along the margin, was coincident with a regional reorganization of ice-flow trajectories, including ice-streaming in Richard Collinson Inlet and the development of a late-glacial ice divide over the Shaler Mountains. It is inferred that rapid changes in ice sheet geometry (i.e. the abrupt deglaciation of M'Clure Strait) occasioned these dynamical changes as a means to re-equilibrate ice sheet surface gradients and stress fields to rapidly changing marine-based glacier margins. This geological record of dynamical changes in the northwest LIS serves as an important glaciological analogue for forecasted changes to the Greenland and Antarctic ice sheets, which are anticipated to dominate levels of eustatic sea level rise in the coming centuries (Meehl et al., 2007; Pardaens et al., 2011; Price et al., 2011; Jevrejeva et al., 2012).

Understanding Quaternary paleoenvironmental variability in the Arctic, future relative sea level changes, and the depositional history of the Arctic Ocean basin, all rely on accurate reconstructions of the extent, thickness, and glacioisostatic signature of Late Wisconsinan glaciation. New surveys of the glacial geology and geomorphology of Banks Island provide important constraints on the Late Wisconsinan configuration of the northwest LIS. These observations also dismiss the previously purported stratigraphy and glacial history of the island (Vincent, 1982, 1983). Consequently, the glacial sediments and landforms are now considered a single depositional sequence relating to Late Wisconsinan glaciation. This record indicates that the LGM limit of the northwest LIS lay west of Banks Island on the Beaufort Sea shelf. The ice sheet was generally thin and cold-based on Banks Island, and was sustained by an ice divide situated over Victoria Island. The character of the northwest LIS on Banks Island contrasts markedly with thick ice streams that occupied Amundsen Gulf and M'Clure Strait, perhaps reaching the shelf break (Stokes et al., 2006, 2009; England et al., 2009; MacLean et al., 2012). This new reconstruction confirms a much more extensive Late Wisconsinan glaciation in the western Canadian Arctic than previously considered, thereby clarifying past climatic and environmental variability in the region during the last glacial-interglacial interval.

The surveyed postglacial marine limit on Banks Island, which is largely a function of the amount of glacioisostatic unloading, complements the newly inferred LGM ice sheet thicknesses and limits. As well, the reconstructed history of postglacial relative sea level change on Banks Island constitutes important new data for regional geophysical models that aim to better understand glacioisostatic crustal adjustments. This knowledge bears on estimates of the geophysical properties of the lithosphere and asthenosphere (i.e. Clague and James, 2002; Peltier and Drummond, 2008), which directly impact modelled forecasts of future relative sea level changes, such as those for several low-lying communities in the western Canadian Arctic (i.e. Paulatuk, Tuktoyuktuk, Sachs Harbour).

The newly recognized extent, thickness, and dynamics of the northwest LIS have implications for our understanding of the Quaternary stratigraphy in the Arctic Ocean basin, where seabed erosion at depths exceeding 1000 m has been attributed to past Quaternary ice sheets, including formerly grounded ice shelves on the Chukchi Borderland (Vogt et al., 1994; Jakobsson, 1999; Polyak et al., 2001, 2007; Kristoffersen et al, 2004; Jakobsson et al., 2005, 2008; Engels et al., 2008). New reconstructions of the thickness and extent of the Late Wisconsinan northwest LIS are in agreement with recent surveying on the Chukchi Borderland suggesting that the limit of seabed erosion during the last glaciation was ~450 m (Polyak et al., 2001, 2007; Jakobsson et al., 2005, 2008). Older erosional landforms at depths exceeding 1000 m, ascribed to older Quaternary ice sheets that occupied the western CAA (Vogt et al., 1994; Jakobsson, 1999; Polyak et al., 2001, 2007; Kristoffersen et al, 2004; Jakobsson et al., 2005, 2008; Engels et al., 2008), provide a proxy for the size of earlier Quaternary ice sheets in Arctic Canada.

The fundamental revision of the Quaternary stratigraphy at Morgan Bluffs constitutes a dismissal of the previous climatostratigraphic framework, which purportedly recorded an elaborate succession of multiple, formally-named glaciations and interglaciations (Vincent 1982, 1983, 1984, 1990; Vincent et al., 1984; Barendregt et al., 1998). A new analysis of the sedimentology and stratigraphy of Morgan Bluffs indicates both former terrestrial and marine depositional environments, including a single phase of glacially-influenced sedimentation. The age of most of the sediments remains loosely constrained to ~ 1 Ma; however, the uppermost stratigraphy is now inferred to record ice-marginal deposition during the last deglaciation, ~12.75 cal ka BP. The revised stratigraphy negates previous correlations between Banks Island and other sites in the circum-Arctic, including the Arctic Ocean basin (Clark et al., 1984; Matthews and Ovenden, 1990) and clarifies a portion of the exceptional geological record of Quaternary environmental change on Banks Island.

This dissertation contributes to our general understanding of high-latitude environmental change and adds to our knowledge of the natural history of the Arctic, which is now unequivocally subject to an unprecedented degree of human influence. The conspicuous decline in summer sea ice extent during the last ~30 years (i.e. Stroeve et al., 2012), perhaps best illustrates the widely documented, non-linear effects of global climate change in the Arctic. Reconstructions of the Quaternary paleoenvironmental evolution of the Canadian Arctic provide an important long-term context for assessing the significance of local and regional manifestations of current and projected global change. A comprehensive geological perspective on high-latitude paleoenvironmental change is necessary for the development of accurate forecasts of future global change.

FUTURE RESEARCH

The recent recognition of Quaternary seabed erosion by thick glacier ice in the Arctic Ocean (Vogt et al., 1994; Jakobsson, 1999; Polyak et al., 2001, 2007; Kristoffersen et al, 2004; Jakobsson et al., 2005, 2008; Engels et al., 2008) places unprecedented constraints on the thickness and extent of circum-Arctic Quaternary ice sheets, including the northwest LIS during the last glaciation. The terrestrial fieldwork presented in this dissertation now warrants future investigations of the Late Wisconsinan limits and thicknesses of the northwest LIS on the Beaufort Sea shelf, which will require extensive marine geophysical surveying and sediment sampling (i.e. MacLean et al., 2010). These observations will bear, particularly, on the extent, thickness, and behaviour of the ice streams that formerly occupied M'Clure Strait and Amundsen Gulf (Stokes et al., 2006, 2009; England et al., 2009; MacLean et al., 2012). Characterizing the former nature of these ice streams will help quantify their significance to Quaternary paleoclimatology, paleoglaciology, paleoceanography, and sea level change, which may be comparable to that postulated for the Hudson Strait ice stream (Heinrich, 1988; Andrews and Tedesco, 1992; Bond et al., 1992, 1993, 1997; Andrews and Barber, 2002). As well, new geological archives of past dynamical changes in the Amundsen Gulf and M'Clure Strait ice streams will add to a rapidly expanding body of geological and geophysical research bearing on the current and future stability of extant ice sheets, particularly the west Antarctic ice sheet (i.e. Weertman, 1974; Mercer, 1978; Joughin and Alley, 2011).

An improved geochronology for the Quaternary stratigraphy on Banks Island will facilitate new, robust chronostratigraphic correlations both among the various exposures and with other geological archives across the Arctic, including Quaternary sediments in the Arctic Ocean basin. The development of such a chronostratigrahic framework spanning the Pliocene and Pleistocene will help clarify the role the Arctic plays in global change. In addition, an improved geochronological framework will bear on our understanding of the geological and environmental evolution of the CAA since the Pliocene when it likely constituted a contiguous landmass adjoined to mainland Canada (England, 1987; Fyles, 1990; Devaney, 1991; Dyke et al., 1992; Fyles et al., 1994). Additional impacts of such fundamental geological research will include new fossil data bearing on the Plio-Pleistocene history of Arctic flora and fauna (i.e. Matthews and Ovenden, 1990; McNeil et al., 2001; Tedford and Harington, 2003; Funder et al., 2009; Ballantyne et al., 2010), new sedimentary records bearing on the tectonic framework of the CAA (i.e. England, 1987; Dyke et al., 1992; McNeil et al., 2001; Harrison et al., 2011), new records of Plio-Pleistocene glaciation and sea level change in the Arctic (i.e. Haug et al., 2005; Funder et al., 2009; Refsnider and Miller, 2010), and additional constraints on Plio-Pliestocene oceanographic reconstructions of the Arctic Ocean (i.e. Sarnthein et al., 2009; Matthiessen et al., 2010).

REFERENCES

Andrews, J.T., Tedesco, K. 1992. Detrital carbonate-rich sediments, northwestern Labrador Sea: implications for ice-sheet dynamics and iceberg rafting (Heinrich) events in the North Atlantic. Geology 20, 1087–1090.

Andrews, J.T., Barber, D.C. 2002. Dansgaard-Oeschger events: is there a signal off the Hudson Strait Ice Stream? Quaternary Science Reviews 21, 443–454. doi:

Ballantyne, A.P., Greenwood, D.R., Sinninghe Damste, J.S., Csank, A.Z., Eberle, J.J., Rybczynski, N. 2010. Significantly warmer Arctic surface temperatures during the Pliocene indicated by multiple independent proxies. Geology 38, 603–606. doi:10.1130/G30815.1.

Barendregt, R.W., Vincent, J.-S., Irving, E., Baker, J. 1998. Magnetostratigraphy of Quaternary and late Tertiary sediments on Banks Island, Canadian Arctic Archipelago. Canadian Journal of Earth Sciences 35, 147–161.

Bentley, M.J. 2010. The Antarctic palaeo record and its role in improving predictions of future Antarctic Ice Sheet change. Journal of Quaternary Science 25, 5–18. doi:10.1002/jqs.1287.

Bond, G., Heinrich, H., Broecker, W.S., Labeyrie, L., McManus, J., Andrews, J.T., Huon, S., Jantschik, R., Clasen, S., Simet, C., Tedesco, K., Klas, M., Bonani, G., Ivy, S. 1992. Evidence for massive discharges of icebergs into the glacial Northern Atlantic. Nature 360, 245–249.

Bond, G., Broecker, W.S., Johnsen, S., McManus, J., Labeyrie, L., Jouzel, J., Bonani, G. 1993. Correlations between climate records from North Atlantic sediments and Greenland Ice. Nature 365, 143–147.

Bond, G., Showers, W., Cheseby, M., Lotti, R., Almasi, P., deMenocal, P., Priore, P., Cullen, H., Hajdas, I., Bonani, G. 1997. A pervasive millennial-scale cycle in North Atlantic Holocene and glacial climates. Science 278, 1257–1266.

Clark, D.L., Vincent, J.-S., Jones, G.A., Morris, W.A. 1984. Correlation of marine and continental glacial and interglacial events, Arctic Ocean and Banks Island. Nature 311, 147–149. doi:10.1038/311147a0.

Deschamps, P., Durand, N., Bard, E., Hamelin, B., Camoin, G., Thomas, A.L., Henderson, G.M., Okuno, J., Yokoyama, Y. 2012. Ice-sheet collapse and sea-level rise at the Blling warming 14,600 years ago. Nature 483, 559–564. doi:10.1038/nature10902.

Devaney, J.R. 1990. Clastic sedimentology of the Beaufort Formation, Prince Patrick Island, Canadian Arctic Islands: Late Tertiary sandy braided river deposits with woody detritus beds. Arctic 44, 206–216.

Dyke, A.S., Morris, T.F., Green, D.E.C., England, J. 1992. Quaternary geology of Prince of Wales Island, Arctic Canada. Geological Survey of Canada, Memoir 433.

Engels, J.L., Edwards, M.H., Polyak, L., Johnson, P.D. 2008. Seafloor evidence for ice shelf flow across the Alaska–Beaufort margin of the Arctic Ocean. Earth Surface Processes and Landforms 33, 1047–1063. doi:10.1002/esp1601.

England, J.H. 1987. Glaciation and the evolution of the Canadian high arctic landscape. Geology 15, 419–424.

England, J.H., Furze, M.F.A., Doupé, J.P. 2009. Revision of the NW Laurentide Ice Sheet: implications for the paleoclimate, the northeast extremity of Beringia, and Arctic Ocean sedimentation. Quaternary Science Reviews 28, 1573–1596.

Funder, S., Bennike, O., Böcher, J., Israelson, C., Strand Petersen, K., Símonarson, L.A. 2009. Late Pliocene Greenland – the Kap København Formation in North Greenland. Bulletin of the Geological Society of Denmark 48, 117–134.

Fyles, J.G. 1990. Beaufort Formation (Late Tertiary) as seen from Prince Patrick Island, Arctic Canada. Arctic 43, 393–403

Fyles, J.G., Hills, L.V., Matthews, Jr., J.V., Barendregt, R., Baker, J., Irving, E., Jette, H. 1994. Ballast Brook and Beaufort Formations (Late Tertiary) on northern Banks Island, Arctic Canada. Quaternary International 22/23, 141–171.

Harrison, J.C., Brent, T.A., Oakey, G.N. 2011. Baffin Fan and its inverted rift system of Arctic eastern Canada: stratigraphy, tectonics and petroleum resource potential. In: A.M. Spencer, A.F. Embry, D.L. Gautier, A.V. Stoupakavoa, K. Sørensen (Eds.), Arctic Petroleum Geology. Geological Society, London, Memoirs 35, 595–626. doi:10.1144/M35.40.

Haug, G.H., Ganopolski, A., Sigman, D.M., Rosell-Mele, A., Swann, G.E.A., Tiedemann, R., Jaccard, S.L., Bollmann, J., Maslin, M.A., Leng, M.J., Eglinton, G. 2005. North Pacific seasonality and the glaciation of North America 2.7 million years ago. Nature 433, 821–825. doi:10.1038/nature03332.

Heinrich, H. 1988. Origin and consequences of cyclic ice rafting in the Northeast Atlantic Ocean during the past 130,000 years. Quaternary Research 29, 143–152.

Jakobsson, M. 1999. First high-resolution chirp sonar profiles from the central Arctic Ocean reveal erosion of the Lomonosov Ridge sediments. Marine Geology 158, 111–123. doi:10.1016/S0025-3227(98)00186-8.

Jakobsson, M., Gardner, J.V., Vogt, P., Mayer, L.A., Armstrong, A., Backman, J., Brennan, R., Calder, B., Hall, J.K., Kraft, B. 2005. Multibeam bathymetric and sediment profiler evidence for ice grounding on the Chukchi Borderland, Arctic Ocean. Quaternary Research 63, 150–160. doi:10.1016/j.yqres.2004.12.004.

Jakobsson, M., Polyak, L., Edwards, M., Kleman, J., Coakley, B. 2008b. Glacial geomorphology of the Central Arctic Ocean: the Chukchi Borderland and the Lomonosove Ridge. Earth Surface Processes and Landforms 33, 526–545. doi:10.1002/esp.1667.

Jevrejeva, S., Moore, J.C., Grinsted, A. 2012. Sea level projections to AD2500 with a new generation of climate change scenarios. Global and Planetary Change 80-81, 14–20. doi:10.1016/j.gloplacha.2011.09.006.

Joughin, I., Alley, R.B. 2011. Stability of the West Antarctic ice sheet in a warming world. Nature Geoscience 4, 506–513. doi:10.1038/NGEO1194.

Kristoffersen, Y., Coakley, B., Jokat, W., Edwards, M., Brekke, H., Gjengedal, J. 2004. Seabed erosion on the Lomonosov Ridge, central Arctic Ocean: a tale of deep draft icebergs in the Eurasia Basin and the influence of Atlantic water inflow on iceberg motion? Paleoceanography 19, PA3006. doi:10.1029/2003PA000985.

Long, A.J., Woodroffe, S.A., Milne, G.A., Bryant, C.L., Simpson, M.J.R., Wake, L.M. 2011. Relative sea-level change in Greenland during the last 700 yrs and ice sheet response to the Little Ice Age. Earth and Planetary Science Letters 315-316, 76–85. doi:10.1016/j.epsl.2011.06.027.

MacLean, B., Blasco, S., Bennett, R., England, J., Rainey, W., Hughes-Clarke, J., Beaudoin, J. 2010. Ice keel seabed features in marine channels of the central Canadian Arctic Archipelago: evidence for former ice streams and iceberg scouring. Quaternary Science Reviews 29, 2280–2301. doi:10.1016/j.quascirev.2010.05.032.

MacLean, B., Blasco, S., Bennett, R., Lakeman, T., Hughes-Clarke, J. 2012. Geological history of Amundsen Gulf over the last ~19,000 years: ameliorating climate transition from glacial to interglacial conditions. Abstract #650. International Polar Year 2012 Conference, Montreal, PQ, April 22–27, 2012.

Matthews, Jr., J.V., Ovenden, L.E. 1990. Late Tertiary plant macrofossils from localities in Arctic/Subarctic North America: a review of the data. Arctic 43, 364–392.

Matthiessen, J., Knies, J., Vogt, C., Stein, R. 2010. Pliocene palaeoceanography of the Arctic Ocean and subarctic seas. Philosophical Transactions of The Royal Society A 367, 21–48. doi:10.1098/rsta.2008.0203.

McNeil, D.H., Duk-Rodkin, A., Dixon, J., Dietrich, J.R., White, J.R., Miller, K.G., Issler, D.R. 2001. Sequence stratigraphy, biotic change, 87Sr/86Sr record, paleoclimatic history, and sedimentation rate change across a regional late Cenozoic unconformity in Arctic Canada. Canadian Journal of Earth Sciences 38, 309–331. doi:10.1139/cjes-38-2-309.

Meehl, G.A., Stocker, T.F., Collins, W.D., Fridlingstein, P., Gaye, A.T., Gregory, J.M., Kitoh, A., Knutti, R., Murphy, J.M., Noda, A., Raper, S.C.B., Watterson, I.G., Weaver, A.J., Zhao, Z.-C. 2007. Global climate projections. In: S. Solomon, D. Qin, M. Manning, Z. Chen, M. Marquis, K.B. Averyt, M. Tignor, H.L. Miller (Eds), Climate Change 2007: The Physical Science Basis. Contribution of Working Group 1 to the Fourth Assessment Report of the IPCC, Cambridge University Press, Cambridge, United Kingdom and New York, NY, USA.

Mercer, J.H., 1978. West Antarctic ice sheet and CO_2 greenhouse effect: a threat of disaster. Nature 271, 321–325. doi:10.1038/271321a0.

Nixon, F.C. 2012. The glacial, sea level, and sea ice histories of Melville and Eglinton islands, western Canadian High Arctic: Last Glacial Maximum to present. Ph.D. thesis, University of Alberta, Edmonton, Canada.

Pardaens, A.K., Lowe, J.A., Brown, S., Nicholls R.J., de Gusmao, D. 2011. Sea-level rise and impacts projections under a future scenario with large greenhouse gas emission reductions. Geophysical Research Letters 38, L12604. doi:10.1029/2011GL047678.

Polyak, L., Edwards, M.H., Coakley, B.J., Jakobsson, M. 2001. Ice shelves in the Pleistocene Arctic Ocean inferred from glaciogenic deep-sea bedforms. Nature 410, 453–457. doi:10.1038/35068536.

Polyak, L., Curry, W.B., Darby, D.A., Bischof, J., Cronin, T.M. 2004. Contrasting glacial/interglacial regimes in the western Arctic Ocean as exemplified by a sedimentary record from the Mendeleev Ridge. Palaeogeography, Palaeoclimatology, Palaeoecology 203, 73–93. doi:10.1016/S0031-0182(03)00661-8.

Polyak, L., Darby, D., Bischof, J., Jakobsson, M. 2007. Stratigraphic constraints on late Pleistocene glacial erosion and deglaciation of the Chukchi margin, Arctic Ocean. Quaternary Research 67, 234–245. doi:10.1016/j.yqres.2006.08.001.

Price, S.F., Payne, A.J., Howat, I.M., Smith, B.E. 2011. Committed sea-level rise for the next century from Greenland ice dynamics during the past decade. Proceedings of the National Academy of Sciences 108, 8978–8983. doi:10.1073/pnas.1017313108.

Refsnider, K.A., Miller, G.H. 2010. Reorganization of ice sheet flow patterns in Arctic Canada and the mid-Pleistocene transition. Geophysical Research Letters 37, L13502. doi:10.1029/2010GL043478.

Sarnthein, M., Bartoli, G., Prange, M., Schmittner, A., Schneider, B., Weinelt, M., Andersen, N., Garbe-Schönberg, D. 2009. Mid-Pliocene shifts in ocean overturning circulation and the onset of Quaternary-style climates. Climates of the Past 5, 269–283. doi:

Siddall, M., Milne, G.A. 2012. Understanding sea-level change is impossible without both insights from paleo studies and working across disciplines. Earth and Planetary Science Letters 315/316, 2–3.

Stokes, C.R., Clark, C.D., Winsborrow, M.C.M. 2006. Subglacial bedform evidence for a major palaeo-ice stream and its retreat phases in Amundsen Gulf, Canadian Arctic Archipelago. Journal of Quaternary Science 21, 399–412.

Stokes, C.R., Clark, C.D., Storrar, R. 2009. Major changes in ice stream dynamics during deglaciation of the north-western margin of the Laurentide Ice Sheet. Quaternary Science Reviews 28, 721–738.

Stroeve, J.C., Serreze, M.C., Holland, M.M., Kay, J.E., Malanik, J., Barrett, A.P. 2012. The Arctic's rapidly shrinking sea ice cover: a research synthesis. Climate Change 110, 1005–1027. doi:10.1007/s10584-011-0101-1.

Tedford, R.H., Harington, C.R. 2003. An Arctic mammal fauna from the Early Pliocene of North America. Nature 425, 388–390. doi:10.1038/nature01892.

Vincent, J. -S. 1982. The Quaternary history of Banks Island, NWT, Canada. Géographie physique et Quaternaire 36, 209–232.

Vincent, J. -S. 1983. La géologie du Quaternaire et la géomorphologie de l'Île Banks, Arctique Canadien. Geological Survey of Canada, Memoir 405.

Vincent, J.-S. 1984. Quaternary stratigraphy of the western Canadian Arctic Archipelago. In: Fulton, R.J. (Ed.), Quaternary Stratigraphy of Canada – A Canadian Contribution To IGCP Project 24. Geological Survey of Canada Paper, 84-10, pp. 87–100.

Vincent, J.-S. 1990. Late Tertiary and Early Pleistocene deposits and history of Banks Island, southwestern Canadian Arctic Archipelago. Arctic 43, 339–363.

Vincent, J.-S., Morris, W.A., Occhietti, S. 1984. Glacial and nonglaical sediments of Matuyama paleomagnetic age on Banks Island, Canadian Arctic Archipelago. Geology 12, 139–142. doi:10.1130/0091-7613(1984)12<139:GANSOM>2.0.CO;2.

Vogt, P.R., Crane, K., Sundvor, E. 1994. Deep Pleistocene iceberg plowmarks on the Yermak Plateau: sidescan and 3.5 kHz evidence for thick calving ice fronts and a possible marine ice sheet in the Arctic Ocean. Geology 22, 403–406. doi:10.1130/0091-7613(1994)022<0403:DPIPOT>2.3.CO;2.

Weertman, J., 1974. Stability of the junction between an ice sheet and an ice shelf. Journal of Glaciology 13, 3–13.

Doubt is thus the space between reality and the application of an idea. it ought to be given over to the weighing of experience, intuition, creativity, ethics, common sense, reason and, of course, knowledge, in balanced consideration of what is to be done. The longer this stage lasts the more we take advantage of our intelligence.

John Ralston Saul